University of Alberta

A new Early Eocene (Lostcabinian) mammal assemblage from the Main Body of the Wasatch Formation, Northern Green River Basin; The Pinnacles, Sweetwater Co., Wyoming

by

Allison Marie Neumann

A thesis submitted to the Faculty of Graduate Studies and Research
in partial fulfillment of the requirements for the degree of

Master of Science

Earth and Atmospheric Sciences

©Allison Marie Neumann
Fall 2013
Edmonton, Alberta

Permission is hereby granted to the University of Alberta Libraries to reproduce single copies of this thesis and to lend or sell such copies for private, scholarly or scientific research purposes only. Where the thesis is converted to, or otherwise made available in digital form, the University of Alberta will advise potential users of the thesis of these terms.

The author reserves all other publication and other rights in association with the copyright in the thesis and, except as herein before provided, neither the thesis nor any substantial portion thereof may be printed or otherwise reproduced in any material form whatsoever without the author's prior written permission.

ABSTRACT

Taphonomy of fluvially deposited microvertebrates and systematic paleontology of the Pinnacles buttes in the northwest Great Divide Basin is examined. The Pinnacles buttes contain an early Eocene mammal assemblage of over 900 cataloged specimens from several prolific University of Michigan localities. The diverse assemblage is represented by a minimum of 56 species of 30 families. Sedimentology of the Main Body of the Wasatch formation in the basin margin of the Great Divide has not previously been examined. This thesis provides the first detailed descriptions and measurements of these specimens and explores the sedimentological and taphonomical environments in which this diverse assemblage accumulated in. The microvertebrate fossils were collected from chute-modified channel bar deposits at two fossiliforous horizons in the uppermost 40-50 m of the Main Body of the Wasatch Formation. Concentration of fossils to discrete horizons vertically associated with crevasse splays and gravel bed streams suggests that proximal channel facies played a pivotal role in preservation of fossils in this setting.

ACKNOWLEDGMENTS

This project nucleated from the collaboration of the University of Alberta, Albion College and University of Michigan, for without the dedicated work of so many collectors and sources of funding over several seasons of fieldwork, the collection would have never become as extensive. I owe much gratitude to Shay Cairns, Cheryl Hodgson and Luke McHugh for all their work measuring section and collecting specimens.

This project has been funded by Albion College's Foundation for Undergraduate Research and Creative Activities (FURSCA), Lawrence Taylor Fund for Undergraduate Research, Dr. Bartel's Langbo Professorship, NSERC Discovery Grant, University of Michigan Museum of Paleontology, Albion College Geology Department and University of Alberta Department of Earth and Atmospheric Sciences.

Drs. Zonneveld, Bartels and Gunnell have provided enormous support and guidance over the duration of my undergraduate and graduate education. I am deeply indebted for the all the opportunities, knowledge and fond memories of collecting at South Pass over the past years.

I would like to thank Prof. Bill Bartels for providing me with a solid foundation of the concepts of biostratigraphy and sedimentary geology. I would also like to thank Dr. Gregg Gunnell for his excellent work identifying the taxa in this collection, enthusiasm and expertise of vertebrate mammalogy.

Most of all, I would like to acknowledge my advisor Dr. JP Zonneveld for providing the opportunities to pursue this research and his unfailing support throughout this project.

TABLE OF CONTENTS

APPENDIX B – MEASURED SECTIONS

LIST OF TABLES

CHAPTER THREE

LIST OF FIGURES

CHAPTER ONE

CHAPTER TWO

CHAPTER THREE

ABBREVIATIONS

Facies

Pgv	Green variegated siltstone
Pgg	Green, Grey or Brown Siltstone-Claystone
Fc	Massive Blue Claystone
Gpo	Petromicitic orthoconglomerate
Goo	Oligomictite orthoconglomerate
Sqt	Tabular quartz arenite sandstone
Sspx	Planar-crossbedded sublitharenite sandstone
Sstx	Trough-crossbedded sublitharenite sandstone
Sst	Tabular sublitharenite sandstone
Svf	Very fine silty sandstone
Ssm	Massive sublitharenite sandstone-siltstone
Sqc	Hummocky-crossbedded quartz arenite sandstone
Smr	Heterolithic rippled sandstone and micrite
Lohx	Cross-bedded oolitic grainstone
Lbm	Bedded micrite
Fpsh	Paper shale
Fosh	Carbonaceous shale

FA1	Mud-dominated distal floodplain
FA2	Sand-gravel based meandering streams
FA3	Levee
FA4	Crevasse splay
FA5	Gravel-base thalweg
FA6	Littoral freshwater lacustrine
FA7	Profundal freshwater lacustrine

Other

UM	University of Michigan
UMMP	University of Michigan Museum of Paleontology
SP	South Pass
NALMA	North American Land Mammal age
EECO	Early Eocene Climate Optimum
MAT	Mean Annual Temperature
MAP	Mean Annual Precipitation

CHAPTER ONE

INTRODUCTION

TIMESCALES AND BIOCHRONOLOGY

Time provides a system to delineate and organize causal relationships in evolution and history. Essentially the creation of a timescale permits correlated episodes of faunal turnover to emerge and shape a perception of the history of life. The philosophical framework of time defines chronology in terms of eternalism, in which time is a phenomenon of reality. The application of eternalism to chronology is justified based on description of B and C-series of time (Mctaggart 1908). In the B-Theory of Time, events are ordered into relative 'before and after' series, in which quantitative measurements allocated to a series are common sufficient (though not necessary) conditions in constructing time. The ordering of a string of events with the C-series needs no temporal allocation, similar to how 'relative time' is used in the construction of biochronology. This in effect makes the past, present and future relative to the time frame of the causational events themselves. Hutton (1788) illuminated the cyclical quality to which "time…is to nature endless and as nothing… The result, therefore, of this physical enquiry is, that we find no vestige of a beginning, – no prospect of an end". In such, deep time theoretically strings infinitely into the past and future without obligation for deterministic boundaries. Unbeknownst to Hutton (Gould 1987), fossils were more than just artifacts of deep time, but the criteria used to define it.

Biostratigraphy was first introduced during development of a chronological scale incorporating the stratigraphic succession of fossils (d'Orbigny 1849-1852, Venec-Peyre 2004). Oppel (1858) subsequently conceived of zones, which were time-stratigraphic units with a distinctive faunal or floral assemblage (Teichert 1958). All taxa are bound to a common denominator of temporal attributes. Understanding time is paramount in understanding biologic change. Without chronology and the element of measured time, the modern synthesis of evolution dissipates.

The chronologic framework of biostratigraphy utilizes lithologic and faunal succession to define changes in deep time. This framework as described by Woodburne (2004b), with from physical stratigraphic data to its correlation and relationship to other physical data sets that correspond to specific ages. Temporal changes in lithology, stratigraphic sequence and fossils, correspond to changes in environmental conditions throughout time. Correlation of similar assemblages records successions of changes in a fauna, which in turn provides an empirical basis by which to study systematics and evolutionary processes (Woodburne 2004b). An understanding of the lithostratigraphy is vital in this process as the temporal range of a biochron depends on the vertical and lateral extent of the strata by which fossils are contained (Woodburne 1987).

According to Walsh (2005), Woodburne advocated the idea of using first and last appearance data (FAD's and LAD's) and overlapping ranges of single taxa as boundary definitions. This concept avoids contradiction with other boundary data by defining the time unit biostratigraphically. Boundary data can be modified with new discoveries, such as the Tiffianian-Clarkforkian boundary (Rose 1981, Walsh 2005). This age was initially proposed from fossils in the Clarks Fork Basin, Wyoming (Wood et al. 1941) but proved contentious due to insufficient documentation of the fauna and its stratigraphic associations (Lofgren et al. 2004). Rose (1981) published the most complete description of the Clark's Fork Basin's Polecat Bench section (in addition to many of the characteristic Clarkforkian fauna), formally reinstating the scientific validity of this mammal age. However only boundaries defined aurichronologically by permanent numerical datums are considered formal ages under the definitions of the North American Commission on Stratigraphic Nomenclature (1983). This method of delineating boundaries may seem valid, but placing permanence to boundary datums defies the concept under which relative time measurements are justified.

Only with continuing discoveries, adjustments to age boundaries and understanding of the association between fossil bearing stratotypes can the Land Mamma Age timescale find adequate resolution to consider placing numerical permanence to these biotic changes.

Biochronologic frameworks are used to correlate stratigraphic successions regionally, continentally and globally. Such timescales are constructed for pollen, invertebrates, vertebrates, foraminifera and notably for this study, continental vertebrates including mammals. Wood et al. (1941) and Savage (1951) defined the eighteen land mammal ages in North America using faunal turnovers in mammal fossils. At the time, stratigraphic type sections were used in conjunction with generic level changes to provide names to these stages. The purpose of this was to both reject the common paradigm of previous decades (Hayden 1869, Granger 1914, Matthew 1909) in using lithologic units to define time-stratigraphic concepts (Walsh 2005). Woodburne (2004a, 1987) later refined and summarized the paleontologic criteria for all Cenozoic land mammals ages.

Constructing timescales based on faunal succession of mammals has been of much interest to paleontologists of the last century (Wood et al. 1941, Savage 1951, 1962, Tedford 1970, McKenna et al. 1973, Prothero 2004, Woodburne 1987, 1996, 2004a). Much emphasis recently has been placed on the latest Early Eocene (Wasatchian-Bridgerian) time intervals in North America (Zonneveld et al. 2000; Gunnell et al. 2009, Woodburne et al. 2009a, Woodburne et al. 2009b, Eberle and Greenwood 2012).

BIOSTRATIGRAPHIC FRAMEWORK OF THE EARLY AND MIDDLE EOCENE

The Eocene Epoch represents an era of dynamic change in North America. During the Eocene, the Green River Basin and greater Uinta Basin of Colorado, Utah and southwestern Wyoming hosted several phases of enormous inland lakes,

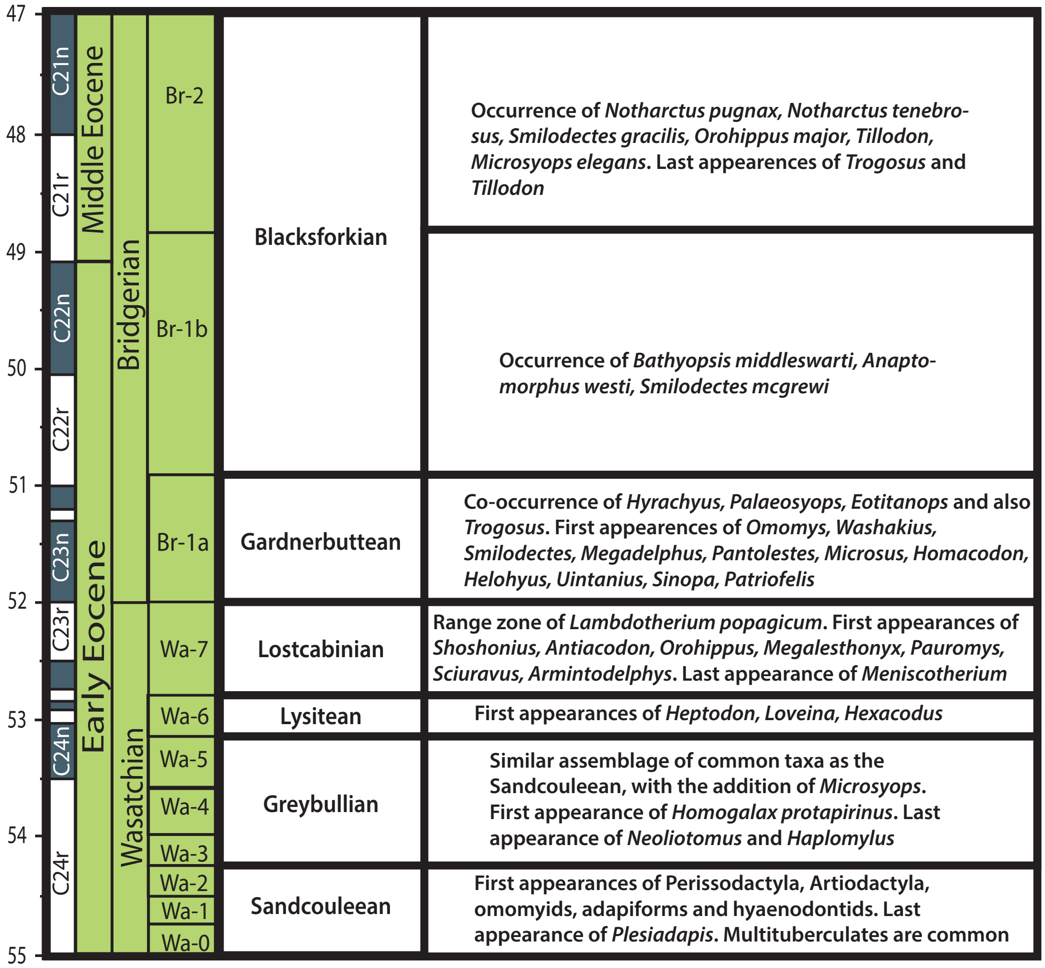

Figure 1.1 - Biostratigraphic framework of the Early and Middle Eocene though the Wa0 to Br2. Chronologic and biochronologic zonation modified from Clyde et al. (1997, 2001) and Tsukui and Clyde (2012). Taxonomic occurrences from Robinson et al. (2004).

effectively shaping the landscape and evolution of animals endemic to these basins. Eutherian mammals began to undergo an adaptive radiation in the earliest Tertiary, and subsequent refinements of this explosion in diversity occurred during the early (Wasatchian) and middle (Bridgerian) Eocene. Unique faunas in the early Tertiary evolution of mammals allow for correlation and relative dating of sedimentary beds based on fossil material. Understanding the assemblages of taxa that define each interval is paramount in accurately associating lithostratigraphic units to a specific biozones. A generalized framework for identifying Wasatchian and Bridgerian subzones is outlined in Fig. 1.1.

Biostratigraphic correlation matched with paleomagnetic and geochronologic results provides a method of absolute dating in sedimentary rocks. Magnetostratigraphic analyses through the Wasatchian-Bridgerian interval have been published on the northern Green River (Clyde et al. 2001), western Green River (Clyde et al. 1997), northern Big Horn (Clyde et al. 1994). Magnetic polarity samples from South Pass in Clyde et al. (2001) place the Wasatchian-Bridgerian boundary at about 52.5 Ma at the beginning of Cr23r. Ar^{40}/Ar^{39} samples from the Grey Tuff of the Wilkins Peak Member of the Green River Formation by Smith et al. (2008) provide a date of 51 Ma for the beginning of the Bridgerian at the end of Cr23r.

WASATCHIAN

The Wasatchian land mammal age at the dawn of the Eocene Epoch experienced vast changes in the ordinal relationships of mammals. Following the Paleocene-Eocene Thermal Maximum (PETM) novel clades formed and further diversified through the Wasatchian. The Paleocene-Eocene Thermal Maximum was a period of climate warming. The mammal faunas in Europe and North America show similar differentiation across the Paleocene-Eocene boundary (Gingerich 2003). The early Sandcouleean (Wa0) was characterized by a dwarfing in mammal size and the appearance of artiodactyls, primates and perissodactyls (Gingerich 2003). *Ectocion, Copecion, Hyracotherium, Prodiacodon, Macrocranon, Lepiacodon, Wyomycteris, Niptomomys* and *Uintacyon* are listed by Woodburne et al. (2009a) to undergo dwarfing across the Paleocene-Eocene boundary. Increased mammal migration (McKenna 1975) and ecological shifts such as an increase in browsing herbivores and decrease in insectivores (Hooker 2000) also occurs at this time. Woodburne et al. (2009a) lists several new genera such as *Arfa, Prototomus, Prolimnocyon, Acarictis, Cantius, Diacodexis, Hyracotherium* and *Macrocranion* that appear as immigrants. The Wa2 through Wa5 represents general climatic stability (Woodburne et al. 2009a) existing between the PETM and EEOC. During the Lysitean subage, mean annual temperature (MAT) increases bring about the origin of new taxa, with *Heptodon* being a possible immigrant (Woodburne et al. 2009a).

Warming during the Early Eocene Climate Optimum (EEOC) lasted from the late Wasatchian (Wa6) to the Bridgerian (Br3) and strongly affected the fauna and flora of the latest Wasatchian (Woodburne et al. 2009a, 2009b, Wilf 2000). By the end of this land mammal age, groups were already being refined and overall change in familial dominance in primates (Muldoon and Gunnell 2002), artidactyls and perrisodactyls is witnessed.

Ages in the Eocene, such as other mammal ages, are commonly named after the formations that host the diagnostic faunas. The four Eocene land mammal ages are based on fossil assemblages from the Green River and Uinta Basins (Robinson et al. 2004) and nomenclature to other sections of Eocene age have been based on lithologic units within the aforementioned basins. The term “Wasatch”, originally by Hayden (1869), refers to fluvial beds from the Bridger basin and southern Fossil basin (Robinson et al. 2004). Hayden (1878) later allocated fossil bearing strata of the Wind River Formation to the Wasatch Group. The discovery of *Coryphodon* in the Bighorn and San Juan Basin by Cope (1877, 1882) provided a Wasatchian affinity to beds outside of the Green River Basin. Granger (1914, 1910) collected in the Bighorn Basin and developed subdivisions of the Wasatchian known as the Sand Coulee, Greybull, Lysite and Lost Cabin (*Lambdotherium* bearing) beds. Gingerich (1983) further refined the biostratigraphy of the Wasatchian (and Paleocene) from extensive collecting within the Willwood Formation of the Bighorn Basin, which allowed for a refined biostratigraphic resolution that previous collecting could not provide. The Wa0 was proposed by Gingerich (1989) as containing faunas characteristically intermediate of the Clarkforkian and other Wasatchian intervals with a marked dominance of hyposodontids and phenacodontids, and the earliest North American occurrence of Artiodactyla. The Gingerich (1983) revision of the Wasatchian in the Clark's Fork Basin included subdivisions of the Greybullian (Schankler 1980) based on distinct turnover events that mark subzone boundaries in the central Bighorn.

Several other mammal bearing early Tertiary localities outside the Rocky Mountain region are known and remain an invaluable asset for faunal comparisons to known type faunas. The San Jose Formation localities of the San Juan Basin, New Mexico contain the genus *Xenicohippus* and thus are assigned a middle Wasatchian (Lysitean, Wa6) age (Robinson et al. 2004, Lucas and Williamson 1993). The earliest Wasatchian (Wa1) Red Hot local fauna (Beard and Dawson 2001) is known from the Tuscahoma Formation in Mississippi. Powder River Basin local fauna (Delson 1971, Robinson and Ivy 1994, Robinson and Williams 1998) contains mammals of the late Sandcouleean to Greybullian (Wa2-Wa3). Pollen from the Wasatch Formation in the Powder River Basin also shows an early Eocene age (Pocknall 1987). Sediments older than Wa3 are not known from the Powder River Basin (Robinson et al. 2004).

BRIDGERIAN

The boundary between the latest Wasatchian (Lostcabinan) and earliest Bridgerian (Gardnerbuttian) is representative of immense climate change in the western cordillera of North America, corresponding to the Early Eocene Climate

Optimum (Gunnell 1997, Woodburne et al. 2009a). Increases in floral diversity were coupled with increased innovation and faunal turnover until the end of the Bridgerian, resulting in dramatic changes to the biodiversity of mammals in the Eocene (Woodburne et al. 2009a).

The term “Bridger” was coined by Hayden (1869). The Bridger Formation was originally divided into various ‘zones’ (A-E) by Matthew (1909) largely based on lithologic distinctions such a “white beds” occurring throughout the formation (Robinson et al. 2004). These have since been distinguished as the lower Blacks Fork Member (A-B), Twin Buttes Member (C-D) (Wood 1934) and Turtle Bluffs Member (E) (Evanoff et al. 1998, Robinson et al. 2004). In the type area Bridger intervals B, C and D are separated by the Sage Creek White Layer and Lone Tree White Layer, respectively (Gunnell and Bartels 2001). As with the Wasatch Formation, faunas from these members came to be considered diagnostic of subdivisions of geological time.

Krishtalka et al. (1987) considered these intervals to be the Blacksforkian and Twinbuttean, respectively. Robinson (1966) designated the earliest Bridgerian as the Gardnerbuttean, which a synonym to the Br1a (Zonneveld et al. 2000; Gunnell and Bartels 2001). In the southern Green River Basin, the first 200m represents the interval A (now known as Br1b, Gunnell and Bartels 2001, Gunnell and Yarborough 2000; Zonneveld et al. 2000). The 150m representing the Bridger B interval is now designated Br2, while the Bridger C-D interval comprise the Br3 (Gunnell and Bartels 2001). Br0 was designated by Gunnell and Bartels (1994) to represent the most of the early Gardnerbuttean (and the *Eotitanops borealis* Assemblage Zone, Gunnell and Yarborough 2000) but has since been abandoned (Gunnell et al. 2009).

During the Br2 interval *Hyopsodus* began to dominant mammalian faunas (Woodburne et al 2009a) which is also known an overal decline in faunal diversity. Rarification analysis of Wa7-Br1age faunas from Stucky (1992) indicate that diversity doubled that of the Wa1-Wa5 interval and then sharply declined by the Br2 (Woodburne et al. 2009).

CLIMATIC SETTING IN THE EARLY AND MIDDLE EOCENE

In the early Cenozoic, most landmasses were separated by seaways (Rose 2006), leaving population exchanges to occur via randomized sweepstakes type (Simpson 1940) dispersal, in which rare and unlikely routes of faunal interchange are used. The Cretaceous epicontinental seaway had largely receded by the early Paleocene, exposing the North American landmass, while global recession of shorelines connected this region with Europe and Asia (Rose 2006). Global warming in the Eocene further permitted migration across high latitude land bridges such as the North De Geer, South Thulean and Beringian Routes (Rose 2006). Population exchange occurred freely between western Europe and North America, particularly across Ellsemere Island (Eberle and Mckenna 2002) while geographic restrictions existed between northern and southern Europe (Rose 2006). Eocene paleogeography also discussed in Mckenna (1975, 1983).

Three distinct turnovers in flora occurred during the early Tertiary in the Rocky Mountain basins based on studies by Wilf (2000). During the early Clarkforkian MAT ranged from 12-19 °C and MAP was 130-150 cm/yr but decreased in the early Wasatchian to 15 °C and 100cm/yr (Wilf 2000). This first turnover was marked by a migration of rare tropical taxa to the basins (Woodburne et al 2009a). The middle and late Wasatchian witnessed another change in flora with a MAT and MAP increase to 23 °C and 140 cm/yr marked by increases in diversity (Wilf 2000). The Latham flora of 53 Ma records a MAT/MAP of 17 °C and 120 cm/yr, and the flora itself was tropical to subtropical with novel plants such as palms, ginger, tree ferns, and aquatic ferns appearing (Woodburne et al. 2009a). The Sourdough flora of 52 Ma records a MAT of 21 °C and 140 cm/yr with presence of dicot plants and thermophilic non-dicots such as plams, gingers, aquatic ferns and tree ferns (Wilf 2000, Woodburne et al.

2009a). Leaves indicate the Sourdough flora was a diverse broad leaved evergreen forest also with hydrophilic plants such as the water lily, horse tails and ferns, but also had subtropical plants such as the alder, poplar and genus *Platycarya* (Woodburne et al. 2009a).

Palynomorphs collected by Roehler (1993) from the Washakie Basin from the Main Body, Lumen, Niland, and Tipton members suggest the climate in this area was warm temperate to subtropical. Leopold and MacGintie (1972) examined the climate during this time from pollen samples, including those referenced in Roehler (1993). The Niland flora of 51.5 Ma records 23 C and 100 cm/yr with a flora similar to the Sourdough, but with less precipitation (Woodburne et al. 2009a).

The third turnover occurred in the Bridgerian at 50 Ma when MAT dropped back to 19.6 C, with less precipitation (75.8 cm/yr) as recorded by the Little Mountain flora (Woodburne et al. 2009a). The Little Mountain flora assemblage included ferns, horsetails, horwort and though species rich, many Niland and Sourdough species (88%) are absent (Woodburne et al. 2009a). Based on Smith et al. (2008), Roehler (1993) and Carroll et al. (2008), Woodburne et al. (2009a) suggested that precipitation changes recorded by the this floral assemblage was coincident with formation of evaporative lacustrine complexes of the Wilkins Peak member. Accord to Roehler (1993) MacGinite reported slight cooling, increased seasonality and decreases in precipitation from the early Eocene to late Eocene. Roehler (1993) suggests that mountains bordering the basin to the east west south and north were likely covered in evergreen and hardwood forests based on conifer and deciduous floras reported by Axelrod (1968) in the Snake River Plain to the west of the Green River Basin.

Although palynological analyses have not been conducted in the study area, aspects of the vertebrate biota are consistent with previous climatic analyses. The presence of abundant, and moderately diverse crocodilian assemblages, several turtle taxa, several lizard taxa, as well as rare snake, amphisbaenid, and amphibian fossils are consistent with warm temperate to subtropical conditions during the Wasatchian-Bridgerian boundary interval in the study area.

EARLY-MIDDLE EOCENE DEPOSITION IN GREEN RIVER BASIN

The Greater Green River Basin covers southwestern Wyoming which is subdivided into the Green River, Sand Wash, Great Divide and Washakie Basins (Love 1961). Green River Basin occupies a 27,000 km^2 region west of the Rock Springs Uplift, east of the Utah-Wyoming Overthrust Range and north of the Unita Range (Roehler 1992a). Love (1961) considered the syncline to the west of the Rock Springs Uplift as the Green River Basin. The Wamsutter Arch and Cherokee Ridge anticlinal structures subdivide the eastern portion of the Greater Green River Basin, north to south, into the Great Divide, Washakie and Sand Wash Basins, respectively. Fossil Basin lies west of the Green River subbasin, and exists as a narrow region within the Overthrust Range.

The Greater Green River Basin formed from structural compression in overlapping events during the Laramide and Sevier Orogenies (Steidmann and Middleton 1991). Thick-skinned deformation (Mederos et al. 2005) during subduction of the Farallon plate occurred along the interior west. The Wind River Range is a 10,000 km^2 body of Laramide-induced basement core uplift thrusted up through Mesozoic strata (Frost et al. 2006). The Wind River thrust complex borders the southern edge of the Wind River Range. These structures were a result of Laramide activity that occurred from the Cretaceous into the Tertiary (Steidtmann and Middleton 1991). During this time, Wyoming and Colorado underwent compression and thrusting of Precambrian basement core formed NW-SE trending complexes across this region (Cerveny and Steidtmann 1993).

The Wind River Thrust Fault maintained activity from the Late Cretaceous through the Eocene (Steidtmann and Middleton 1991). Fragmentation of the

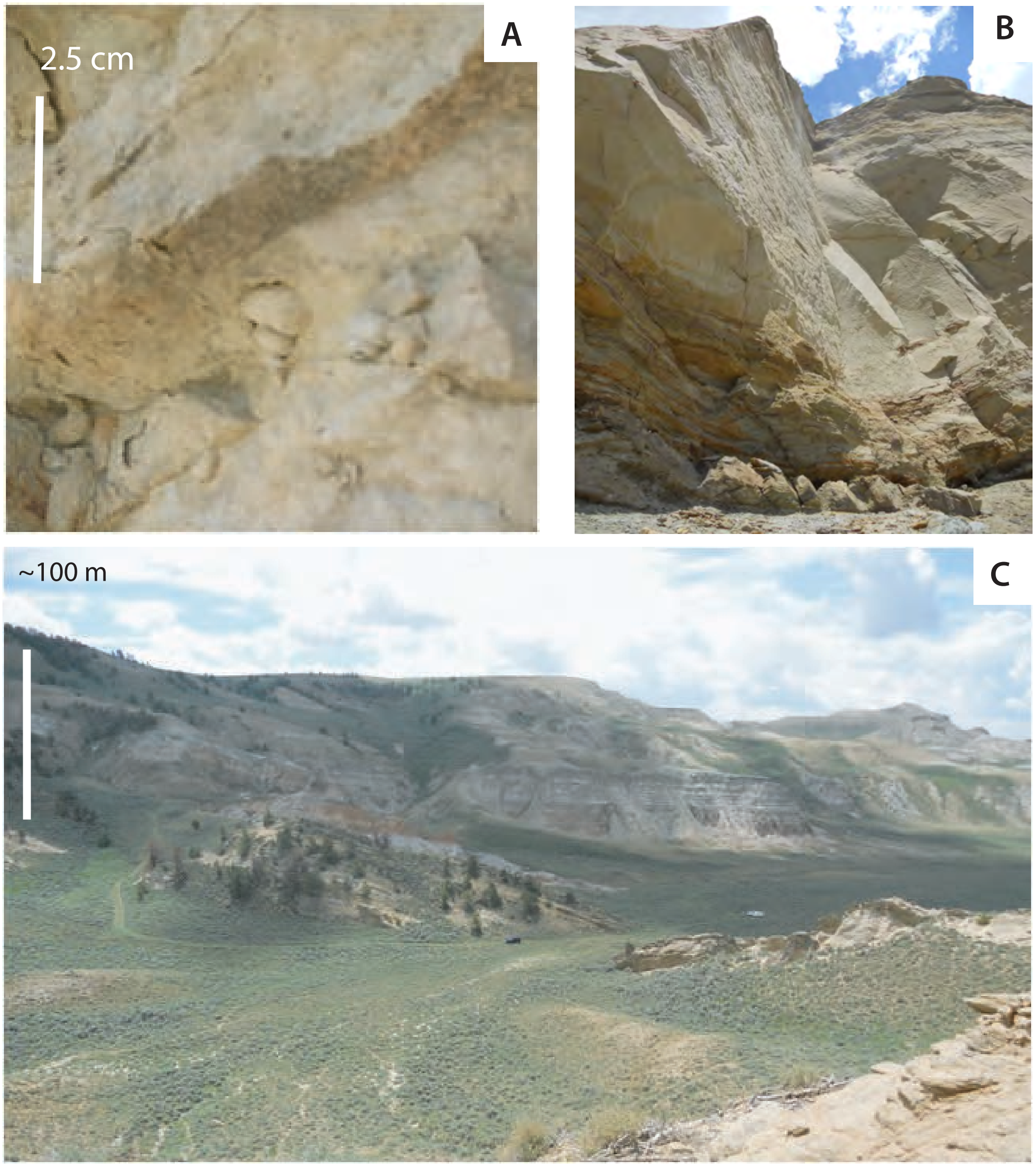

Figure 1.2 - Wind River Thrust Fault and Farson Sandstone bed at Reds Cabin Monocline near Pacific Butte, Fremont Co., Wy. A: Land snail *Vivviparus* sp. at base of the Farson Sandstone. B: Farson Sandstone bed of the Tipton Member. C: Cathedral Bluffs member draped over offset beds of the Main Body of the Wasatch Formation.

hanging wall on the western flank of Wind River Fault produced the Eocene age Continental fault (Steidtmann and Middleton 1991). Continental Fault broaches surface along the base of the Wind River Mountains in South Pass near Pacific Butte at Red's Cabin Monocline. Faulting along this hanging wall reverse fault ended during deposition of the Cathedral Bluffs Member (Steidtmann and Middleton 1991). Reds Cabin Monocline shows displacement up to the Cathedral Bluffs member, but only the Main Body here is offset, and a delta has formed during the Tipton interval known as the Farson Sandstone Member (Figure 1.3) (McHugh 2012).

WASATCH FORMATION

In the central Greater Green River Basin, along the Rock Springs Uplift, the Paleocene Fort Union Formation rests and lies unconformably upon the Lance Formation of the Late Cretaceous (Winterfeld 1982) and conformably grades upwards into the Eocene Wasatch Formation. The Fort Union outcrops along the base of the Rock Springs Uplift, where the base is marked by thick channel sandstone units and a well developed paleosol horizon (Winterfeld 1982). Winterfeld (1982) also discussed problems with delineating the lower boundary of the Wasatch Formation. The lithofacies of the Fort Union change from dominantly paludal to fluvial as it grades into the overlying Wasatch Fm. Due to gradational change in facies from the Fort Union to the Wasatch Fm, the lower boundary of the Wasatch Formation on the eastern side of the Green River Basin is not clearly defined.

In the Green River Basin, tongues of the Green River Formation occur intercalated with the Wasatch Formation. The Main Body outcrops in the central (Pipiringos 1961), east (Masursky 1962) and west (Roehler 1992b) Great Divide Basin (Fig. 1.2). Roehler (1992b) described the beds in this region as grey-green mudstones containing golden sandstone units. The Niland Tongue, described by Pipiringos (1955) formed from paudal and fluvial environments. These deposits

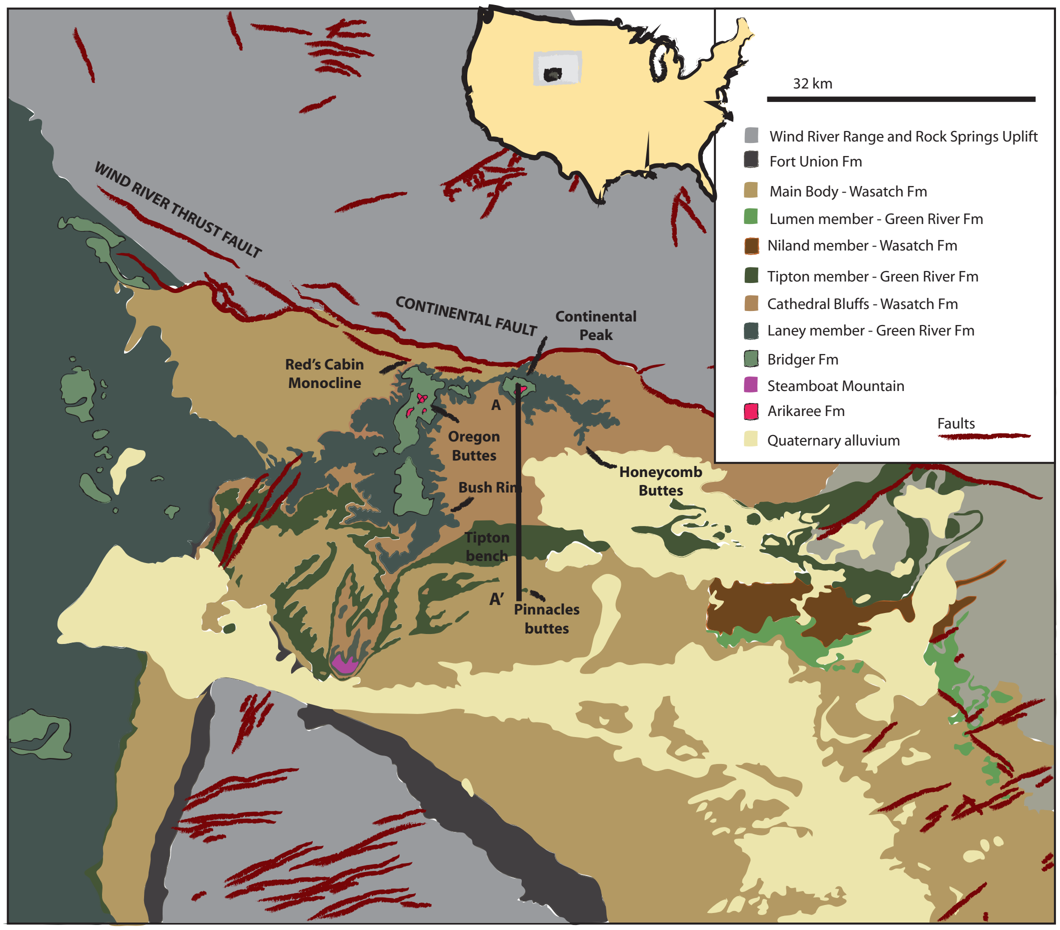

Figure 1.3 - Geologic map of the north-central Green River Basin, modified from Love and Christensen (1985). The South Pass region includes Oregon Buttes, Continental Peak, Bush Rim, the Pinnacles and Reds Cabin Monocline.

lie laterally adjacent to facies of the Lumen Tongue and are situated vertically between the Lumen and Tipton shale units. Likewise the Main Body comprises fluvial facies that lie adjacent to the Tipton, but not vertically underlain by the Lumen Tongue. The Main Body of the Wasatch Formation underlies Scheggs and Rife Beds of the Tipton Member, Green River Formation (Roheler 1992b). The Battle Spring Formation outcrops in the western Great Divide Basin and is an approximate stratigraphic equivalent to the Wasatch Formation (Roehler 1992b).

The Cathedral Bluffs Tongue overlies the Tipton Member in the northern Green River Basin, except in the Bridger Basin, where underfilled lake deposits of the Wilkins Peak Member occur (Chetel and Carroll 2010). In the northern Great Divide Basin, the Cathedral Bluffs sediment at Honeycomb Buttes and Bush Rim have mixed alluvial and lacustrine provenance as movement on the fault interplayed with transgression of the lake margin (McHugh et al. 2010).

GREEN RIVER FORMATION

The position of the shoreline of Lake Gosiute in the continental Green River Basin has resulted from changes in climate, tectonic movement of the faults bounding Laramide uplifts (Surdam and Stanley 1980, Carroll and Bohacs 1999) and geomorphology of the landscape (Carroll et al. 2006).). During the later stages of the Laramide Orogeny, pulses of uplift on previously induced fault complexes along the periphery of the greater Green River and Uinta basins subjugated these basins to intense compressional forces. Subsequent erosion of the Precambrian and Paleozoic core of the Laramide uplifts produced approximately half the sediment thatwas preserved during deposition in the Paleocene (Carroll et al. 2006). According to Carroll et al. (2006) sediment starvation also influenced fluvial deposition on the basin margin and lacustrine deposition in the basin center during the Eocene.

Four main depositional phases occurred in the Green River Formation, first of which is the Lumen tongue, followed by the Tipton, Wilkins Peak and Laney Members (Pietras et al. 2002). The members represent significant shoreline transgressions of Lake Gosiute during the Early to Middle Eocene (Smith et al. 2008). The Tipton Shale is further subdivided into the Scheggs Bed, the Farson Sandstone and the Rife Bed (Pietras et al. 2002, Roehler 1992b). The Scheggs and Rife beds are known from the northern (Roehler 1992b) and southern (Roehler 1991). The Scheggs bed of the Tipton member is regionally continuous and occurs in the Sand Wash Basin at Hargrove Rim (Roehler 1990), in the Bridger Basin (Zonneveld et al. 2005) and in the Great Divide Basin at South Pass (Gunnell and Bartels 2001). Oil shale and fish fossils are also characteristic found in Scheggs and Rife Beds (Pietras et al. 2003, Roehler 1990, Culbertson 1969), but the gastropod *Elimia* (formerly *Goniobasis,* Hartman and Roth 1998) is common throughout Scheggs bed occurrences (Hanley 1976). These unitsare considered to represent freshwater shoreface successionsin the Scheggs bed and saline lacustrine conditions in the Rife bed (Roehler 1992b).

The Tipton Member outcrops in the southwest area of South Pass at the Pinnacles buttes, near Bush Rim and Oregon Buttes, in the Bridger Basin (Zonneveld et al. 2003) and within the central Great Divide Basin (Pipiringos 1961). A thick fossiliferous carbonate sandstone occurs at the base of the Tipton Member in both the Oregon Buttes (Zeller and Stephens 1969) and central basin (Pipiringos 1961). The fossiliferous base of the Scheggs bed is composed of fragmented *Elimia sp.*, *Viviparus sp., Lampsillis sp.* and ostracods. Zeller and Stephens (1969) identified the base of the Tipton as possessing a '*Goniobasis* bed', as also noted in Roehler (1992b) as the base of the Scheggs bed. Shoreface deposits of the Scheggs bed are overlain by oil shale, which are then overlain by, and interbedded with, stromatolites. Stromatolitic beds at the top of the Tipton Member have also been noted by Zeller and Stevens (1969), Schultz (1920), Bradley (1926) and Roehler and Stanton (1992).

PREVIOUS INVESTIGATIONS IN THE NORTHERN GREEN RIVER BASIN

The study area is located in South Pass at the northern region of the Greater Green River Basin between the Wind River Mountains and the Rock Springs Uplift (Fig. 1.3). Sections of the Wasatch Formation, Green River Formation and Bridger Formation are exposed at the Pinnacles, Oregon Buttes and Continental Peak (Fig. 1.3, 1.4).

Recent investigations in South Pass have focused on the chronologic (Clyde et al. 2001, Tsukui and Clyde 2012) and biostratigraphic significance (Bartels and Gunnell 1997, 2001) of the Green River, Bridger and Wasatch Formations in this area. Known fossil occurrence at South Pass preserves a unique biostratigraphic framework in which the Lostcabinian, Gardnerbuttean and Blacksforkian intervals are represented within the Main Body, Cathedral Bluffs and Bridger Formation, respectively (Gunnell and Bartels 2001).

Unusual faunal elements and biodiversity 'hotspots' at basin margins have also been discussed in Gunnell and Bartels (1994), Gunnell and Yarborough (2000), Bartels and Gunnell (1997, 2001) and Gunnell (2012). Ongoing research of basin margin vertebrate assemblages provides new data that may be utilized to examine the role of geographic location on composition of vertebrate faunas.

Early and Middle Eocene fossil localities in the northern Green River Basin were investigated by West (1969, 1970, 1973), Gazin (1952, 1962, 1965) and Pipiringos (1961). Vertebrate occurrences at South Pass were discussed by Zonneveld et al. (2001), Bartels et al. (2004, 2011) Gunnell et al. (2004) and Neumann et al. (2010, 2011) but have not, as yet, been described in detail. Vertebrate fossils from the South Pass area have also served as research material for undergraduate theses by Millhouse (2007), Adams (2008), Neumann (2010), Light (2010), Mahoney (2011), Fontana (2012) and Jacisin (2012). Early Eocene vertebrate localities from the Pinnacles were discussed briefly by Roehler (1991) and in Gunnell and Bartels (2001). These faunas were also the focus of several

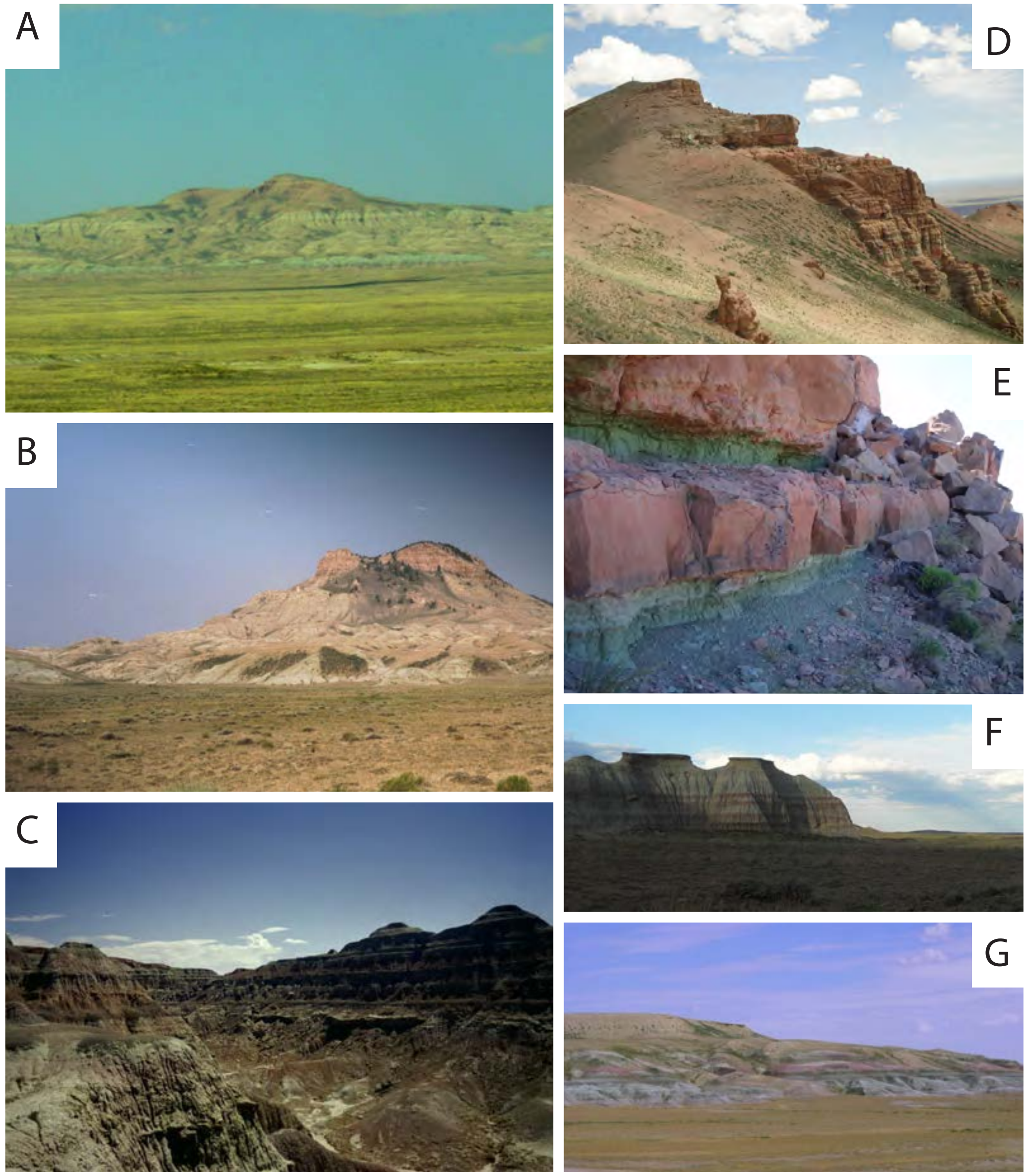

Figure 1.4 - Exposure of Cathedral Bluffs Member, Laney Shale and Bridger Formation at South Pass. A: Wasatch, Green River and Bridger Formations at Continental Peak B: Wasatch, Green River and Bridger Formations at Oregon Buttes. C: Cathedral Bluffs member at Honeycomb Buttes. D-E: Alterations of red and green sediment of the upper Bridger Formation, Continental Peak. F: Cathedral Bluffs member at the base of Oregon Buttes. E: Cathedral Bluffs member and Laney shale at Bush Rim.

conference presentations (Gunnell et al. 2004; Anemone et al. 2008, 2010; Van Regenmorter and Anemone 2008).The sedimentology, taphonomy and taxonomy of Early Eocene vertebrate fossils from the Main Body of the Wasatch Formation have not previously been described from the Pinnacles Buttes. This thesis addresses these issues and provides the first descriptions and measurements of well preserved mammal specimens from the University of Michigan localities.

Detailed lithologic descriptions are provided to determine the stratigraphic relationship of fossil horizons and sedimentological nature of fluvial facies of the uppermost Main Body of the Wasatch Formation and lacustrine facies of the Scheggs bed, Tipton Shale, Green River Formation. The vertebrate assemblage confirms the late Wasatchian age affinity of the uppermost Main Body.

REFERENCES

Adams JK. 2008. Morphometric Analysis and Systematics of Hyopsodus (Mammalia; Condylarthra) from the Early to Middle Eocene of the Green River Basin, Wyoming. Albion College Undergraduate Research Papers, volume 63. Albion College Publishing. Albion, Michigan: 1-270.

Axelrod DI. 1968. Tertiary floras and topographic history of the Snake River Basin, Idaho: Geological Society of America Bulletin. 79: 713-734.

Anemone R., Watkins R., Nachman B., Moore W., Dirks W., Held T., Kersbergen V. 2010. Early Eocene mammalian fossils from an extraordinarily rich new locality in the Great Divide Basin, SW Wyoming. American Journal of Physical Anthropology, Supplement 50: 56.

Anemone R, Dirks W, Nachman B. 2008. Geology and vertebrate paleontology of Paleocene and Eocene deposits in the Great Divide Basin of southwestern Wyoming. 68th Annual Meeting of the Society of Vertebrate Paleontology. 28(3 supplement):45A.

Bartels WS, Gunnell GF. 1997. Basin margin faunas and the origin of North American Land Mammal Age faunal turnover. Journal of Vertebrate Paleontology. 17(3 supplement):31A

Bartels WS, Zonneveld JP, Gunnell GF. 2004. Early fluvial (Cathedral Bluffs) deposition into a lacustrine basin (Green River) and the resulting preservation of an unusual terrestrial vertebrate assemblage, Honeycomb Buttes, Wyoming. Geological Society of America Abstracts with Programs. Denver, Colorado. 36(5): 527.

Bartels WS, McHugh LP, Fontana TM. 2001. An unusual vertebrate assemblage preserved in distal alluvial fan and lake margin deposits of the Cathedral Bluffs Tongue, Wasatch Formation, Bush Rim, Red Desert, Wyoming. Geological Society of America Abstracts with Programs. Minneapolis, Minnesota. 43(5): 264.

Beard KC, Dawson MR. 2001. Early Wasatchian mammas from the Gulf Coast Plain of Mississippi: Biostratigraphic and paleobiogeographic implications. In Eocene Biodiversity: Unusual occurrences and rarely sampled habitats. Ed Gunnell GF. Topics in Geobiology Series, Kluwer/Plenum, New York: 75-94.

Bradley WH. 1964. Geology of the Green River Formation and associated Eocene rocks in southwestern Wyoming and adjacent parts of Colorado and Utah: USGS Professional Paper 496-A. 86p. pl. 1, scale 1:25000

Carroll AR, Bohacs KM. 1999. Stratigraphic classification of ancient lakes: Balancing tectonic and climatic controls. Geology. 27(2): 99-102

Carroll AR, Chetel LM, Smith ME. 2006. Feast to famine: sediment supply control on Laramide basin fill. Geology. 34(3): 197-200

Carroll AR, Doebbert AC, Booth AL, Chamberlain, Rhodes-Carson MK, Smith ME, Johnson CM, Beard BL. 2008. Capture of high-altitude precipitation by a low-altitude Eocene lake, western US. Geology. 36: 791-794.

Cerveny PF, Steidtmann JR. 1993. Fission track thermochronology of the Wind River Range, Wyoming: Evidence for timing and magnitude of Laramide exhumation. Tectonics. 12 (1): p. 77-91

Chetel LM, Carroll AR. 2010. Terminal infill of Eocene Lake Gosiute, Wyoming, USA. Journal of Sedimentary Research. 80: 492-514.

Clyde WC., Stamatakos J., Gingerich PD. 1994. Chronology of the Wasatchian Land Mammal Age (Early Eocene): Magnetostratigraphic Results from the McCullough Peaks Section, Northern Bighorn Basin, Wyoming. Journal of Geology. 102: 367-377.

Clyde WC., Zonneveld JP., Stamatakos J., Gunnell GF., Bartels WS. 1997. Magnetostratigraphy across the Wasatchian/Bridgerian NALMA Boundary (Early to Middle Eocene) in the Western Green River Basin, Wyoming. Journal of Geology. 105: 657-669

Clyde WC., Sheldon ND., Koch PL., Gunnell GF., Bartels WS. 2001. Linking the Wasatchian/Bridgerian boundary to the Cenozoic Global Climate Optimum: new magnetostratigraphic and isotopic results from South Pass, Wyoming. Paleogeography, Paleoclimateology, Paleoecology. 75: 175-199.

Cope ED. 1877. Report upon the extinct Vertebrata obtained in New Mexico by parties of the expedition of 1874. Chapter 12: Fossils of the Eocene period. Geographical Surveys West of the 100th Meridian. Ed, GM Wheeler. Government Printing Office, Washington, DC:37-282.

Cope ED. 1882. Contributions to the history of the Vertebrata of the lower Eocene of Wyoming and New Mexico, made during 1881. Proceedings of the American Philosophical Society. 20(111): 139-197

Culbertson WC. 1969. Oil shale in the Green River Formation, Green River Basin, Wyoming. Wyoming Geological Association Guidebook, 21st Annual Field Conference. Wyoming Geological Society, Casper. 191-195.

Delson E. 1971. Fossil mammals of the early Wasatchian Powder River local fauna, Eocene of northeast Wyoming. Bulletin of the American Museum of Natural History 146: 305-364.

d 'Orbigny A. 1849-1852. Cours elementaire de Paleontologie et de Geologie stratigraphiques, v. 1-2. V. Masson, Paris, France. v 1: 1-299. v 2: 1-847.

Eberle JJ and Mckenna MC. Early Eocene Leptictida, Pantolesta, Creodonta, Carnivora, and Mesonychidae (Mammalia) from the Eureka Sound Group, Ellesmere Island, Nunavut. Canadian Journal of Earth Sciences. 39: 899-910.

Eberle JJ, Greenwood DR. 2012. Life at the top of the greenhouse Eocene world – A review of the Eocene flora and vertebrate fauna from Canada's High Arctic. Geological Society of America Bulletin. 124(1/2): 3-23.

Evanoff E, Robinson P, Murphey C, Kron DG, Engard D, Monaco P. 1994. An early Uintan fauna from Bridger E. Journal of Vertebrate Paleontology. 14(supp 3):24A.

Fontana TM. 2012. Eocene Turtles from the Distal Deposits of the Cathedral Bluffs Tongue (Wasatch Formation), Red Desert, Wyoming. Albion College Undergraduate Research Papers, volume 67. Albion College Publishing. Albion, Michigan: 1-198.

Frost ER, Frost CD, Cornia M, Chamberlain KR, Kirkwood R. 2006. The Teton – Wind River domain: a 2.68-2.67 Ga active margin in the western Wyoming Province. Canadian Journal of Earth Science. 43:1489-1510.

Gazin CL. 1956. The occurrence of Paleocene mammalian in the Fossil Basin of southwestern Wyoming. Journal of Paleontology. 30(3): 707-711.

Gazin CL. 1962. A further study of the lower Eocene mammalian faunas of southwestern Wyoming. Smithsonian Miscellaneous Collections. 144(1): p. 1-46.

Gazin CL. 1965. Early Eocene Mammalian Faunas and Their Environment in the vicinity of the Rock Springs Uplift, Wyoming. Sedimentation of Late Cretaceous and Tertiary Outcrops, Rock Springs Uplift, 19th Annual Field Conference Guidebook. 171-180.

Gould SJ. 1987. Time's Arrow, Time's cycle. Harvard University Press. 1-222.

Granger W. 1914. On the names of lower Eocene faunal horizons of Wyoming and New Mexico. Bulletin of the American Museum of Natural History. 33:201-207.

Granger W. 1910. Tertiary faunal horizons in the Wind River Basin, Wyoming with descriptions of new Eocene mammals. Bulletin of the American Museum of Natural History. 28: 235-251.

Gingerich PD. 1983. Paleocene-Eocene faunal zones and a preliminary analysis of Laramide structural deformation in the Clark's Fork Basin, Wyoming. Wyoming Geological Associaltion Guidebook, Thirty-fourth Annual Field Conference, p. 185-195

Gingerich PD. 1989. New earliest Wasatchian mammalian fauna from the Eocene of northwestern Wyoming: Composition and diversity in a rarely sampled high-floodplain assemblage. University of Michigan Papers on Paleontology 28:1-97.

Gingerich PD. 2003. Mammalian response to climate change at the Paleocene-Eocene boundary: Polcat Bench record in the northern Bighorn Basin, Wyoming. Geological Society of America Special Paper 369. 463-478.

Gunnell GF. 1997. Wasatchian-Bridgerian (Eocene) paleoecology of the western interior of North America: changing paleoenvironments and taxonomic composition of omomyid (Tarsiiformes) primates. Journal of Human Evolution. 32: 105-132.

Gunnell GF. 2012. New Uintasoricine (?Primates, Plesiadapiformes) from the Earliest Bridgerian, Latest Early Eocene of Wyoming. Journal of Paleontology. 86(6):973-978.

Gunnell GF, Bartels WS. 1994. Early Bridgerian (middle Eocene) vertebrates, paleontology and paleoecology of the sourthern Green River Basin, Wyoming. University of Wyoming, Contributions to Geology. 30: 57-70.

Gunnell GF, Bartels WS. 2001. Basin margins, biodiversity, evolutionary innovation, and the origin of new taxa. Gunnell GF. Ed. Eocene Biodiversity: Unusual occurrences and rarely sampled habitats. Topics in Geobiology Series. Kluwer/Plenum, New York. 403-440.

Gunnell GF, Yarborough VL. 2000. Brontotheriidae (Perissodactyla from the late Early and Middle Eocene (Bridgerian) Wasatch and Bridger Formations, Southern Green River Basin, southwestern Wyoming. Journal of Vertebrate Paleontology. 20: 349-368.

Gunnell GF., Bartels WS., Zonneveld JP. 2004. A late Wasatchian (Late Early Eocene) vertebrate assemblage preserved in meandering stream channel deposits, Northern Red Desert, Wyoming: Geological Society of America Abstracts with Programs. Denver, Colorado. 36(5): p. 92.

Gunnell GF., Murphy PC., Stucky RK., Townsend KEB., Robinson P., Zonneveld JP., Bartels WS. 2009. Biostratigraphy and Biochronology of the Latest Wasatchian, Bridgerian, and Uintan North American Land Mammal "Ages". Papers on Geology, Vertebrate Paleontology, and Biostratigraphy in Honor of Michael O. Woodburne. Museum of Northern Arizona Bulletin 65. 279-330.

Hanley JH. Lithostratigraphic relations, nonmarine Molluska and depositional environments of a portion of the Green River and Wasatch formations south of the Rock Springs Uplift, Sweetwater County, Wyoming, with appendices of measured stratigraphic sections. US Geological Survey Open File Report 77-588. 1-233

Hartman JH, Roth B. (1998). Late Paleocene and Early Eocene Nonmarine Molluscan Faunal Change in the Bighorn Basin, Northwestern Wyoming and South-Central Montana. Late Paleocene-Early Eocene climatic and biotic events in the marine and terrestrial record. Ed. Aubry MP, Lucas SG, Berggren WA. Columbia University Press, New York.

Hayden FV. 1869. Chapter 11, Review of Leading Groups, etc. Preliminary Field Report of the United States Geological Survey of Colorado and New Mexico. Washington, DC: 89-99.

Hayden FV. 1878. Wasatch group. In General notes, Geology and Paleontology. American Naturalist. 12: 831.

Hooker JJ. 2000. Ecological response of mammals to global warming in the late Paleocene and early Eocene. Geologiska Foreningens I Stockholm Forhandlingar. 122: 77-79.

Hutton J. 1788. Theory of the Earth; or an investigation of the laws observable in the compostion, dissolution and restoration of land upon the Globe. Transactions of the Royal Society of Edinburgh. 1(2): 209-304.

Jacisin JJ. 2012. Fossil Reptiles from the late Early Eocene (Wasatchian, Lostcabinian) of the Red Desert, Wyoming. Albion College Undergraduate Research Papers, volume 67. Albion College Publishing. Albion, Michigan: 1-132.

Krishtalka L, West RM, Black CC, Dawson MR, Flynn JJ, Turnbull, Stucky RK, McKenna MC, Bown TM, Gloz J, Lillegraven JA. 1987. Eocene (Wasatchian through Duchesnean) biochronology of North America. Woodburne MO. Ed. 1987. Cenozoic Mammals of North America: Biostratigraphy and Geochronology. University of California Press, Berkeley. 1-336.

Leopold EB, MacGinitie HD. 1972. Development and affinities of Tertiary floras in the Rocky Mountians. In Floristics and paleofloristics of Asia and eastern North America. Elsevier, Amsterdam. 147-200.

Light MA. 2010. Evolution and Systematics of the Eocene Alligator *Procaimanoidea*. Albion College Undergraduate Research Papers, volume 65. Albion College Publishing. Albion, Michigan: 1-160.

Lofgren DL, Lillegraven JA, Clemens WA, Gingerich PD, Williamson TE. 2004. Paleocene Biochronology: The Puercan through Clarkforkian Land Mammal Ages. Woodburne MO. Ed. Late Cretaceous and Cenozoic Mammals of North America: Biostratigraphy and Geochronology. Columbia University Press, New York. 1-343.

Love JD. 1961. Definition of Green River, Great Divide and Washakie Basins, southwestern Wyoming. AAPG Bulletin. 45(10): 1749-1755

Love JD, Christiansen AC. 1985. Geologic Map of Wyoming. U. S. Geological Survey, 1: 500,000

Lucas SG, Williamson TE. 1993. Eocene vertebrates and late Laramide stratigraphy of New Mexico. In Vertebrate paleontology in New Mexico. Ed. Lucans SG, Zidek J. Bulletin of the New Mexico Museum of Natural History and Science 2: 145-158.

Mahony ME. 2011. Comparison of Eocene Basin-margin and Basin-center Crocodiles from the Bridger Formation, Green River Basin, Wyoming. Albion College Undergraduate Research Papers, volume 66. Albion College Publishing. Albion, Michigan: 1-118.

Masursky H. 1962. Uranium-bearing coal in the eastern part of the Red Desert area, Wyoming: US Geological Society Bulletin 1099-B, 152p. pl.1,

Matthew WD. 1909. The Carnivora and Insectivora of the Bridger Basin, middle Eocene. Memoir of the American Museum of Natural History. 9: 291-567.

McHugh LP, Zonneveld JP, Bartels WS, Gunnell GF. Sedimentology, Stratigraphy and ichnology of the Cathedral Bluffs Tongue of the Wasatch Formation. Geological Society of America Abstracts with Programs. Denver, Colorado. 42(5): 135

McKenna MC, Russell DE, West RM, Black CC, Turnbull WD, Dawson MR, Lillegraven JA. 1973. K/Ar recalibration of Eocene North American land mammal “ages” and European ages. Geological Society of America Abstracts with Programs. 5(7):733.

McKenna MC. 1975. Fossil mammals and early Eocene North Atlantic land continuity. Annals of the Missouri Botanical Garden 62: 335-353.

McKenna MC. 1983. Holoarctic landmass rearrangement, cosmic events, and Cenozoic terrestrial organisms. Annals of the Missouri Botanical Garden 70: 459-489.

McTaggart JME. 1908. The Unreality of Time. Mind. 17: 457-474.

Muldoon KM, Gunnell GF. 2002. Omomyid primates (Tarsiiformes) from the Early Middle Eocene at South Pass, Greater Green River Basin, Wyoming. Journal of Human Evolution. 43(4):479-511.

Mederos S, Tikoff B, Bankey V. 2005. Geometry, timing, and continuity of the Rock Springs uplift, Wyoming, and Douglas Creek arch, Colorado: Implications for uplift mechanisms in the Rocky Mountain foreland, USA. Rocky Mountain Geology. 40(2): p. 167-191

Millhouse AM. 2007. Morphometric Analysis of Emydid Turtles from the Eocene of South Pass, Wyoming. Albion College Undergraduate Research Papers, volume 62. Albion College Publishing. Albion, Michigan: 1-162.

Neumann AM. 2010. Systematics and Taphonomy of Microvertebrate Faunas from the Early Eocene of the Pinnacles, Green River Basin, Wyoming. Albion College Undergraduate Research Papers, volume 65. Albion College Publishing. Albion, Michigan: 1-230

Neumann AM., Bartels WS., Gunnell GF., Zonneveld JP. 2010. Comparison of Lostcabinian (Late Early Eocene) mammalian assemblages from the Green River and Wind River Basins, Wyoming. Geological Society of America Abstracts with Programs. Denver, Colorado. 42(5): p. 464

Neumann AM, Zonneveld JP, Bartels WS, Gunnell GF. 2011. Stratigraphy of a fossiliferous late Wasatchian (Lostcabinian) fluvial section in the Red Desert, north eastern Green River Basin, Wyoming. Journal of Vertebrate Paleontology. 31(3 supplement):166

North American Commission on Stratigraphic Nomenclature. 1983. North American Stratigraphic Code. American Association of Petroleum Geology Bulletin. 67: 213-219.

Oppel A. 1858. Die Juranformation Englands, Frankreichs und des sudwestlichen Deutschlands: nach ihren einzelnen Gliedern eingetheilt und verglichen. Ebner and Seubert, Stuttgart, Baden-Wuttemberg. 1-857.

Pietras JT, Carroll AR, Rhodes MK. 2003. Lake basin response to tectonic drainage diversion: Eocene Green River Formation, Wyoming. Journal of Paleolimnology. 30: p. 115-125

Pipiringos GN. 1961. Uranium-bearing coal in the central part of the Great Divide Basin, Wyoming: US Geological Society Bulletin 1099-A, p. A1-A104

Pipiringos GN. 1955. Tertiary rocks in the central part of the Great Divide Basin, Sweetwater County, Wyoming. In Wyoming Geological Association Guidebook, 10th Annual Field Conference, 1955. 100-104.

Pocknall DT. 1987. Paleoenvironments and Age of the Wasatch Formation (Eocene), Powder River Basin, Wyoming. Palaios. 2(4): 368-376.

Prothero DR. 2004. Chapter 18: North American mammalian chronostratigraphy: The contributions of Malcolm C. McKenna. Bulletin of the American Museum of Natural History. 285: 238-245.

Roehler HW. 1990. Sedimentology of freshwater lacustrine shorelines in the Eocene Scheggs bed of the Tipton Tongue of the Green River Formation, Sand Wash Basin, northwest Colorado. US Geological Survey Bulletin 1911, p. 1-12

Roehler HW. 1991. Revised stratigraphic nomenclature for the Wasatch and Green River Formations of Eocene age, Wyoming, Utah and Colorado. US Geological Survey Professional Paper 1506-B. p. B1-B38

Roehler HW. 1992a. Introduction to the Greater Green River Basin. Geology, Physiography and History of Investigations. US Geological Survey Professional Paper 1506-A. p. A1-A14

Roehler HW. 1992b. Description and correlation of Eocene rocks in stratigraphic reference sections for Green River and Washakie Basins, southwest Wyoming. US Geological Survey Professional Paper 1506-D. p. D1-D83.

Roehler HW. 1993. Eocene climates, depositional environments and geography, Greater Green River Basin, Wyoming, Utah and Colorado. US Geological Survey Professional Paper 1506-F. p. F1-F72.

Roehler HW, Stanton RW. 1992. Geological investigations of the Wamsutter Rim Canneloid Coal Bed in the Eocene Niland Tongue of the Wasatch Formation, Northern Washakie Basin, Southwest Wyoming. US Geological Survey Bulletin 2018: 1-16.

Robinson P, Ivy LD. 1994. Paromomyida (Dermoptera?) from the Powder River Basin, Wyoming, and a discussion of microevolution in closely related species. University of Wyoming, Contributions to Geology 30: 91-116.

Robinson P. 1966. Fossil mammals of the Huerfano Formation, Eocene of Colorado. Peabody Museum of Natural History Yale University Bulletin. 21.

Robinson P, Williams BA. 1998. Species diversity, tooth size, and shape of *Haplomylus* (Condylarthra, Hyopsodontidae) from the Powder River Basin, northeastern Wyoming. University of Wyoming, Contributions to Geology 31: 59-78.

Robinson P, Gunnell GF, Walsh SL, Clyde WC, Storer JE, Stucky RK, Froehlich DJ, Ferrusquia-Villafranca I, McKenna MC. 2004. Wasatchian through Duchesnean Biochronology. Woodburne MO. Ed. Late Cretaceous and Cenozoic Mammals of North America: Biostratigraphy and Geochronology. Columbia University Press, New York. 1-343.

Rose KD. 1981. The Clarkforkian land-mammal age and mammalian faunal composition across the Paleocene-Eocene boundary. University of Michigan Papers on Paleontology. 26: 1-197.

Rose KD. 2006. Introduction. The Beginning of the Age of Mammals. John Hopkins University Press, Baltimore. 1-22.

Savage DE. 1951. Late Cenozoic vertebrates of the San Francisco Bay region. University of California Publication of Geological Science. 28: 215– 314.

Savage DE. 1962. Cenozoic geochronology of the fossil mammals of the Western Hemisphere. Revista Museo Argentino Ciencias Naturales. 8: 53-67.

Schultz AR. 1920. Oil possibilities in and around Baxter Basin, in the Rock Springs Uplift, Sweetwater County, Wyoming: US Geological Survey Bulletin. 702: 1-107.

Simpson GG. (1940). Mammals and Land Bridges. Journal of the Washington Academy of Sciences. 30: 147-163.

Smith EM, Carroll AR, Singer BS. 2008. Synoptic reconstruction of a major ancient lake system: Eocene Green River Formation, western United States. Geological Society of America Bulletin. 120(1/2):54-84.

Steidtmann RJ, Middleton LT. 1991. Fault chronology and uplift history of the southern Wind River Range, Wyoming: Implications for Laramide and post-Laramide deformation in the Rocky Mountain foreland. Geological Society of America Bulletin. 103: p. 472-485.

Stucky RK. 1992. Mammalian faunas in North America of Bridgerian to early Arikareean “ages” (Eocene and Oligocene). In Eocene-Oligocene Climatic and Biotic Evolution. Ed.Prothero DR, Berggren WA. Princeton University Press. 464-493.

Surdam RC, Stanley KO. Effects of changes in drainage-basin boundaries on sedimentation in Eocene Lakes Gosiute and Uinta of Wyoming, Utah and Colorado. Geology. 8: 135-139.

Tedford RH. 1970. Principles and practices of mammalian geochronology in North America. Proceedins of the North American Paleontological Convention 2F: 666-703.

Teichert C. 1958. Some Biostratigraphical concepts. Geological Society of America Bulletin. 69: 99-120.

Tsukui K, Clyde WC. Fine-tuning the calibration of the early to middle Eocene geomagnetic polarity time scale: Paleomagnetism of radioisotopically dated tuffs from Laramide foreland basins. Geological Society of America Bulletin. 124(5/6): 870-885.

Van Regenmorter J., Anemone R. 2008. Biostratigraphy of the Freighter Gap and Pinnacles areas, Great Divide Basin, southwestern Wyoming. Journal of Vertebrate Paleontology. 28 (3 supplement):156A.

Venec-Peyre M. 2004. Beyond frontiers and time: the scientific and cultural heritage of Alcide d’Orbigny (1802-1857). Marine Micropaleontology. 50: 149-159.

Walsh SL. 2005. The role of stratotypes in stratigraphy Part 3. The Wood Committee, the Bereley school of North American mammalian stratigraphic paleontology, and the status of provincial golden spikes. Earth-Science Reviews 70. 75-101.

West RM. 1969. Geology and vertebrate paleontology of the northeastern Green River Basin, Wyoming. Wyoming Geological Association Guidebook, 21st Annual Field Conference, p. 77-92.

West RM. 1970. Sequence of mammalian faunas of Eocene age in the Northern Green River Basin, Wyoming. Journal of Paleontology. 44(1): 142-147.

West RM. 1973. Geology and mammalian paleontology of the New Fork-Big Sandy area, Sublette County, Wyoming. Fieldiana. Geology. 29: 1-193.

Winterfeld GF. 1982. Mammalian paleontology of the Fort Union Formation (Paleocene), eastern Rocky Springs Uplift, Sweetwater County, Wyoming. Contributions to Geology, University of Wyoming. 21(1): 73-112.

Wilf P. 2000. Late Paleocene-early Eocene climate changes in southwestern Wyoming: Paleobotanical analysis. Geological Society of America Bulletin 112: 292-307.

Wood HE, Chaney RW, Clark J, Colbert EH, Jepsen GL, Reeside JB, and Stock C. 1941. Nomenclature and correlation of the North American continental Tertiary. Geological Society of America Bulletin. 52:1-48.

Woodburne MO. Ed. 1987. Cenozoic Mammals of North America: Biostratigraphy and Geochronology. University of California Press, Berkeley. 1-336.

Woodburne MO. 1996. Precision and resolution in mammalian chronostratigraphy: principles, practices, examples. Journal of Vertebrate Paleonotology 16(3): 531-555.

Woodburne MO. 2004a. Introduction. Woodburne MO. Ed. Late Cretaceous and Cenozoic Mammals of North America: Biostratigraphy and Geochronology. Columbia University Press, New York. 1-343.

Woodburne MO. 2004b. Principles and Procedures. Woodburne MO. Ed. Late Cretaceous and Cenozoic Mammals of North America: Biostratigraphy and Geochronology. Columbia University Press, New York. 1-343.

Woodburne MO, Gunnell GF, Stucky RK. 2009a. Land mammal faunas of North America rise and fall during the Early Eocene Climatic Optimum. Denver Museum of Nature and Science Annals, No 1, p. 1-74.

Woodburne MO, Gunnell GF, Stucky RK. 2009b. Climate directly influences Eocene mammal faunal dynamics in North America. Proceedings of the National Academy of Sciences. 106 (32): 13399-13403.

Zeller HD, Stephens EV. 1969. Geology of the Oregon Buttes Area Sweetwater, Sublette and Fremont Counties Southwestern Wyoming. United States Geological Survey Bulletin 1256:1-60.

Zonneveld JP, Bartels WS, Wolfe SD. 2001. The occurrence of fossil vertebrates along strandlines of Paleolake Gosiute, Wasatch Formation, South Pass, Wyoming. Journal of Vertebrate Paleontology. 21(3 supplement):117A.

CHAPTER TWO

THE PINNACLES BUTTES MAMMAL ASSEMBLAGE OF THE UPPER MAIN BODY OF THE WASATCH FORMATION, NORTHERN GREEN RIVER BASIN, SWEETWATER CO, WYOMING

INTRODUCTION

Mammal biostratigraphy merges biological and stratigraphic information as a method of correlating rocks of similar age on a continental scale. Faunal turnovers, known temporal ranges of mammal genera and overlapping intervals are used to construct timescales that can be applied to sequences of an unknown age affinity based on the fossil assemblage. The first framework for the North American Land Mammal Ages was defined by continental wide turnover events which occurred from the Paleocene to the early Pleistocene (Wood et al. 1941). After the Wood Committee corroborated findings of previous paleontologists (Matthew 1909, Osborn and Matthew 1909, Granger 1914, Simpson 1933) subsequent authors sought to refine and correlate these ages throughout the Rocky Mountain Basins.The endeavor to define age affinity based on mammal assemblages and pursuits to refine such timescales has lead to various discoveries of temporal faunal change in the Green River (Gingerich 1979, Gunnell 1998b, Zonneveld et al. 2000), Wind River (Stucky et al. 1990), Clarks Fork (Badgley and Gingerich 1988) and Bighorn basins (Gingerich 1983, 1989, Gingerich and Clyde 2001, Gunnell et al. 1992).

The Green River Basin contains stratigraphically continuous fluvial and lacustrine deposits of Eocene age and remains a primary area for the exploration of undescribed fossil assemblages. The objective of this study is to provide descriptions of the fossil fauna from a unique, previously unsampled, fluvial deposit on the northern margin Greater Green River Basin. Early Eocene localities are known from the eastern region of the Greater Green River Basin in the Great

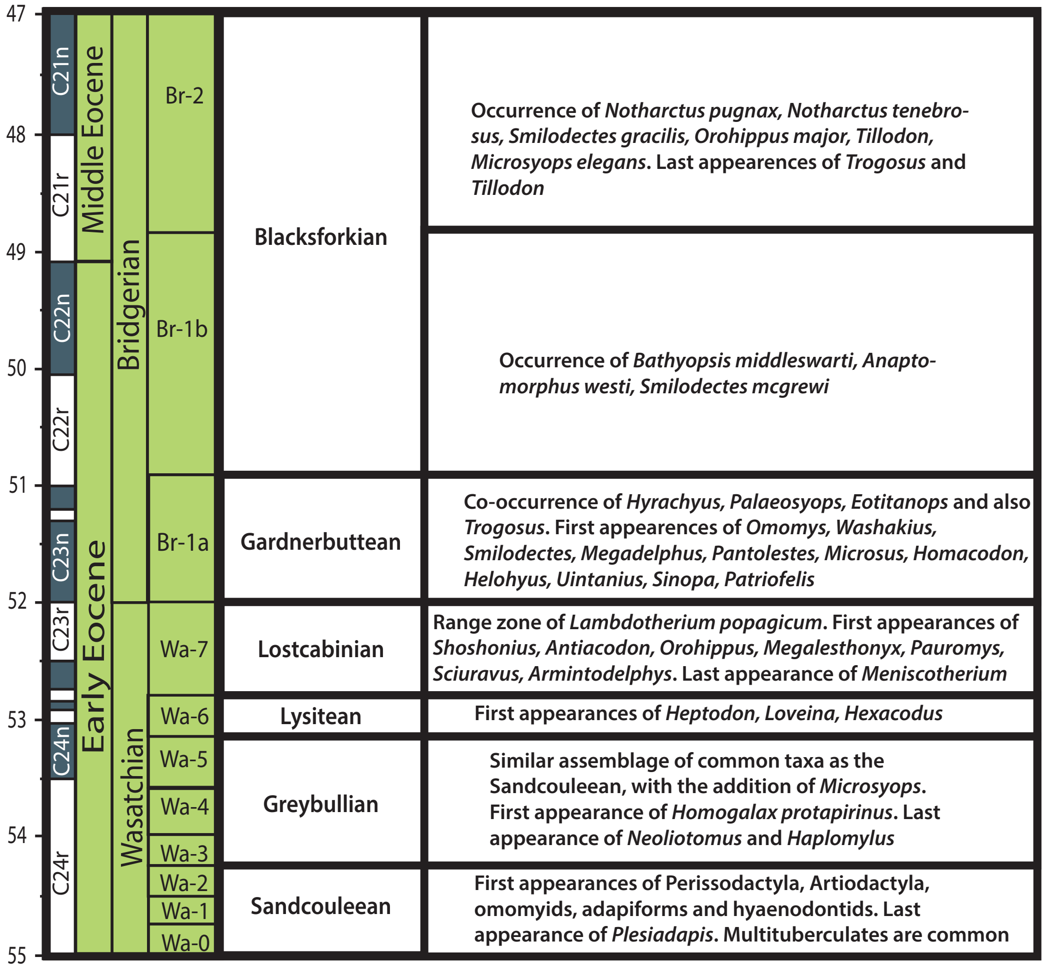

Figure 2.1 - Early to Middle Eocene timescale with biostratigraphic framework of the Wasatchian and Bridgerian. Chronologic and biochronologic framework modified from Clyde et al. (1997, 2001) and Tsukui and Clyde (2012). Taxonomic occurrences from Robinson et al. (2004).

Divide (Gunnell and Bartels 2001, Van Regenmorter and Anemone 2008, Gunnell et al. 2004) and Washakie basins (Honey 1988). Roehler (1991) also mentions a few early Eocene localities (including the Pinnacles, White Mountain and Parnell Creek near Reds Cabin Monocline) in the Great Divide Basin. Vertebrate localities in the northern Green River Basin have also been discussed by Gazin (1952, 1962, 1965), Pipiringos (1961) and West (1969, 1970, 1973). This contribution focuses on the taxonomy of mammalian faunas in the Pinnacles area of South Pass, Wyoming. These faunas provide tight age constraints for the age of the Main Body of the Wasatch Formation and clearly indicate a late Wasatchian (Lostcabinian; Wa7) age for this interval.

GEOGRAPHIC AND GEOLOGIC SETTING

The intermontane Greater Green River Basin occupies the southwestern corner of Wyoming, northeastern Colorado and northwestern Utah (Fig. 2.2). Basement core uplifts from the Laramide Orogeny (Steidmann and Middleton 1991) such as the Wind River Range enclose the basin to the north and the Uinta Range, to the south. South Pass resides geographically in the central-north region of the Green River Basin between the Rock Spring's Uplift and Wind River Range at the northwest corner of the Great Divide Basin.

The South Pass region is composed of lacustrine to fluvial strata of the Wasatch, Green River and Bridger Formations. The Main Body of the Wasatch Formation and Tipton Shale Member of the Green River Formation outcrop in the southeast corner of South Pass at the Pinnacles buttes and to the northwest at Reds Cabin Monocline (Fig. 2.3). The Cathedral Bluffs tongue of the Wasatch Formation, Laney shale of the Green River Formation and Bridger Formation outcrop to the north and west at Oregon Buttes and Continental Peak. Vertebrate localities are known from the Wasatch and Bridger formations at South Pass, yielding assemblages of an early and middle Eocene age (Gunnell and Bartels 2001).

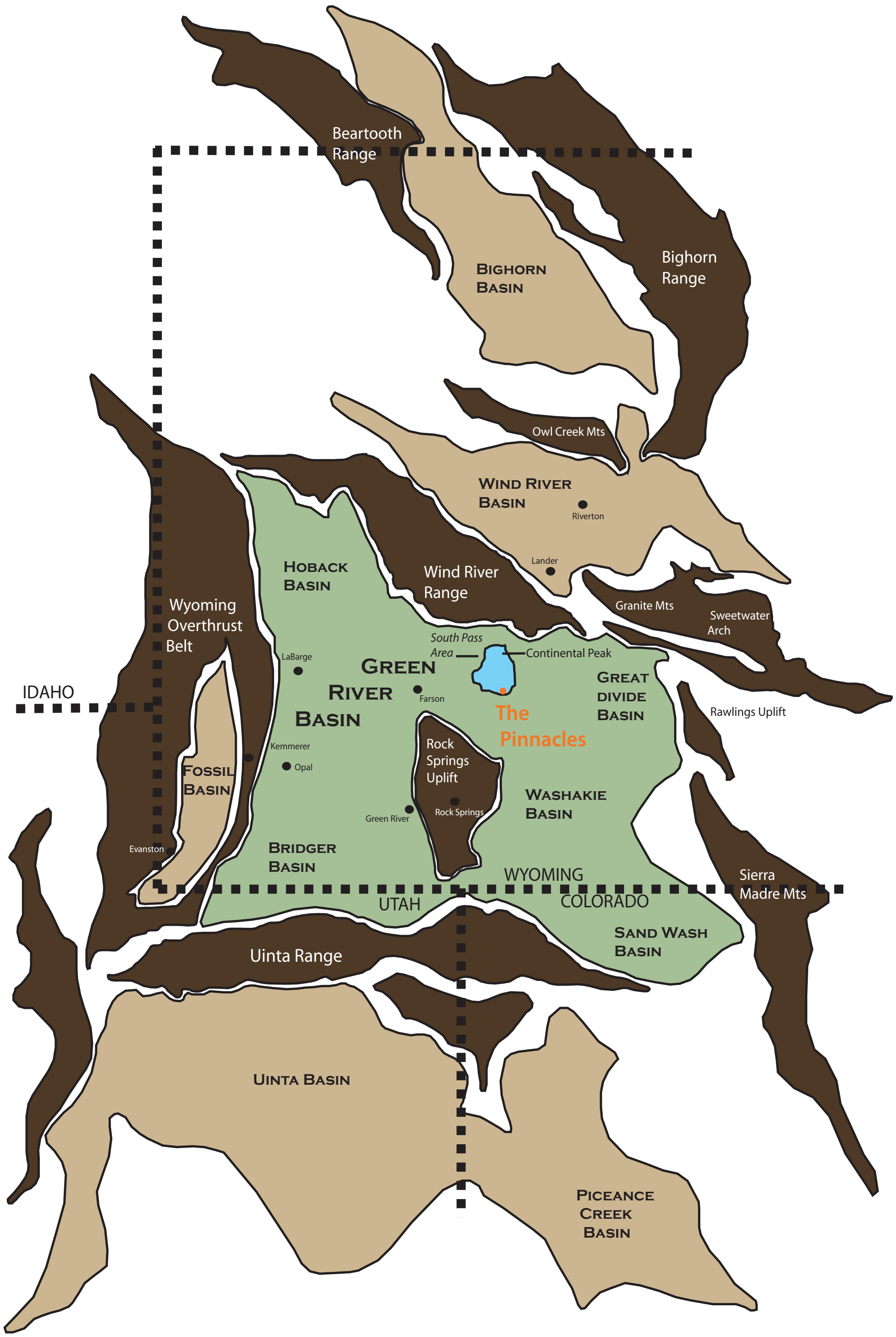

Figure 2.2 - Location of South Pass and the Pinnacles in relation to the Greater Green River Basin and adjacent intermontane basins in the Rocky Mountains. Modified from Smith et al. (2008).

METHODS

The molar specimens of each taxonwere measured and simple descriptions of the general appearance were made to compare specimens of the same genera. Length and width of isolated tooth specimens in the catalogued collection were measured with a Vernier caliper and raw measurements are presented in the Appendix (A1-A16). Photographs, digitally illustrated or graphite drawings are provided for all genera.

Measurements are presented in the following manner: (catalogue number) description = width x length. Length is considered the longest measurement parallel to the anterioposterior axis of the tooth and width is considered the widest part of the tooth perpendicular to this axis. Premolars were described and measured for genera with either small sample sizes or when considered diagnostic fora particular taxon, such as *Microsyops*. Subjective terms used to describe characters on specimens such as ‘small’, ‘distinct’, ‘indistinct’, ‘tall’ were used forsizes of cusps for particular specimen or genera.

FOSSIL LOCALITIES

Eighteen University of Michigan localities were designated for collecting based on prospecting from several field seasons (1999 -2011) (Fig. 2.4). Previous fieldwork at the Pinnacles has lead to the recovery of over 900 specimens of teeth, jaws, postcrania; including 35 miscellaneous(zmisc) samples consisting of broken specimens and those not identifiable to the generic level and numeroussamples of anthill wash and quarry block. Western Michigan University also has localities in this area, which have produced over 200 specimens (Van Regenmorter and Anemone 2008). This study includes the specimens in the collection at the University of Michigan Museum of Paleontology.

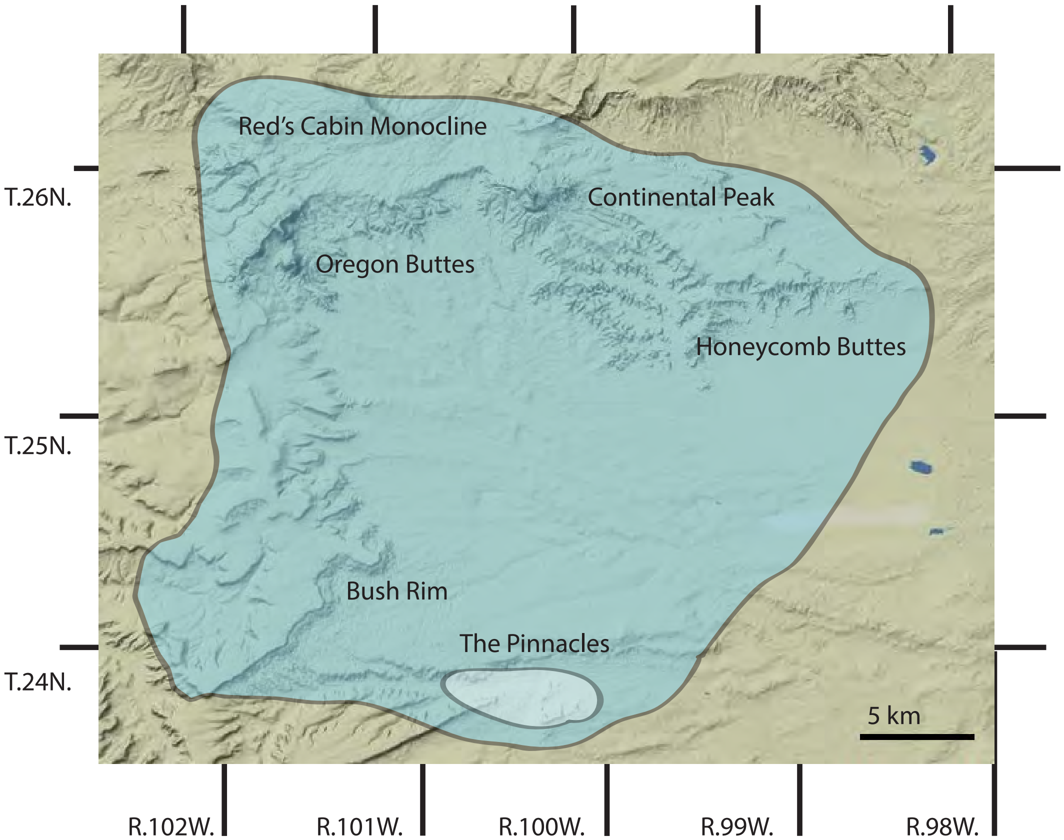

Figure 2.3 - South Pass and fossil bearing areas including Continental Peak, Honeycomb Buttes, Bush Rim and the Pinnacles. Pinnacles Quadrangle is T.24N. R.100W. Terrain map modified from Google Maps (2013).

SYSTEMATIC PALEONTOLOGY OF THE PINNACLES BUTTES ASSEMBLAGE

The Pinnacles buttes assemblage consists of at least 46 species of mammal within 46 genera and 30 families. The Pinnacles has also produced specimens of booid snakes (*Boavus*); emydid (*Echmatemys*), trionychid (*Aymda*) and dermatemydid (*Baptemys*) turtles; and squamate lizards such as xantusiids (*Restes*), xantusids (*Paleoxantusia*), iguanids (*Parasauromalus*), varanids (*Saniwa*) and glyptosaurines (*Odaxosaurus, Xestops* and *Glyptosaurus*) (Neumann 2010). The reptile assemblage was discussed further in Jacisin (2012). Bird fossils are limited to one known genus, the anseriform *Presbyornis*. Isolated fish scales (most likely from the gar-fish *Lepisosteus*) are also a common element in the recovered fossil material.

University of Michigan is abbreviated UM and South Pass is SP. Tooth type is abbreviated with an upper or lower case to designate either position on the dentary or maxilla. M or m stands for molars, I or i for inscisors, C or c for canine and P or p for premolar. Letter abbreviations are followed by a numeral position, either 1,2,3 or 4 (ie. Rm4, or right lower fourth molar); an X signifies an indeterminate tooth position (ie. LMX, or left upper molar)

Class MAMMALIA

Order ARTIODACTYLA

Family DICHOBUNIDAE, Gill 1872

***Bunophorus,* Cope 1882**

Referred Specimens—(103529) left m1; (104496) left P3; (115684) left p4; (103538) right MX; (104524) left astragalus; (104698) right MX; (109065) right m1 and possibly associated right p4; (112101) right p4; (112133) left M1; (112174) right M2; (116245) left m3; (115810) right m3; (116100) right m3; (116263) left P3 and unassociated left P4; (115724) left p3; (115725) left m1.

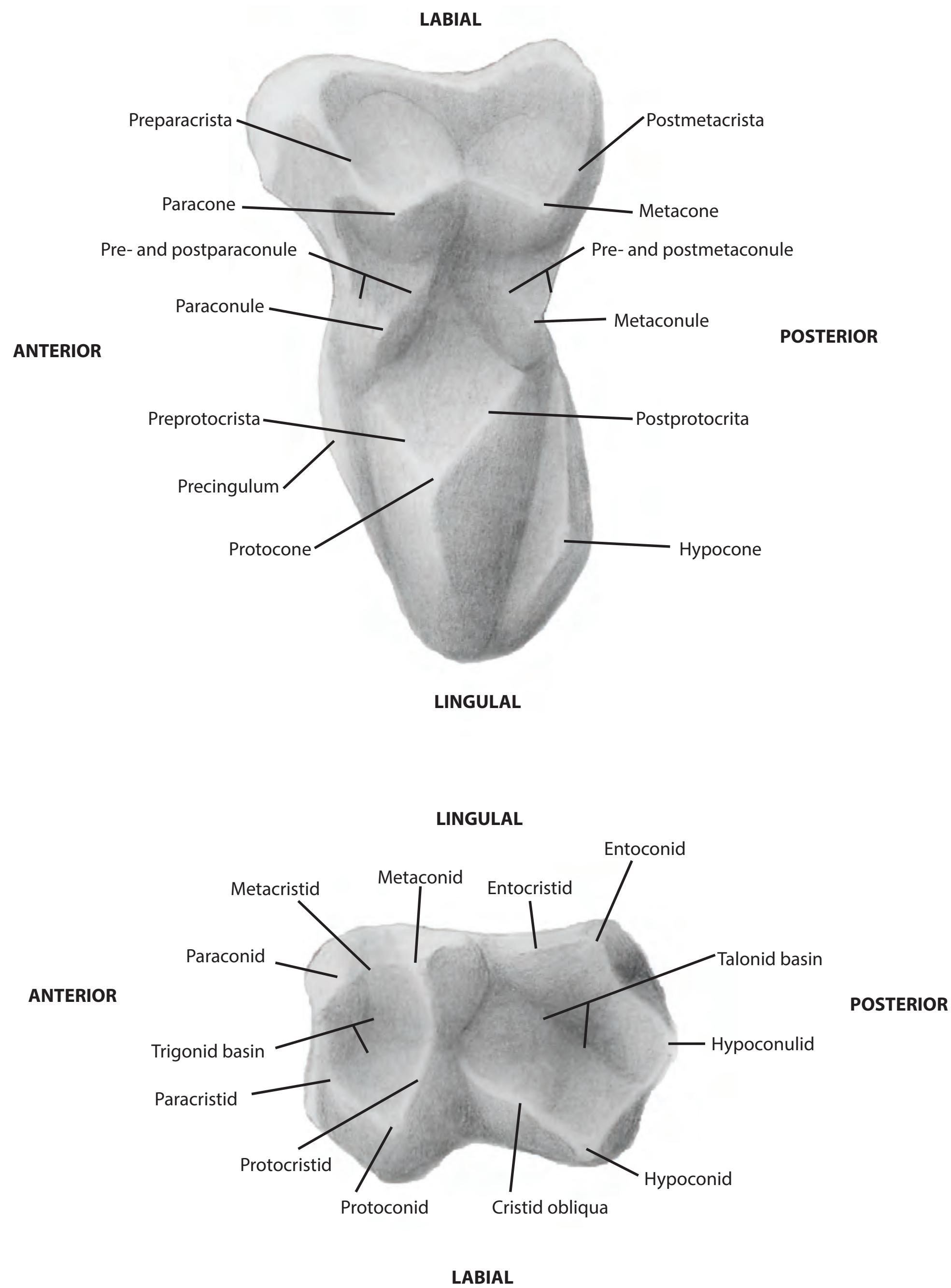

Figure 2.4 - Left upper molar and lower molar morphology, modified from Bown and Kraus (1979), Rose (2006)

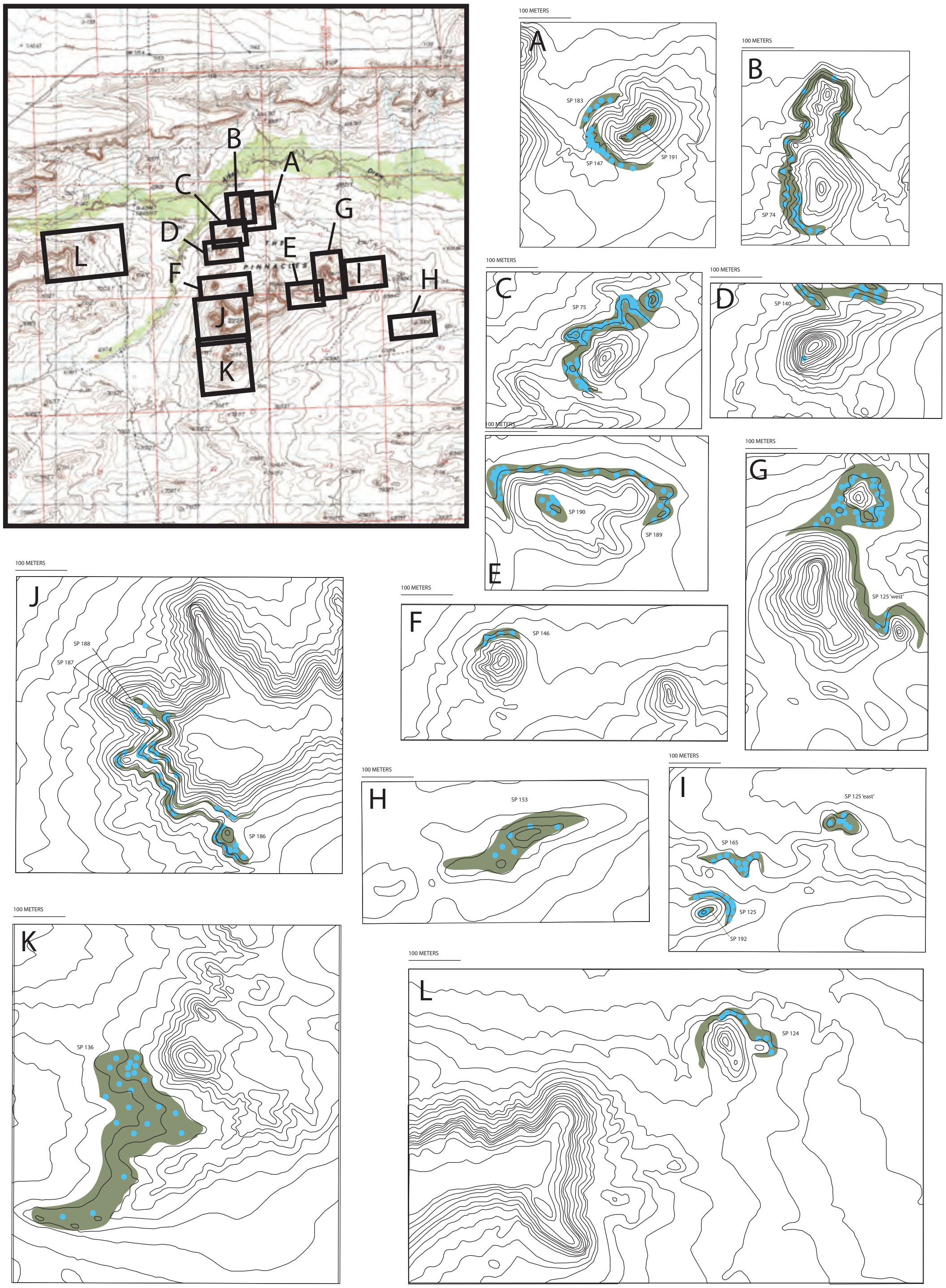

Figure 2.5 - Map of localities in the northern Pinnacles Quadrangle and distribution across each butte. A: SP 183, 147, 191. B: SP 74. C: SP 75. D: SP 140 E: SP 189, 190. F: SP 146. G: SP 125 'west'. H: SP 153. I: SP 165, 165 'east', 125, 192. J: SP 186, 187, 188. K: SP 136. Scale equals 100 meters

Known species—*Bunophorus etsagicus* Cope 1882, *B. sinclairi, B. macropternus, B. granger, B. pattersoni* and *B. robustus.*

Occurrence—SP 74, SP 75, SP 136, SP 147, SP 125

Description—Cusps on the upper and lower molars of *Bunophorus* are more rounded than *Diacodexis* (Rose 2006). The UMMP specimens generally have low bunodont to bulbous cusps. The lower third molars have an elongate talonid (UM 116100, 116245). The hypocone is reduced on the upper first molar (UM 112133) and also on MX specimen UM 103538, which is also likely an M1.

Discussion—*Bunophorus* is known from the early Wasatchian to early Bridgerian (Janis et al. 1998). The molars more suited for omnivory and herbivory and possess bunodont and brachydont shapes (Rose 2006).

Measurements—(104698) right MX = 7.90 x 5.65; (112133) left M1 = 6.30 x 5.70; (112174) right M2 = 8.10 x 5.60; (103529) left m1 = 7.35 x 6.45; (115725) left m1 = 5.30 x 6.00; (116245) left m3 = 5.95 x 8.35; (115810) right m3 = 5.10 x 7.45; (116100) right m3 = 5.85 x 8.60

***Bunophorus sinclairi,* Guthrie 1966**

Referred Specimen—(104530) right m1

Occurrence—SP locality 75

Description— A distinct metaconid is present on the upper fourth premolars, which remains absent in all other Eocene artiodactyls (Guthrie 1966). The crista obliqua that is commonly found on the lower molars of other dichobunids is absent in *B. sinclairi* and reduced in *B. estagicus* (Guthrie 1966). The talonid is

completely separated from the trigonid by a deep trough, which would be separated by the crista obliqua in other genera (Guthrie 1966).
UM 104530 has a deep medial trough which distinguishes it as *B. sinclairi*. This specimen has bulbous cusps, tall metaconid and a large hypoconid.

Measurements—(104530) right m1 = 6.45 x 7.30

***Diacodexis*, Cope 1881**

***Diacodexis* cf. *D. secans*, Cope 1881**

Referred Specimens—(103524) left M1; (104687) right M1; (104692) left p3; (109050) right M3; (112117) right p4; (112137) left m1; (112193) left M3; (115162) left m2; (115163) left MX; (115702) right M1; (111902) left P4; (115834) left p4; (116109) right M3; (116255) right m2; (112863) right M3; (112879) left m3; (115183) left P4; (115723) left P4; (112837) left M3; (116123) left M3

Known species—*Diacodexis secans* Cope 1881, *D antunesi, D. gazini, D. gracillis, D. ilicis, D. indicus, D. kelleyi, D. metaiacu, D. minutes, D. pakistanensis, D. parvus, D. primus, D. woltonensis*

Occurrence—SP 74, SP 75, SP 135, SP 125, SP 153, SP 136, SP 147

Description— *Diacodexis* possesses more sharp acute cusps than *Bunophorus* (Rose 2006). The lower molars have three distinct trigonid cusps and a broad basined talonid; the m3 has an extended hypoconulid lobe (Rose 2006). UM 112879 however has no paraconid but a posteriorly protruding hypoconulid. The upper molars typically lack a hypocone (Rose 2006) and have distinct conules with a strong anterior and posterior cingulum (115702, 116109).

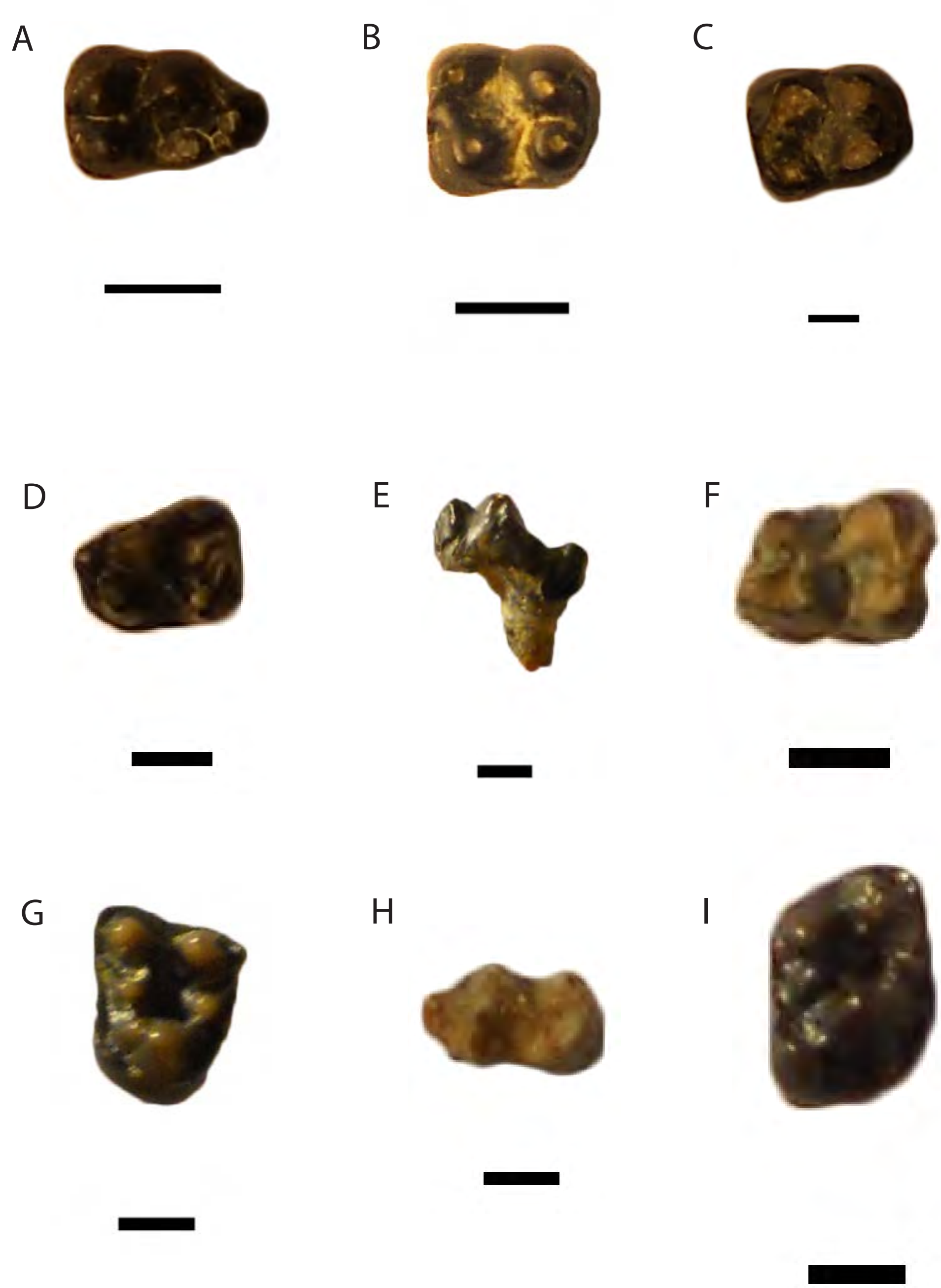

Figure 2.6 - Artiodactyla. A: *Bunophorus* sp., 116110, right m3 in occlusal view, scale equals 5mm. B: *Bunophorus sinclairi*, 104530, right m1 in occlusal view, scale equals 5mm. C: *Bunophorus* sp., left m1 in occlusal view, scale equals 2mm. D: *Antiacodon vanvaleni*, 115196, left m1 in occlusal view, scale equals 2mm. E: *Antiacodon vanvaleni*, 104700, right p3 in labial view, scale equals 2mm. F: *Hexacodus pelodes*, 115886, right m2 in occlusal view, scale equals 2mm. G:*Diacodexis* sp., 115702, right M1 in occlusal view, scale equals 2mm. H: *Diacodexis* sp., 112879, left m3 in occlusal view, scale equals 2mm. I: *Hexacodus pelodes*, 116271, right MX in occlusal view, scal equals 2mm.

Discussion— *Diacodexis* is known from the early Wasatchian (Wa0) to Early Bridgerian (Janis et al. 1998) and has a dental formula of 3.1.4.3/ 3.1.4.3 (Rose 2006). *Diacodexis* is a pentadactyl rabbit sized animal with a vestigial hallux on the foot and vestigial clavicle (Rose 2006).

Measurements—(103524) left M1 = 4.95 x 4.00; (104687) right M1 = 4.95 x 3.60; (115702) right M1 = 4.65 x 3.75; (109050) right M3 = 5.70 x 4.20; (112193) left M3 = 4.95 x 3.20; (116109) right M3 = 5.65 x 3.95; (112863) right M3 = 5.50 x 4.30; (112837) left M3 = 5.55 x 3.90; (116123) left M3 = 5.70 x 4.25; (115162) left m2 = 3.55 x 4.20; (112879) left m3 = 2.70 x 4.60.

Family HOMACODONTIDAE, Marsh 1849

***Hexacodus,* Gazin 1952**

***Hexacodus pelodes,* Gazin 1952**

Referred Specimens—(104490) right M1 or M2; (115165) left p4; (116246) right M1 or M2; (116271) right MX; (115653) left m1; (115656) left MX; (115886) right m2; (115157) left P4

Known species— *Hexacodus pelodes* Gazin 1952, *H. uintensis*

Occurrence—SP 75, SP 147, SP 136

Description—*Hexacodus* has a robust and broad P3, p4 and P4, although the P3 is shorter and longer and p4 has an indistinct to absent metaconid (Stucky 1998). The lower molars possess a tall, pointed entoconid which lies lingual to the hypoconid on the m1-2 (Stucky 1998). The paraconid and metaconid are closely joined on the m2-3, elevated above the protoconid, though the paraconid is smaller than the metaconid (Stucky 1998). On the upper molars of *Hexacodus*, the protocone resides midline on the tooth, the hypocone is small, the mesostyle is weak and the preparaconule crista and preprotocrista form a shearing crest

(Stucky 1998). The upper molars (116246, 116271, 115656) display a reduced hypocones and strong preprotocrista. *H. pelodes* is distinguished from *H. uintensis* by twinning of the paraconid and metaconid on the premolars (Stucky 1998). Of the UM specimens, 115165 showed a twinned paraconid.

Discussion— *Hexacodus* is a selenoform artiodactyl (Stucky 1998) and known from the Middle Wasatchian to Late Wasatchian (Janis et al. 1998). The selenodont type teeth were adapted for grazing and browsing (Rose 2006). An enlarged metaconule and anterior protocone on the upper molars as well as a hypoconulid on the posterior cingulum and a distinct posterior crest are characters possessed by all selenodont forms (Stucky 1998).

Measurements— (115656) left MX = 4.25 x 2.80; (116271) right MX = 4.90 x 3.40; (104490) right M1 or M2 = 5.05 x 4.25; (116246) right M1 or M2 = 5.10 x 4.10; (115653) left m1 = 3.05 x 4.20; (115886) right m2 = 2.80 x 3.65.

Antiacodon, **Marsh 1872**
Antiacodon vanvaleni, **Guthrie 1971**

Referred Specimens—(104700) right p3; (115718) left m2; (115746) right m1; (116103) right p4; (115196) left m1

Known species— *Antiacodon venustus* Marsh 1872, *A. vanvaleni, A. pygmaeus, A. huerfanensis*

Occurrence— SP 136, SP 75

Description—The lower molar m1 (115196) possess a distinct paraconid and the m2 (115718) has a narrow trigonid. The upper M1 in this assemblage (115746) showed strong preprotocrista and postprotocrista, with a reduced hypocone.

Discussion—*Antiacodon* is known from the latest Wasatchian (Wa7) (Stucky 1998) to late Bridgerian (Br3) (Janis et al. 1998). *Antiacodon* shows variation of the cristid obliqua and intersection with the metaconid, which also appears in most antiacodonts (Stucky 1998). Lostcabinian *Antiacodon* has an equally sized paraconid and metaconid, unlike Bridgerian and later forms which possess a reduced metaconid, with a weak to absent mesostyle and hypocone (Stucky 1998).

Measurements—(115746) right M1 = 6.30 x 5.05; (115196) left m1 = 3.15 x 3.75; (115718) left m2 = 4.05 x 4.95

Order CARNIVORA

Family MIACIDAE, Cope 1880

***Vulpavus,* Marsh 1871**

Referred Specimens—(115194) right m2

Known species— *Vulpavus palustris* Marsh 1871, *V. australis, V. canavus, V. ovatus, V. profectus*

Occurrence – SP 74, SP 75, SP 136

Description— The lower molars possess low trigonids and a very broad talonid basin (Flynn 1998). UM 115194 has tall protoconid, twinned metaconid, distinct paraconid with an anterior crest. The talonid is low and narrow with serration on the entocristid.

Discussion— *Vulpavus* is known from the early Wasatchian (Wa0) to late Bridgerian (Br3) (Flynn 1998). *Vulpavus* belongs to a clade of caniforms possessing low, rounded and quadrate upper molars where shearing is reduced or absent due to lack of carnassiform P4 (Flynn 1998). *Vulpavus australis* has the smallest dentition of any other Wasatchian *Vulpavus*, with a taller m1 trigonid than Bridgerian forms (Rich and Collinson 1973).

Measurements—(115194) right m2 = 2.60 x 3.55

Vulpavus australis, Matthew 1915

Referred Specimens—(103532) right dentary with m2; (112170) right M2; (116251) left M2

Occurrence— SP 75, SP 136, SP 159

Description –*V. australis* possesses a serrated entoconid crest on the m2 (Gingerich 1983). UM 103532 is a left lower dentary fragment with an intact m2, and m3 root. The m2 possesses low rounded cusps, deep wear to the enamel on the protoconid and mesoconid and a weakly developed hypoconulid on a low talonid. The protoconid is large and the paraconid is distinct. The M2 specimens have a labially protruding parastyle and while the hypocone on 116251 is situated lingual to the protocone, the hypocone on the large 112170 specimen is posteriolingual.

Measurements— (112170) right M2 = 6.60 x 3.65; (116251) left M2 = 4.40 x 2.15; (103532) right dentary with m2 = 3.20 x 4.30 with the total length of the dentary fragment being 16.35 mm.

Miacis, Cope 1872

Referred Specimens—(115121) right p4

Figure 2.7 - Carnivora and Creodonta. A-B. *Viverravus* sp., 116272, left m1 in lateral and occlusal views , scale is 1mm. C: *Viverravus*, 115730, right M1 in occlusal view, scale is 1mm. D:*Viverravus*, 115713, left M1 in occlusal view, scale is 1mm. E: *Miacis latidens*, 104688, left M2 in occlusal view, scale is 5mm. F-E: *Uintacyon* sp., 115779, left m3 in occlusal view, scale is 1mm. H-I: *Vulpavus australis*, 103532, right dentary m2 in occlusal and labial views, scale is 10mm. J: *Didymictis* sp., 116275, right mX in labial view, scale 5mm. K: P*rolimnocyon antiques*, 115126 left m2 in labial view, scale is 5mm. L: *Tritemnodon whitiae*, 116260, left c1 in labial view, scale is 5mm.

Known species—*Miacis parvivorus* Cope 1872, *M. australis, M. cognitus, M. deutschi, M. exiguus, M. gracilis, M. jepseni, M. latidens, M. medius, M. petilus, M. sylvestris, M. uintensis, M. washakius, M. winkleri*

Occurrence—SP 136, SP 75, SP 135, SP 124

Description— *Miacis* has moderate to large carnassials and premolars, tubercular dentition is small, and lower molars possess basined heels (Flynn 1998). The p4 (115121) has a tall sectoral protoconid with the metaconid taller than the paraconid.

Discussion— *Miacis* is known from the *e*arly Wasatchian (Wa0) to middle Chadronian (Flynn 1998). *Miacis* is generally a primitive caniform, probably constituting a paraphyletic genus which is distinguished from other caniforms by the lack of derived characters diagnositic of later Cenozoic forms (Flynn 1998).

Measurements—(115121) right p4 = 1.55 x 4.60

Miacis latidens, Matthew 1915

Referred Specimens—(104688) left M2

Occurrence—SP 75

Description— UM 104688 has a labially protruding parastyle with strong postparacrista and an inflated protocone (larger than the metacone). The M2 also has no hypocone, but strong preprotocrista and postprotocrista.

Measurements—(104688) left M2 = 7.10 x 4.60

Uintacyon, Leidy 1873

Referred Specimens—(115779) left m3

Known species— *Uintacyon edax* Leidy 1873, *U. acutus, U. asodes, U. bathygnathus, U. jugulans, U. major, U. massetericus, U. pugnax, U. rudis, U. vorax*

Occurrence—SP 153

Description— The mandible of *Uintacyon* is shortened with a deep symphyseal region (Flynn 1998). All lower molars have trenchant talonids and both upper and lower third molars are reduced (Flynn 1998). The m3 UM 115779 is reduced and has a tall trigonid with a distinct paraconid, in addition to small talonid with no discernable entoconid or hypoconulid.

Discussion—*Uintacyon* is known from the Clarkforkian (Cf2) to Duchesnian (Flynn 1998).

Measurements—(115779) left m3 = 1.45 x 1.85

Family VIVERRAVIDAE, Wortman and Matthew 1899

***Viverravus*, Marsh 1872**

Referred Specimens—(115730) right M1; (105195) left M2; (109071) right p4; (112103) right m2 or m3; (115713) left M1; (115765) right p3; (116247) right P4; (108048) left P4; (112893) right p4; (116125) left p4; (116126) left m1; (116127) right M1 fragment; (116136) left m2; (116272) left m1; (112854) left p3; (112856) right p3; (115112) left p3; (115875) left p2; (115887) left M2

Known species— *Viverravus gracilis* Marsh 1872*, V. acutus, V. bowni, V. lutosus, V. minutes, V. politus, V. sicarius*

Occurrence—SP 75, SP 74, SP 125, SP 136

Description— *Viverravus* possesses trenchant talonids on m1-2, where the cristid obliqua is aligned more anterioposteriorly (parallel to the axis of the tooth) then other feliforms, and the sulcus obliquus is narrow and deep (Flynn 1998). Presence of a hypocone on the upper molars is an advanced condition in some species (Flynn 1998). A crest-like hypocone is observed on the P4 (108048, 116247) and on the p4 the metaconid is larger than the paraconid (112893, 116125). Labially protruding parastyle, inflated protocone, strong postparacrista, postprotocrista and preprotocrista were observed on M2 (115887, 105195) and M1 (115713, 116127) specimens. Metaconids typically dominate the paraconid in size on lower premolars (115765, 112893, 116125, 115112). Lower molars have inflated trigonids with tall protoconids and low talonids (116126, 116272, 116136).

Discussion—*Viverravus* is known from the Clarkforkian (Cf2) to Late Uintan (Flynn 1998). Mandible on *Viverravus* is elongate and slender associated with an elongate skull (Flynn 1998). The m1 is a shearing blade which is accentuated on paralophid but reduced on trigonid (where metacone is reduced and paracone is enlarged) (Flynn 1998). This shear on the protolophid is more transverse because metaconid rests labial instead of postlingual to the protoconid, which produces great shearing ability (Flynn 1998).

Measurements— (116247) right P4 = 6.70 x 3.40; (108048) left P4 = 6.10 x 3.20; (115713) left M1 = 6.10 x 3.70; (115887) left M2 = 4.90 x 3.10; (105195) left M2 = 3.65 x 1.70; (115765) right p3 = 1.50 x 5.45; (112854) left p3 = 1.50 x 3.60; (115112) left p3 = 1.30 x 3.65; (109071) right p4 = 2.20 x 5.90; (116125) left p4 = 1.60 x 4.65; (112893) right p4 = 1.60 x 4.55; (116272) left m1 = 2.80 x 5.10; (116136) left m2 = 1.60 x 2.70; (112103) right m2 or m3 = 2.15 x 4.15

***Didymictis,* Cope 1875**

Referred Specimens—(116275) right mX trigonid

Known species— *Bryanictis (=Didymictis) microlestes* Simpson 1935

Occurrence—SP 125

Description—UM 116275 has a lobate paraconid, strong paracristed with an inflated protoconid.

Discussion—*Didymictis* is known from the Tiffanian to the Duchesnean (Flynn 1998). *Didymictis microlestes* was assigned as the type by Simpson (1935) and later reassigned to *Bryanictis* by Gingerich and Winkler (1985).

Order CIMOLESTA

Family APATEMYIDAE, Matthew 1909

***Apatemys,* Marsh 1872**

***Apatemys* c.f. *A. bellus,* Marsh 1872**

Referred Specimens—(105199) right M1; (116278) right I1; (115111) left I1; (115123) left I1; (115660) left i1, (115847) left I1, (115150) right I1

Known species—*Apatemys bellus* Marsh 1872*, A. chardini, A. hendry, A. rodens, A. uintensis*

Occurrence—SP 75, SP 135, SP 136

Description— *Apatemys* has a dental formula of 2.0.2.3/1.0.3.3. *Apatemys* possesses an enlarged front tooth with a reduced number of small teeth between the front of the dentition and the (Gunnell et al. 2008a). I_1 is procumbent and

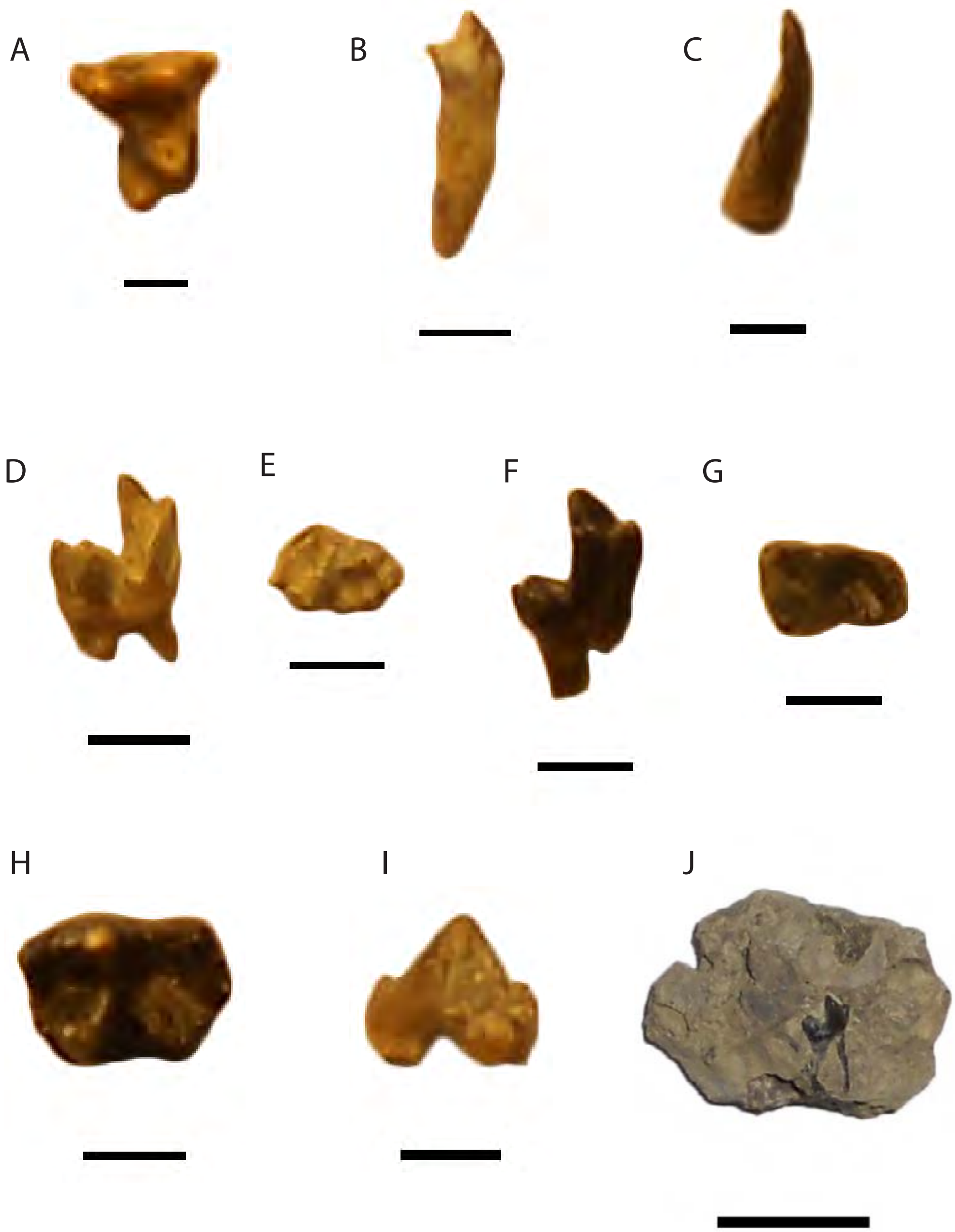

Figure 2.8 - Cimolesta. A: *Apatemys* sp., 105199, right M1 in occlusal view, scale equals 1mm. B: *Apatemys* sp., 115111, left I1 in lateral view, scale equals 2mm. C: *Apatemys* sp., 115150, right i1 in occlusal view, scale equals 2mm. D-E: *Didelphodus* sp., 115127, right m3 in occlusal and lateral view, scale equals 2mm. F-G: *Didelphodus* sp., 115652, left m3 in occlusal and labial view, scale equals 2mm. H: *Paleosinopa* cf. *lutreola*, 116092, left m1 or m2 in occlusal view, scale equals 2mm. I: *Paleosinopa* cf. *lutreola*, 115132, left p3 in labial view, scale equals 2mm. J: *Paleosinopa* cf. *lutreola*, 116254, left mX in labial view, scale equals 10mm.

large while the I^1 rests vertically (Rose 2006). Trigonids are low relative to talonids on lower molars and 2 lower premolars are retained (Gunnell et al. 2008a). UM 105199 has a distinctly triangular upper molar with a hypocone, posteriorly protruding metastyle and anteriorly protruding parastyle.

Discussion—*Apatemys* is known from the earliest Wasatchian (Wa0) to Duchesnian and the temporal range may even be extended from Ti5 – Ch1 (Gunnell et al. 2008a). *Apatemys* resembles a squirrel to mouse sized (small to medium) animal that maintains terminal phalanges that are short, deep and laterally compressed with an elongated IV digit (Rose 2006).

Measurements—(105199) right M1 = 2.70 x 2.45

Family CIMOLESTIDAE, Marsh 1889

***Didelphodus,* Cope 1882**

***Didelphodus* c.f. *D. altidens,* Marsh 1872**

Referred Specimens—(115832) left m3; (115127) right m3; (115652) left m3

Known species— *Didelphodus absarokae* Cope 1882, *D. altidens, D. serus*

Occurrence— SP 125, SP 136

Description— *Didelphodus* has a dental formula of X.1.4.3/3.1.4.3 (number of upper incisors is not known) (Rose 2006). The m1 the trigonid is short relative to the talonid and m2-3 are reduced relative to m1 (Gunnell et al. 2008a). The m3 (115832, 115127, 115652) possesses an inflated trigonid with a reduced talonid and distinct hypoconulid.

Discussion— *Didelphodus* is known from the Wasatchian (Wa1) to Duchesnian (Gunnell et al. 2008a).

Measurements—(115832) left m3 = 1.85 x 2.95; (115127) right m3 = 1.90 x 2.85; (115652) left m3 = 1.90 x 3.10

Family PANTOLESTIDAE, Cope 1884

***Palaeosinopa*, Matthew 1901**

***Palaeosinopa* cf. *P. lutreola*, Matthew 1918**

Referred Specimens— (115819) right M3; (116254) mX, (115132) left P3; (116092) left m1 or m2

Known species— *Palaeosinopa veterrima* Matthew 1901*, P. didelphoides, P. dorri, P. incerta, P. lutreola, P. nunavutensis*

Occurrence— SP 125, SP 136

Description— *Palaeosinopa* has a dental Formula of 3.1.4.3/3.1.4.3. Upper molars of *Palaeosinopa* are tritubercular, have strong postlingual cingular ledge, high and cresentic protocone, sharp and conical metacone and paracone, well developed labial cingular shelf with a crest curving anteriorlabially from paracone to posterolabial end of tooth (Gunnell et al. 2008a). The P3 has a small protocone that is more prominent on the P4 (Gunnell et al. 2008a). The upper third molar has a vestigial metacone (Gunnell et al. 2008a). Lower molars possess equal trigonid cusps, larger talonid than trigonid, strong hypoconid and entoconid (Gunnell et al. 2008). The lower molar cusps are distinct with a tall trigonid (116092, 116254). The hypocone on the M3 (115819) is small and the paracone protrudes labially.

Discussion—*Paleosinopa* is known from the Tiffanian (Ti3) to early Bridgerian (Br1) (Gunnell et al. 2008a)

Measurements— (115132) left P3 = 3.55 x 2.25; (116092) left m1 or m2 = 2.70 x 4.10

Order CONDYLARTHRA

Family HYOPSODONTIDAE, Trouessart 1879

***Hyopsodus,* Leidy 1870**

Referred Specimens—103528, 103534, 104491, 104492, 104494, 104498, 104500, 103545, 103550, 104516, 104517, 104519, 104525, 104527, 104528, 104531, 104532, 104533, 104685, 104699, 104900, 104901, 109048, 109051, 109057, 109059, 109062, 109064, 109070, 109072, 112094, 112096, 112102, 112104, 112105, 112106, 112107, 112124, 112135, 112139, 112171, 112178, 112179, 112184, 112186, 112194, 112195, 112197, 112198, 112200, 115164, 115688, 115689, 115690, 115696, 115703, 115704, 115706, 115707, 115708, 115709, 115710, 115711, 115714, 115715, 115736, 115738, 115739, 115750, 115757, 115758, 115759, 115760, 115764, 115767, 108042, 108043, 111906, 112886, 112891, 112894, 115215, 115786, 115789, 115803, 115817, 115818, 115821, 115823, 115824, 115828, 115829, 115836, 115838, 116098, 116102, 116105, 116108, 116112, 116122, 116130, 116132, 116133, 116135, 111919, 111921, 111922, 111923, 111924, 111931, 111932, 111936, 111943, 111948, 112850, 112852, 112853, 112855, 112860, 112862, 112867, 112870, 112871, 112876, 112878, 112916, 112925, 112926, 112927, 112928, 115092, 115186, 115201, 115657, 115658, 115661, 115665, 115666, 115669, 115672, 115674, 115675, 115676, 115843, 115850, 115851, 115854, 115856, 115857, 115860, 115870, 115874, 115876, 115881, 115884, 115885, 116086, 116090, 116093, 116095, 112076, 112077, 112941, 112081, 112166, 115153, 115155, 115801, 112838, 112840, 112843, 112844, 115773, 115776, 115782, 115784, 115146, 115147, 109028, 115151, 108047, 109014, 109026, 115149 (see appendix for individual descriptions)

Known species— *Hyopsodus paulus* Leidy 1870*, H. fastigatus, H.itinerans, H.lepidus, H.loomisi, H. lysitensis, H. markmani, H. mentalis, H.minor, H. minusculus, H. pauxillus, H. powellianus, H. sholemi, H.simplex, H.tonksi, H. uintensis, H. walcottianus, H. wardi, H. wortmani*

Occurrence—SP 74, SP 75, SP 125, SP 136, SP 146, SP 147, SP 153, SP 159

Description—*Hyopsodus* possesses simple inscisors and canines in addition to first premolars which are similar, single rooted teeth that increase in size posteriorly (Archibald 1998). P2 is double rooted and more elongate than P1 (as in lower first and second premolars) while P3 is triple rooted with prominent deuterocone and lingual talonid (Archibald 1998, Gazin 1968). P4 deuterocone and primary cusp are equal in height while the p4 is double rooted with a distinctive metaconid (Archibald 1998) The upper molars are conical bunodont with six well defined cusps (prominent conules) (Achibald 1998, Matthew 1915). The M1-2 are similar but the M2 is transversly wider and more oblique (Gazin 1968). The anterior molars have a paracone and metacone of equal height, prominent metastyle and parastyle (no mesostyle), labial cingulum and crest which joins the anterior cusps (Gazin 1968). The M3 is more oblique than the anterior molars, with a small metacone compared to the paracone (Gazin 1968). The lower molars have high cusps and a more selenodont tooth pattern (Archibald 1998). The trigonid consists of dominant protoconid and metaconid with a sharp anterior crest and no paraconid, while the talonid portion possesses a tall hypoconid (equi-height to the protoconid) shorter entoconid and cristid oblique extending to join the metaconid, leaving a depression separating the protoconid from the hypoconid (Gazin 1968).

Discussion—*Hyopsodus* is known from the Clarkforkian (Cf3) to Middle Chadronian (Archibald 1998). Classification of *Hyopsodus* species are difficult based on morphological parameters, but size of the molars, particularly the length of the m2, is a more useful method of distinguishing various forms (Gazin 1968, Zonneveld et al. 2000). Two late Wasatchian species are mentioned by Gazin

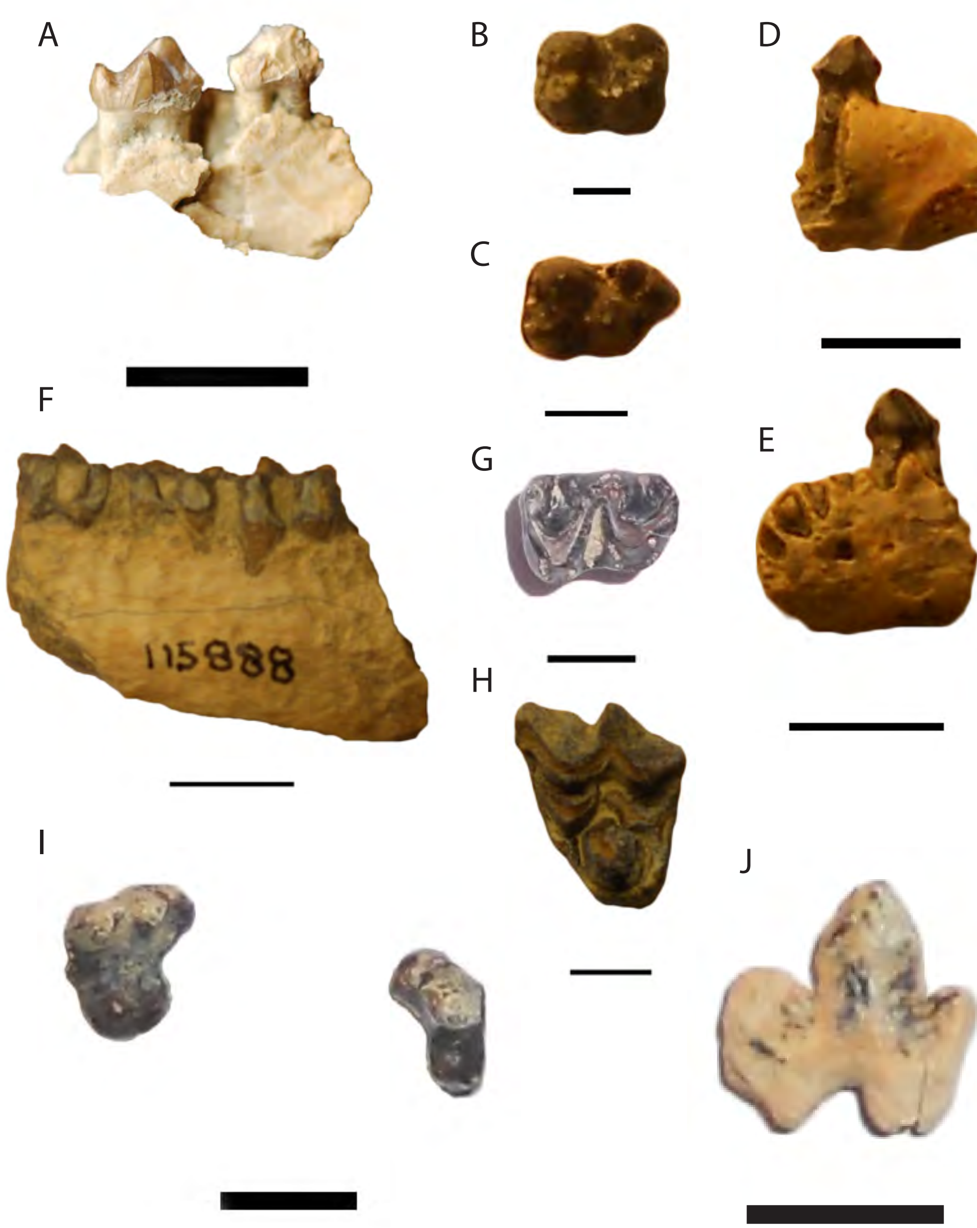

Figure 2.9 - Condylarthra and Cete. A: *Hyopsodus* sp., 103534, left dentary p3-4 in labial view, scale equals 5mm. B: *Hyopsodus* sp., 109042, left m2 in occlusal view, scale equals 2mm. C: *Hyopsodus* sp., 111922, left m3 in occlusal view, scale equals 2mm. D-E: *Hyopsodus* sp., 104533, left dentary p3 in lateral and labial views, scale equals 5mm. F: *Meniscotherium* sp., 115888, left dentary p4-m2 in labial view, scale equals 10mm. G: *Meniscotherium* sp., 115769, right m1 in occlusal view, scale equals 5mm. H: *Meniscotherium* sp., 111916, left M3 in occlusal view, scale equals 5mm. I: *Hapalodectes* sp., 104691, left P3-4 in occlusal view, scale equals 5mm. J: *Hapalodectes* sp., 112080, right m2 in lateral view, scale equals 5mm.

(1968); *Hyopsodus walcottianus* (Matthew 1915b) and *Hyopsodus wortmani* (Osborn 1902) both described from the Wind River Basin. According to Gazin's (1968, figure 2, 5) figures, *H. wortmani* has a size distribution of the m2 length between 3-4mm while *H. walcottianus* is approximately 6.5mm. Two size variations are witnessed in the m1 specimens but few approximate the size of *H. walcottianus. H. paulus* is represented alongside a slightly smaller species, possibly *H. wortmani.* The m1 and m2 are extremely difficult to distinguish as isolated specimens. A possible difference witnessed in the isolated teeth described herein is a lingually protruding entoconid (producing a slightly expanded talonid) on the m1.

Family MENISCOTHERIDAE, Cope 1882

***Meniscotherium,* Cope 1874**

***Meniscotherium* c.f. *M. robustus*, Cope 1874**

Referred Specimens—(115733) left m1; (107995) left MX fragment; (107996) left m1 talonid; (111899) left M3; (111916) left M3; (115888) left dentary p4-m2; (112939) left M3; (115769) right m1

Known species—*Meniscotherium chamense* Cope 1874*, M. terraerubrae, M. tapiacitum, M. robustus*

Occurrence—SP 75, SP 124, SP 125, SP 136, SP 146, SP 147

Description—*Mensicotherium* has a metaconule-hypocone metaloph and valley separating the protocone and paraconule (Archibald 1998). Cristid obliqua of the lower cheek teeth in *Meniscotherium* meets the metaconid at the lingual edge producing a pronounced metastylid (Archibald 1998). The upper third molars (111899, 111916) have a distinct parastyle and mesostyle, no hypocone and distinct conules (112939). The lower molars on UM115888 are heavily worn and produce distinct triangular crests on the trigonid, which forms the metastylid on the talonid.

Discussion—*Meniscotherium* is known from the Clarkforkian (Cf3) to Middle Bridgerian (Br2) (Archibald 1998). *Meniscotherium* is a small to medium sized phenacodontid (ungulate condylarth), with lophodont to selenodont cheek teeth (Archibald 1998).

Measurements— (111899) left M3 = 10.70 x 8.90; (111916) left M3 = 9.40 x 11.90; (115888) left dentary p4-m2: p4 = 5.20 x 7.45, m1 = 6.20 x 7.80; m2 = 6.35 x 8.05; (115769) right m1= 5.60 x 8.50

Order CREODONTA

Family HYAENODONTIDAE, Wortman 1902

***Prolimnocyon* Matthew 1915**

***Prolimnocyon antiquus* Matthew 1915**

Referred Specimens—(104495) left m1 or m2

Known species— *Prolimnocyon atavus* Matthew 1915*, P. antiquus, P. haematus, P. eerius, P. elisabethae, P. ludei, P. chowi*

Occurrence—SP 74

Description—Dental Formula for *Prolimnocyon* is X.1.4.3/3.1.4.3 (upper incisors not known) (Gunnell 1998a). The m1 is wide and smaller to equal in size with m2 with an unreduced protocone (Gunnell 1998a). The upper and lower third molars are generally small and m2 has a short parastyle but distinct metacone (Gunnell 1998a). UM 104495 has a very tall inflated trigonid and low talonid. The trigonid has a distinct paraconid with a lingually protruding vertical crest. The talonid has a serrated postcristid extending from a small hypoconid.

Discussion—*Prolimnocyon* is known from the Clarkforkian (Cf2?) or early Wasatachian (Wa0) to late Wasatchian (Wa7) (Gunnell 1998a).

Measurements—(104495) left m1 or m2 = 3.70 x 6.40

***Tritemnodon* Matthew 1906**

Tritemnodon whitiae* Matthew 1915 *(=strenuus* Guthrie 1967*)

Referred Specimens—(116260) left c1

Known species— *Tritemnodon agilis* Matthew 1906*, T. strenuous, T. whitiae (strenuus)*

Occurrence—SP 125

Description—UM 116260 is a posteriorly curved large canine, approximately 19 mm tall from the base of the crown.

Discussion—*Tritemnodon* is known from the early Wasatachian (Wa0), possibly as early as the Clarkforkian (Cf2) to Late Wasatchian (Wa7) (Gunnell 1998a). The taxonomic name *T.whitiae* comes from *Stypolophus whitiae* (Cope 1882), Matthew (1915a) synominized Cope's *Stypolophus* with *Tritemnodon.* Guthrie (1967) later used *T. strenuus* synonymously with *T. whitiae*.

Measurements—(116260) left c1 = 5.65 x 7.50 and 19 mm tall

Order LEPTICTIDA

Family LEPTICTIDAE, Gill 1872

***Palaeictops*, Matthew 1899**

***Palaeictops* c.f. *P. bicuspis*, Matthew 1899**

Referred Specimens—(116282) left mX; (116261) broken right MX; (112931) left m3; (115093) right M1; (115095) right p3; (115097) right m1 or m2; (115098) right m1 or m2; (115099) left m1 or m2; (115108) right P4; (115115) right m1 or m2; (115198) right p4; (115844) left M1; (116088) left p3; (116096) left m2; (112923) left m2

Known species—*Palaeictops bicuspis* Matthew 1899*, P. bridgeri, P. borealis, P. matthewi, P. muticuspis, P. pineyensis*

Occurrence—SP 75, SP 125, SP 136

Description— The lower molars have anterioposteriorly narrow trigonids and large, broad talonids and an entoconid, while the m3 possesses a protruding hypoconulid (Novacek 1977). The paracone, metacone, paraconule, metaconule, hypocone, precingula, postcingula and narrow ectocingulum are all present on the upper molars (Novacek 1977). The upper molars possess conules at the labial base of the paracone and metacone, short anterior cingulae, distinct hypocones, narrow stylar shelves, shallow extoflexus on the M2-3 and low bulbous cusps (Gunnell et al. 2008b, Novacek 1977). M2 is not wider than M1, and the lower molar trigonids are relatively low compared to *Prodiacodon* (Gunnell et al. 2008b). The lower molars (112923, 116096, 115115, 115099) have tall trigonids with distinct paraconids and a low talonid with tall entoconid, hypoconid and hypoconulid. The M1 (115093) posseses a distinct hypocone, strong pre and post protocrista, deep talon, small parastyle and protruding postmetacrista.

Discussion—*Palaeictops* is known from the Wasatchian (Wa1) or as early as the Puercan (Pu2?), to Duchesnian (Gunnell et al. 2008b). Leptictids are generally recognized by a dental formula of 2.1.3.3/3.1.3.3 (Novacek 1977). Novacek (1977) remarks that *Palaeictops* can be distinguished from other leptictids by lack of tall, sharp cusps that denote occlusional piercing.

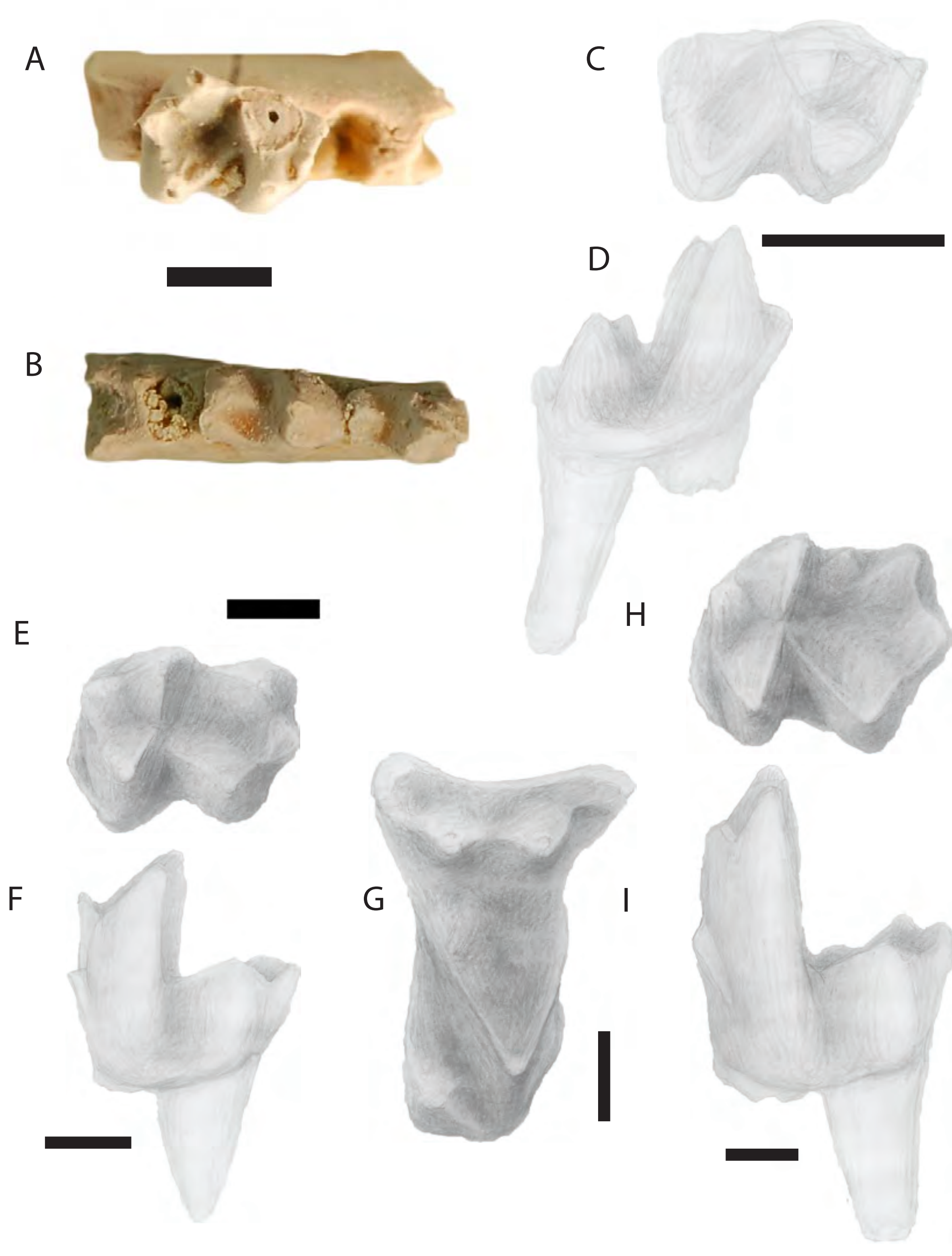

Figure 2.10 - Insectivore groups Leptictida and Erinaceomorpha. *Scenopagus* sp., 105198, right m1 in occlusal view, scale is 1mm. B: *Scenopagus* sp., 115852, left dentary p3-4 in occlusal view, scale is 1mm. C-D: *Talpavus* sp., 115125, right m1 in lateral and occlusal views, scale is 1mm. E-F: *Palaeictops* sp., 112923, left m2 in occlusal and lateral view, scale is 1mm. G: *Palaeictops* sp., 115093, right M1 in occlusal view, scale is 1mm. H-I: *Prodiacodon* sp., 115808, left m2 in lateral and occlusal view, scale is 1mm.

Measurements— (115844) left M1 = 4.05 x 2.30; (115093) right M1 = 4.35 x 3.85; (115097) right m1 or m2 = 1.80 x 2.65; (115098) right m1 or m2 = 1.75 x 2.65; (115099) left m1 or m2 = 1.90 x 2.40; (115115) right m1 or m2 = 1.80 x 2.60; (116096) left m2 = 1.80 x 2.65; (112923) left m2 = 2.12 x 2.70; (112931) left m3 = 1.65 x 2.65;

***Prodiacodon,* Matthew 1929**

Referred Specimen—(115808) left m2

Known species— *Prodiacodon puercensis* Matthew 1929, *P. concordiarcensis, P. crustulum, furor, P. puercensis, P. tauricinerei*

Occurrence—SP 125

Description— *Palaeictops* does not have transverse or anterioposteriorly compressed upper molars like *Proiacodon,* and the molar trigonids of *Prodicodon* are taller than on the molars of *Palaeictops* (Novacek 1977). UM 115808 has a tall and narrow trigonid, taller than *Palaeictops* but more labialingually elongate. 115808 also has a wide, compressed talonid with protruding hypoconulid and small cusp anterior to the entoconid.

Measurements—(115808) left m2 = 2.10 x 3.60

Order ERINACEOMORPHA

Family SESPEDECTIDAE, Novacek 1985

Scenopagus,* Mckenna and Simpson *1959

***Scenopagus* cf. *S. edenensis*, McGrew et al. 1959**

Referred Specimens—(105185) right m3; (10518) left mX; (105198) right dentary with m1; (105207) left p4; (116138) left MX; (115096) left MX; (115114) left M1 or M2; (115116) left P4; (115852) left dentary with p3-4?; (116315) left MX; (116322) two unassociated left mX

Known species—*Scenopagus mcgrewi* McGrew et al. 1959, *S. curtidens, S. edenensis, S. hewettensis, S. priscus*

Occurrence— SP localities 136, 75, 125

Description— The P3 of *Scenopagus*, is triangular with a small protocone, while the P4 lacks a separate metacone, but the paracone maintains a shearing metastylar crest and the protocone has a posterior crest with low hypocone (Gunnell et al. 2008c). The M1-2 are transverse with a small metacone, anteriorposterly compressed trigons, crescentic paraconules that have wings extending toward the paracones and parastyles (Gunnell et al. 2008c). These upper molars M1-2 also possess labially protruding parastylar and metastylar lobes and a small hypocone, lacking crests, that projects as a small lobe from the elevated lingual ends of the postcingulum (Gunnell et al.2008c). The M3 is not reduced relative to the other molars and also possesses a parastylar lobe (Gunnell et al. 2008c). The upper molar specimens (116138, 115096, 115114, 116315) have distinct hypocones, tiny conules, strong postparacrista and an anteriorly protruding parastyle (1163150). The m1 (105198) has a tall trigonid, distinct paraconid and tall entoconid. The m2-3 (116322, 105185) have tall trigonids with distinct paraconids and low talonids which are elongate with a protruding hypoconulid on the m3 (116322, 105185). The m3 specimens also have a distinct anterior crest.

Discussion—*Scenopagus* is known from the Wasatchian (Wa0) to Uintan (Ui3) (Gunnell et al. 2008c)

Measurements—(115114) left M1 or M2 = 1.50 x 0.95; (116315) left MX = 1.55 x 1.15; (116138) left MX = 2.00 x 1.15; (115096) left MX = 2.00 x 1.15; (115852) left dentary with p3-p4?: p3 = 0.35 x 0.95, p4 = 0.70 x 1.30; (105198) right dentary with m1 = 0.95 x 1.45; (105185) right m3 = 1.00 x 1.50; (116322) two unassociated left mX: m2? = 1.75 x 2.45, m3? 1.65 x 2.80; (10518) left mX = 0.75 x 1.30

Family ERINACEIDAE, Fischer von Waldheim 1817

***Talpavus,* Marsh 1872**

Referred Specimen—(115125) right m1

Known species— *Talpavus nitidus* Marsh 1872*, T. conjectus, T. duplus, T. sullivani*

Occurrence— SP locality 136

Description—Lower molar entoconids are higher than the hypoconid on *Talpavus* while trigonids and talonids are of equal size and width (Gunnell et al. 2008c). The m2 paraconid is compressed anterioposteriorly into a thin high crest and hypoconulids of the lower molars are small but occur at the posteriolabial base of the entoconid, while a small notch distinguishes the two cusps (Gunnell et al. 2008c). The m1 (115125) specimen has a small paraconid with sharp anterior crest, tall metaconid and distinct talonid cusps.

Discussion — *Talpavus* is known from the Wasatchian (Wa5) or even as early as the Tiffanian (Ti4?) to Duchesnian (Gunnell et al. 2008c).

Measurements—(115125) right m1 = 0.80 x 1.40

Order MARSUPIALIA

Family DIDELPHIDAE, Gray 1821

***Herpetotherium,* Aymard 1850 (=*Peratherium*)**

Referred Specimen —(105182) right mX trigonid; (105189) right mx; (105203) left mX; (116248) left MX; (115094) right MX; (115100) left MX; (115156) right MX

Known species—*P. constans, P. cuvieri, P. edwardi, P. giselense, P. lavergnense, P. macgrewi, P. comstocki, P. marsupium*

Occurrence—SP localities 75, 136, 147

Description—The upper molars (115094, 115100, 115156) have a wide protocone, broad metastylar shelf, parastyle and tiny conules. The lower molar specimen (105203) has a narrow trigonid with anteriorly protruding paraconid and lingually situated hypoconulid. The upper molars, M1-2 has stylar cusp D as the central, dominant cusp (fused with stylar cusp C), while on the M3-4 this is stylar cusp C (Korth 2008). According to Korth (2008), *Peratherium* is allotted to European genera while most North American specimens are considered to be *Herpetotherium.*

Discussion— *Herpetotherium* is known from the Wasatchian, possibly as early as the Tiffanian, to Early Miocene (Hemingfordian, He2) (Korth 2008).

Measurements— (115094) right MX = 2.10 x 2.45; (115100) left MX = 2.75 x 2.65; (115156) right MX = 3.10 x 3.30; (105189) right mX = 1.65 x 2.40; (105203) left mX = 1.25 x 2.45

***Peradectes,* Matthew and Granger 1921**

***Peradectes* cf. *P. chesteri*, Matthew and Granger 1921**

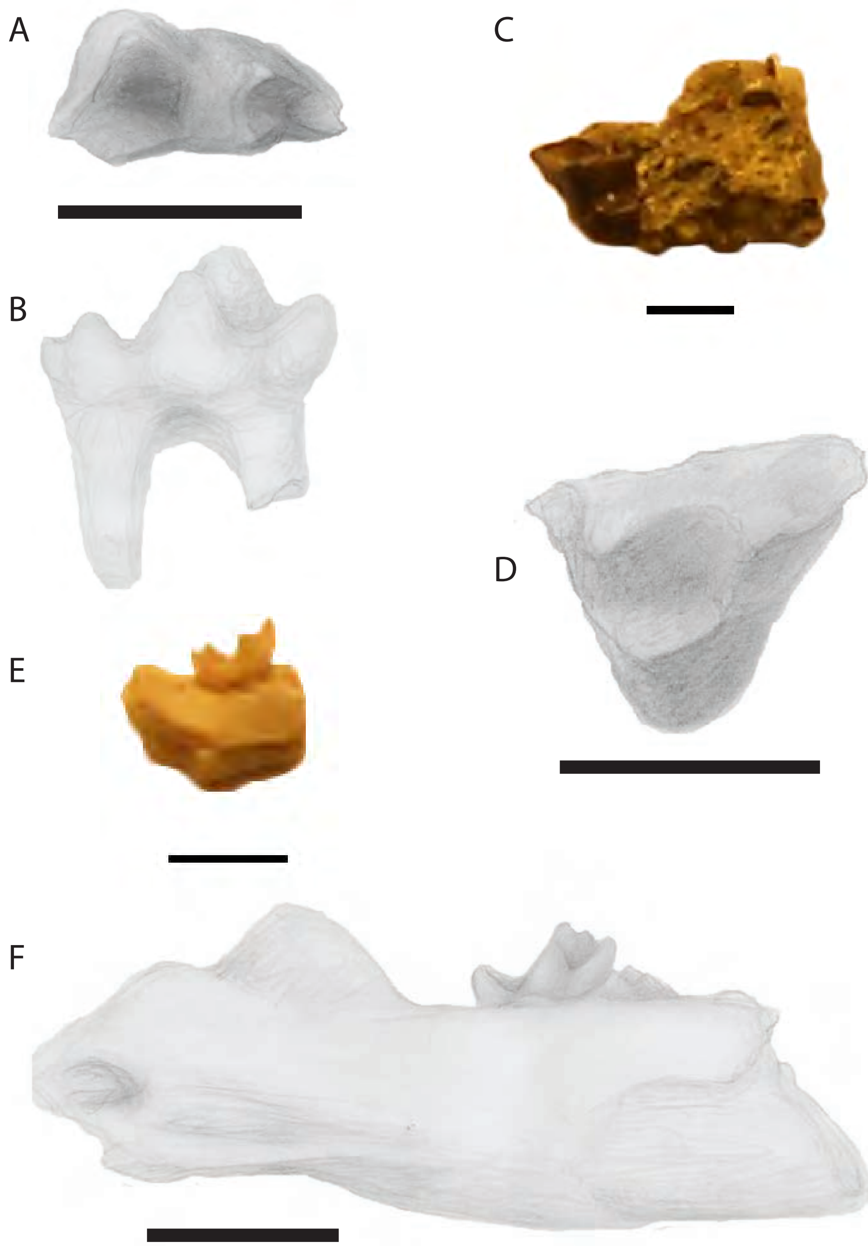

Figure 2.11 - Marsupiala. A-B: *Herpetotherium* sp., 105203, left mX in occlusal and labial views, 2mm. C: *Herpetotherium* sp., 115156, right MX in occlusal views, scale is 2mm. D: *Herpetotherium* sp., 115100, left MX in occlusal view, scale is 2mm. E: *Peradectes* sp., 115131, right m4 in labial view, scale is 2mm. F: *Peradectes* sp., 115089, left dentary m3(talonid)-m4 in labial view, scale is 2mm.

Referred Specimens—(105193) left MX; (115089) left dentary m3-m4 talonid; (115119) right mX; (115131) right m4; (116021) right maxilla MX

Known species— *Peradectes minor* Clemons 2006, *P. elegans, P. californicus, P. chesteri, P. pauli, P. protinnominatus.*

Occurrence—SP localities 75, 136

Description— On the upper molars the paracone and protocone of M1-3 are equal in size and the posterorlingual side of the protocone is not expanded (Korth 2008). On the lower m1-3 the talonid is short and the hypoconulid and entoconulid are equal in height (Korth 2008). The upper molar specimen (105193) has a labially protruding paracone. The lower molar specimens (115089, 115119, 115131) have a distinct and tall paraconid and hypoconid with a reduced to elongate talonid.

Discussion— *Peradectes* is known from the Puercan (Pu1) to Chadronian (Ch3) (Korth 2008). *Peradectes elegans (*Matthew and Granger 1921) was the first species named but *Peradectes minor* is the type species. *Peradectes* is distinguished from *Thylacoden* (early Paleocene) by progressively reduced stylar cusps and conules (lost in Oligocene *Nanodelphys*) (Korth 2008). These genera produce one of two clades which share the trend toward loss of stylar cusps and conules (Korth 2008).

Measurements—(105193) left MX = 1.75 x 1.10; (116021) right maxilla MX = 1.10 x 0.95; (115089) left dentary m3-m4 talonid: m3 = 0.45 x 1.05; (115131) right m4 = 0.50 x 1.25; (115119) right mX = 0.70 x 1.25

Order CETE

Suborder ACREODI, Matthew 1909

Family HAPLODECTIDAE, Ting and Li 1987

Hapalodectes, Matthew 1909

Hapalodectes cf. *H. leptognathus,* Matthew 1909

Referred Specimens—(104691) associated? P3 and P4; (111926) left mX; (115766) left p3; (115218) right mX; (116110) P3; (112080) right m2

Known species— *Haplodectes leptognathus* Matthew 1909*, H. anthracinus*

Occurrence—SP localities 75, 125, 136, 147

Description— Lower Dental Formula: 0.1.4.3 *Hapalodectes* possesses a slender jaw and highly compressed teeth where the talonids are generally high and sharp, metaconids are small and m1-3 has well developed paraconids (Archibald 1998). The lower molars (111926, 115218, 112080) have rounded, compressed cusps with the paraconid larger than metaconid on the m2 (112080). The upper premolars (104691, 116110) have small lingual cusps.

Discussion—*Hapalodectes* is known from the early Wasatchian to Middle Bridgerian (Archibald 1998).

Measurements—(104691) associated? P3 and P4: P3 = 4.65 x 5.40; (111926) left mX = 1.25 x 3.95; (115766) left p3 = 1.80 x 3.10; (115218) right mX = 1.35 x 4.55; (116110) P3 = 2.60 x 3.60; (112080) right m2 = 1.70 x 6.20

Order PALAEANODONTA

Family METACHEIROMYIDAE, Wortman 1903

Palaeanodon, Matthew 1918

Referred Specimens—(116283) metatarsal II; (116128) dentary fragment with no teeth; (116257) left c1; (116265) metacarpal II; (112100) metatarsal fragment; (115814) right c1; (112875) distal radius

Included species— *Palaeanodon ignavus* Matthew 1918*, P. nievetti, P. parvulus*

Occurrence—SP 75, SP 125, SP 136

Description— The dentary possesses a prominent medial buttress with five teeth and about four on the maxilla (Rose 2008). Premolars and molars are single rooted, vestigial, peg-like and possess rounded crowns while canines are robust with a distinct triangular cross section (Rose 2008).

Discussion— *Palaeanodon* is known from the Clarkforkian (Cf2) to late Wasatchian (Wa7) (Rose 2008).

Family EPOICOTHERIIDAE, Simpson 1927

***Pentapassalus* Gazin 1952 (=*Tubulodon* Jepson 1932)**

Referred Specimens—(104504) phalanx; (115673) second metacarpal

Known species— *Pentapassalus pearcei* Gazin 1952

Description— UM 115673 is a second left metacarpal in which the proximolateral edge of the metacarpal which attaches to the trapezoid is elongated to the left. UM 104504 is a proximal or middle phalanx.

Discussion— The proposed name *Pentapassalus pearcei* by Gazin (1952) was synonymized as *Tubulodon pearcei* by Rose et al. (1991) and Rose and Lucas (2000).

Order PANTODONTA

Family CORYPHODONTIDAE, Marsh 1876

***Coryphodon*, Owen 1845**

Figure 2.12 - Paleanodonta, Pantodonta, Rodentia and Tillodonta. A: *Coryphodon* sp., 112936, pX fragments in lateral view, scale equals 20mm. B: *Palaeanodon* sp., 115814, right c1 in lateral view, scale equals 5mm. C: *Palaeanodon* sp., 116128, right dentary fragment, scale equals 10mm. D: *Pentapassalus* sp., 104504, phalanx, scale equals 1mm. E: *Esthonyx acutidens*, 115815, left i2 in lateral view, scale equals 5mm. F: *Paramys* sp., 115770, right m1 in occlusal views, scale equals 1mm. G: *Paramys* sp., 105194, right mX in occlusal views, scale equals 1mm. H: *Sciuravus* sp., 112919, right m1 in occlusal view, scale equals 1mm. I: *Sciuravus* sp., 112932, right M1 in occlusal view, scale equals 1mm. J: *Microparamys* sp., 115128, right m3 in occlusal view, scale equals 1mm. K: *Microparamys* sp., 115772, left m1 in occlusal view, scale equals 1mm.

Referred Specimens—(107979) skull and tooth fragments; (116107) various tooth fragments; (116115) various tooth fragments; (116129) right astragalar fragment; (116258) right lower molar trigonid; (112936) upper premolar fragments; (109003) tooth fragments

Known species— *Coryphodon eocaenus* Owen 1846, *C. simus, C. molestus, C. anthracoideus, C. oweni, C. lobatus, C. subquadratus, C. proterus*

Occurrence—SP localities 124, 125, 135, 146

Description -- *Coryphodon* still possess postprotocristae or metaconules, and the premetacristae is short (Lucas 1998). *Coryphodon* has long trigonids and ectolophs on p2-4, while the P2-4 protocones are not as isolated as other pantodont genera (*Asiocorphyphodon* and *Eudinoceras*) (Lucas 1998). The m3 is oval shaped with a distinctive posterior crest making the teeth less bilophodont (Lucas 1998). The lower canine does not curve outward, while iscisors are not extremely broad, and m1-3 paracristids and cristid obliqua are well developed (Lucas 1998).

Discussion— *Coryphodon* is known from the Clarkforkian (Cf1) to Early Bridgerian and remains the only North American genus of its family (*Hypercoryphodon, Heterocoryphodon, Asiocorphyphodon* and *Eudinoceras* are from Eocene of Asia) (Lucas 1998). *Coryphodon* is a small to medium coryphodontid (large pantodonts), though larger than most other Eocene mammals with a m1-3 length of 70-99mm (Lucas 1998). These also have the least bilophodont (two transverse lophs) teeth than any other genus of coryphodontid (Lucas 1998). *Coryphodon* is known from the Pinnacles assemblage as an astragalar and various tooth fragments. Due to *Coryphodon*'s large tooth size, fragmentation was an inevitability of reworking.

Order PERISSODACTYLA

Superfamily EQUOIDEA, Hay 1902

Family EQUIDAE, Gray 1821

***Hyracotherium*, Owen 1841**

Referred Specimens—103525, 103526, 103530, 104502, 104505, 112088, 112089, 112090, 115683, 115685, 115731, 103540, 103542, 103546, 103549, 104515, 104520, 104523, 104529, 104680, 104681, 104682, 104683, 104686, 104696, 104697, 104701, 109045, 109049, 109053, 109055, 109069, 112093, 112095, 112098, 112125, 112126, 112132,112134, 112172, 112173, 112202, 115160, 115691, 115692, 115694, 115698, 115705, 115734, 115743, 115744, 115752, 115754, 115755, 115756, 116249, 107981, 107983, 107988, 107991, 111912, 115805, 115809, 115822, 115826, 115830, 115833, 116101, 116111, 116114, 116119, 116121, 116137, 116139, 116140, 116141, 116143, 116266, 116274, 111917, 111950, 112848, 112861, 115861, 112082, 112084, 112085, 112086, 112167, 115154, 115726, 115727 (See appendix for descriptions of individual specimens)

Known species— *Hyracotherium leporinum* Owen 1840*, H. seekinsi, H. angustidens, H. sandrae, H. index, H. grangeri, H. vasacciense, H. aemulor, H. pernix, H. cristatum, H. craspedotum*

Occurrence—SP 74, SP 75, SP 124, SP 125, SP 135, SP 136, SP 147

Description— The known dental formula for *Hyracotherium* is 3.1.4.3 with a diastema occurring between the I3, C, p1 and p2, at various lengths in different species (Kitts 1956). The upper molars are quadrate and lingually tapered. The protocone and hypocone are steep and of equal height to the paracone and metacone, with the paracone positioned anteriolabially to the metacone (Kitts 1956). An ectoloph is present, the protoloph is more prominent than the metaloph and a paraconule protrudes as a thickening in the protoloph (Kitts 1956). The paraconule is more cone shaped on the M1 and progressively more lophate towards the M3 (Kitts 1956). The M3 is generally more obliquely shaped than the M1-2 with a prominent posterior shelf (Kitts 1956). The m1-3 are rectangular and anterioposteriorly elongate. The protoconid and metaconid are steep, slight twinning is present in the metaconid, a tall protolophid connects the metaconid and protoconid and a paralophid extends anteriorly from the protoconid forming an anteriomedial shelf (Kitts 1956). The protolophid is present and a metalophid extends diagonally joining the hypoconid and the protolophid. The m3 has a large, distinct posteriolabially offset hypoconulid with a posteriolingual shelf which may possess smaller cuspules (Kitts 1956).

Discussion—*Hyracotherium* is known from the early Wasatchian (Wa0) to Early Bridgerian (MacFadden 1998). According to Kitts (1956) the m3 hypoconulid is a distinguishable character between some *Hyracotherium* species. The hypoconulid heel is long and narrow in *H. craspedotum* but short and broad in *H. vasacciense* and *H. angustidens* (Kitts 1956). *Hyracotherium* is relatively small, possesses a manus of four digits (II – V) and pes of three digits (II-IV) and has unmolarized premolars (MacFadden 1998).

***Orohippus*, Marsh 1872**

***Orohippus* cf. *O. pumulus*, Marsh 1871**

Referred Specimens—(112839) right dp2?

Included species— *Orohippus pumulis* Marsh 1871, *O. major, O. progressus, O. agilis, O. sylvaticus, O. proteros*

Occurrence—SP 153

Description— *Orohippus* differs from *Hyracotherium* by fully molariform teeth and P3-4 with four equally sized cusps, while the p3-4 have an entoconid

(MacFadden 1998). *Orohippus* is small and similar to *Hyracotherium* except it possesses a slightly more advanced dentition (MacFadden 1998). The deciduous premolar specimen (112839) is elongate with a large protoconid, no metaconid and distinct paraconid, entoconid and hypoconid.

Discussion— *Orohippus* is known from the late Wasatchian to Early Uintain (MacFadden 1998).

Measurements—(112839) right dp2? = 2.20 x 4.60

Family BRONTOTHERIIDAE, Marsh 1873

***Lambdotherium,* Cope 1880**

***Lambdotherium popoagicum,* Cope 1880**

Referred Specimens— (103527) unassociated left P2, right P3and right M3; (112118) right m3; (107976) left astragalus; (111907) right p4; (111913) left M3; (115807) left M1; (115825) right mX; (116113) right m1 or m2; (116118) left p4; (116262) left P3; (116267) right m3

Known species— *Lambdotherium popoagicum* Cope 1880

Occurrence—SP 74, SP 75, SP 124, SP 125

Description— *L. popoagicum* is characterized by a W-shaped ectoloph and weak cross-lophs on the upper molars (Rose 2006). Distinguished from *Eotitanops* and other early brontotheres by *Lambdotherium*'s smaller size, lack of a strong preprotocrista, but strong postprotocrista on the P2 and the paracones and metacones of the premolars in this genus are buccally inflated (Eberle 2006). The protocone and hypocone of the upper molars are nearly equal in size with a strong anterior cingulum (Eberle 2006). *L. popoagicum* is characterized by a simple paraconid and metaconid on the p3 (Bonillas 1936).

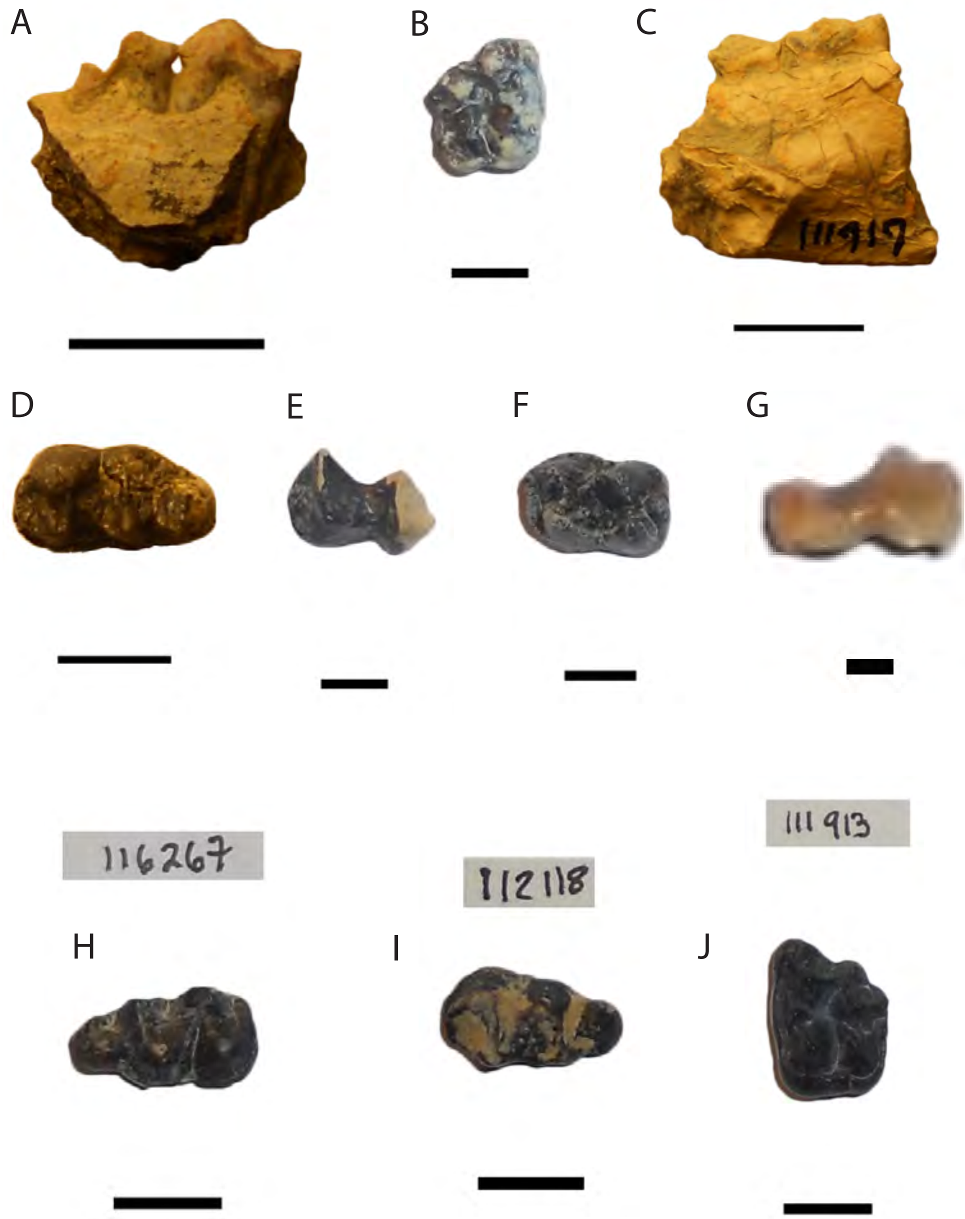

Figure 2.13 - Perissodactyla. A: *Hyracotherium* sp., 116143, left dentary p1-2 in labial view, scale equals 10mm. B: *Hyracotherium* sp., 112085, right M1 in occlusal view, scale equals 5mm. C: *Hyracotherium* sp., 111917, right dentary p3-4 in labial view, scale equals 10mm. D: *Hyracotherium* sp., 115154, left m3 in occlusal view, scale equals 5mm. E: *Helaletes* sp., 115728, right mX in occlusal view, scale equals 5mm. F: *Heptodon* sp., 112165, left m1 in occlusal view, scale equals 5mm. G: *Orohippus* sp., 112839, right dp2 in lateral view, scale equals 1mm. H: *Lambdotherium popoagicum*, 116267, right m3 in occlusal view, scale equals 10mm. I: *Lambdotherium popoagicum*, 112118, right m3 in occlusal view, scale equals 10mm. J: *Lambdotherium popoagicum*, 111913, left M3 in occlusal view, scale equals 10mm.

Discussion— *Lamdotherium* is found exclusively in the Late Wasatchian and thus the index fossil for the Wa7 Lostcabinian zone (Gunnell et al. 2009). (Rose 2006). *Lambdotherium* is considered to either be some primitive brontothere (along with *Eotitanops*) (Rose 2006) or a paleothere (Gunnell et al. 2009).

Measurements—(103527) unassociated left P2, right P3and right M3: P2 = 8.20 x 7.95, P3 = 10.00 x 8.85, M3 = 16.80 x 12.85; (112118) right m3 = 8.10 x 15.95; (111907) right p4 = 7.25 x 9.95; (111913) left M3 = 17.80 x 13.05; (115807) left M1 = 14.65 x 12.65; (116113) right m1 or m2 = 9.40 x 12.90; (116118) left p4 = 6.60 x 8.90; (116262) left P3 = 10.50 x 9.45; (116267) right m3 = 9.00 x 17.00

Superfamily TAPIROIDEA, Gill 1872

Family HELALETIDAE, Osborn 1892

***Helaletes,* Marsh 1872**

***Helaletes nanus,* Marsh 1872**

Referred Specimens—(115728) right mX

Known species— *Helaletes nanus* Marsh 1872

Occurrence—SP 75, SP 147

Description— The hypocone on the upper molars is separate from the protocone, M1-2 metacones are convex/flat, while M3 has relatively short metaloph and m3 has short hypoconulid (Colbert and Schoch 1998).

Discussion—*Helaletes* is known from the early Bridgerian to late Uintan (Colbert and Schoch 1998). *Helaletes* differs from *Heptodon* and *Tapris* by a higher greater trochanter at the femur and a longer illium indicative of a more cursorial habitat (Colbert and Schoch 1998).

Heptodon, **Cope 1882**

Referred Specimens— (115192) left p4; (112165) left m1

Known species— *Heptodon calciculus* Cope 1880*, H. posticus*

Occurrence— SP 136, SP 147

Description—*Heptodon* possesses a p2 which is a labiolingually compressed shearing blade, while the p3-4 have high trigonids (Colbert and Schoch 1998).

Discussion—*Heptodon* is a small to medium sized ceratomorph known from the early Wasatchian to early Bridgerian (Colbert and Schoch 1998) . The distinguishing features of *Heptodon* from other isectolophids (small cursorial Meropomorphs) include a long postcanine diastema, lack of paraconules and metaconules on M1-3, and a long and narrow M3 which has a reduced metacone (Colbert and Schoch 1998).

Measurements—(115192) left p4 = 6.55 x 9.55; (112165) left m1 = 6.60 x 10.10

Order PLESIADAPIFORMES

Family MICROSYOPIDAE, Osborn and Wortman 1892

Microsyops, **Leidy 1872**

Referred Specimens—115845, 115849, 1158 55, 115862, 115863, 115867, 115871, 115873, 115878, 116094, 112940, 115780, 115144, 112869, 112877, 112920, 112930, 112933, 112934, 115091, 115181, 115184, 115191, 115195, 115654, 115655, 115662, 111945, 112866, 112868, 115219, 115787, 115788, 115806, 115835, 116116, 116120, 116134, 116145, 116253, 116279, 111920, 111929, 111933, 111935, 111937, 111938, 112091, 115679, 115682, 104510, 104690, 105197, 105201, 109058, 109061, 109067, 112119, 112123, 112138, 112177, 112190, 115712, 115735, 115741, 115747, 115761, 115762, 107990, 108049, 108050, 111900, 111903, 111910, 112885, 112888, 112889, 112892, 112895, 112896, 11289 7, 115216, 115217 (See appendix for descriptions of individual specimens)

Known species— *Microsyops elegans* Marsh 1871 (=*M.gracilis* Leidy 1872), *M. angustidens, M. kratos, M. annectens, M. cardiorestes, M. knightensis, M. latidens, M. scottianus, M. knightensis*

Occurrence—SP 74, SP 75, SP 124, SP 125, SP 135, SP 136, SP 145, SP 153, SP 159, SP 165

Description— Central incisors are enlarged, bladelike, fully lanceolate and rotated mesially (Silcox and Gunnell 2008). Also, *Microsyops* lacks upper and lower P1, the p2 is single rooted, while upper canines are reduced and double rooted (Silcox and Gunnell 2008). Upper molars possess a mesostyle, a very small paraconule and metaconule, and either lack a hypocone or have a small cusp on the postcingulum (Silcox and Gunnell 2008). The lower p4 has a distinct paraconid, lingually set hypoconid, and weak paracristid (Gunnell 1989). A strong metacone and mesostyle are present on the upper P4 (Gunnell 1989). Drawings of the lower molars of Bridger Basin specimens (Matthew 1915c figure 39, 40) show low, small trigonids and broad talonids with a distinct hypoconulid on the m2-3 and a narrow cingulum located posteriolabially on m1-3.

Discussion—*Microsyops* is known from the *e*arly Wasatchian (Wa0) to middle Uintan (Ui2) (Silcox and Gunnell 2008). Cranial features of *Microsyops* are similar to characters of Microsyopidae such as a strong sagittal crest, broad zygomatic arches and constriction of the postorbital (Silcox and Gunnell 2008).

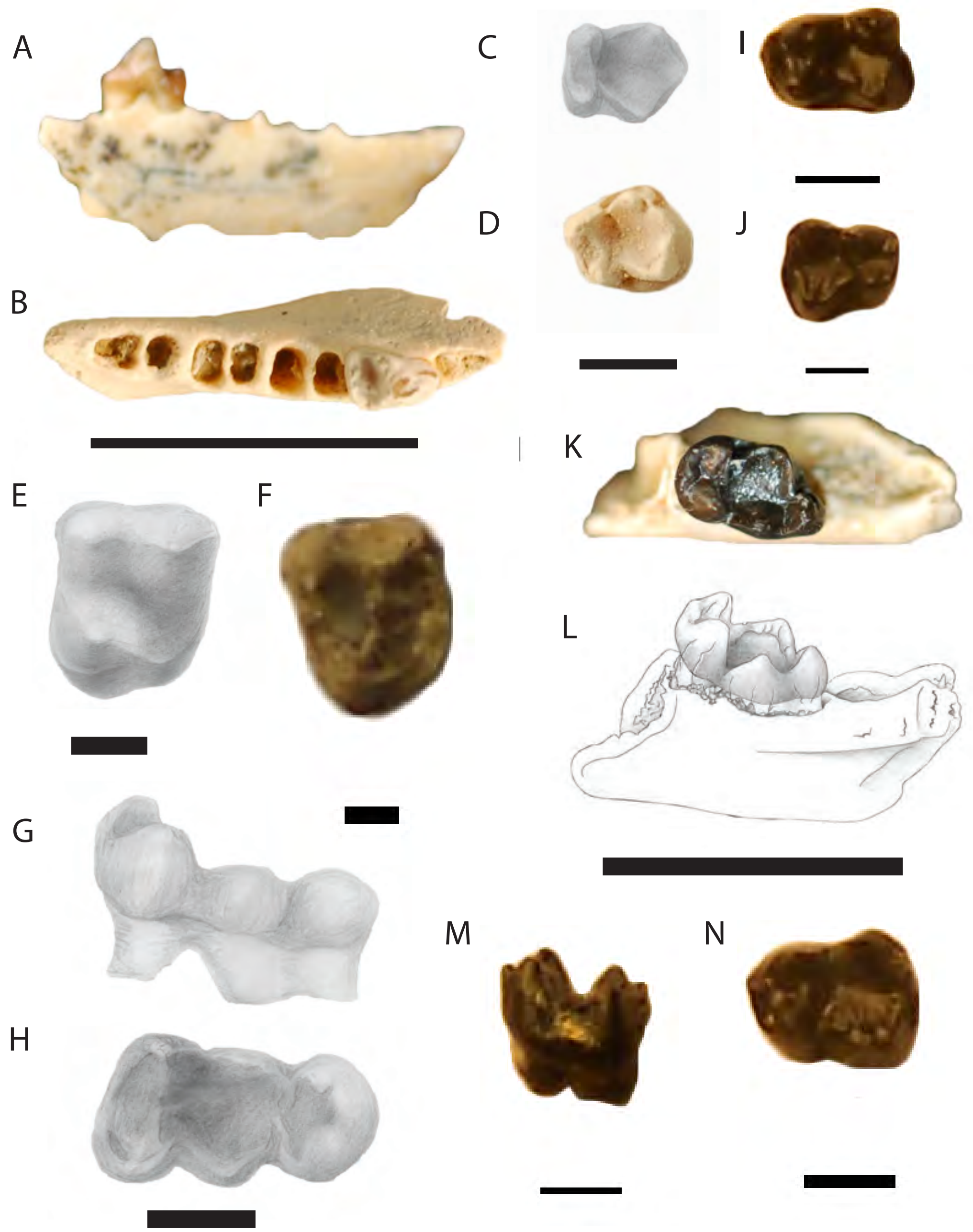

Figure 2.14 - Plesiadapiformes. A-B: *Niptomomys* sp., 115763, left dentary p4 in lateral and occlusal views, scale is 5mm. C-D: *Niptomomys* sp., 116314, left m2 in occlusal view, scale is 1mm. E: *Phenacolemur* sp., 115804, left M1 in occlusal view, scale is 1mm. F: *Phenacolemur* sp., 116319 left MX in occlusal view, scale is 1mm. G-H: *Phenacolemur* sp.,109008, left m3 in lateral and occlusal views, scale is 1mm. I: *Microsyops* sp., 112940, left m1 in occlusal veiw, scale equals 2mm. J: *Microsyops* sp., 115873, right m2 in occlusal view, scale equals 2mm. K-L: *Microsyops* sp., 115735, right dentary m3 in labial and occlusal views, scale is 10mm. M-N: *Microsyops knightensis*, 103548, left m2 in lateral and occlusal views, scale equals 2mm.

Microsyops knightensis, Gazin 1952

Referred Specimens—(103543) left M1; (103544) right p4; (103548) left m2; (115107) right M1

Occurrence—SP 75

Description— *M. knightensis* has dilambdont teeth, a molariform P4 with a broad talonid basin. The p4 of *M. knightensis* has a centered hypoconulid, and is larger than *M. scottianus*, which has a hypoconulid positioned closer to the entoconid (Gunnell 1989). The p4 (103544) is molariform and the m2 (103548) has a tall trigonid with low paraconid and lingualmedially placed hypoconulid. The upper molars (115107, 103543) have a distinct hypocone, metaconule and paraconule with a tiny mesostyle and metastyle.

Discussion— *M. knightensis* represents one of three linaeages microsyopids present in the Early Bridgerian (Br1a) (Gunnell 1998). *M. knightensis* was described from material of the Labarge-Big Piney area of the Green River Basin and is known specifically to the Lostcabinian (Wa7) and Gardnerbuttean (Br1a) (Gunnell 1989).

Measurements—(103543) left M1 = 4.10 x 3.54; (103544) right p4 = 2.10 x 3.25; (103548) left m2 = 2.65 x 3.60; (115107) right M1 = 3.70 x 3.10

Niptomomys, McKenna 1960

Niptomomys cf. *N. thelmae,* Gunnell and Gingerich 1981

Referred Specimens—(115763) right dentary p4; (116314) left m2

Known species— *Niptomomys doreenae* Mckenna 1960, *N. favorum, N. thelmae*

Occurrence—SP 75

Description— *Niptomomys* possesses enlarged upper and lower forth premolars with an absence of a paraconid on the p4 (Silcox and Gunnell 2008). The m2 specimen (116314) has a narrow trigonid with no paraconid and wide talonid with lingually placed hypoconulid.

Discussion— *Niptomomys* is known from the Clarkforkian (Cf1) to Middle Wasatchian (Wa5) (Silcox and Gunnell 2008).

Measurements—(115763) right dentary p4 = 0.60 x 1.10; (116314) left m2 = 0.80 x 0.90

Family PAROMOMYIDAE, Simpson 1940

***Phenacolemur*, Matthew 1915**

Referred Specimens—(111901) left MX; (115804) left M1; (115118) right m3; (115126) left dentary fragment m2; (116074) left M3; (116316) right MX; (116319) right I1; (109008) left m3

Known species— *Phenacolemur praecox* Matthew 1915, *P. citatus, P. foritior, P.jepseni, P. pagei, P. shifrae, P. simonsi*

Occurrence—SP 135, SP 125, SP 136

Description— Lower Dental formula for *Phenacolemur* is 1.0.1.3. The upper molars (111901, 115804, 116074, 116316) possess a broad posterior cingulum, no conules and inflated paracone on the M3 (116074). The m2 (115126) has a tall trigonid with no paraconid and distinct lingual cingulum. The m3 specimens

(109008, 115118) have a tall trigonid with large metaconid and elongate talonid with bulbous and inflated hypoconulid.

Discussion— *Phenacolemur* is known from the middle Tiffanian (Ti2) to middle Uintan (Ui2) (Silcox and Gunnell 2008)

Measurements—(111901) left MX = 3.55 x 2.90; (116316) right MX = 2.15 x 1.65; (115804) left M1 = 2.60 x 2.00; (116074) left M3 = 2.20 x 1.40; (115126) left dentary fragment m2 = 1.60 x 1.95; (115118) right m3 = 1.10 x 2.55; (109008) left m3 = 1.90 x 3.80

Order PRIMATA

Family NOTHARCTIDAE, Trouessart 1879

***Notharctus,* Leidy 1870**

Referred Specimens—(109056) right m2; (109068) left M2; (116252) left m2; (116259) unassociated lot: right P4, right m1 or m2, left M1, left M2; (116264) left m3; (116276) right m1; (116277) right m3; (115105) right m3

Known species— *Notharctus tenebrosus* Leidy 1870, *N. pugnax, N. robinsoni, N. robustor, N. venticolus*

Occurrence— SP 74, SP 75, SP 124, SP 125, SP 135, SP 136

Description— *Notharctus* possesses long lower molar paracristids that curve posteriorly and expand anteriorly (Gunnell et al. 2008d). Upper molars have large, distinct and lobate hypocones which are separated from the protocones by a distinct notch (Gunnell et al. 2008d). The strong hypocone and mesostyle distinguish *Notharctus* from *Copolemur* and other genera such as *Pelycodus* (Gingerich 1979). Well developed upper molar mesostyles, a small paraconid, open or narrow entoconid notch, and discontinuous cristid obliqua distinguish

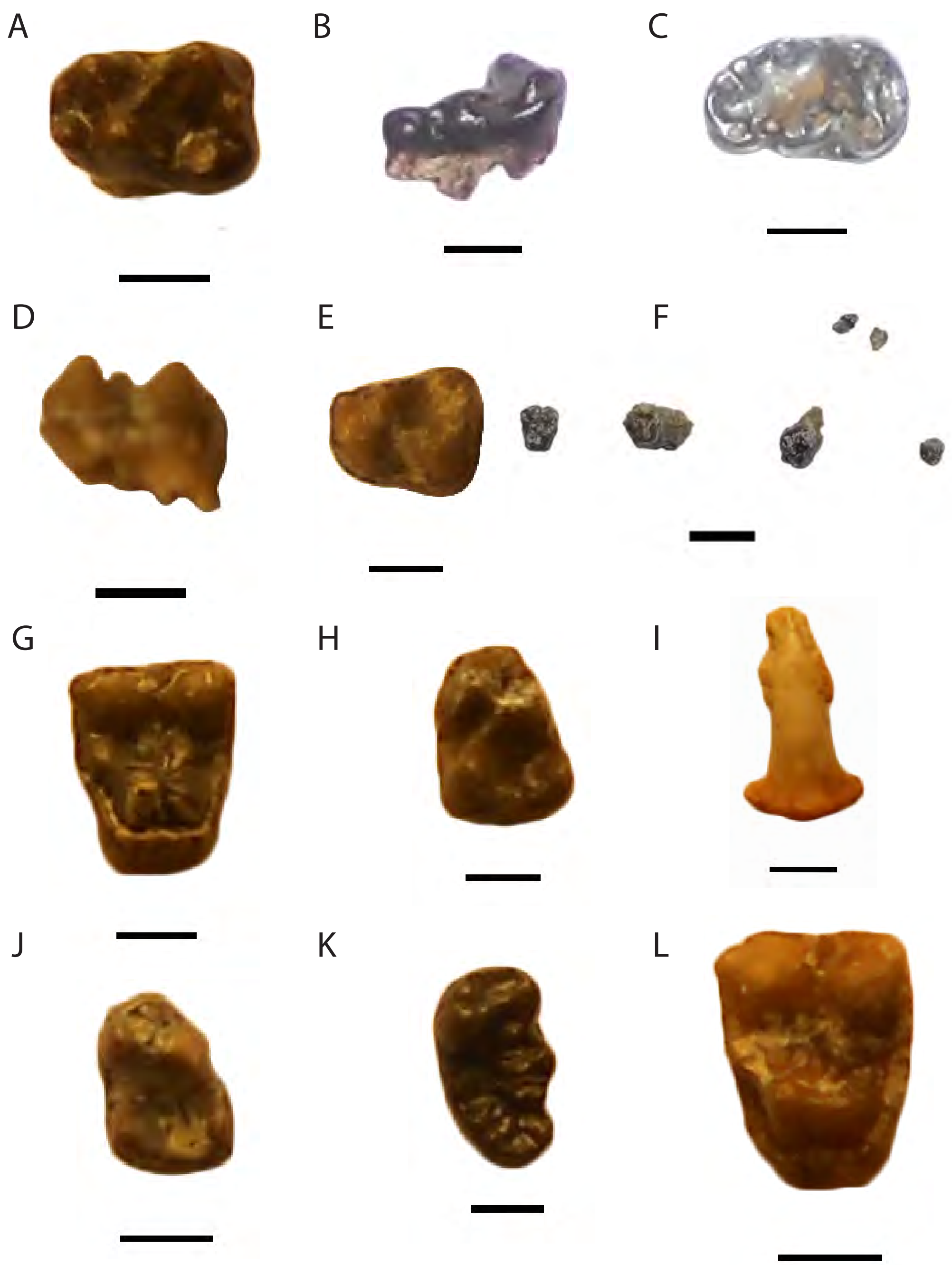

Figure 2.15 - Notharctine primates. A: *Notharctus* sp., 116276, right m1 in occlusal view, scale is 2mm. B-C: *Notharctus* sp., 116277, right m3 in lateral and occlusal views, scale is 2mm. D-E: *Notharctus venticolis*, 115088, left m1 in lateral and occlusal views, scale is 2mm. F: *Notharctus venticolis*, 104506, right P4-M3 in occlusal views, scale is 10mm. G: *Cantius* sp., 112131, left M1 in occlusal view, scale is 2mm. H: *Cantius* sp., 115687, left m1 in occlusal view, scale is 2mm. I: *Cantius* sp., 112882, distal phalanx, scale is 2mm. J: *Cantius nunienus*, 116320, left m1 in occlusal view, scale is 2mm. K: *Copelemur* sp., 109019, left M1 in occlusal view, scale is 2mm.

Notharctus from *Cantius* which posseses well defined paraconids (Gunnell et al. 2008d). The upper molars also possess a large M1 and M3 metaconules while the postprotocrista is not inflated (Gunnell 2002). *Notharctus* is distinguished from *Copolemur* by a lack of labiolingually compressed and blade-like postcingula on the upper molars and lower molar entoconids that are more posterior with straighter entocristids (Gunnell et al. 2008d). The upper molars have a distinct cingulum medially coupled protocone and metacone, with a mesostyle on the M1 (116259) and distinct conules, mesostyle, parastyle and metastyle on the M2 (116259, 109068). The m1 (116276) has a narrow trigonid with a lingual paraconid, assessory cusp on the paracristid and taller metaconid than protoconid; the wide talonid basin has a large hypoconid and cristid obiqua which meets the protocristid at the base of the metaconid. The m2 has a narrow trigonid with indistinct or lingual paraconid and paracristid cusp, lingually protruding entoconid and a cristid obliqua that meets the protocristid medially (109056) or at the base of the protoconid (116252, 116259). The m3 (115105, 116277, 116264) has a narrow precingulum, posteriolabially protruding hypoconulid with serrated posteriolingual crest and short cristid obliqua that extends to the base of the protoconid.

Discussion—*Notharctus* is known from the early Wasatchian (Wa0) to (Br1) (Gunnell et al. 2008). *Notharctus* is relatively large compared to other adapiforms, and has sharp crested and defined cheek teeth and a folivorous diet (Gunnell et al. 2008d).

Measurements— (109068) left M2 = 6.45 x 4.45; (116259) unassociated lot: right P4 = 4.65 x 3.45, right m1 or m2 = 3.20 x 3.55, left M1 = 6.10 x 3.55, left M2 = 5.60 x 4.15; (116276) right m1 = 3.20 x 4.50; (109056) right m2 = 3.95 x 4.70; (116252) left m2 = 3.25 x 4.20; (116264) left m3 = 3.15 x 5.40; (116277) right m3 = 3.05 x 5.05; (115105) right m3 = 2.95 x 5.30

***Notharctus venticolus,* Osborn 1902**

Referred Specimens—(112192) right p4; (115088) left m1; (104506) right P4-M3 and cranial fragments; (107977) right MX fragment; (108041) right dP4; (109020) right M2

Occurrence—SP 74, SP 75, SP 124, SP 125, SP 135, SP 136

Description—*N. venticolus* has variable development of molar mesostyles, the P4 paracristid is lower and more distinct than in *Notharctus* sp. and m1 cristid obliqua is continuous to the metaconid (Gunnell 2002).

Discussion—One of the first notharctines to appear in the Late Wasatchian (Wa7) (Gunnell 2002). *N. venticolus* was allotted as a species of *Cantius* by Gingerich and Haskin (1981) who claimed that either affinity to *Northarctus* or *Cantius* is valid (Gunnell 2002).

Measurements—(109020) right M2 = 6.30 x 4.10; (115088) left m1 = 3.20 x 4.20; (104506) (112192) right p4 = 3.30 x 4.35

Copelemur, Gingerich and Simons 1977

***Copelemur* cf. *C. australotutus*, Beard 1988**

Referred Specimens—(109019) left M1

Known species—*Copelemur tutus* Cope 1877*, C. australotutus, C. praetutus*

Occurrence—SP 135

Description—On the lower molars, *Copelemur* possess an m3 paraconid, anteriolingualy paracristid, and anteriolabial entoconid with a short and curving entocristid (Gunnell et al. 2008d). A distinct parastyle is present on the M1-2 along with a small M1 metaconule, strong M1-2 postprotocigula, distinct metastyles and parastyles (metastyle smaller on the M3) and no hypocone (Gunnell 2002). *Copelemur* is distinguished from all other notharctines by possession of a well developed, posteriorly extended, linguolabially compressed postprotocingulum on upper molars (Gunnell et al. 2008d). *Copelemur* also shares a distinctly open entoconid notch present in only some species of *Cantius*, *Notharctus* and *Smilodectes* (Gunnell et al. 2008d). The M1 (109019) possesses a distinct cingulum, medially placed protocone with strong postprotocrista, indistinct hypocone and conules, but distinct stylar cusps.

Discussion—*Copelemur* is known from the Wasatchian (Wa1 – Wa7) (Gunnell et al. 2008d). The type species of *Copelemur, C. tutus,* was originally named by Cope (1877) as *Tomitherium tutus* and later grouped into *Copelemur* by Gingerich and Simons (1977).

Measurements—(109019) left M1 = 5.00 x 3.80

***Cantius,* Simons 1962**

Referred Specimens—(112131) left M1; (112140) right m3; (112175) right m3; (112180) right M3; (112185) right M3; (112189) right M3; (112196) left m1; (115687) left m1; (115697) (115748) (115749) left m3; (115753) (115213) right M1; (115214) right p4; (115831) left m1; (111930) right M1; (111934) (112880) right M1; (112882) distal phalanx; (112915) right m3; (112929) (115187) left P4; (115670) left m1; (115840) right m1; (115858) right m3; (115859) left M1; (115868) (115869) right m1; (115872) left M3; (112083) left m1; (115158) (115777) left MX 115781, 115145, (116621) left M3

Known species—*Cantius angulatus* Cope 1875, *C. abditus, C. frugivorus, C. mckennai, C. nunienus, C. ralstoni, C. torresi, C. trigonodus, C. simonsi*

Occurrence—SP 75, SP 136, SP 125, SP 147, SP 153, SP 159

Description— The incisors are anteriorly inclined and this genus trends toward a progressive development of a mesostyle and hypocone, incipent selenodonty and increases in size (Rose 2006). Lower molars are bunodont with three distinct cusps on the trigonid (the paraconid may be reduced and lost in later forms) and an m3 with an expanded hypoconulid lobe (Rose 2006). The lower molars m1-2 possess a closed entoconid notch, the m1 cristid obliqua connects the hyopconid to the metaconid, and the m3 entoconid is distinct; variation on the lower molars exists on the m3 entoconid and entoconid notch (Gunnell 2002). The paraconid is very small on the m3 but the entonconid is distinct (Gunnell 2002). On the M1-2 the mesostyle is either an indistinct cresenctric cusp or not present at all and the hypocone is also very small, converging with the protocone on the nannopithex fold or remotely separated (Gunnell 2002). A low posterior cingulum extends from the protocone on all upper molars (Gunnell 2002). *Cantius* has less selenodont molars than *Notharctus* (more coarse herbivorous diet) and smaller hypocones, absent to small mesostyles, shallow or absent entoconid notches and distinct paraconids (Gunnell et al. 2008d). Possesses posteriorly placed entoconids and shallower entoconid notches than *Smilodectes* and *Copelemur* (Gunnell et al 2008d). Short paracristids in *Cantius* close the trigonids lingually and curving entocristids are present (Gunnell et al. 2008d). *Cantius* may also possess an M1 metaconule and M2 paraconule.

Discussion—*Cantius* is known from the early Wasatchian (Wa0) to early Bridgerian (Br1) (Gunnell et al. 2008d). *Cantius* is generally smaller than other notharctines (except for derived species) and very primitive, though some possess the distinctive entoconid notch and appear similar to *Notharctus* such a *C. nunienus* (Gunnell et al. 2008d). Due to its primitive nature and early appearance in Wasatchian, *Cantius* is paraphyletic and may have given rise to both *Notharctus* and *Copelemur* (Gunnell et al 2008d). Smaller Wind River Basin

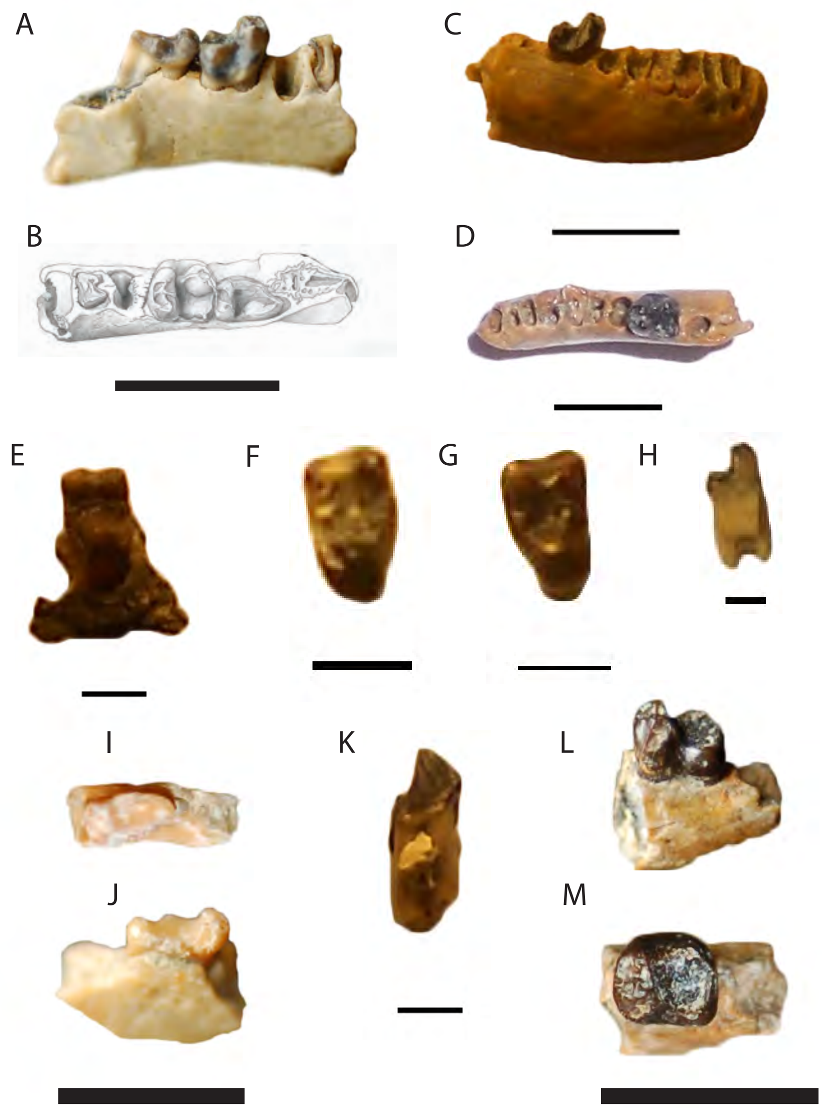

Figure 2.16 - Omomyine primates. A-B: *Artimonius nocerai*, 109063, right dentary m2-3 in labial and occlusal views, scale is 5mm. C-D: *Artimonius nocerai*, 104678, right dentary m2 in lateral and occlusal views, scale is 5mm. E: *Artimonius nocerai*, 109011, left maxilla M2 in occlusal view, scale is 2mm. F: *Anemorhysis sublettensis*, 115113, right M2 in occlusal view, scale is 2mm. G: *Anemorhysis* sp., 115837, left M1 in occlusal view, scale equals 2mm. H: Loveina zephyri, 116030, left m2 in labial view, scale is 1mm. I-J: *Trogolemur* sp., 111942, left dentary m3 in labial and occlusal views, scale is 5mm. K: *Absarokius gazini*, 115745, left p4 in labial view, scale is 2mm. L-M: *Absarokius* sp., 116268, right dentary m2 in labial and occlusal views, scale is 5mm

notharctine taxa are generally assigned to *Cantius* and the larger to *Notharctus* (Gunnell 2002).

Measurements—(115187) left P4 = 3.80 x 2.80; (115777) left MX = 3.20 x 2.75; (111930) right M1 = 5.70 x 3.60; (112131) left M1 = 5.60 x 4.15; (115859) left M1 = 4.90 x 2.90; (112880) right M1 = 5.15 x 3.85; (115213) right M1 = 5.60 x 3.80; (116621) left M3 = 4.60 x 3.10; (112180) right M3 = 5.35 x 3.60; (112185) right M3 = 4.20 x 3.35; (112189) right M3 = 3.95 x 2.70; (115872) left M3 = 4.90 x 3.60; (115214) right p4 = 2.20 x 3.55; (112196) left m1 = 3.10 x 4.15; (115687) left m1 = 3.20 x 4.15; (115670) left m1 = 3.15 x 3.95; (115840) right m1 = 3.20 x 4.15; (112083) left m1 = 3.20 x 4.25; (115869) right m1 = 3.10 x 4.00; (115858) right m3 = 3.10 x 5.35; (112140) right m3 = 3.10 x 4.65; (112175) right m3 = 3.15 x 4.55; (112915) right m3 = 2.70 x 4.65

***Cantius nunienus* Cope 1881**

Referred Specimens—(103539) (103541) right m3; (103547) (104684) left m2; (112865) right M3; (116317) left m3; (116318) left P4; (116320) left m1; (115142)

Occurrence—SP 75, SP 136, SP 159

Description—While *Cantius* has a relatively closed entoconid notch, *C. nunienus* possesses a more narrow but open notch (Gunnell 2002).

Measurements—(116318) left P4 = 4.20 x 3.10; (112865) right M3 = 3.10 x 4.60; (116320) left m1 = 2.70 x 4.00; (104684) left m2 = 3.15 x 3.80; (103541) right m3 = 3.05 x 4.60; (116317) left m3 = 3.05 x 4.60

Family OMOMYIDAE, Gazin 1958

Subfamily ANAPTOMORPHINAE, Cope 1883

Tribe TROGOLEMURINI, Szalay 1976

***Trogolemur*, Matthew 1909**

***Trogolemur* cf. *T. amplior*, Matthew 1909**

Referred Specimens—111942, left dentary m3

Known species—*Trogolemur myodes* Matthew 1909*, T. amplior, T. fragilis, T. leonardi*

Occurrence—SP 136

Description—*Trogolemur* is the smallest anaptomorphine known (Gunnell et al. 2008d). The m2-3 possesses a small, occasionally absent paraconid which is distinct on the m1 and trigonids are compressed anterioposteriorly (Gunnell et al. 2008d). One specimen of *Trogolemur* is known from the late Wasatchian at South Pass. The left dentary fragment is about 3.8 mm with a single lower molar. The m3 is small with a tall and narrow trigonid, no paraconid, and a metaconid which is taller than the protooconid. The talonid is low and posteriorly elongate

Discussion—*Trogolemur* is known from the Wasatchian (Wa6) to Duchesnian (Gunnell et al. 2008d)

Measurements—111942, left dentary m3 = 0.90 x 1.80

.

Tribe ANAPTOMORPHINI, Cope 1883

***Artimonius*, Muldoon and Gunnell 2002**

***Artimonius nocerai*, Muldoon and Gunnell 2002**

Referred Specimens—(104501) left m3; (104678) right dentary with m2; (109063) right dentary with m2-3; (109011) left maxilla with M2

Known species— *Artimonius witteri* Morris 1954, *A. australis, A. nocerai*

Occurrence—SP localities 74, 75, 135

Description—*Artimonius* molars are relatively large compared to other *Absarokius* species and the upper molars are more transverse with larger, crenulated basins. (Gunnell and Muldoon 2002). *Artimonius* is distinguished from other species of *Absarokius* by a the lack of a p2, a single rooted p3, and a enlarged p4 (Gunnell and Muldoon 2002). Three primary cusps are present on the upper molars along with distinct conules (Rose 2006). The M2 is larger than the M3, transverse, with paracone and metacone of equal height, a relatively smaller protocone and equal development of the paraconule and metaconule (*A. witteri* has a larger metaconule) (Gunnell and Muldoon 2002). The hypocone is small to absent, a narrow stylar shelf and mesostyle are present and a postprotocingulum runs posteriorly to the protocone (Rose 2006). Four late Wasatchian specimens are known from South Pass. The m2 (104678, 109063) both possess tall and narrow trigonids with paraconid shifted lingually toward the metaconid. The m3 (109063, 104501).

Discussion—*Artimonius* is known from the Wasatchian (Wa6) to early Bridgerian (Br1a) (Gunnell et al. 2008) and belongs to the Omomyidae which have simple, low crowned molars and resemble modern tarsiers (Rose 2006). *Artimonius witteri* was originally named *Absarokius witteri* by Morris (1954) and later renamed as the type for *Artimonius* by Muldoon and Gunnell (2002). *Artimonius nocerai* was originally described as *Absarokius noctivagus nocerai* by Robinson (1966), given species status as *Absarokius nocerai* by Bown and Rose (1987) and finally reallocated to *Artimonius* (Muldoon and Gunnell 2002). The late Wasatchian specimens listed here are also referenced in Muldoon and Gunnell (2002).

Measurements—(104501) left m3 = 1.35 x 2.10; (104678) right dentary with m2 = 1.75 x 2.10; (109063) right dentary with m2-3: m2 = 1.80 x 1.90, m3 = 1.20 x 1.75; (109011) left maxilla with M2 = 3.60 x 1.90

Tribe TETONIINA, Abel 1931

***Absarokius*, Matthew 1915**

***Absarokius gazini*, Bown and Rose 1987**

Referred Specimens—(116268) right dentary m2; (116269) left p4; (115745) left p4 (116270); left M1 fragment

Included species—*Absarokius abbotti* Loomis 1906*, A. gazini, A. metoecus*

Occurrence—SP locality 75

Description—*Absarokius* has a lower dental formula of 2.1.3.3 (Gunnell et al. 2008d). Upper and lower third molars in *Absarokius* are relatively reduced (Gunnell et al. 2008d). Matthew (1915c) describes the lower molars as wide, low cusped, with a notable paraconid on the m1. The m3 is smaller than m1 or m2 with slender talonid and very small hypoconulid and entoconid (Matthew 1915c). *Absarokius* retains a p2, lacks extreme enlargement of the p4, upper molars are narrow and possess small trigon basins, which distinguish it from *Artimonius* (Gunnell et al. 2008d). The m2 (116268) has a very tall and narrow trigonid, comprising of a small protoconid and metacond and no paraconid. The talonid of UM 116268 has a narrow labial cingulum, short cristid obliqua and no hypoconulid. *A. gazini* is generally smaller than most other species of *Absarokius* other than *A. metoecus*, but differs from this species by possessing a larger, more hypertrophied p4 (Gunnell and Rose 2002).

Discussion— *Absarokius* is known from the early Wasatchian (Wa1) to early Bridgerian (Br1) (Gunnell et al. 2008d). *Absarokius abbotti* was originally named

Anaptomorphus abbotti by Loomis (1906) and renamed under the genus *Absarokius* by Matthew (1915c).

Measurements— (116269) left p4 = 2.10 x 2.20; (115745) left p4 = 2.00 x 1.85; (116268) right dentary m2 = 1.90 x 2.15

Anemorhysis, Gazin 1958

Referred Specimens—(115220) left M1; (115837) left M2

Known species— *Anemorhysis sublettensis* Gazin 1952*, A. natronensis, A. pearcei, A. pattersoni, A. savage, A. wortimani*

Occurrence— SP 125, SP 136

Description— *Anemorhysis* possesses sharply defined molar cusps that are not enlarged near the base with straight postcristids on m1-2 (Gunnell et al. 2008d). *Anemorhysis* can also be distinguished from other anaptomorphines (namely *Teilhardina* and *Tetonius*) by a semi-molariform p4 (Gunnell et al. 2008d). The M1 (115220) has a lingually elongate protocone and a weakly developed metaconule and paraconule. The M2 (115837) is similar in size as the M1 (115220) but has a very small paracone and metacone with no conules.

Discussion—*Anemorhysis* is known from the Wasatchian (Wa1 – Wa7) (Gunnell et al. 2008d). *A. sublettensis* was originally named *Paratetonius* sublettensis by Gazin (1952) and later renamed by Gazin (1958) as the type for *Anemorhysis.*

Measurements—(115220) left M1 = 2.85 x 1.80; (115837) left M2 = 2.80 x 1.65

Anemorhysis sublettensis Gazin 1952

Referred Specimens—(115101) left M1; (115109) right M1; (115110) left m1; (115113) right M2

Occurrence—SP 136

Description— *A. sublettensis* is one of the smaller species of *Anemorhysis* (Bown and Rose 1987). The upper M1 (115101, 115109) have a distinct metaconule and paraconule, sharp postprotocristae and weak metastyle (115101). The M2 (115113) is similar to M1 specimen UM 115220 in that it possesses a broad posterior cingulum, distinct conules and lingually elongate protocone. The lower m1 (115110) has a tall trigonid with distinct paraconid and an enlarged metaconid situated posteriolingually to the protoconid. The hypoconulid on UM 115110 is situated labially on the talonid, closely paired to the hypoconid.

Measurements—(115113) right M2 = 3.15 x 1.80; (115101) left M1 = 2.05 x 1.50; (115109) right M1 = 2.85 x 1.75; (115110) left m1 = 1.65 x 2.30

Subfamily OMOMYINAE, Trouessart 1879

Tribe WASHAKIINI, Szalay 1976

***Loveina*, Simpson 1940**

***Loveina zephyri*, Simpson 1940**

Referred Specimens—(115700) right m1; (105184) right P4; (116030) left m2

Known species— *Loveina zephyri* Simpson 1940*, L. minuta, L. sheai, L. wapitiensis*

Occurrence—SP 75, SP 136

Description— *Lovina* is considered more primitive than other washakiins including *Shoshonius, Dyseolemur* and *Washakius* (Gunnell et al. 2008d). *Lovina* may occasionally possess minor metastylids on m1-3 (Gunnell et al. 2008d).

Discussion— *Lovina* is known from the Wasatchian (Wa5 – Wa7) (Gunnell et al. 2008). The right m1 (105184) is slightly smaller than the type specimen (AMNH 32517) *Lovina zephyri* (Simpson 1940). The m1 (105184) differs from the m2 (116030) in that the paraconid is small but present, and the cristid obliqua intersects medially on the protocristid. The m1 is slightly smaller than other specimens of *L. zephyri* but the length falls close to the size of *L. minutes* which is 1.85 mm (Holroyd and Strait 2008). The m2 (116030) has a tall trigonid, wide talonid and no paraconid or hypoconulid. The metaconid on this molar is twinned and the crista obliqua intersects the protocristid at the base of the protoconid. The size of this m2 is smaller than other described specimens of *L. zephyri* (Holroyd and Strait 2008).

Measurements—(105184) right P4 = 2.15 x 1.15; (115700) right m1 = 1.20 x 1.90; (116030) left m2 = 1.15 x 1.25

Order RODENTIA

Family SCIURAVIDAE, Miller and Gidley 1918

***Sciuravus*, Marsh 1871**

Referred Specimens—(105183) left p4; (105188) left mX; (105190) right p4; (105192) left MX; (105200) left MX; (105205) right P4; (105206) right mX; (108044) right MX; (112849) right mX; (112851) right mX; (112857) left p4; (112859) left p4; (112918) left p4; (112919) right m1; (112932) left M1; (112841) right MX

Known species— *Sciuravus nitidus* Marsh 1871, *S. altidens, S. bridger, S. popi, S. wilsoni*

Occurrence—SP 74, SP 75, SP 125, SP 135, SP 153, SP 136

Description—The M1-2 have short metalophs that are transverse on M3, while the m1 has no metastylid crest and the entoconid connects to the mesolophid (Walten and Porter 2008). The m2 has a short ectolophid (not connected to protoconid) and hypoconulid does not connect to the hypolophid (Walten and Porter 2008). The upper molars are relatively quadrate, the hypocone may be smaller or equal in size to the protocone. Metaconules and paraconules are present (115101, 115109, 115113, 105205, 108044, 112932) and vary in development. A distinct mesostyle (112932, 108044) and occasional small parastyle to distinct stylar crest may also be present. The lower molars (112849, 112851, 112919) are generally square shaped with low pointed cusps, tall metaconid and occasional mesoconid (105188). UM 105206 and 115188 are small with low to worn cusps and a broad shallow talonid.

Discussion—*Sciuravus* is known from the Wasatchian (Wa3) to Duchesian (Walten and Porter 2008).

Measurements—(112841) right MX = 2.35 x 1.95; (105192) left MX = 1.35 x 1.35; (105200) left MX = 1.55 x 1.45; (108044) right MX = 2.15 x 1.70; (112932) left M1 = 2.15 x 2.20; (105188) left mX = 1.40 x 1.60; (105206) right mX = 0.90 x 1.05; (112849) right mX = 1.60 x 2.10; (112851) right mX = 2.10 x 2.15; (112919) right m1 = 1.65 x 1.95;

Family ISCHYROMYIDAE, Alston 1876

Subfamily PARAMYINAE, Haeckel 1895

***Paramys*, Leidy 1871**

Referred Specimens—(105194) right mX; (105209) right mX; (115770) right m1

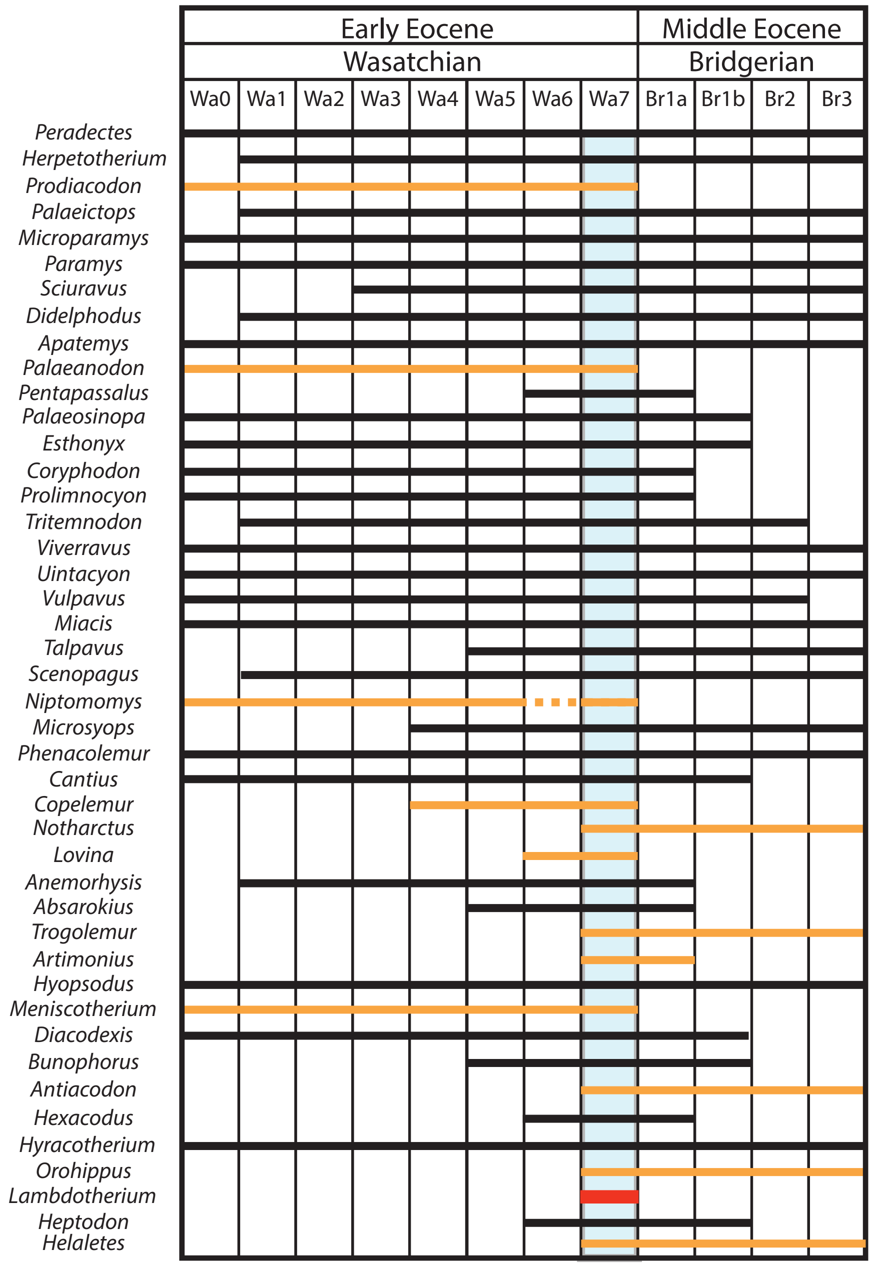

Figure 2.17 - Wasatchian and Bridgerian ranges of genera found at the Pinnacles buttes modified from Woodburne et al. (2009a). Lambdotherium is indicated in red. Orange indicates taxa with either a first or last appearance in the Wa7 zone. Ranges contributed from Lofgren et al. (2004), Korth (2008), Gunnell et al. (2008a, 2008b, 2008c, 2008d), Anderson (2008), Gunnell and Bartels (1999), Walton and Porter (2008), Storer (1996), Rose (2008), Gingerich and Clyde (2001), Lucas and Schoch (1998), Gingerich (1989), Lucas (1998), Gunnell (1998), Morlo and Gunnell (2003), Flynn (1998), Robinson et al. (2004), Heinrich et al. (2008), Wang and Tedford (1994), Silcox and Gunnell (2008), Archibald (1998), Stucky (1998), Krishtalka et al. (1987), MacFadden (1998), Mader (1998), Mihlbachler (2008).

Included species— *Paramys delicatus* Leidy 1871*, P. compressidens, P. copei, P. delicatior, P. excavates, P. hunti, P. nini, P. pycnus, "P."simpsoni, P. Taurus*

Occurrence—SP 75, SP 147

Description— *Paramys* possesses oval shaped lower incisors that have enamel on the anteriolateral side (Anderson 2008). On lower molars, trigonid basins are opened posteriorly, posterorlophids connect to the hypoconid, the metaconid and protoconid are connected by the anterior cingulum and the mesoconid remains distinct (Anderson 2008). The lower molars (105194, 105209, 115770) are square shaped with rounded cusps and low trigonid with no hypoconuid or paraconid. The metaconid is taller than the protoconid and a mesoconid is discernable on UM 115770 and 105209.

Discussion— *Paramys* is found in the Clarkforkian (Cf2) to Chadronian (Ch1) and medium to large for a rodent, with a heavy mandibular ramus (Anderson 2008).

Measurements—(105194) right mX = 2.10 x 2.30; (105209) right mX = 2.25 x 2.90; (115770) right m1 = 2.80 x 3.10

Family ISCHYROMYIDAE, Alston 1876

Subfamily MICROPARAMYINAE, Wood 1962

***Microparamys,* Wood 1959**

Referred Specimens—(105204) right mX; (115719) left mX; (116104) right M3; (115128) right m3; (115130) left M1 or M2; (115651) left m3; (115883) left p4; (116087) right p4; (115772) left m1

Known species— *Microparamys hottingeri* Marandat 1989*, M. cheradius, M. dubius, M. hunterae, M. minutes, M. nanus, M. nimius, M. paisi, M. perfossus, M. sambucus, M. scopaiodon, M. solidus, M. tricus, M. woodi*

Occurrence—SP 75, SP 136, SP 153, SP 125

Description— The lower molars have a distinct anterior cingulum, a distinct metastylid and mesoconid is present, in addition to well developed metalophs and protolophs (Anderson 2008). *Microparamys* is characterized by an absence of a hypocone on the P4 that is present on M1-2 (Anderson 2008). The upper molars (115130, 116104) are generally small with a protruding parastyle and hypocone on the M3. The lower molars have low pointed to heavily worn (115651) cusps, with a wide talonid (105204, 115719). A mesoconid is occasionally present on some of the lower molars (115772, 115719) but can also be absent as in UM 105204.

Discussion— *Microparamys* is one of the smallest individuals in the family isochromyidae (Anderson 2008).

Measurements—(115130) left M1 or M2 = 1.30 x 1.15; (116104) right M3 = 1.80 x 2.20; (105204) right mX = 0.70 x 0.80; (115719) left mX = 2.35 x 2.35; (115772) left m1 = 1.20 x 1.40; (115128) right m3 = 1.20 x 1.60; (115651) left m3 = 1.05 x 1.25;

ORDER TILLODONTIA

FAMILY ESTHONYCHIDAE, Cope 1883

Subfamily ESTHONYCHINAE, Zittel and Schlosser 1911

***Esthonyx*, Cope 1874**

***Esthonyx acutidens*, Cope 1881**

Referred Specimens—(115815) left i2

Known species—*Esthonyx bisculcatus* Cope 1874*, E. xenicus, E. ancylion, E. granger, E. gunnelli, E. spatularis, E. acutidens*

Occurrence—SP 125

Description—The lower incisor crown is 9.30mm tall, robust and slightly curved with a transverse crest on the anteriolingual surface. The labial surface of the inscisor maintains a thick enamel, while the lingual surface is worn.

Discussion— *Esthonyx* is known from the Clarkforkian (Cf1) to early Bridgerian (Gingerich and Gunnell 1979) and is a medium to large esthonychine (small to medium tilliodonts, possessing a skull length of 10-20 cm (Lucas and Schoch 1998). Upper molars of *Esthonyx* are narrower than other trogosines, slightly larger tilliodonts, which included *Meiostylodon* and *Plesiesthonyx* (Lucas and Schoch 1998). Trogosines replaced esthonychine tillodonts in the early Bridgerian (Gingerich and Gunnell 1979). *E. acutidens* is known specifically to the Lostcabinian and may have arisen from or lived along side populations of *E.bisulcatus* during this time (Gingerich and Gunnell 1979). According to Gunnell and Gingerich (1979) the wear on *Esthonyx*'s inscisors and molars may be indicative of ground foraging and a rhizophagous diet.

AGE AND CORRELATION OF PINNACLES ASSEMBLAGE

Gunnell et al. (2009) provide the most contemporary review of the Lostcabinian (latest Wasatchian, Wa7) to Gardnerbuttean (early Bridgerian, Br1a) since Robinson et al. (2004). The Lostcabinian is recognized as the interval range zone of the species *Lambdotherium popoagicum* as described by Stucky (1984) from the type section at Buck Springs Quarry of Lost Cabin Member of the Wind River Formation. *Eotitanops borealis* lies stratigraphically above occurrences of

L. popoagicum, and occurs with other known earliest Bridgerian mammals such as *Trogosus* and *Hyrachyus* (Gunnell et al. 2009).

The presence of *Lambdotherium popoagicum* and *Lovina zephryi* with the absence of *Eotitanops borealis, Hyrachyus* and *Trogosus* is an indication of Lostcabinian affinity. Of the Pinnacles assemblage in particular, overlapping last appearance datums (LAD) of *Palaeanodon, Copeleumur, Loveina, Mensicotherium* and *Heptodon* in the late Wasatchian with the first appearance datums (FAD) of *Antiacodon, Orohippus, Trogoleumur, Artimonius* and *Northarctus* (Woodburne et al. 2009a) support the late Wasatchian (Wa7; Lostcabinian) age assignment.

FAUNAL CHARACTERISTICS OF THE LATE WASATCHIAN

The Wa7 was characterized by faunal reorganization with increases in rodent, artiodactyl, and perissodactyl diversity and a high number of LAD's with one immigrant (*L. popoagicum*) (Woodburne et al. 2009a, 2009b). In contrast, later expansion of the Br1a fauna resulted in far more FAD's than LAD's (Woodburne et al. 2009a, 2009b). Beginning in the late Wasatchian, the Bridgerian witnessed a major radiation of carnivores and rodents, change in dominant families of omomyid primates (omomyine over anaptomorphine, Gunnell 1997), the addition of homoacodine artiodactyls and also diversification of Brontitheridae (four subfamilies) (Woodburne et al. 2009b).

In contrast to the Paleocene-Eocene Thermal Maximum (PETM), which saw large scale migration events (Rose 2006), the Early Eocene Climate Optimum (EECO) was dominated by cladiogenesis and evolutionary innovation (Woodburne et al. 2009b). The EECO during subzones Wa7-Br1a is also coincident with increased levels of insectivory, scansoriality and arboreality (Hooker 2000). While the PETM interval was marked by an increase in taxa, the EEOC also had a diversification in flora and northward migration of tropical zones into the mid-latitudes (Woodburne et al. 2009a). The origination of new taxa at lake margins in the Green River Basin may have also contributed (Gunnell and Bartels 1994, 2001, Bartels and Gunnell 1997).

DISCUSSION

The late Wasatchian is represented within North America in the Lost Cabin Member of the Wind River Formation (Stucky 1984, Stucky et al. 1990); Huerfano basin in Colorado (Robinson 1966); upper Main Body of the Wasatch Formation in the northern Great Divide Basin at the Pinnacles near South Pass, Wyoming (Neumann et al. 2011, Gunnell et al. 2004) and Freighter Gap (Van Regenmorter and Anemone 2008); the New Fork tongue of the Wasatch Formation in the northern Green River Basin (West 1973); at Little Muddy in the western Green River Basin (Zonneveld et al. 2000); Cathedral Bulffs tongue of the Wasatch Formation, Cottonwood Creek area, Washakie Basin (Honey 1988); Lost Cabin beds of the Willwood Formation in the Big Horn Basin (Gunnell et al. 1992, Schankler 1980); Piceance Creek basin, Colorado (Kihm 1984); the Eureka Sound Group in Nunavut Territory, Canada (Eberleand McKenna 2002); Hannold Hill Formation in Big Bend National Park, Texas (Maxwell et al. 1967). Other localities in North America thought to contain Wasatchian-Bridgerian taxa have since been reexamined. A premolar from Pumpkin Buttes in the Powder River Basin once considered *Lamdotherium* (Soister 1968) has now been reassigned to Wa3 perrisodactyl *Homogalax* (Robinson and Ivy 1994). The brontothere *Eotitanops,* collected from the dominantly early Wasatchian localities of the Lomas las Tetas de Cabra Formation in Baja California, may be either a truly early representative of the Br1a taxa or the result of downhill contamination (Novacek et al. 1991).

Lambdotherium and *Eotitanops* were suspected to overlap in select areas of the northern Green River Basin (Gunnell and Yarborough 2000, West 1973). Novacek et al. (1991) mentions one specimen of *Eotitanops* in the Loma las tetas de Cabra fauna in Baja California. A Yale Peabody Museum (YPM) specimen of *Eotitanops* was supposedly recovered from Lostcabinian age beds in the Bighorn Basin (Gunnell and Yarborough 2000). Smith and Holroyd (2003) confirmed the validity of this occurrence the YPM specimen in the Lostcabinian, but the anomalous specimen from Big Piney, Green River Basin has since been regarded as misidentification (Gunnell et al. 2009).

An anomalous co-occurrence of *Lambdotherium* and *Eotitanops* can be explained by misidentification, downhill contamination or even possibly the intersection of migrating populations. This does not diminish the utility of these taxa as biostratigraphic indicators. *Eotitanops* occurs above *Lamdotherium* in the Cathedral Bluffs member at South Pass and New Fork member of the Wasatch, Wyoming; Little Muddy faunas I-III of the Wasatch and Green River Formations; Hiland-Raptor Heights, Red Creek and Deadman Buttes in the Wind River Formation; Huerfano Formation and Debeque Formation, Colorado; and Eureka Sound Formation, Ellesmere Island (Gunnell et al. 2009, Bartels and Gunnell 2001, West 1973, Zonneveld et al. 2000, Robinson 1966, Stucky 1984, Kihm 1984, Eberle 2006). Realistically, the age determination of a unit should not be based solely upon the index taxa, but also supported by FADs and LADs of other genera recovered from localities.

The type section in the Lost Cabin Member of the Wind River Formation is composed of approximately 66 mammal species from 30 families (Stucky et al. 1990, Stucky 1984, Stucky and Gunnell per comm. 2010). Notable differences between the Buck Springs assemblage and the Pinnacles assemblage include a higher diversity of insectivores at and absence of *Meniscotherium, Loveina* and metacheiromyids at Buck Springs. The Pinnacles assemblage has a higher diversity of omomyids and lacks multituberculates, *Phenacodus, Shoshonius, Alveojunctus* and *Uintasorex.* Also, carnivores, perrisodactyls, marsupials, microsyopids and omomyids are represented in each area by different taxa.

The omomyid primates in the study area consist of 5 genera (*Trogolemur, Absarokius, Anemorhysis, Artimonius, Loveina*) and are more diverse than the notharctine primates, which comprise 3 genera (*Notharctus, Cantius, Copelemur*). This suggests that familial dominance in the primates favors omomyids by the latest Wasatchian at this location. Variation is witnessed in the position of the hypoconulid on the lower molars of *Microsyops.* The hypoconulid is either medially positioned in reference to the trigonid, or placed lingually near the entoconid. The large *Microsyops* sample may be represented by more than one species. *Hyopsodus* may be represented by the two species *Hyopsodus paulus* and *Hyopsodus wortmani.*

Anachronistic taxa such as *Orohippus*, co-occurring with its ancestor taxon *Hyracotherium,* occur at some Pinnacles localities. Collecting has reveled thus far that the diagnostic Wa7 (*Lambdotherium*) and Br1a (*Eotitanops, Trogosus, Hyrachyus*) taxa do not share stratigraphic ranges at the Pinnacles, Red's Cabin Monocline or Cathedral Bluffs. The Wasatchian-Bridgerian (Lostcabinian-Gardnerbuttean) boundary is herein interpreted to occur within the uppermost beds of the Main Body of the Wasatch Formation, just below its contact with the Tipton Shale Member, Green River Formation.

CONCLUSIONS

The Lostcabinian and Gardnerbuttean mark the onset of incredible evolutionary change during the Early Eocene Climate Optimum (EECO) onset by increased floral diversity, mid-latitude tropicality and faunal reorganization (Woodburne et al. 2009a, 2009b). Measurements and detailed descriptions of specimens from the Lostcabinian provide an empirical basis by which future authors can compare Pinnacles faunas with coeval Lostcabinian assemblages and to assemblages from overlying Gardnerbuttean successions.

The assemblage is represented by 56 species from 46 genera and 30 families. The collection is comparable in diversity to the type Lostcabinian fauna, which is represented by 66 species. The Pinnacles sample is more diverse than the coeval Little Muddy sample which consists of 20 species from 19 genera.The Pinnacles fauna provides the largest known Lostcabinian fossil vertebrate sample from the northern Green River Basin.

The age affinity is confirmed by two Lostcabinian index taxa – *Loveina zephyri* and *Lambdotherium popoagicum* (Gunnell et al. 2009). The overlapping temporal ranges of other taxa with last appearances in the Lostcabinian (*Palaeanodon, Copeleumur, Loveina, Mensicotherium* and *Heptodon*) to others with first appearances (*Antiacodon, Orohippus, Trogoleumur, Artimonius* and *Notharctus*) support the Lostcabinian age assignment.

REFERENCES

Anderson D. 2008. Ischyromyidae. Evolution of Tertiary Mammals of North America Volume 2: Small Mammals, Xenarthrans and Marine Mammals. Ed. Janis CM, Gunnell GF, Uhen MD. Cambridge University Press, New York.

Archibald DJ. 1998. Archaic Ungulates ("Condylarthra"). Evolution of Tertiary Mammals of North America Volume 1: Terrestrial Carnivores, Ungulates and Ungulatelike Mammals. Ed. Janis CM, Scott KM, Jacobs LL. Cambridge University Press, New York.

Badgley C, Gingerich PD. 1988. Sampling and faunal turnover in Early Eocene mammals. Paleogeography, Paleoclimatology, Paleoecology. 63: 141-157.

Bartels WS, Gunnell GF. 1997. Basin margin faunas and the origin of North American Land Mammal Age faunal turnover. Journal of Vertebrate Paleontology. 17(3 supplement):31A

Bonillas Y. 1936. Dentition of Lamdotherium. *Journal of Mammalogy.* 17(2): 139-142.

Bown TM, Rose KD. 1987. Patterns of dental evolution in early Eocene anaptomorphine primates (Omomyidae) from the Bighorn Basin, Wyoming. Paleontological Society Memoir. 23:1-162.

Clyde WC., Zonneveld JP., Stamatakos J., Gunnell GF., Bartels WS. 1997. Magnetostratigraphy across the Wasatchian/Bridgerian NALMA Boundary (Early to Middle Eocene) in the Western Green River Basin, Wyoming. Journal of Geology. 105: 657-669

Clyde WC., Sheldon ND., Koch PL., Gunnell GF., Bartels WS. 2001. Linking the Wasatchian/Bridgerian boundary to the Cenozoic Global Climate Optimum: new magnetostratigraphic and isotopic results from South Pass, Wyoming. Paleogeography, Paleoclimateology, Paleoecology. 75: 175-199.

Colbert and Schoch . 1998. Tapiroidea and other moropomorphs. North America Volume 1: Terrestrial Carnivores, Ungulates and Ungulatelike Mammals. Ed. Janis CM, Scott KM, Jacobs LL. Cambridge University Press, New York.

Cope ED. 1877. Report upon the extinct Vertebrata obtained in New Mexico by parties of the expedition of 1874. Chapter 12: Fossils of the Eocene period. Geographical Surveys West of the 100th Meridian. Ed, GM Wheeler. Government Printing Office, Washington, DC:37-282.

Cope ED. 1882. Contributions to the history of the Vertebrata of the lower Eocene of Wyoming and New Mexico, made during 1881. Proceedings of the American Philosophical Society. 20(111): 139-197

Eberle JJ. 2006. Early Eocene Brontotheriidae (Perissodactyla) from the Eureka Sound Group, Ellesmere Island, Canadian High Arctic – Implications for Brontothere origins and high-latitude dispersal. *Journal of Vertebrate Paleontology*. 26 (2). 381-386.

Eberle JJ and Mckenna MC. Early Eocene Leptictida, Pantolesta, Creodonta, Carnivora, and Mesonychidae (Mammalia) from the Eureka Sound Group, Ellesmere Island, Nunavut. Canadian Journal of Earth Sciences. 39: 899-910.

Flynn JJ. 1998. Early Cenozoic Carnivora ("Miacoidea"). Evolution of Tertiary Mammals of North America Volume 1: Terrestrial Carnivores, Ungulates and Ungulatelike Mammals. Ed. Janis CM, Scott KM, Jacobs LL. Cambridge University Press, New York.

Gazin CL. 1956. The occurrence of Paleocene mammalian in the Fossil Basin of southwestern Wyoming. Journal of Paleontology. 30(3): 707-711.

Gazin CL. 1962. A further study of the lower Eocene mammalian faunas of southwestern Wyoming. Smithsonian Miscellaneous Collections. 144(1): p. 1-46.

Gazin CL. 1965. Early Eocene Mammalian Faunas and Their Environment in the vicinity of the Rock Springs Uplift, Wyoming. Sedimentation of Late Cretaceous and Tertiary Outcrops, Rock Springs Uplift, 19th Annual Field Conference Guidebook. 171-180.

Gazin CL. 1968. A study of the Eocene condylarthran mammal *Hyopsodus*. Smithsonian Miscellaneous Collections. 153(4): 1-89.

Gingerich PD. 1979. Phylogeny of middle Eocene Adapidae (Mammalia, Primates) in North America: *Smilodectes* and *Notharctus*. Journal of Paleontology. 53: 153-163.

Gingerich PD. 1983a. Paleocene-Eocene faunal zones and a preliminary analysis of Laramide structural deformation in the Clark's Fork Basin, Wyoming. Wyoming Geological Associaltion Guidebook, Thirty-fourth Annual Field Conference, p. 185-195

Gingerich PD. 1983b. Systematics of early Eocene Miacidae (Mammalia, Carnivora) in the Clark's Fork Basin, Wyoming. Contributions from the Museum of Paleonotology, University of Michigan. 26(10): 197-225.

Gingerich PD. 1989. New earliest Wasatchian mammalian fauna from the Eocene of northwestern Wyoming: Composition and diversity in a rarely sampled high-floodplain assemblage. University of Michigan Papers on Paleontology 28:1-97.

Gingerich PD, Simons EL. 1977. Systematics, phylogeny and evolution of early Eocene Adapidae (Mammalia, Primates) in North America. Contributions from the Museum of Paleontology, University of Michigan. 24(22):245-279.

Gingerich PD, Haskin RA. 1981. Dentition of early Eocene *Pelycodus jarrovii* (Mammalia, Primates) and the generic attribution of species formally referred to *Pelycodus*. Contributions by the Museum of Paleontology, University of Michigan. 25: 327-337.

Gingerich PD, Winkler DA. 1985. Systematics of Paleocene Viverravidae (Mammalia, Carnivora) in the Bighorn Basin and Clark's Fork Basin, Wyoming. Contributions from the Museum of Paleontology, University of Michigan. 27(4): 87-128.

Gingerich PD, Gunnell GF. 1979. Systematics and evolution of the genus *Esthonyx* (Mammalia, Tillodontia) in the Early Eocene of North America. Contributions from the Museum of Paleontology, University of Michigan. 25(7): 125-153.

Gingerich PD, Clyde WC. 2001. Overview of mammalian biostratigraphy in the Paleocene-Eocene Fort Union and Willwood formations of the Bighorn and Clark's Fork basins. University of Michigan Papers on Paleontology 33 Gingerich PD, ed. Paleocene-Eocene Stratigraphy and Biotic change in the Bighorn and Clarks Fork Basins, Wyoming. 1.14.

Google Maps. 2013. Southwest Wyoming. https://maps.google.com/maps?q=reference+google+maps&um=1&ie=UTF-8&hl=en&sa=N&tab=wl

Granger W. 1914. On the names of lower Eocene faunal horizons of Wyoming and New Mexico. Bulletin of the American Museum of Natural History. 33:201-207.

Gunnell GF. 1989. Evolutionary history of Microsyopoidea (Mammalia, ?Primates) and the relationship beween Plesiadapiforms and Primates. University of Michigan Papers in Paleontology. 27: 1-157.

Gunnell GF. 1997. Wasatchian-Bridgerian (Eocene) paleoecology of the western interior of North America: changing paleoenvironments and taxonomic composition of omomyid (Tarsiiformes) primates. Journal of Human Evolution. 32: 105-132.

Gunnell GF. 1998a. Creodonta. Evolution of Tertiary Mammals of North America Volume 1: Terrestrial Carnivores, Ungulates and Ungulatelike Mammals. Ed. Janis CM, Scott KM, Jacobs LL. Cambridge University Press, New York.

Gunnell GF. 1998b. Mammalian fauna from the lower Bridger Formation (Bridger A, early middle Eocene) of the southern Green River Basin, Wyoming. Contributions from the Museum of Paleontology, University of Michigan 30:83–130

Gunnell GF. 2002. Notharctine primates (Adapiformes) from the early to middle Eocene (Wasatchian–Bridgerian) of Wyoming: transitional species and the origins of *Notharctus* and *Smilodectes. Journal of Human Evolution.* 43(3): 353-380.

Gunnell GF., Bartels WS., Gingerich PD., Torres V. 1992. Wapiti Valley Faunas: Early and Middle Eocene fossil vertebrates from the North Fork of the Shoshone River, Park County, Wyoming. Contributions from the Museum of Paleontology, University of Michigan. 28(11): 247-287.

Gunnell GF, Bartels WS. 1994. Early Bridgerian (middle Eocene) vertebrates, paleontology and paleoecology of the sourthern Green River Basin, Wyoming. University of Wyoming, Contributions to Geology. 30: 57-70.

Gunnell GF, Bartels WS. 1999. Middle Eocene vertebrates from the Uinta Basin, Utah and their relationships with faunas fro mthe southern Green River Basin, Wyoming. Utah Geological Survey Miscellaneous Publication 99-1. Gillette DD, ed. Vertebrate Paleontology in Utah. 429-442.

Gunnell GF, Bartels WS. 2001. Basin margins, biodiversity, evolutionary innovation, and the origin of new taxa. Gunnell GF. Ed. Eocene Biodiversity: Unusual occurrences and rarely sampled habitats. Topics in Geobiology Series. Kluwer/Plenum, New York. 403-440.

Gunnell GF, Yarborough VL. 2000. Brontotheriidae (Perissodactyla from the late Early and Middle Eocene (Bridgerian) Wasatch and Bridger Formations, Southern Green River Basin, southwestern Wyoming. Journal of Vertebrate Paleontology. 20: 349-368.

Gunnell GF and Rose KD. 2002. Tarsiiformes: Evolutionary history and adaptation. The Primate Fossil Record. Ed. Hartwig WC. Cambridge University Press, New York.

Gunnell, GF, Bartels WS, Zonneveld JP. 2004. A late Wasatchian (late early Eocene) vertebrate assemblage preserved in meandering stream channel deposits, Northern Red Desert, Wyoming. GSA Abstracts with Programs, 2004: A-92

Gunnell GF, Bown TM, Bloch JI, Boyer DM. 2008a. “Protoeutheria”. Evolution of Tertiary Mammals of North America Volume 2: Small Mammals, Xenarthrans and Marine Mammals. Ed. Janis CM, Gunnell GF, Uhen MD. Cambridge University Press, New York.

Gunnell GF, Bown TM, Bloch JI. 2008b. Leptictida. Evolution of Tertiary Mammals of North America Volume 2: Small Mammals, Xenarthrans and Marine Mammals. Ed. Janis CM, Gunnell GF, Uhen MD. Cambridge University Press, New York.

Gunnell GF, Bown TM, Hutchison JH, Bloch JI. 2008c. Lipotyphla. Evolution of Tertiary Mammals of North America Volume 2: Small Mammals, Xenarthrans and Marine Mammals. Ed. Janis CM, Gunnell GF, Uhen MD. Cambridge University Press, New York.

Gunnell GF, Rose KD, Rasmussen DT. 2008d. Euprimates. Evolution of Tertiary Mammals of North America Volume 2: Small Mammals, Xenarthrans and Marine Mammals. Ed. Janis CM, Gunnell GF, Uhen MD. Cambridge University Press, New York.

Gunnell GF., Murphy PC., Stucky RK., Townsend KEB., Robinson P., Zonneveld JP., Bartels WS. 2009. Biostratigraphy and Biochronology of the Latest Wasatchian, Bridgerian, and Uintan North American Land Mammal "Ages". Papers on Geology, Vertebrate Paleontology, and Biostratigraphy in Honor of Michael O. Woodburne. Museum of Northern Arizona Bulletin 65. 279-330.

Guthrie DA. 1966. A New Species of Dichobunid Artiodactyl from the Early Eocene of Wyoming. *Journal of Mammology.* 47(3): 487-490

Guthrie DA. 1967. The mammalian fauna of the Lysite Member, Wind River Formation (early Eocene) of Wyoming. Memoirs of the Southern California Academy of Sciences. 5: 1-53.

Heinrich RE, Strait SG, Houde P. 2008. Earliest Eocene Miacidae (Mammalia: Carnivora) from northwestern Wyoming. Journal of Paleontology. 82: 154-162.

Holroyd PA, Strait SG. New data on *Loveina* (Primates: Omomyidae) from the early Eocene Wasatch Formation and Implcations for Washakiin relationships. Elwyn Simons: A search for Origins. Ed Fleagle JG, Glibert CC. Springer. 243-257.

Honey JG. 1988. A mammalian fauna from the base of the Eocene Cathedral Bluffs Tongue of the Wasatch Formation, Cottonwood Creek area, southeast Washakie Basin, Wyoming. In Geology and paleoecology of the Cottonwood Creek Delta in the Eocene Tipton Tongue of the Green River Formation and a mammalian fauna from the Eocene Cathedral Bluffs Tongue of the Wasatch Formation, southeast Washakie Basin, Wyoming. US Geological Survey Bulletin 1669-C: C1-C14.

Hooker JJ. 2000. Ecological response of mammals to global warming in the late Paleocene and early Eocene. Geologiska Foreningens I Stockholm Forhandlingar. 122: 77-79.

Jacisin JJ. 2012. Fossil Reptiles from the late Early Eocene (Wasatchian, Lostcabinian) of the Red Desert, Wyoming. Albion College Undergraduate Research Papers, volume 67. Albion College Publishing. Albion, Michigan: 1-132.

Janis CM, Effinger JA, Harrison JA, Honey JG, Kron DG, Lander B, Manning E, Prothero DR, Stevens MS, Stucky RK, Webb SD, Wright DB. (1998). Artiodactyla. Evolution of Tertiary Mammals of North America Volume 1: Terrestrial Carnivores, Ungulates and Ungulatelike Mammals. Ed. Janis CM, Scott KM, Jacobs LL. Cambridge University Press, New York.

Kihm AJ. 1984. Early Eocene mammalian faunas of the Piceance Creek Basin northwestern Colorado. Ph.D Dissertation, University of Colorado, Boulder.

Kitts DB. 1956. American *Hyracotherium* (Perissodactyla, Equidae). Bulletin of the American Museum of Natural History. 110(1): 7-58.

Krishtalka L, West RM, Black CC, Dawson MR, Flynn JJ, Turnbull, Stucky RK, McKenna MC, Bown TM, Gloz J, Lillegraven JA. 1987. Eocene (Wasatchian through Duchesnean) biochronology of North America. Woodburne MO. Ed. 1987. Cenozoic Mammals of North America: Biostratigraphy and Geochronology. University of California Press, Berkeley. 1-336.

Korth WW. 2008. Marsupialia. Evolution of Tertiary Mammals of North America Volume 2: Small Mammals, Xenarthrans and Marine Mammals. Ed. Janis CM, Gunnell GF, Uhen MD. Cambridge University Press, New York.

Lofgren DL, Lillegraven JA, Clemens WA, Gingerich PD, Williamson TE. 2004. Paleocene Biochronology: The Puercan through Clarkforkian Land Mammal Ages. Woodburne MO. Ed. Late Cretaceous and Cenozoic Mammals of North America: Biostratigraphy and Geochronology. Columbia University Press, New York. 1-343.

Lucas SG. 1998. Pantodonta. Evolution of Tertiary Mammals of North America Volume 1: Terrestrial Carnivores, Ungulates and Ungulatelike Mammals. Ed. Janis CM, Scott KM, Jacobs LL. Cambridge University Press, New York.

Lucas SG and Schoch . 1998. Tillodontia. Evolution of Tertiary Mammals of North America Volume 1: Terrestrial Carnivores, Ungulates and Ungulatelike Mammals. Ed. Janis CM, Scott KM, Jacobs LL. Cambridge University Press, New York.

MacFadden BJ. 1998. Equidae. Evolution of Tertiary Mammals of North America Volume 1: Terrestrial Carnivores, Ungulates and Ungulatelike Mammals. Ed. Janis CM, Scott KM, Jacobs LL. Cambridge University Press, New York.

Madar B. 1998. Brontotheriidae. Evolution of Tertiary Mammals of North America Volume 1: Terrestrial Carnivores, Ungulates and Ungulatelike Mammals. Janis CM, Scott KM, Jacobs LL, ed. Cambridge University Press, New York. 525-559.

Matthew WD. 1909. The Carnivora and Insectivora of the Bridger Basin, middle Eocene. Memoir of the American Museum of Natural History. 9: 291-567.

Matthew WD. 1915. Part I: Order Ferae (Carnivora) Suborder Creodonta. A revision of the lower Eocene Wasatch and Wind River faunas Bulletin of the American Museum of Natural History. 34(1):1-103

Matthew WD. 1915. Part II: Order Condylarthra, Family Hyopsodontidae. A revision of the lower Eocene Wasatch and Wind River faunas. Bulletin of the American Museum of Natural History. 34(9): 311-328

Matthew WD. 1915. Part IV: Entelonychia, Primates, Insectivora (part). A revision of the lower Eocene Wasatch and Wind River faunas. Bulletin of the American Museum of Natural History. 34(10):429-483

Matthew WD, Granger W. 1921. New genera of Paleocene mammals. American Museum Novitates. 13:1-7

Maxwell RA, Lonsdale JT, Hazzard RT, Wilson JA. 1967. Geology of Big Bend National Park, Brewster County, Texas. University of Texas, 6711: 1-320.

Mihlbachler MC. 2008. Species taxonomy, phylogeny, and biogeography of the Brontotheriidae (Mammalia: Perissodactyla). Bulletin of the American Museum of Natural History 311: 1-475.

Morris WJ. 1954. An Eocene fauna from the Cathedral Bluffs tongue of the Washakie Basin, Wyoming. Journal of Paleontology. 28(2): 195-203.

Morlo M, Gunnell GF. 2003. Small limnocyonines (Hyaenodontidae, Mammalia) from the Bridgerian middle Eocene of Wyoming: *Thinocyon, Prolimnocyon* and *Iridodon*, new genus. Contributions of Museum of Paleontology, The University of Michigan 31: 43-78.

Muldoon KM, Gunnell GF. 2002. Omomyid primates (Tarsiiformes) from the Early Middle Eocene at South Pass, Greater Green River Basin, Wyoming. Journal of Human Evolution. 43(4):479-511.

Neumann AM. 2010. Systematics and Taphonomy of Microvertebrate Faunas from the Early Eocene of the Pinnacles, Green River Basin, Wyoming. Albion College Undergraduate Research Papers, volume 65. Albion College Publishing. Albion, Michigan: 1-230

Neumann AM, Zonneveld JP, Bartels WS, Gunnell GF. 2011. Stratigraphy of a fossiliferous late Wasatchian (Lostcabinian) fluvial section in the Red Desert, north eastern Green River Basin, Wyoming. Journal of Vertebrate Paleontology. 31(3 supplement):166

Novacek MJ. 1977. A review of Paleocene and Eocene Lepticidae (Eutheria: Mammalia) from North America. Paleobios. 24: 1-42.

Novacek MJ, Ferrusquia-Villafranca I, Flynn JJ, Wyss AR, Norell M. 1991. Wasatchian (early Eocene) mammals and other vertebrates from Baja California, Mexico: the Lomas las Tetas de Cabra fauna. American Museum of Natural History Bulletin 208: 1-88.

Osborn HF. 1902. The four phyla of Oligocene titanotheres. Bulletin of the American Museum of Natural History. 16(8):91-109

Osborn HF, Matthew WD. 1909. Cenozoic mammal horizons of western North America. U.S. Geological Survey Bulletin. 36:1-38.

Pipiringos GN. 1961. Uranium-bearing coal in the central part of the Great Divide Basin, Wyoming: US Geological Society Bulletin 1099-A, p. A1-A104

Rich TH and Collinson JW. 1973. First Mammalian Fossil from the Flagstaff Limestone, Central Utah: Vulpavus australis (Carnivora: Miacidae). *Journal of Paleontology*. 47(5): 854-860.

Robinson P. 1966. Fossil mammals of the Huerfano Formation, Eocene of Colorado. Peabody Museum of Natural History Yale University Bulletin. 21.

Robinson P, Ivy LD. 1994. Paromomyidae (Dermoptera?) from the Powder River Basin, Wyoming and a discussion of microevolution in closely related species. University of Wyoming, Contributions to Geology 30: 91-116.

Robinson P, Gunnell GF, Walsh SL, Clyde WC, Storer JE, Stucky RK, Froehlich DJ, Ferrusquia-Villafranca I, McKenna MC. 2004. Wasatchian through Duchesnean Biochronology. Woodburne MO. Ed. Late Cretaceous and Cenozoic Mammals of North America: Biostratigraphy and Geochronology. Columbia University Press, New York. 1-343.

Rose KD. 2006. The Beginning of the Age of Mammals. John Hopkins University Press, Baltimore. 1-428.

Rose KD. 2008. Palaeanodonta and Pholidota. Evolution of Tertiary Mammals of North America Volume 2: Small Mammals, Xenarthrans and Marine

Mammals. Ed. Janis CM, Gunnell GF, Uhen MD. Cambridge University Press, New York.

Rose KD, Krishtalka L, Stucky RK. 1991. Revision of the Wind River faunas, early Eocene of central Wyoming. Part 11: Palaeanodonta (Mammalia). Annals of the Carnegie Museum. 60(1)

Rose KD, Lucas SG. 2000. An early Paleocene palaeanodont (Mammalia, ?Pholidonta) from New Mexico, and the origin of Palaeanodonta. Journal of Vertebrate Paleontology. 20(1):139-156

Roehler HW. 1991. Revised stratigraphic nomenclature for the Wasatch and Green River Formations of Eocene age, Wyoming, Utah and Colorado. US Geological Survey Professional Paper 1506-B. p. B1-B38

Schankler, D. M. 1980. Faunal zonation of the Willwood Formation in the central Bighorn Basin, Wyoming. Papers on Paleontology, University of Michigan. 24:99-114.

Silcox MT and Gunnell GF. (2008). Plesiadapiformes. Evolution of Tertiary Mammals of North America Volume 2: Small Mammals, Xenarthrans and Marine Mammals. Ed. Janis CM, Gunnell GF, Uhen MD. Cambridge University Press, New York.

Steidtmann RJ, Middleton LT. 1991. Fault chronology and uplift history of the southern Wind River Range, Wyoming: Implications for Laramide and post-Laramide deformation in the Rocky Mountain foreland. Geological Society of America Bulletin. 103: p. 472-485.

Simpson GG. 1933. Glossary and correlation charts of North American Tertiary mammal-bearing formations. Bulletin of the American Museum of Natural History. 67: 79-121.

Simpson GG. 1935.The Tiffany fauna, Upper Paleocene: Multituberculata, Marsupialia, Insectivora and ?Chiroptera, Volume1. American Museum novitiates. 795: 1-19.

Simpson GG. 1940. Studies on the earliest primates. Bulletin of the American Museum of Natural History. 77(4):185-212.

Smith KT, Holroyd PA. 2003. Rare taxa, Biostratigraphy and the Wasatchian-Bridgerian Boundary in North America. Causes and consequences of Globally Warm Climates in the Early Paleogene. Ed Wing SL, Gingerich PD, Schmitz B, Thomas E. Geological Society of America Special Paper 369. 501-511.

Soister PE. 1968. Stratigraphy of the Wind River Formation in south-central Wind River Basin, Wyoming. US Geological Survey Professional Paper 594-A.

Storer JE. 1996. Eocene-Oligocene faunas of the Cypress Hills Formation, Saskatchewan. The Terrestrial Eocene-Oligocene Transition in North America. Cambridge University Press. 240-261.

Stucky RK. 1984. Revision of the Wind River faunas, Early Eocene of central Wyoming. Part 5. Geology and mammalian biostratigraphy of the upper part of the Wind River Formation. Annals of Carnegie Museum. 53:231-294.

Stucky RK, Krishtalka L, Redline AD. 1990. Geology, vertebrate fauna and paleoecology of the Buck Spring Quarries (early Eocene, Wind River Formation), Wyoming.

Stucky RK. 1998. Eocene bunodont and bunoselenodont Artiodactyla (“dinobunids”). Evolution of Tertiary Mammals of North America Volume 1: Terrestrial Carnivores, Ungulates and Ungulatelike Mammals. Ed. Janis CM, Scott KM, Jacobs LL. Cambridge University Press, New York.

Tsukui K, Clyde WC. Fine-tuning the calibration of the early to middle Eocene geomagnetic polarity time scale: Paleomagnetism of radioisotopically dated tuffs from Laramide foreland basins. Geological Society of America Bulletin. 124(5/6): 870-885.

Van Regenmorter J., Anemone R. 2008. Biostratigraphy of the Freighter Gap and Pinnacles areas, Great Divide Basin, southwestern Wyoming. Journal of Vertebrate Paleontology. 28 (3 supplement):156A.

Walten AH and Porter RM. 2008. Sciuravidae. Evolution of Tertiary Mammals of North America Volume 2: Small Mammals, Xenarthrans and Marine Mammals. Ed. Janis CM, Gunnell GF, Uhen MD. Cambridge University Press, New York.

Wang X and Tedford RH. 1994. Basicranial anatomy and phylogeny of primitive canids and closely related miacids (Carnivora: Mammalia. American Museum Novitates 3092: 1-34.

West RM. 1969. Geology and vertebrate paleontology of the northeastern Green River Basin, Wyoming. Wyoming Geological Association Guidebook, 21st Annual Field Conference, p. 77-92.

West RM. 1970. Sequence of mammalian faunas of Eocene age in the Northern Green River Basin, Wyoming. Journal of Paleontology. 44(1): 142-147.

West RM. 1973. Geology and mammalian paleontology of the New Fork-Big Sandy area, Sublette County, Wyoming. Fieldiana. Geology. 29: 1-193.

Wood HE, Chaney RW, Clark J, Colbert EH, Jepsen GL, Reeside JB, and Stock C. 1941. Nomenclature and correlation of the North American continental Tertiary. Geological Society of America Bulletin. 52:1-48.

Woodburne MO, Gunnell GF, Stucky RK. 2009a. Land mammal faunas of North America rise and fall during the Early Eocene Climatic Optimum. Denver Museum of Nature and Science Annals, No 1, p. 1-74.

Woodburne MO, Gunnell GF, Stucky RK. 2009b. Climate directly influences Eocene mammal faunal dynamics in North America. Proceedings of the National Academy of Sciences. 106 (32): 13399-13403.

Zonneveld JP, Gunnell GF., Bartels WS. 2000. Early Eocene fossil vertebrates from the southwestern Green River Basin, Lincoln and Uinta counties, Wyoming. Journal of Vertebrate Paleontology. 20(2): 369-386.

CHAPTER THREE

SEDIMENTOLOGY OF THE WASATCH AND GREEN RIVER FORMATIONS AND FLUVIAL REWORKING ON MICROVERTEBRATE BONEBED ASSEMBLAGES, PINNACLES BUTTES, SWEETWATER CO, WY

INTRODUCTION

The Wasatchian-Bridgerian boundary interval in the Green River Basin occurs contemporaneous with the formation of large regional lakes, climate change and the end of the Laramide Orogeny (Smith et al. 2008, Pietras et al. 2003, Roehler 1993). Intermontane basins of the Rocky Mountain region contain some of the most continuous early and middle Eocene successionsin North America and remain a premier location for sedimentary sequences throughthe Wasatchian-Bridgerian boundary. The Pinnacles Buttes assemblage has produced a collection of over 1100 specimens (900 from the University Of Michigan Museum Of Paleontology and 200 from Western Michigan University) of comparable diversity to the Lostcabinian type section (Neumann et al. 2010, Van Regenmorter and Anemone 2008). Detailed descriptions of the fluvial and lacustrine facies from the Main Body of the Wasatch Formation and Tipton Tongue of the Green River Formation assist in understanding conditions of deposition, which led to high mammalian diversityin this area. Abrasion and weathering scales compare modes of accumulation in different facies. Measured sections provide an empirical basis to examine fluvial channel stacking and stratigraphic location of fossiliferous horizons.

STUDY AREA

The study area occurs in the South Pass area of west central Wyoming, on the northeastern margin of the Green River Basin. South Pass forms a 40km (25 mile) pass from the southern edge of the Wind River Range to the Rock Springs Uplift, at the northwest corner of the Great Divide Basin. The study area occurs within the Jack Morrow Hills region, which encompasses fossiliferous strata of the historic Oregon Buttes, Pacific Butte and Continental Peak landmarks (Fig. 3.1). This area also extends southwestward into the basin to include the Pinnacles Buttes and Red's Cabin Monocline areas (Fig. 3.2).

The Oregon, California and Emigrant Trails, which provided conduits for early emigration across the continental United States to the western states region, traverse through South Pass, allowing for geographical and geological exploration since the early 19th century (Zeller and Stephens 1969). Expeditions by Fremont from 1842-1844 may have been the first published geologic endeavors through this area (Fremont 1845a, 1845b, 1848). Endlich (1879) and the expedition party of 1877 were assigned the Sweetwater district (41.75 to 43° N, 107 to 109.5° W) which included Steamboat Mountain, Oregon Buttes, Continental Peak and the central and east Great Divide Basin. Additional maps and geologic descriptions of South Pass and the surrounding areas were produced during expeditions to the northern Green River Basin by Endlich (1879), Nace (1939), Bradley (1964), Zeller and Stevens (1969) and Roehler (1992, 1993).

The present study area occurs in the Pinnacles area on the southwestern margin of the South Pass study area. The Pinnacles comprise a co llection of isolated buttes located in the northern Red Desert Basin about 20 miles south of the foothills of the Wind River Mountains and 22km (13 miles) southeast of Continental Peak. The Red Desert resides in the northern corner of the Great Divide Basin, an endorheic intramontane basin. Snowmelt and sporadic summer rains are responsible for a majority of the precipitation in the Red Desert (only 20 cm/yr White et al. 1989) and whatever water accumulates here is readily evaporated. The elevation, desiccation and wind compose a modern aeolian environment and landscape of mesas, pinnacles and buttes. Scarce vegetation allows for exposed butte faces in some areas where. Windblown sediments shed

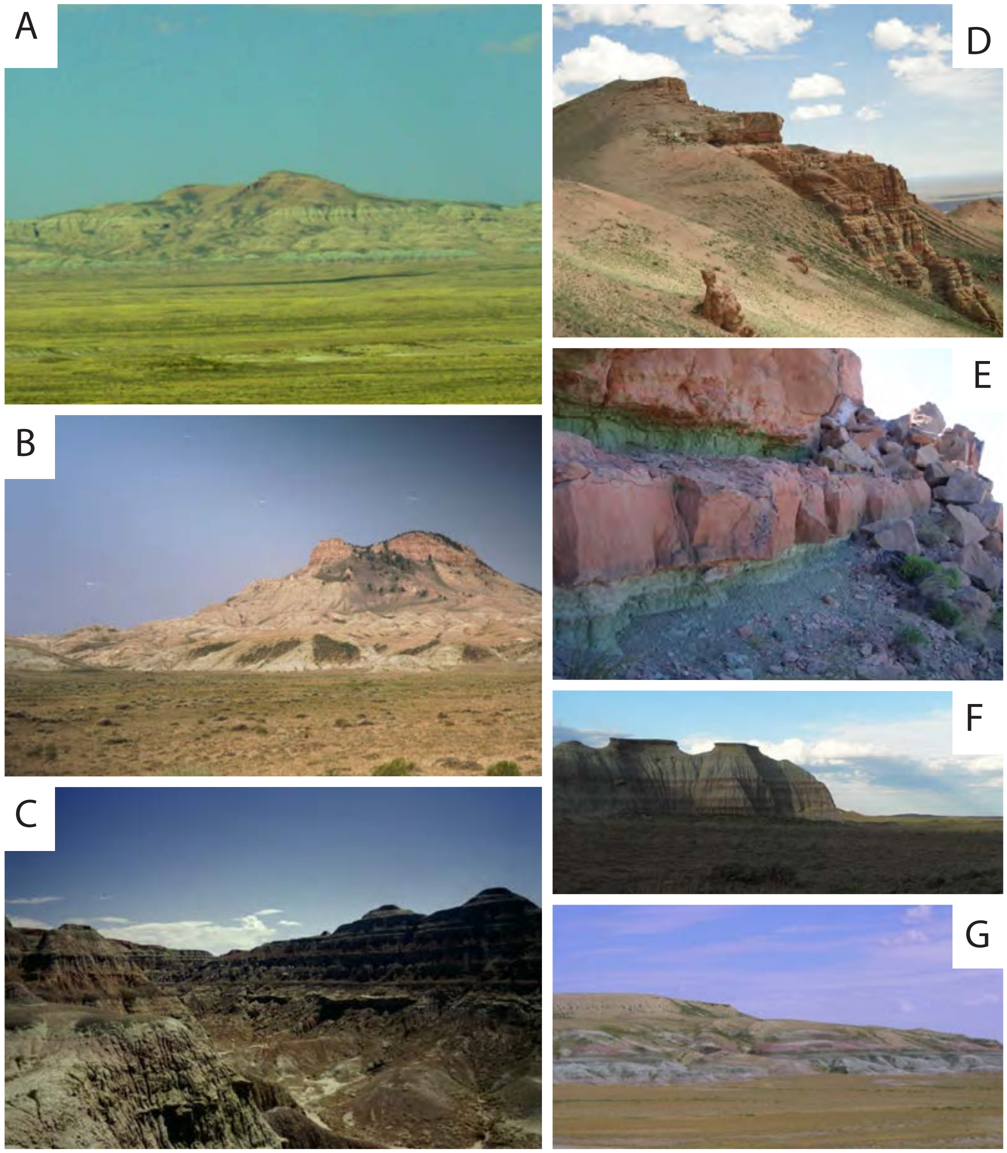

Figure 3.1 - Representative outcrop photographs of Early Eocene sediments at South Pass. A: Continental Peak section showing the Wasatch, Green River and Bridger Formations. B: Oregon Buttes showing the Wasatch, Green River and Bridger Formations C: Cathedral Bluffs member at Honeycomb Buttes. D-E: Alterations of red and green sediment of the upper Bridger Formation, Continental Peak. F: Cathedral Bluffs member at the base of Oregon Buttes. E: Cathedral Bluffs member and Laney shale at Bush Rim.

from thick (5-9m) sandstone deposits are abundantly fossiliferous, with occurrences of *in situ* bonebeds. The badlands erosion in this area provides an exposed section of the upper Main Body of the Wasatch Formation through the base of the Tipton Shale.

The region is divided into sixteen individual conical buttes (Fig. 3.3). A northern cluster of four buttes (Fig. 3.4), where sections 1001, 1101, 1102 and 1103 were measured, is also the location of the collecting sites SP 75, 74, 147, 183 and 191 (Fig. 3.5). To the south lies the main Pinnacles butte 13 surrounded by four isolated buttes, where the anthill locality SP 136 is found (Fig 3.7). Buttes 5-9 comprise the east Pinnacles (Fig. 3.6) where sections 1104 ABC and 1105 ABC were measured and also the location of collecting sites SP 165, 125, 189, 190 and 192 (Fig. 3.5). Across Alkali Draw, the west buttes 15 and 16 are the location of sections 1106 AB and the site of SP 124. The top of butte 16 contains a thick outcrop of Scheggs bed and is also a prime location for collecting stromatolites and other invertebrates. The Tipton shale caps many of the buttes and is best exposed on butte 13 and 16. The face of this Tipton bench shows a sequence of paleosols, sand and paleosols, overlain by limestone and shale.

The vertical succession in South Pass (Fig. 3.8), from oldest to youngest formation, is as follows: Main Body Member (Wasatch), Tipton Member (Green River), Cathedral Bluffs Member (Wasatch), Laney Member (Green River), Bridger and Arikaree formations (Gunnell and Bartels 2001). Wasatch, Green River and Bridger were defined in Hayden's (1869) USGS report of the Territories and further examined by Roehler (1992). The fluvial Wasatch and Bridger formations consist of sandstone and mudstone beds overprinted by red, green or grey paleosols. Thinly bedded limestone, evaporites and lacustrine shale of the Green River Formation attribute to the characteristic bench topography atop the Pinnacles and Honeycomb buttes. Trangressional phases of the Green River Formation (Laney, Tipton and Lumen Members) interbed with the Wasatch and Bridger formations, interpreted as expansion of lacustrine environments into the

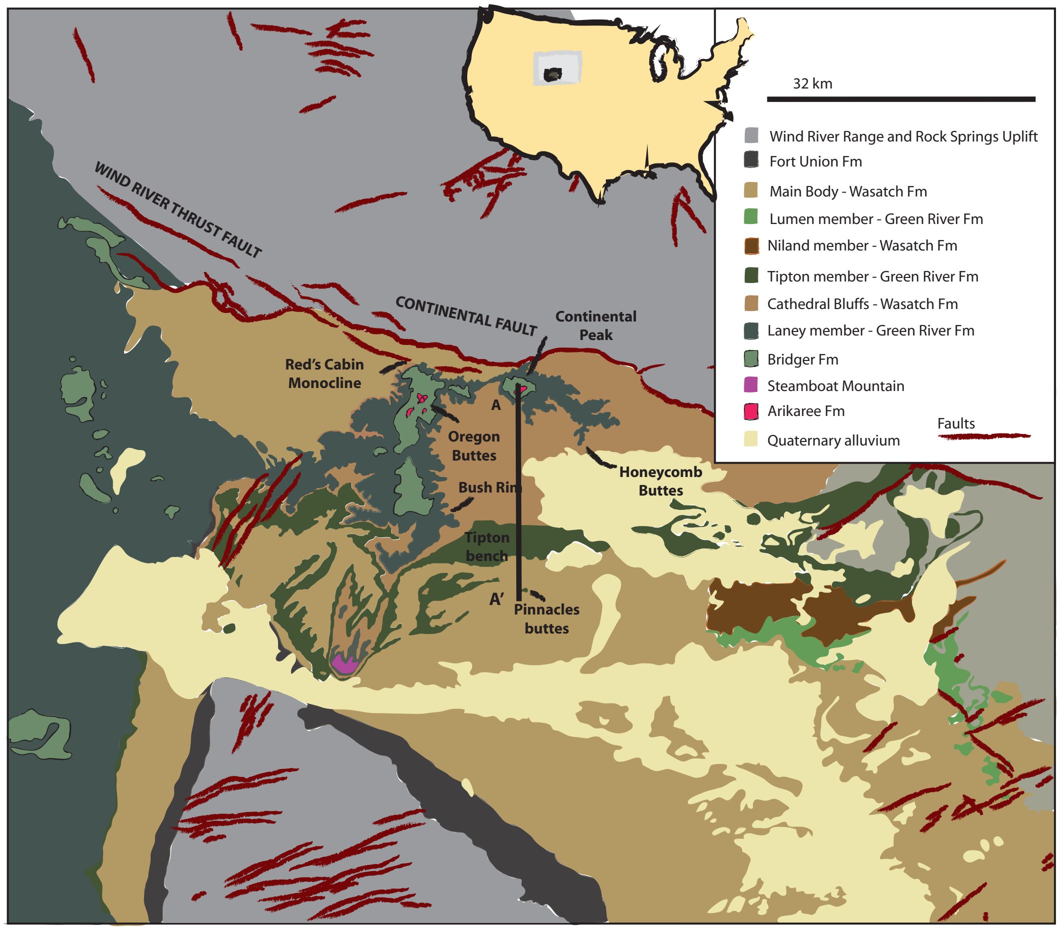

Figure 3.2 - Geologic map of the North-central Green River Basin, modified from Love and Christensen (1985). The South Pass Paleontological Field Area includes Oregon Buttes, Red's Cabin Monocline, Continental Peak, Bush Rim, Honeycomb buttes and the Pinnacles buttes.

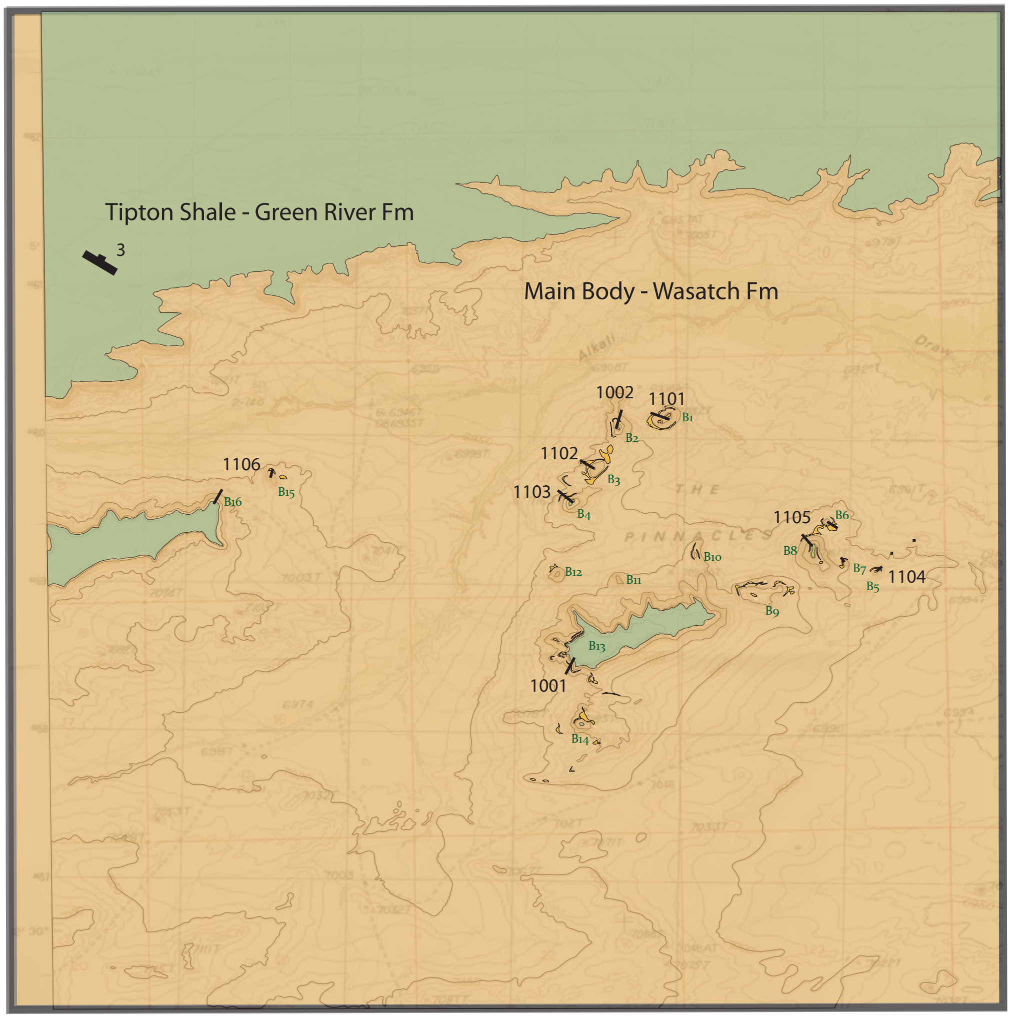

Figure 3.3 - Topographic map of The Pinnacles buttes, surrounding area and contact between the Main Body and Tipton Members. Sections and buttes are numerically labeled. Extent of golden sandstone bodies are outlined in yellow and appear at the 7020-7040 ft level.

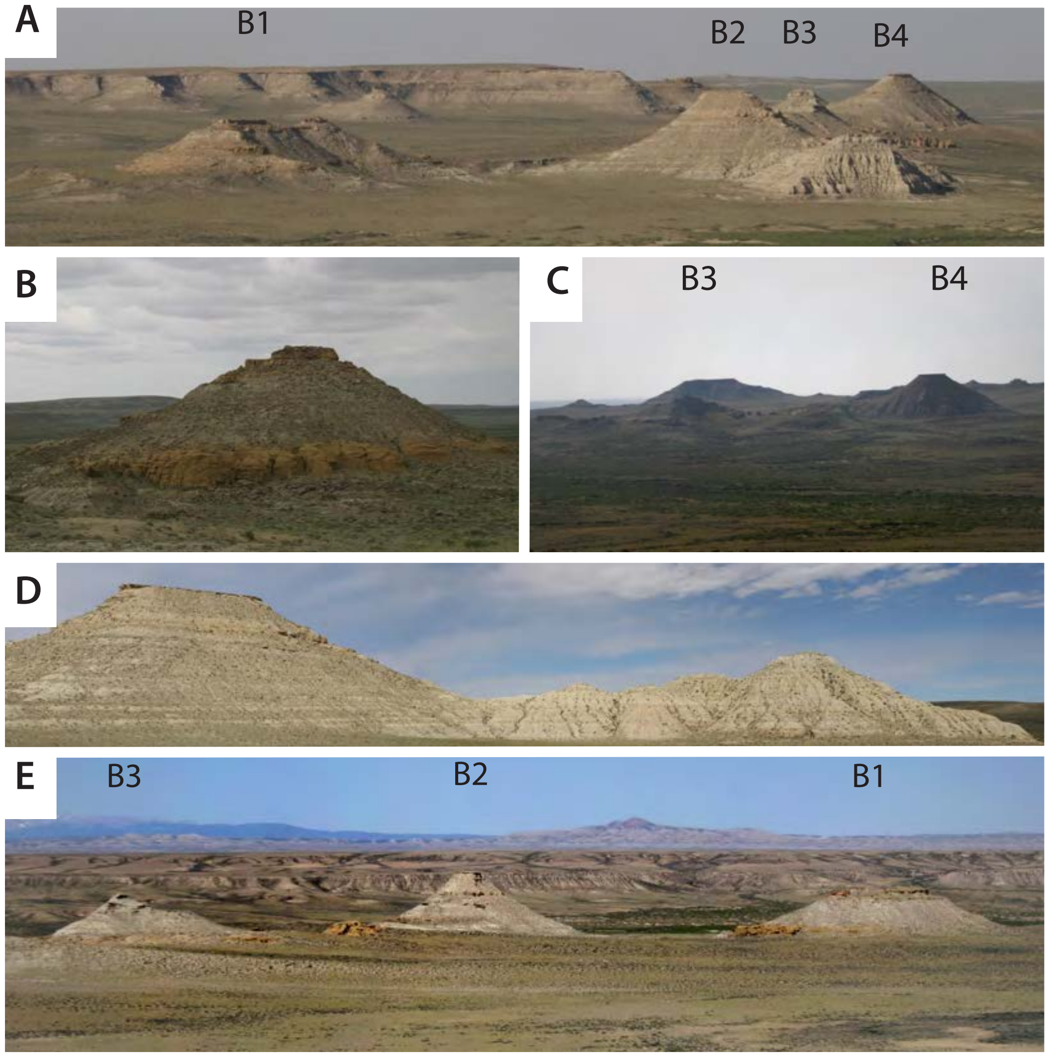

Figure 3.4 - North Pinnacles buttes. A: North face of the buttes. B: south face of B1 at section 1101. C: west face of B3 at section 1102 and B4 at section 1103. D: east face of B2 at section 1001 E: south face of buttes.

northern basin margin during the early and middle Eocene. Shifting depositional settings causes the Green River Formation to appear twice as the Tipton and Laney shale units are separated by fluvial units of the Cathedral Bluffs member. The Bridger Formation, a relatively thick fluvial-volcanoclastic unit, outcrops in South Pass along Oregon Buttes and Continental Peak, consisting of the section beneath an Eocene-Miocene unconformity. The Bridger Formation at Continental Peak consists of several repeating beds of green and red mudstones. Vertebrate localities at Continental Peak are known within 10m of the Bridger-Arikaree contact. *Omomys carteri* (field expedition 2008), perrisodactyl, crocodilian teeth, *Xestops sp.* and turtle remnants have been recovered from green horizons in the uppermost localities on this summit (Fig. 3.1). The peach colored tuffaceous sandstone of the Miocene age Arikaree Formation outcrops at the summit of Continental Peak and Oregon Buttes. White ash layers are visible within the Arikaree at Oregon Buttes from a distance, also noted by Zeller and Stevens (1969).

The deposits of South Pass are considered basin margin based upon proximity to the Continental Fault of the Wind River Range, relative immaturity of the sediment and occurrence of unusual faunal elements (Bartels and Gunnell 2001). This succession represents a fluctuating fluvial-lacustrine environment in the northeastern corner of the Green River Basin during the Wasatchian and Bridgerian. Eocene strata in South Pass provide a continuous biostratigraphic sequence from the late Wasatchian (Wa7) through the middle to Upper Bridgerian (Br2 or Br3) (Fig. 3.8). The Main body of the Wasatch Formation is the base of the exposed stratigraphic section in the Pinnacles study area and is confidently identified as Lostcabinian (Wa7) based on the occurrence of *Lambdotheriam popoagicium* and *Loveina zephyri* (see chapter 2). Also *Palaeanodon, Copeleumur, Loveina, Mensicotherium* and *Heptodon* all have a last appearance in the late Wasatchian while *Antiacodon, Orohippus, Trogoleumur, Artimonius* and *Northarctus,* (Woodburne et al. 2009) first appear in this time with the overlapping ranges of these taxa confirming the age assignment. Other taxa recovered at the Pinnacles such as *Artimonius, Cantius, Paramys, Hyracotherium* and *Diacodexis* are listed as common in Lostcabinian assemblages by Gunnell et al. (2009).

METHODS

Lithofacies analysis – This study is based on joint University of Alberta – University of Michigan – Albion College field investigations conducted between 2007 and 2011.The vertebrate collection from the Pinnacles buttes was assembled during collecting seasons between1999 and 2011 resulting from surface prospecting at all horizons. Most of the fossils in the collection were collected from localities at the bases of the buttes and anthill collecting assisted in prospecting for fossiliferous horizons. Some localities occur in fine-grained paleosol horizons such as SP 74, SP 183 or 165 in part; other localities occur in, or adjacent to, gold-colored sandstone beds.

Thirteen individual sections were measured at six fossiliferous localities in The Pinnacles area (Figure 4). Strata were measured with a standard 1.5m Jacob's staff and Brunton field compass. Most of the sectionswererelatively well-exposed although fine-grained intervals were characterized by up to 30 cm of cover. Lithology, grain size, sorting, sedimentary and biogenic structures, weathering pattern and color were recorded and facies were recorded.

Correlations between sections utilized the contact between Green River and Wasatch formations as a datum as this surface is interpreted to be a regionally consistent lacustrine flooding surface. Incorporated outcrop data and photographic mosaics were used to correlate individual beds. Color was used as a basis to distinguish paleosol horizons where extensive banding can be seen in outcrop. Some color horizons are clearly visually correlatable between different buttes using high-resolution photographs. Sections 1001, 1002, 1103, 1105C, 1106B are correlated by the Wasatch and Green River contact. GPS location, elevation and

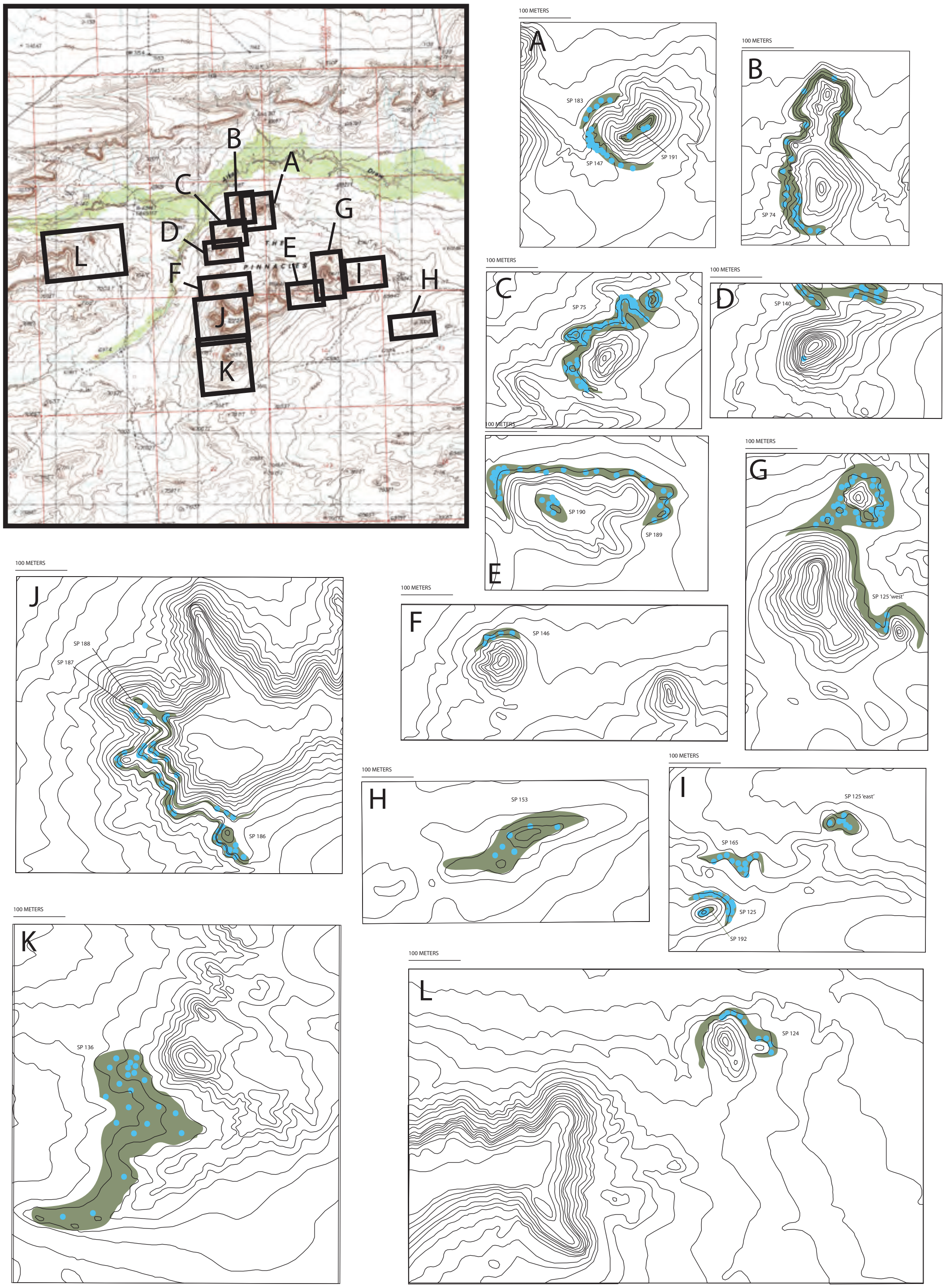

Figure 3.5 - Reference of Pinnacles localities and fossil occurrence. A: SP 183, 147, 191. B: SP 74. C: SP 75. D: SP 140 E: SP 189, 190. F: SP 146. G: SP 125 'west'. H: SP 153. I: SP 165, 165 'east', 125, 192. J: SP 186, 187, 188. K: SP 136. Blue dots show relative distribution of vertebrate fossils and green areas indicate general boundaries of the indicated locality.

satellite photos were used to correlate sections without a preserved Green River-Wasatch contact.

Sediment was sampled at 50 cm intervals in sections 1101, 1104, 1105; 1 m intervals in 1106; and at lithologic boundaries in sections 1102 and 1103. Samples of clay-silt from selected horizons in sections 1101, 1103, 1104A, 1104B, 1104C and 1106B were powdered for mineralogical analysis. Overbank clay and silt samples were tested using X-ray defraction (XRD) to detect mineral composition.

Taphofacies analysis–Fossil vertebrate collections in the study area include individually catalogued specimens (identifiable to the level of genus) and 'misc' (miscellaneous) specimens which include all other bone material from a locality. Z misc samples were sorted based on weathering, element type and abrasion. Voorhies (1969) described three groups in which disarticulated elements are transported via hydraulic sorting. Voorhies Group I represents low density, easily transportable material such as ribs and vertebrae, Group II includes slightly more dense material and Group III represents the densest material such as teeth (Behrensmeyer 1975, Fiorillo 1988), skulls and jaws (Voorhies 1969, Fiorillo 1988). However in microvertebrate assemblages, size differences between element types differ wildly (such as a piece of turtle vertebrae vs a snake vertebra) and may not be the best indicator of depositional conditions. Abrasion stages are scaled from 0-3 (Fiorillo 1988, Hunt 1978). Stage 0 includes angular elements with sharp edges; stage 1 pertains to slightly abraded subangular elements; stage 2 includes well polished subrounded bones; stage 3 represents rounded and indiscriminable bones (Fiorillo 1988). The abrasion scale provides an estimate of level of transport which in turn can discern whether the assemblage is autochthonous. Both zmisc samples and the catalogue contain fragmented and whole bones. Photographs show the different proportions of abraded elements recovered from paleosol and channel localities.

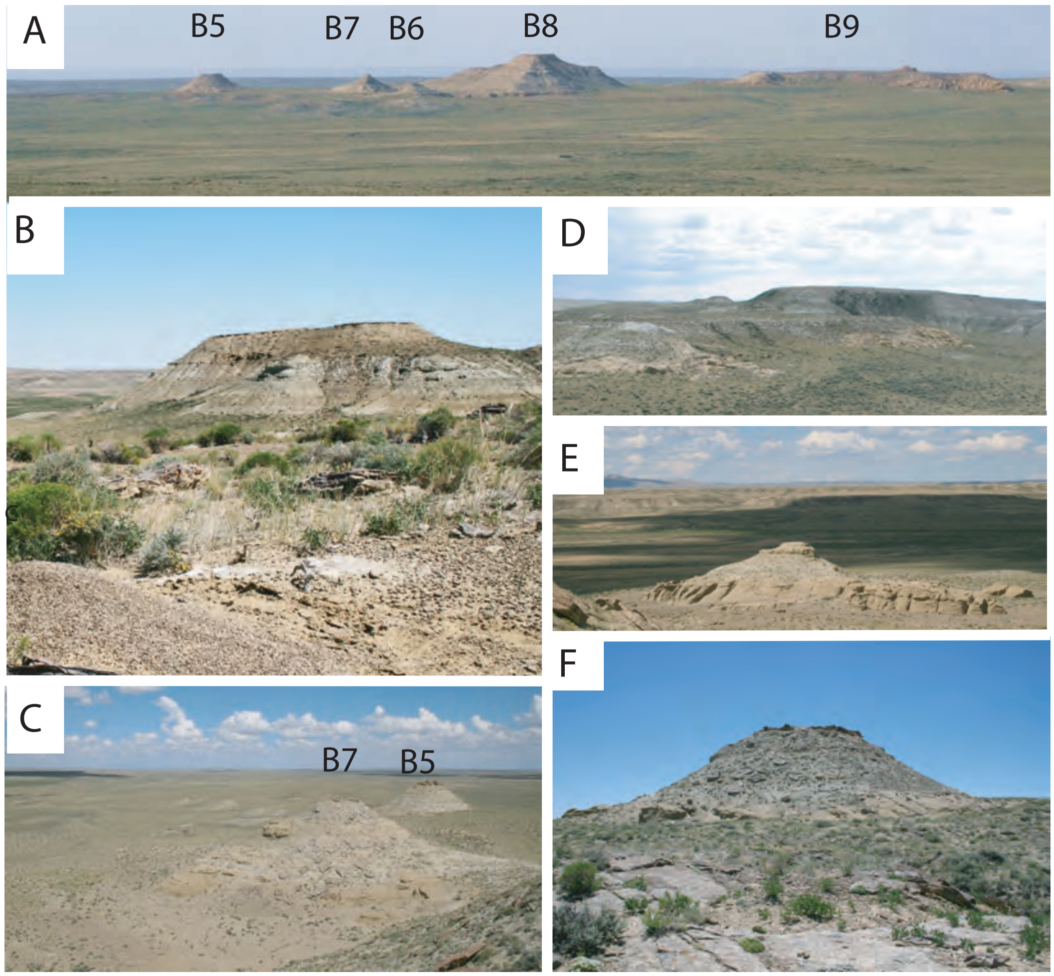

Figure 3.6 - East Pinnacles buttes. A: North face of the buttes B: West face of B8, at section 1105C C: West face of B7 at 1105B D: Golden sandstones at B9 or SP-189 E: South face of B6 at section 1105A F: North face of B5 at section 1104C

FLUVIAL AND LACUSTRINE FACIES

Sedimentary facies are mapable beds or suites of beds thatshare lithological, biological or ichnological characteristics which distinguish it from other beds and indicative of a distinctive depositional process. Facies are based off of objective non-genetic visual characters. The definition of a 'facies' has undergone debate, but the consensus of the term (Miall 1977, 1978, Hicken 1993) is a description of bedform level lithologies and textures with similar characteristics. Classification abbreviations of the lithofacies reflect those in outcrop but are inspired from Miall (1996) and Keighley et al. (2003).

Fluvial facies models have undergone significant revision since Allen's (1964, 1965) original fining upward model. Architectural element analysis, described in Miall (1985, 1988) remains an essential component in describing fluvial deposits (Hicken 1993). Miall (1985) discussed problematic fluvial facies are derived when methodology and interpretation relies heavily on vertical profiles and lacks independent controls on grain size and channel morphology. Miall (1985) iterates that three-dimensional characters are absent if facies are based exclusively on vertical succession. Miall (1985) also outlined constraints on scale which were described in Jackson (1975) such as microforms, mesoforms and macroforms are used to delineate first, second and third order surfaces. Fluvial system architectural elements include overbank fines, lateral accretions bedforms, sandy sheets, channels (vertically aggregating), gravelly bars, laminated sand and sandy bedforms (Miall 1985). The lateral form in Table 1 is described as either lenticular, lense, tabular or sheet (Fig. 3.9). The combinations of this terminology is scale dependent – for instance, a unit can consist of first order cross bedded lenses in a tabular or lenticular shaped complex. Facies models for carbonate lakes (Platt and Wright 1991) including Eocene Lake Uinta, are discussed in Keighley et al. (2003), Cole and Picard (1978), Tanavsuu-Milkeviciene and Sarg (2012). Buchheim et al. (2000), Carroll and Bohacs (1999), Smith et al. (2008) discussed lacustrine facies of the Lake Gosiute.

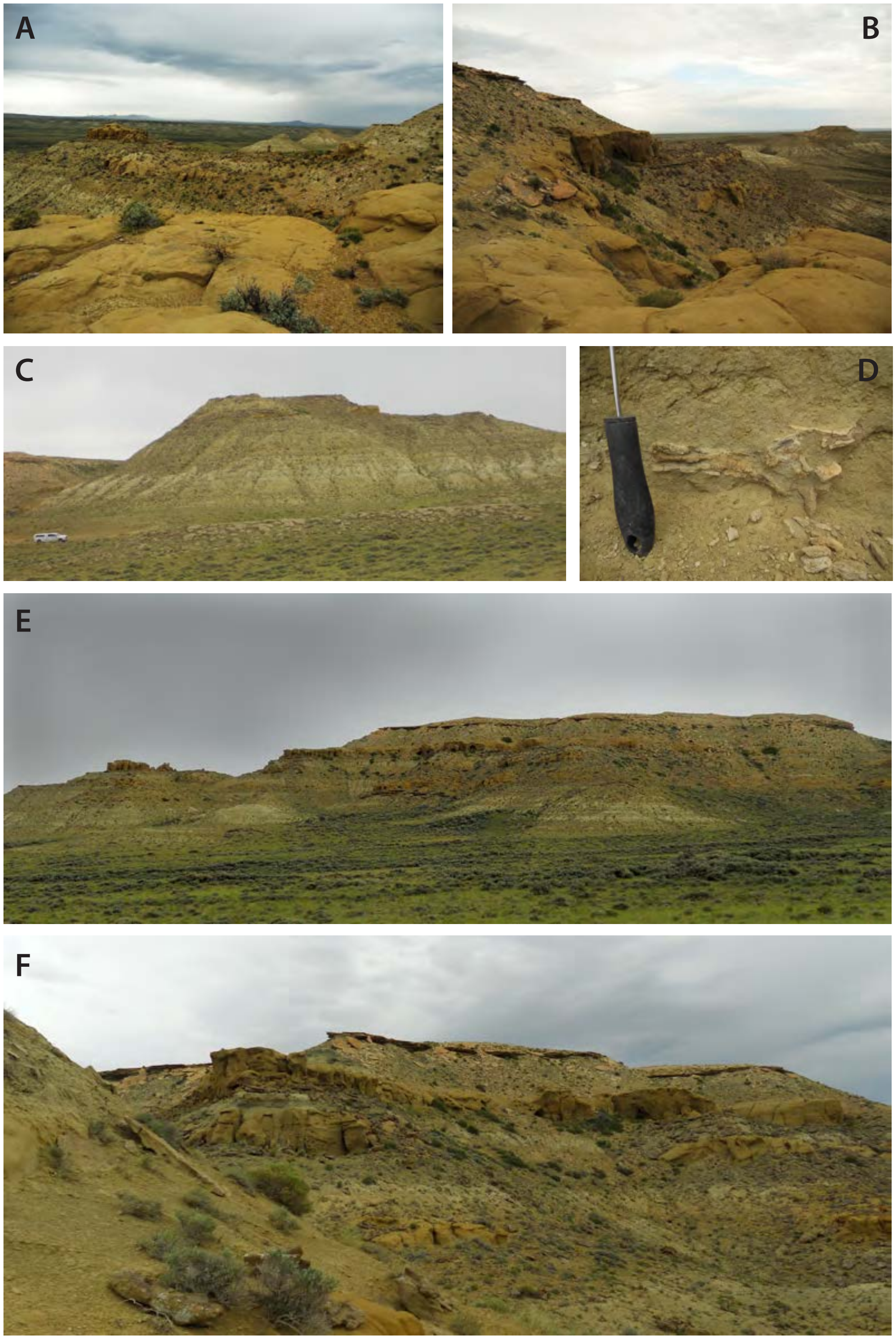

Figure 3.7 - South Pinnacles buttes. A-B: Southwest and southeast face of the butte 13 taken from top of highest lenticular sandstone C: west face of B14 D: Crocodile skull in mudstone below lowest lenticular sandstone E-F: south face of butte13 at section 1002

Table 3.1. Facies descriptions of various lithologies in The Pinnacles section. Lithologic names based on Folk's (1974) classification of clastics and Dunham's (1962) classification of carbonates.

FACIES	LITHOLOGY	SEDIMENTARY STRUCTURES	BIOGENIC STRUCTURES	LATERAL FORM	FOSSILS
Pgv	Siltstone; green variegated, grey horizon at top	pedogenic slicken-sides, hydromorphic mottling, calcrete nodules, ovular peds	-	Continuous; extends from section 1104B to 1102, tabular to sheet shaped	Biofacies 1; localities 165, 125; very high abundance
Pgg	Siltstone-claystone; green, grey and brown	Massive to bedded	-	Continuous; tabular shaped	Fragmented unident. Amniote; low abundance
Fc	Claystone; blue, grey, brown or green	Massive to laminated, <1m overall thickness	-	Constrained; tabular shaped	Fragmented unident. Amniote; low abundance
Gom	Monomictite orthoconglome rate; 9-14cm green clay clasts, quartz sand matrix	Parallel bedded to planar cross bedded, imbricated clasts	-	Continuous; tabular to sheet shaped, up to 1km	Biofacies 1; localities 165, 125; high abundance
Goo	Oligomictite orthoconglome rate; 0.5-2cm green clay quartz and chert clasts, quartz sand matrix	Trough crossbedded, parallel bedded, imbricated clasts, current ripples	-	Constrained; lense shaped, channelized	Biofacies 1; Localities 165,125; high to moderate abundance
Sqt	Quartz arenite andstone; medium to coarse, mica lithics, clean	Parallel bedded, current ripples, climbing ripples	Vertical unlined tube traces	Continuous; tabular to sheet shaped, up to 1km	Biofacies 1; localities 75, 147,125, 189; high abundance
Sstx	Sublitharenite sandstone; medium to coarse, mica and chert lithics, muddy matrix	Trough cross bedded, imbricated clasts, heterolithic cross beds (biotite/sand), cross bedded mudclasts	Unlined branching, unlined vertical and branching, root casts, iron concretions, meniscate burrows	Constrained; lenticular shaped scours, vertically stacked	Biofacies 1; localities 74,75, 124, 125, 136, 147, 187, 188, 189; very high abundance

Sspx	Sublitharenite sandstone; medium to coarse, mica and chert lithics, muddy matrix	Planar cross bedded to rippled	-	Constrained; lenticular to tabular shaped	Biofacies 1; localities 74,75, 124, 125, 136, 147, 187, 188, 189; very high abundance
Sst	Sublitharenite sandstone; medium to fine, mica lithics, muddy matrix	Massive to bedded, rippled	-	Continuous; lobe to sheet shaped	Low to no abundance
Svf	Sandstone; very fine	Massive	-	Continuous; lobe to sheet shaped	Low to no abundance
Ssm	Sublitharenite sandstone to siltstone; mica lithics, grey	Massive, boulbous weathering pattern, >1m thickness	-	Continuous; lobe to sheet shaped	Low to no abundance
Sqc	Quartz arenite sandstone; fine to coarse, clean	cross beds, rippled	-	Constrained; lenticular to tabular shaped scours, variable thickness	Biofacies 2
Smr	Sandstone and micrite; fine to medium	Laminated, lentincular beds of sand with silty drapes, rippled	-	Constrained; lenticular to sheet shaped	Fragmented gastropod and mollusk shells, moderate to low abundance
Lohx	Grainstone to packstone; 0.1-4cm fossil clasts and ooids	crossbeds, parallel beds, rippled	-	Continuous; tabular to sheet shaped	Biofacies 2
Lbm	Micrite; white	Parallel bedded	Trail traces	Continuous; sheet shaped	Fragmented invertebrate, low abundance
Fpsh	Micrite shale; white to grey	Parallel bedded to laminated, papery	-	Continuous; sheet shaped	Low to no abundance of macroinvertebrates
Fosh	Carbonaceous shale; black, brown and grey	Parallel bedded to laminated	-	Continuous; sheet shaped	Low to no abundance of macroinvertebrates

Each unique lithology and architectural form in the study interval has been assigned to a lithofacies. The sandstone facies are separated into golden muddy coarse sandstone, coarse quartz rich tabular sheets, quartzose sandstone and various grey to tan micaceous silty sandstone units. Clay and silt facies are described on the basis of color and composition. Calcareous facies include fossiliferous limestone, calcareous siltstone, and algal interbedded carbonaceous shale. Facies characteristics of the study area are summarized in Table 1.

FACIES ASSOCIATIONS

FA1 - Mud-dominated distal floodbasin/alluvial plain - The floodbasin and alluvial plain association includes green-variegated paleosol (Pgv), green-grey paleosol (Pgg), tabular silty sand (Ssm), massive clay (Fc).Brightly colored variegated green siltstone occurs at the base of sections 1104A and B, 1001 and 1002. This siltstone in sections 1104 A and B is overlain by Goo and Gom orthoconglomerates. Pgv siltstone is distinguished from other siltstone units by its striking green hue and pedogenic purples. Calcrete nodules and hydromorphic mottling are indicative of pedogenic maturity (Kraus 1999). Grey A horizons are occasionally exposed (Fig. 11). Green siltstone at this stratigraphic level is also highly fossiliferous with *in situ* Biofacies 1 taxa including *Lambdotherium popoagicum*. Chrome-green siltstone and claystone underlie the lowest stacked sandstone lenses at sections 1001, 1002 and 1104ABC. Evidence of pedogenesis, mudcracks, bioturbation (*Thalassinoides, Glossifungities, Skolithos*-type traces) (Fig. 3.10) and calcrete nodules are observed. Punctuated parallel bedded to rippled sands are interbedded with the green siltstone. *Thalassinoides*-like branching traces occur in siltstone deposits underlying the second stacked channel sandstone at section 1002 (Fig. 3.10). The FA1 unit is generally mud dominated with approximately 15% sand beds.

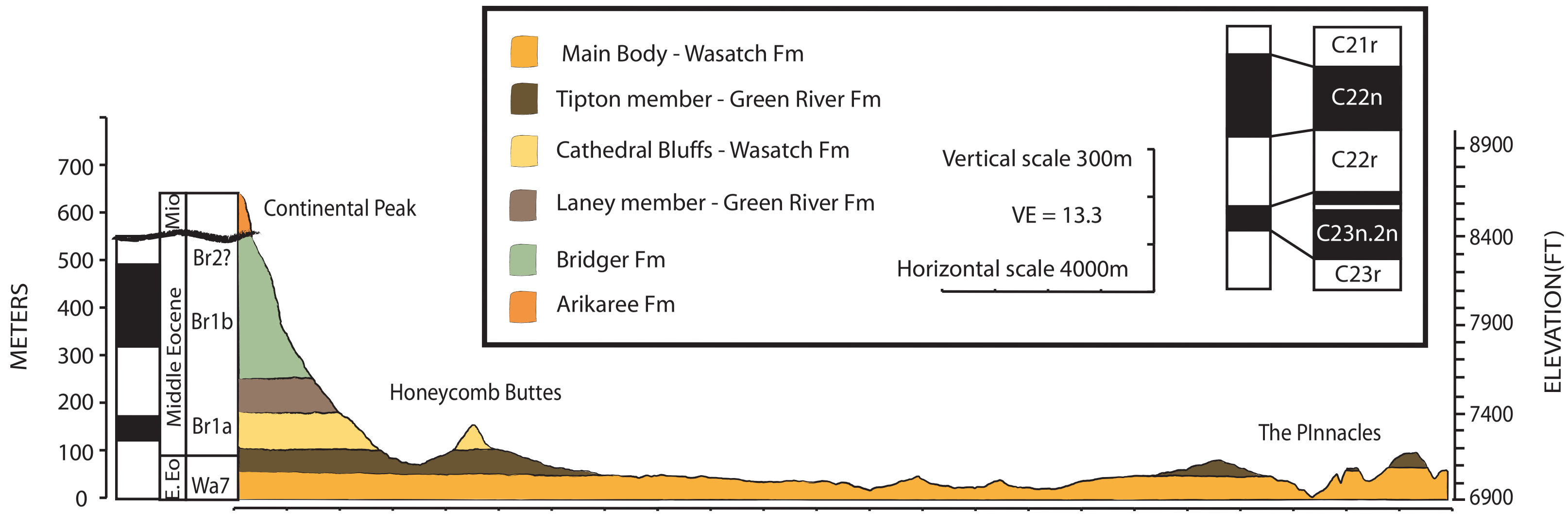
METERS
700
600
500
400
300
200
100
0
Mio
Middle Eocene
E. Eo
Br2?
Br1b
Br1a
Wa7
Continental Peak
Honeycomb Buttes
The PInnacles
Main Body - Wasatch Fm
Tipton member - Green River Fm
Cathedral Bluffs - Wasatch Fm
Laney member - Green River Fm
Bridger Fm
Arikaree Fm
Vertical scale 300m
VE = 13.3
Horizontal scale 4000m
C21r
C22n
C22r
C23n.2n
C23r
8900
8400
7900
7400
6900
ELEVATION(FT)

Figure 3.8 - A-A’ Cross section of South Pass stratigraphy from The Pinnacles to Continental Peak. Biostratigraphy modified from Gunnell and Bartels (2001) and projected chonologic correlation based on results by Clyde et al. (1997, 2001) and Tsukui and Clyde (2012). Measurements from South Pass show the Cr23n interval to occur in the Cathedral Bluffs member and the Cr22n interval begins less than 100m from the base of the Bridger Formation (Clyde et al. 2001). Based on measurements by Tsukui and Clyde (2012) the top of the Bridger Formation at Continental Peak was deposited during Cr21r.

Table 2.2. XRD summary of selected claystone and siltstone samples selected from sections 1104B, 1104C, 1104A, 1101, 1102, 1103, 1106. Measurements represent level the sample was collected from in each section. Specific bed the sample belongs to is indicated on sections, see Appendix.

Section	0.2m - Green silt	4.78m - Green Clay			
1104A	Quartz Ankerite Calcite Clinochlore Muscovite Orthoclase Albite	Quartz Clinochlore Orthoclase Albite Phengite			
1104B	0.0 - Green Silt-clay	5.75 - Green clay	7.75 - Sand-silt		
	Quartz Ankerite Calcite Clinochlore Muscovite Orthoclase	Quartz Calcite Clinochlore Orthoclase Albite Phengite	Quartz Muscovite Albite Clinochlore Orthoclase Calcite Dolomite		
1104C	5.50 - Grey silt	12.08 - Blue clay	20.0 - Green silt-clay		
	Quartz Muscovite Clinochlore Orthoclase Calcite Albite	Quartz Clinochlore Muscovite Albite Orthoclase Gypsum	Quartz Muscovite Nontronite Albite Anorthite	Quartz Muscovite Albite Clinochlore Dolomite Calcite Orthoclase	
1101	3.0 - Green silt	3.75 - Mottled horizon Green silt	7.0 - Grey silt	22.6 - Green grey silt-clay	25.25 - Grey clay
	Quartz Calcite Clinochlore Muscovite Orthoclase Albite Dolomite	Quartz Clinochlore Orthoclase Albite Beldellite Muscovite Anorthoclase	Quartz Muscovite Orthoclase Albite Clinochlore	Quartz Muscovite Clinochlore Orthoclase Dolomite	
1103	7.5 - Yellow green clay	23.0 - Green grey silt	43.65 - Blue-yellow clay		
	Quartz Muscovite Albite Clinochlore Orthoclase	Quartz Muscovite Albite Clinochlore Orthoclase Ankerite Beldellite	Montmorillonite Quartz Muscovite Orthoclase Albite		
1106B	1.0 - Green grey clay-silt	6.0 - Green grey clay	21.0 - Grey silt-clay		
	Quartz Calcite Clinochlore Muscovite Orthoclase Albite Dolomite	Quartz Muscovite Clinochlore Ankerite Orthoclase Albite	Quartz Muscovite Albite Clinochlore Dolomite Calcite Orthoclase		

Paleosol horizons are thicker and brightly colored (blue, grey, green, orange) to the southeast while the northwest have numerous alternations of sandstone and siltstone beds with thinner, drab-colored beds (Fig. 3.4B and 3.6B). Thickness of the paleosol is proportional to the amount of time allotted before burial and distance from an active stream (Kraus 1999). Thick paleosols develop on distal floodplain siltstone or claystone (Fig. 3.6B). Thin sheets of sandstone and siltstone (Fig. 3.4B) and poorly develop colors indicate episodic deposition and proximity to the stream (Kraus 1999).

Roehler (1993) described two distinct color patterns in the Main Body of the Wasatch Formation in the Green River Basin; red or variegated paleosols and grey or green paleosols. The red hues indicate oxidation of iron induced by well-drained conditions and grey or greens by the reduction of iron in saturated soils (Roehler 1993). The greenish nature of the fine sediment at the Pinnacles is also suggestive of proximality to area of Niland and Lumen deposition (Fig. 3.12) The clay in fine-grainedPinnacles lithologies consists of high amounts of quartz, clinochlore, muscovite and feldspar (Table 2). Carbonate lithics such calcite, dolomite and ankerite were also detected, which may be explained by the development of calcrete nodules and the occurrence of Paleozoic carbonate strata in the fluvial source area. Fc claystone is generally well-compacted, occasionally fissile and orange weathering may or may not be present (Fig. 3.10). Claystone beds are generally thin but can also be up to a meter in thickness. Clay also deposits fromsuspension during overbank flooding in levee and floodplain environments. Thick sections of Fc mudstone are interpreted as channel fill if directly overlying fining upward Sstx and Sspx sandstone beds. Claystone is interbedded with Sqt quartz arenite and siltstone in section 1103.

FA2 - Sand-gravel based meandering streams - Trough cross bedded sublitharenite (Sstx), planar cross bedded sublitharenite (Sspx) and massive claystone (Fc) are associated with point bar accretion and channel avulsion. Accumulation of point bar sediments within the meandering system form first order planar and trough cross bed sets of cm (ripples marks) to 0.5m (dune forms) and second order meter scale cosets (Miall 1985). Third order surfaces (Miall 1985) are erosional at the base of the sandstone lense and gradational with overlying siltstone beds. The gradational upper surfaces may also be truncated by other channels forming multiple stacked lenses or interbedded with quartz sandstone beds of FA4.

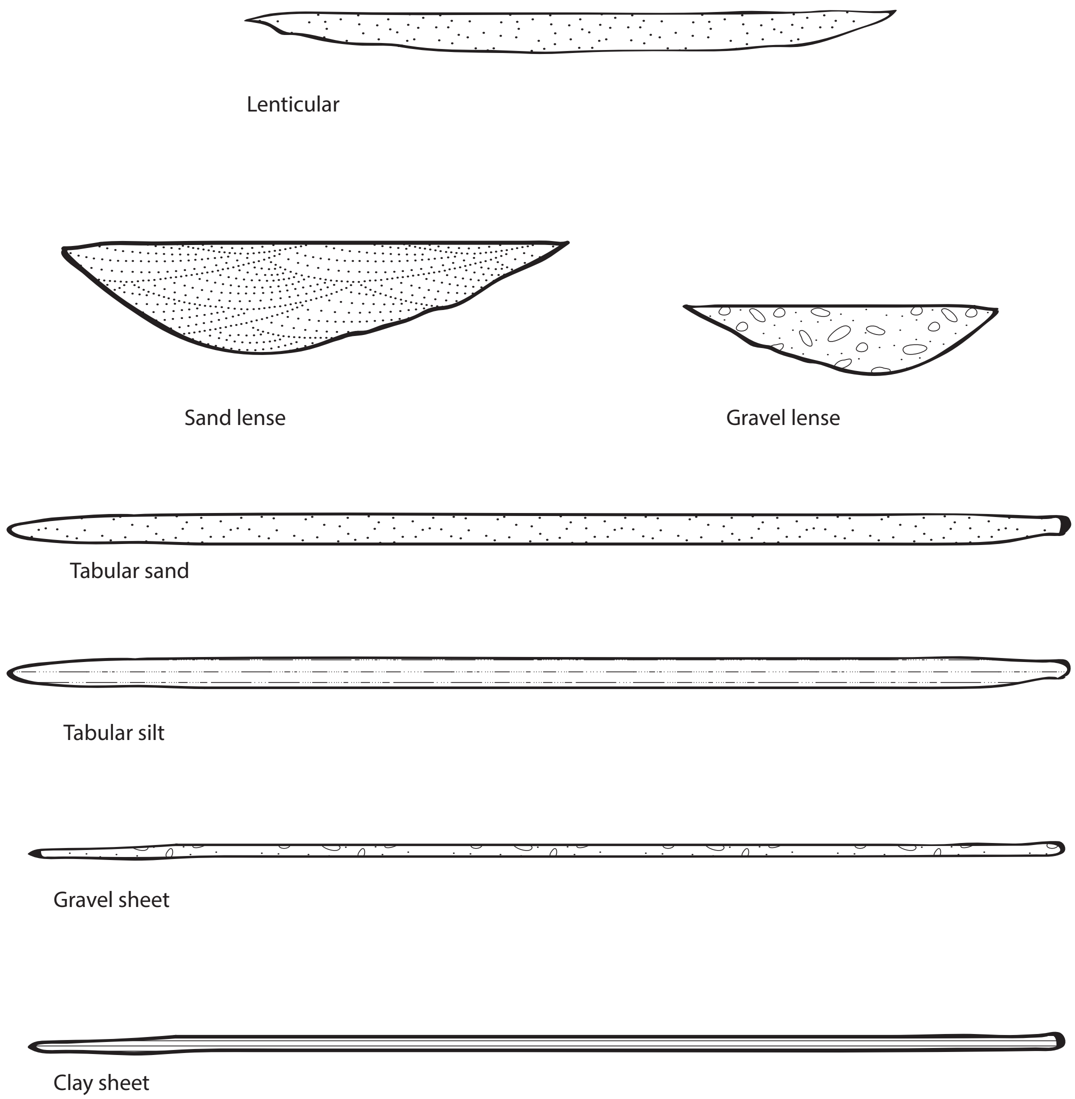

Figure 3.9 - Reference diagram of architectural forms for clay, silt, sand and gravel beds in the upper Main Body of the Pinnacles section.

Cross-bedded sublitharenite sandstone beds are golden-amber in color and biotite rich. Large-scale (0.1-1.0 m sets) cross-bedded biotite occurs within second order cosets in sandstone bodies at Sect 1105A (Fig. 3.13). Cross-bedded mudclast lenses occur within 1-2m of the base of the sandstone lense in Sect 1106A. Root traces and orange iron concretions are also common (Fig. 3.11). Crescent shaped burrows with thin meniscae, very similar to *Naktodemasis* described in (Smith et al. 2008b,c) occur at the top of the sandstone lense complex at section 147. Lined teardrop shaped burrows infilled with sand are observed at the base of the sandstone lenses at section 1105B and SP-189 (Fig. 3.11). The *Glossifungites* ichnofacies includes burrows produced on firmground surfaces, an indicator in marine settings for subarieal exposure and also used to demarcate sequence boundaries (Zonneveld et al. 2003). *Glossifungites*-like traces indicate compaction, burial and subaerial exhumation prior to infaunal activity and located at the base of channel complexes in fluvial settings (Zonneveld et al. 2003). The term *Glossifungites* surface is used conservatively as burrows below the fluvial channels in this study are restricted to isolated occurrences and not ubiquitous across a mappable surface.

Scours and irregularities are common in crossbedded cosets (Fig. 3.14) and truncate lateral accretion bedforms in the multistory complex. Chutes are typically crossbedd with a coarse bedload such as imbricated gravel (Fig. 3.14D, clay clasts (Fig. 3.14 E-F), or biotite (Fig. 3.13 D). These scours and chutes are composed of muddy sublitharenite to quartz arenite sandstone and may show various forms of differential erosion from the surrounding channel outcrop (Fig.3.14 C, D, G). Scours and chutes occur at sandstone outcrops from section 1101, 1106, 1105A and in highest frequency at 1102.

Multistoried sublitharenite lenses with erosional bases at the bottom of the sections show a maximum of 13 meters of incision. Thick (5-9m) isolated wedge-shaped bodies are similar to ribbon-bodied sandstones described by Kraus (1987).

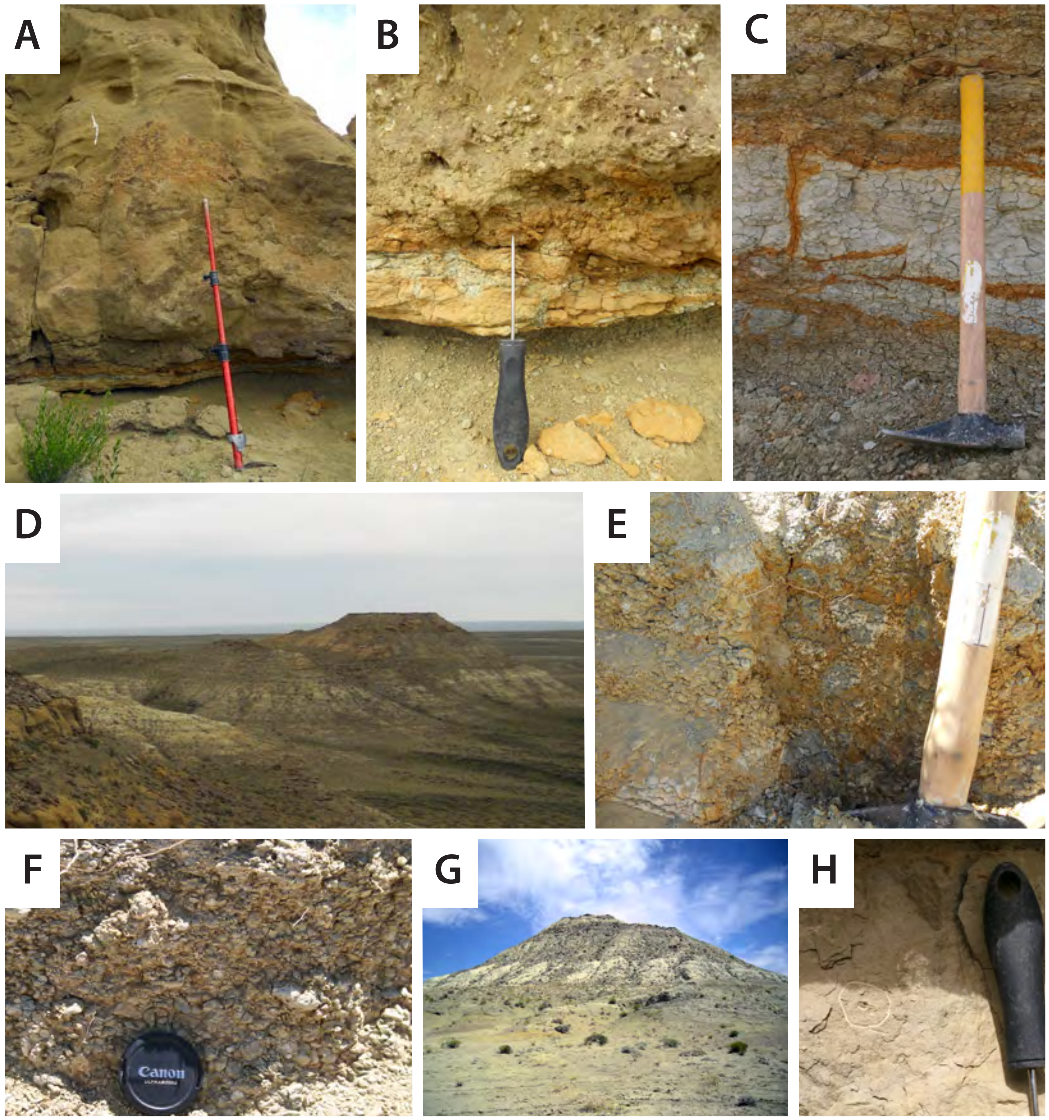

Figure 3.10 - Paleosol and floodplain associations. A-B: Laminated siltstone with branching trace. C: Blue siltstone with orange mottling in section 1104C. D: Thick grey horizon extending from butte 13 to 14. E: Grey claystone with orange mottles in section 1103. F: granular peds in green siltstone at section 1104B. G: Grey horizon at SP 136, butte 14. H: Inscisor in grey siltstone below a sandstone lense at SP 189.

Multistoried and vertically aggregating scours are interpreted by Kraus (1987) as laterally fixed distributary channels. Cross bedded sandstone bodies are also fashioned as laterally extensive lenticular belts. Lenticular sandstone outcrops from butte 13, section 1002 have first and second order surfaces identical to the ribbon bodied sandstone lenses, except with a lateral extent of 300-400 m. The lenticular sandstone bodies were deposited under dominantly laterally shifting (Kraus 1987) rather than vertically aggregating point bars. Ori (1982) developed width and height thresholds for vertical and lateral accretion, in which lateral accretion was dominant if the ratio of width divided by height was greater than 15. Vertical aggradation dominated under ratios of less than 7 (Ori, 1982). Lenticular and lense type sand complexes suit Ori's criteria for lateral accretion.

Laterally extensive and constrained sandstone complexes occur along three horizons measuring up to the base of the Tipton shale. In Sect 1002, butte 13, three stacked sandstone units are well exposed and separated by roughly 1.5-3m of Fgg siltstone-claystone. Upper and lower sandstone complexes on butte 1, 3 and 5 (sections 1101, 1102, 1104C) correlate to the second and third lenticular outcrop. Evidence a lower sandstone complex below the first sheet exists at SP 153 (Fig. 5) where only the top 1-2 meters of the complex is exposed.

Several of the sandstone bodies that occur at the base of each sections 1101, 1001, 1102, 1103, 1002, 1105ABC, 1106A and 1104C, contain microvertebrate fossils of Biofacies 1. The assemblage of taxa includes *Lambdotherium popoagicum*, *Microsyops, Cantius* and *Hyopsodus* at high frequency.

FA3 - *Levee* - Very fine sandstone (Svf), tabular sublitharenite sandstone (Sst) and green grey siltstone (Pgg) are associated with levee progradation.Grey to brown silt form cm scale interbeds with thinly-bedded, very fine to fine-grained sandstone. Sandstone belonging to this facies lack of significant cross-bedding (though ripples may be present) and possess a yellow, tan or grey color instead of

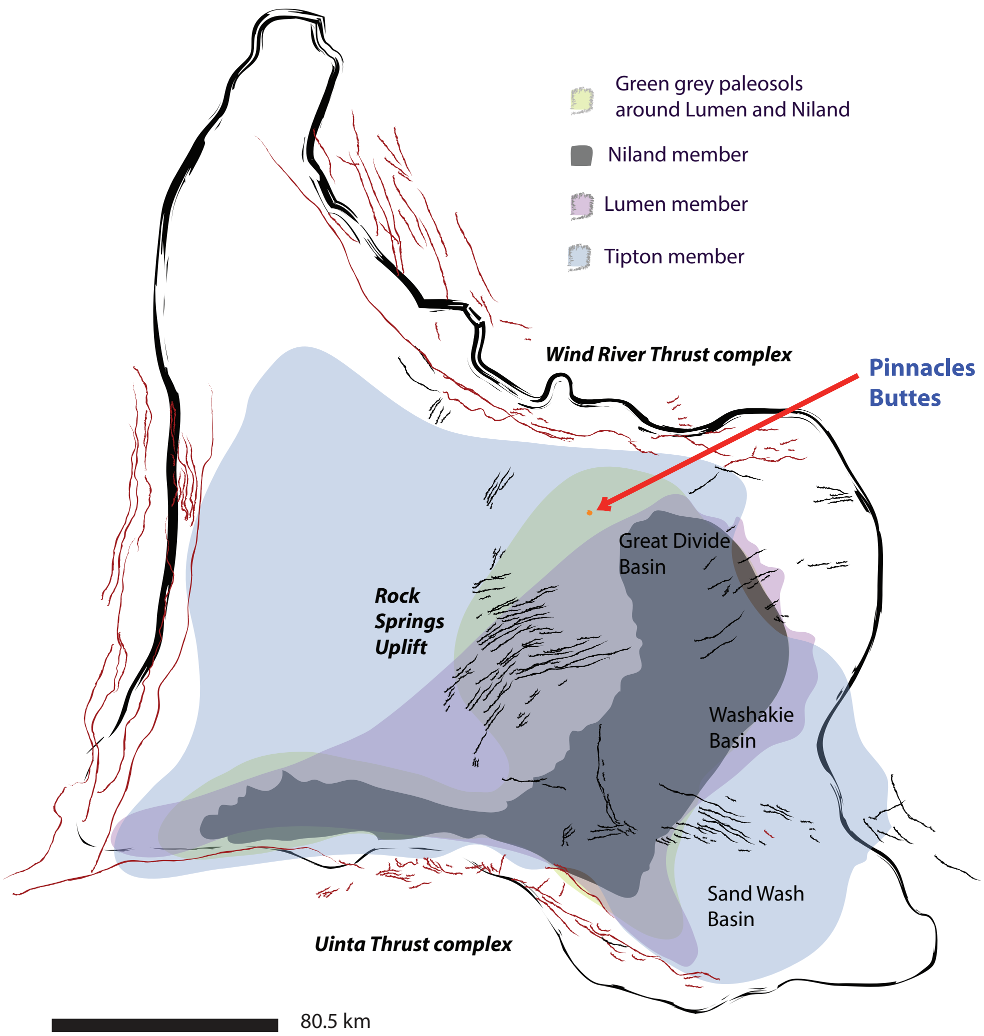

Figure 3.11 - Geography of the eastern greater Green River Basin and paleogeography of the Lumen, Niland and Tipton members based on outcrop exposure of Love and Christenson (1985) and modified from Roehler (1993). Red and black lines represent faults which compose the relevant structural boundaries in the eastern Green River Basin. The Lumen and Tipton Members belong to the Green River Formation while the Niland Member is Wasatch Formation.

a golden hue. Soil horizons are generally thin and not as brightly colored as Pgv siltstone. Coarsening upward sandstone, siltstone and claystone couplets mark cyclical progradation of levees. The couplets are typified by thin, tabular to sheet-like sandstone beds interbedded with up to 1 m of siltstone. Levees prograde close to the channel margin, adjacent to point bars and sequences appear vertically associated and interbedded with channel sandstone successions. Ssm sandstone refers to beige and tan micaceous silty very fine to medium-grained sandstone (Fig. 15). The sandstone is massive to blocky with a sheet to lenticular architecture, and is typically >1 m in thickness. The sandstone is well-lithified, producing distinctive escarpments with a bulbous weathering pattern. The sheet to tabular shape, lithics and mixed sand-silt lithology suggest suspended load material. Laterally continuous silty sand lobes are similar to crevasse splay material of distal levee deposits described by Ferguson and Brierley (1999).

FA4 - Crevasse splay - Tabular and sheet-like beds of iron stained quartz arenite (Sqt) is associated with fluvial flooding events. The Sqt sandstone is lithified, well-cemented, tabular to sheet-like and forms resistant benches. It is composed of coarse-medium grained quartz and less than 10-15% mica lithics with common biotite. Meter-scale current and climbing ripples are present at 1104C (Fig. 16). Tabular to sheet bodied quartz rich sandstone occasionally contain gravel and underlie FA2 associated sandstone are interpreted as proximal crevasse splay sheets (Kraus 1999). Thin, cm scale iron stained quartz sandstone sheets punctuate interbedded levee and floodplain associations in section 1103. Sqt sandstone underlies and occurs within the basal lag of thick Sstx and Sspx sandstone (Fig. 13) and interbeds in some sections with laminated sand-silt. Two extensive Sqt sheets are exposed at SP 125/189 and SP 147/75. The SP-125/189 sheet is approximately 854 m x 233 m, truncates the upper sandstone lense at section 1104C and is bounded by two cross-bedded sandstone bodies at SP-189. The SP-147/75 sheet is 451 m x 168 m, underlies the several sandstone lenses at SP-147 and is truncated by the sandstone lense at SP-75. An exposed Sqt sandstone splay in the upper 1101, 1102 and 1103 sections, if continuous, extends

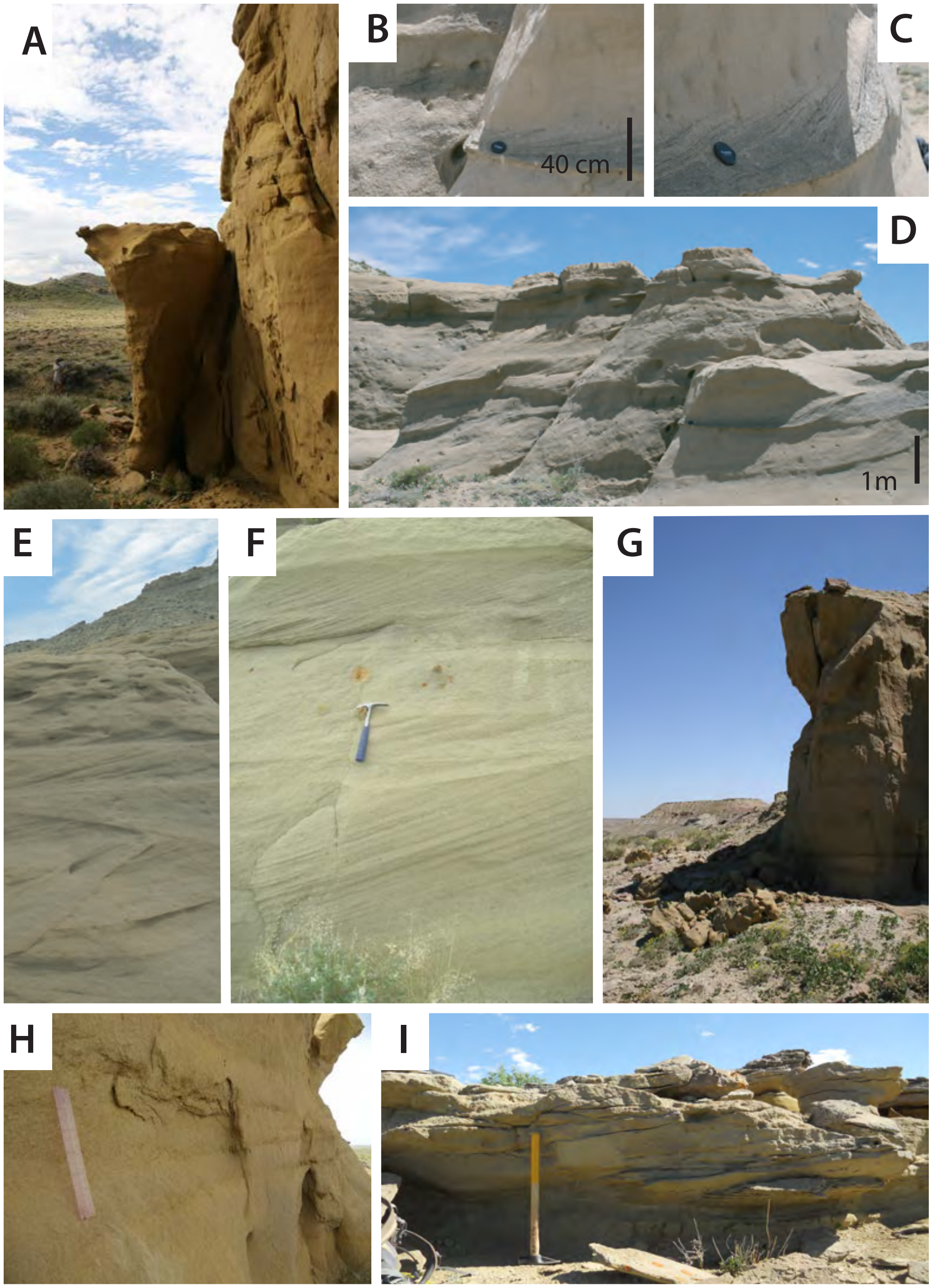

Figure 3.12 - Channel facies associations. A, G: Multistoried sand lenses from butte 9. B-D: Heterolithic biotite and sand crossbed cosets from base of section 1105A. E: Trough crossbedded sandstone (SStx) from section 1102. F: Planar crossbeds (SSpx) in sandstone from section 1102. H: 3 cm crossbeds on first order surfaces in sandstone lense from section 1102. I: Incising planar crossbeds at top of section 1104C.

laterally 860 m. Sqt sandstone at the top of section 1101 and 1104C occur 20-25 m above the base of the butte.

FA5–Gravel based thalweg – petromictic orthoconglomerate (Gpo) and oligomictic orthoconglomerate (Goo). The Goo orthoconglomerate consists of a coarse-medium grained quartz sand matrix, with pebble sized clasts (0.5-2 cm) composed of chert and quartz. At section 1104B Goo conglomerate forms shallow 20 cm lenses beneath lenticular beds lithifiedGpopetromictite which grade into Sqt sandstone (Fig. 3.17 B). The Gpo orthoconglomerate consists of lithified coarse to medium grained quartz and mud matrix with (9-14cm) variable mixture of green clay, siltstone and chert clasts (Fig. 3.17 C). Both orthoconglomerate types overlie and incise into clay bearing Fgv paleosol at sections 1104 A and B. Bedding sets are 2-3 cm with imbricated clasts, shallow scours and parallel bedding. Gpo orthoconglomerate beds possess a well lithified matrix The Gom conglomerate is abundantly fossiliferous in Biofacies 1 taxa and *Lambdotherium popoagicum*. At the east buttes the areal exposure of Gpo and Goo conglomerate sheet like complex is approximately 600 x 400m. The sand-gravel meandering stream model (Miall 1996) consists of gravel sheets overlain by internally-fining lateral accretion bodies. Goo and Gpo conglomerates underlie, and interbed with, the bases of channel sandstone lenses at the base and top of 1104C (Fig. 3.17 C-E).

FA6 - Littoral freshwater lacustrine-The shallow freshwater and marginal terrestrial zone consists of blue silt-clay (Fbc), sand-silt ripples (Smr), cross-bedded quartz arenite (Sqc), fossiliferous packstone (Lohx) and bedded micrite (Lbm). The base of the Green River Fm is composed of 0.5-4 meters of resistant packstone, thinly interbedded with white siltstone and overlain by >3 meters of carbonaceous ‘paper’ shale. Abundant ostracods, gastropods and mollusks (*Elimia tenera, Viviparus* sp., *Lampsilis* sp.) occur in the interbedded packstone. The contact between the Wasatch and Green River Formation at the Pinnacles occurs at shoreface sandstone beds that underlie the first lithified and resistant laminated

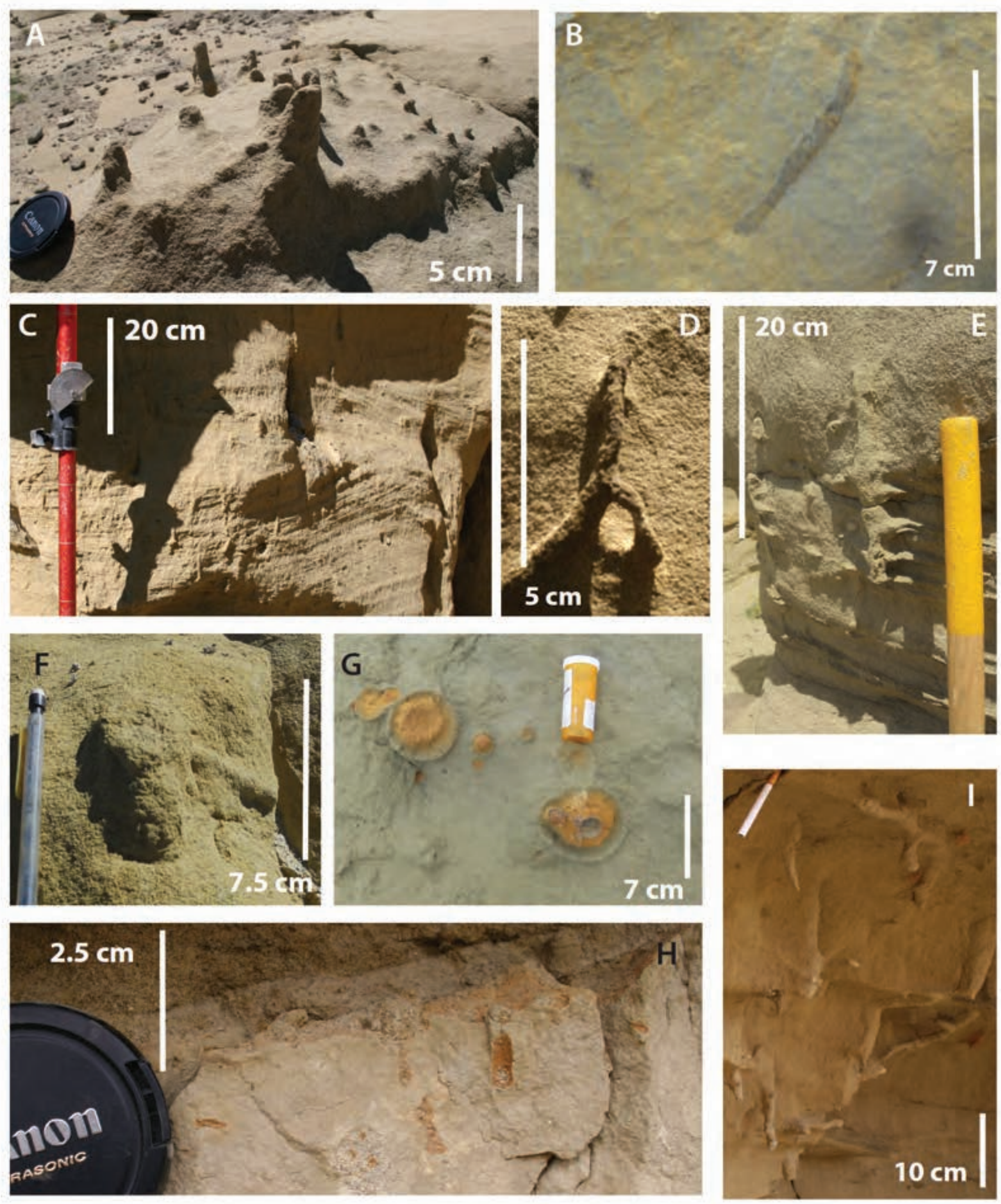

Figure 3.13 - Bioturbation in ribbon bodied sandstone lenses. A: Root traces at section 1105A. B: mud infilled burrow at section 1103. C: root traces through trough cross bedding at section 1106A. D: root trace at section 1105B E: Unlined branching trace at section 1102, follows cross lamination. F: chamber cast at section 1103 G: iron concretion at butte 14. H: *Glossifungites*-like lined borings in massive silt, infilled with overlying sand at SP 189. I: root traces weathering out of sandstone at section 1101

limestone beds containing abundant *Elimia sp.* typical of the basal Scheggs Bed of the Tipton Shale Member (Roehler 1992).Soils which formed immediately prior to transgression of the lake margin may have undergone subaqueous alteration processes. Monmorillonite is a smectitic clay unique in the study interval to a claystone deposit in the uppermost beds of the fluvial phase in section 1103. Montmorillonite, kaolinite, mica and sodium-feldspar (such as albite) are principle minerals in soils of quaternary Nile delta alluvium and develop under alkaline conditions in poorly drained soils (El-attar and Jackson, 1973). The presence of Na-rich feldspar is indicative of weathering from a source, which contained diabase, trachyte or dolerite, while a K-rich feldspar suggestsan origination from granite bearing sources (Et-attar and Jackson 1973). The Fbc siltstone and claystone pertains to the uppermost fine-grained unit in Sect 1103 and 1105C. Fbc is laterally continuous between sections 1103 and 1105C and also exposed along the north face of butte 13. XRD analysis (Table 2) of a yellow clay horizon in this unit at section 1103 illustrates thepresence of montmorillonite. Fbc is interpreted as a transitional fluvial-lacustrine unit. The clay and silt was likely transported via overbank flooding, but was post-depositionallyaltered by the approaching lake and high water table.

The Lohx clastic limestone coquina is dominantly freshwater fossils with a micritic matrix and interbedded with Lbm micrite. Cross-bedding and truncation of underlying Smr sandstone-siltstone is also present. The distinctive ostracod beds are underlain by pebble and fossil bearing sand dominated beds at Butte 13 (Fig. 3.18). Lohx limestone contains abundant fossils of Biofacies 2. Fish skeletal debris, including dentaries, spines and vertebrae of fish occur in the coquina, along with gastropods (*Elimia* sp., *Lampsilis* sp.) and ostracods. These beds weather to purple/sienna and form distinct escarpments on t he buttes and at Tipton bench. The appearance of ostracods, *Elimia* sp and fish remnants indicate established subaqueous to shallow lacustrine conditions (Roehler 1992). Lohx facies overlies Sqc and Smr shoreface deposits. The fragmentary nature of the fossils and cross-bedding suggest deposition above wave base. The interbedding

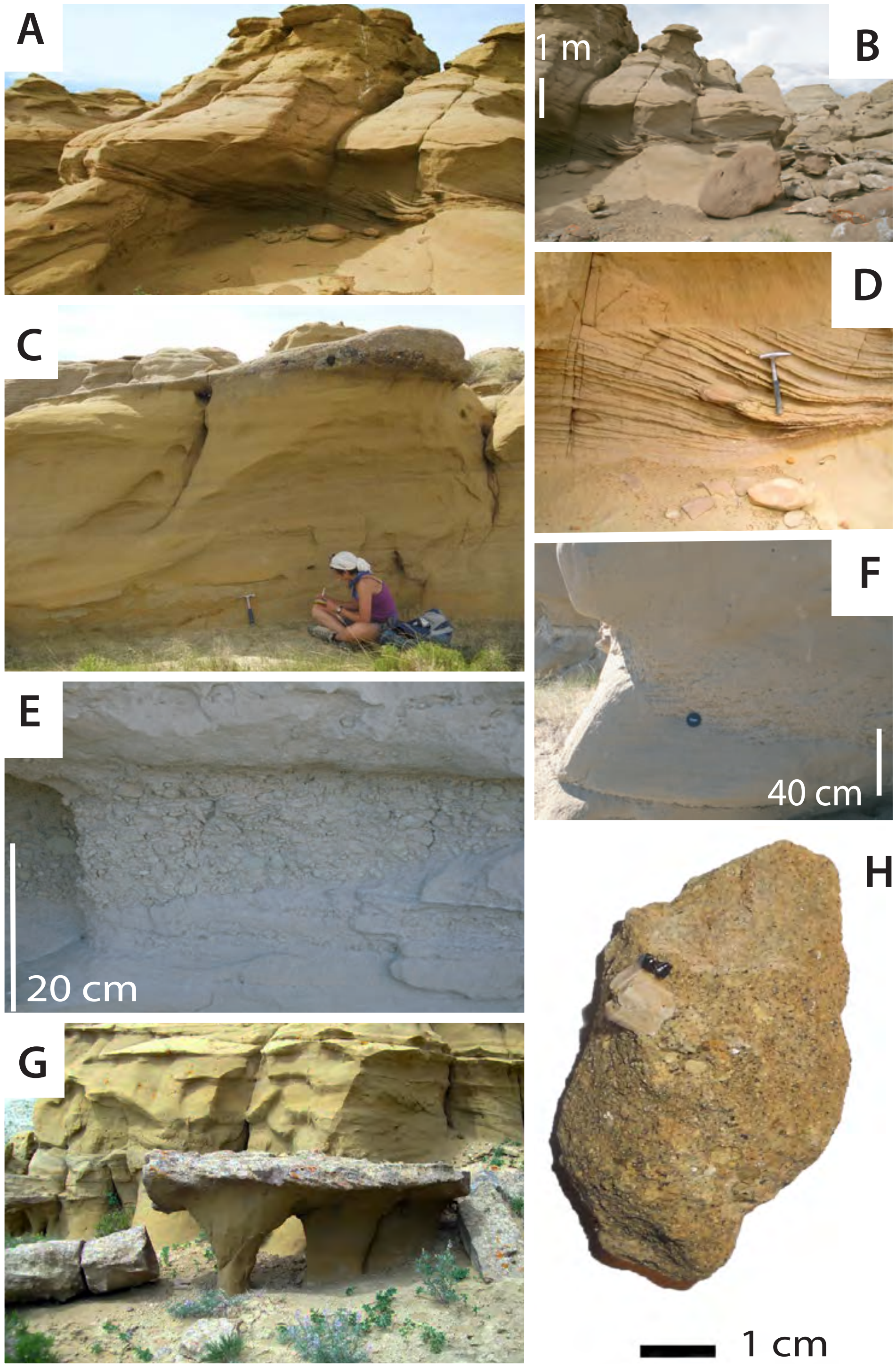

Figure 3.14 - Chutes and scours in channel facies associations. A-B,D: Gravel bearing chute in Sspx sandstone from section 1102. C: Iron stained sandstone chute from section 1102. E-F: Trough crossbedded clay clast gravel at section 1106A. G: Cross bedded iron stained sandstone eroding out of multistoried lense sandstone at section 1101 H: Hyopsodus sp. in sandstone from section 1101/SP 147.

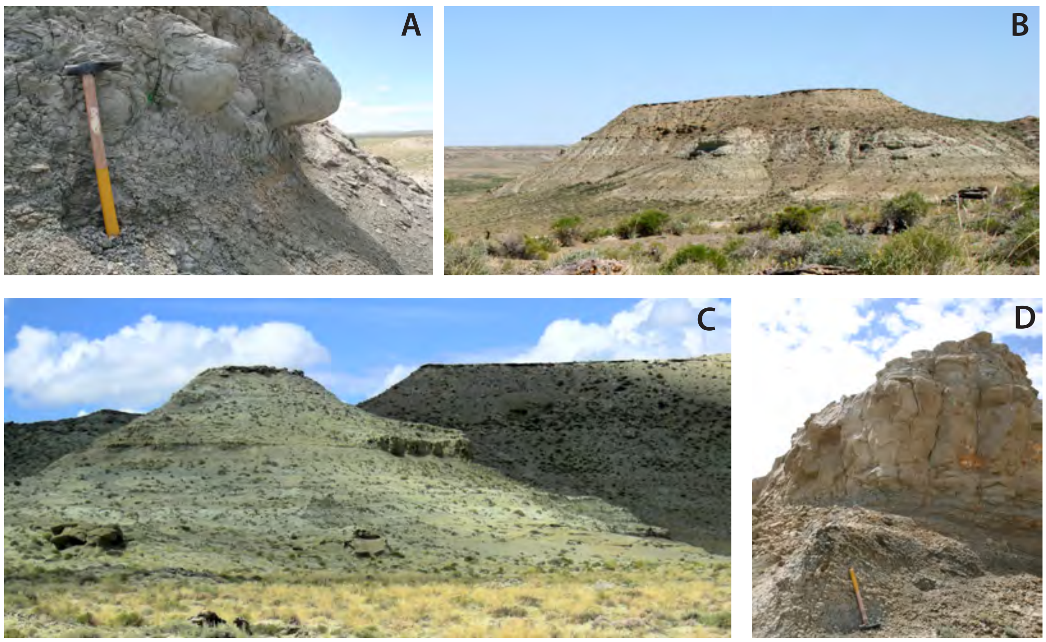

Figure 3.15 - Levee facies association. A: Ssm sandstone from section 1105B. B: Ssm sandsone and interbedded Svf and Pgg siltstone on 1105C. C: Two packages of interbedded Ssm, Sst sandstones and siltstone at section 1105B. D: Coarsening upward Sst sandstone outcrops underlain by bedded clay and siltstone at section 1105B.

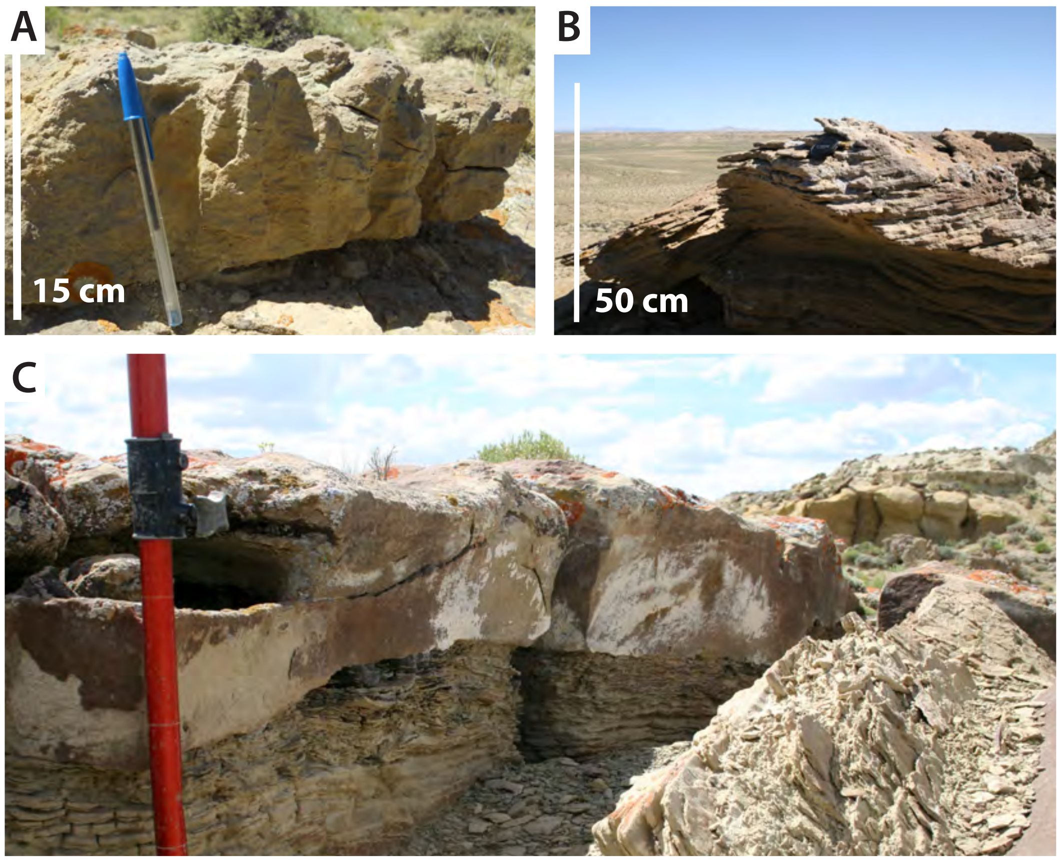

Figure 3.16 - Tabular andstone beds of crevasse splay association. B: Laminated sand overlain by Goo conglomerate at section 1104B. C: Laminated Goo conglomerate overlain by crossbedded Sqt sandstone. D: unlined *Skolithos*-like vertical trace in Sqt sandstone. E: Climbing ripples in Sqt sandstone at the top of section 1104C. F: Sqt sandstone overlying laminated siltstone on butte 8.

with micrite indicates a lateral relationship to offshore carbonate units deposited below wave base. The coquina likely formed on a carbonate breaker bar at the interface between nearshore and proximal offshore environments.

Rippled fine sandstone with silt drapes and fragmented invertebrate shells outcrops along butte 13, overlain by limestone coquina dominated by fragmentary *Elimiasp.* This unit is underlain in some sections by quartz arenite. At butte 4, section 1103 and butte 8, section 1105C, thin beds of clean white sand contain gastropod shells and underlie the Lohx limestone. Along butte 13 these beds are up to a meter in thickness. Fragmentary *Elimia* sp. shells, fish spines and clam shells suggest these beds are reworked shoreface sand. Lbm micrite consists of tabular, massively bedded to rippled carbonate mud and 0.1-10cminterbeds of Lohx packstone, paper and oil shale. Massive bedding maybe the result of bioturbation. Trail trace impressions are present (Fig. 3.18 D). Laterally continuous beds of micrite outcrop at the top of buttes 4, 8, 13, 16 (sections 1103, 1105C, 1002 and 1106B respectively, see Appendix). Micrite forms on broad platforms, in lagoons and environments with constricted flow and calm currents (Folk 1974). Low energy deposition below wave base between littoral-profundal zones would result in mm to cm scale interbeds of packstone, micrite and paper shale.

FA7 - Profundal freshwater lacustrine - The deeper water lacustrine zone includes deposition of paper shale (Fpsh), bedded micrite (Lbm), oil shale (Fosh). Thin, fissile beds of calcareous white shale are overlain by brown shale and interbedded with bedded micrite. The thin laminae and lack of bioturbation in paper shale successions indicate quiescent depositional conditions (below storm wave base).Fosh shale is dark grey/black and laminated with an organic to kerogen aroma. Carbonaceous shale is underlain and interbedded with white paper shale, micrite and stromatolitic limestone. Stromatolites are increasingly common at the top of the Tipton on Butte 16, section 1106B. Laminated black and grey layers of shale result from accumulation of organic matter in the

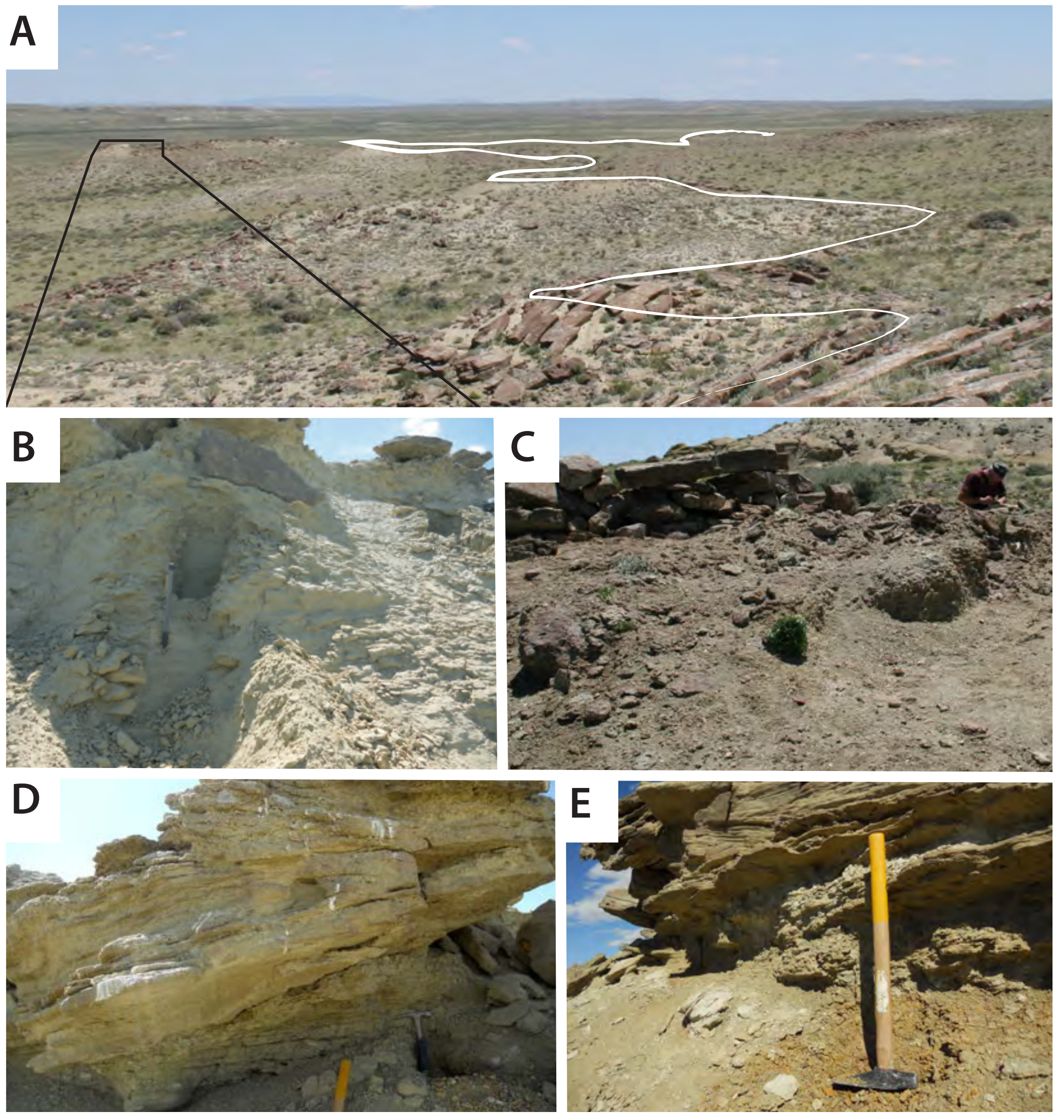

Figure 3.17 - Conglomeratic sheet complex and trough scours of thalwag or braided stream facies association. A: Gom conglomerate overlain by sandstone sheet at section 1104 AB. B: Petromictite (Gpo) overlying oligomictite (Goo) at section 1104B. C: Gpo overlying variegated paleosol (Pgv). D-E: Goo and Gpo conglomerates interbeded with and underlying multistoried sandstone lenses at the top of section 1104C.

Figure 3.18 - Littoral and profundal associations at the base of the Tipton member of the Green River Fm, Scheggs bed on the northern face of butte 13. A: Fbc claystone at the uppermost Main Body overlain by basal Scheggs bed. B: Paper shale and Lohx limestone overlying laminated sand and silt. C: laminated sand silt with very small scale ripples and pebbles. D: Trail traces in bedded micrite. E: Fosh and Fpsh with bedded micrite and algal limestone. F: Sqc sandstone overlain by Smr sandstone-siltstone.

hypolimnion of the lake (Flugel 2010). Interbeds of shale, micrite and stromatolites indicate fluctuation of between littoral and profundal zones while the lake migrated toward the basin margin.

TAPHONOMY OF PINNACLES VERTEBRATES FOSSIL HORIZONS A AND B

During previous expeditions to the Pinnacles, (1999-2011) fossiliferous beds were discovered at the base of the buttes, with vertebrates being most abundant in golden hued sandstone outcrops. Thin basal conglomerate beds are also known for containing abundant vertebrates at two discrete stratigraphic levels (Fossil horizons A, B Fig. 3.17). Microvertebrate specimens typically include disarticulated carapace and plastron, phalangeal elements, calcanea, vertebrae, teeth, osteoderms and cranial fragments. The catalogued collection is dominated by mammal teeth and jaws, though the reptile specimens also remain an important component. Fish fossils are also represented by gar scales.

The material collected from the Pinnacles represents a diverse assemblage, based largely on isolated elements. Fossils were collected via three methods: surface prospecting, anthill picking and small-scale quarry excavation. A majority of the sampled material comes from densely fossiliferous localities SP 75, 125, 147, 165 and 136 located at different sides of the study area (Fig. 3.5). The stratigraphic correlation between these localities and the lateral extent of fossiliferous beds at the Pinnacles buttes had not been previously well constrained.

Localities 74, 75, 125, 147, 165, 136, 146, 186 and 153 correspond to fossil horizon A while 187, 189, 190 and 191 correspond to fossil horizon B. One locality 188 belongs to the location of fossil horizon C, but very little material has been recovered at this level thus far. Fossil horizons A and B are vertically associated with the appearance of both point bar (Sstx, Sspx lenses) and crevasse

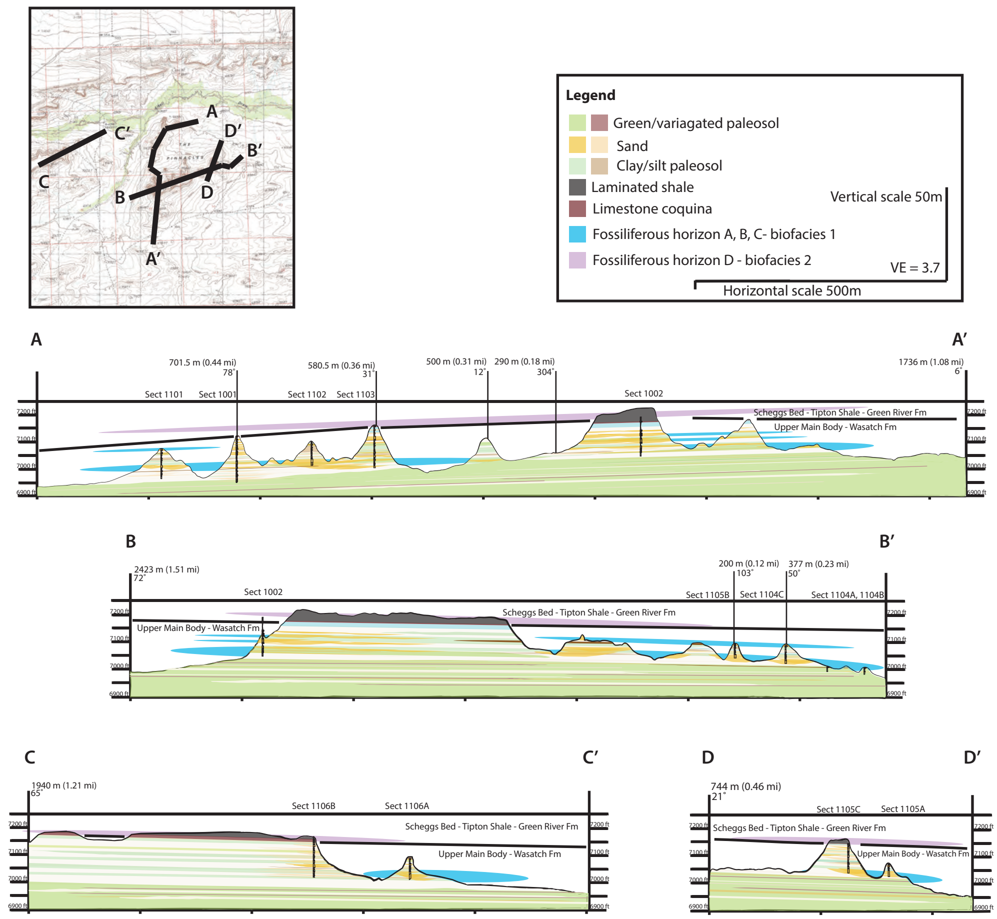

Figure 3.19 - Cross sections of the east, west, north and south buttes. Cross sections A-A', B-B', C-C', D-D' shows the relationship of sections, facies associations and fossil horizons. Correlation between measured sections 1103, 1105, 1106, 1001, 1002 is based on a synchronous lacustrine flooding surface, co-occuring with the appearance of Elimia sp. and calcareous sediments. The Green River-Wasatch Fm contact dips at approximately 3° to the northeast.

splay associations (Sqt, Gom, Goo sheets). Horizons A-D occur with approximately 5-25 m of stratigraphic separation. Fossil horizon A rests at the bottom of the measured exposed sections. Horizon B is 25 m above horizon A at sections 1101 and 1104C and 5-10 m above A at section 1002.Horizon C lies 8 m above horizon B at section 1002. Horizon D is found at the top of the exposed section roughly 35-45 m above horizon A.

The vertebrate and invertebrate assemblages segregate the section into two distinct biofacies. Biofacies 1 consists of mostly vertebrate fossils including mammal, reptile, ave and fish. FA2, FA 4 and FA5 type sandstone and gravel complexes are heavily concentrated in mammal teeth and fragmented postcrania of BF1 affinity. The stratigraphic location of such facies associations determines the level at which horizon A, B, or C occur. Key taxa of this biofacies are *Lamdotherium popoagicum* and *Lovina zephyri*, with common taxa including *Microsyops, Hyracotherium, Cantius* and *Hyopsodus.* The Biofacies 2 assemblage is dominantly invertebrates (gastropods, mollusks, stromatolites and ostracods) with a low abundance of fish jaws, teeth and spines. Key taxa of this biofacies are *Elimia* sp., *Lampsilis* and ostracods. This also includes stomatolitic algal beds at the top of the Tipton. Ostracods in Lohx limestone comprise a significant component of the basal Scheggs bed, the location of horizon D.

Cross sections A-A', B-B', C-C' and D-D' (Fig. 3.19) show the approximate strata occurance of horizons A-D in relation to facies associations. The uppermost Wasatch section of the buttes is underlain by green variegated paleosol horizons of FA1, with a sand dominated unit of FA2, FA3 and FA4 overlain by FA5 and FA6 of the Green River Formation. Blue markers show the vertical placement of fossil horizons A, B and C belonging to Biofacies 1 and fossil horizon D belonging to Biofacies 2. The shift in ecology and fossil abundance preserved in the Pinnacles section corresponds to formational boundaries and symbolizes the change from subaerial to aqueous deposition.

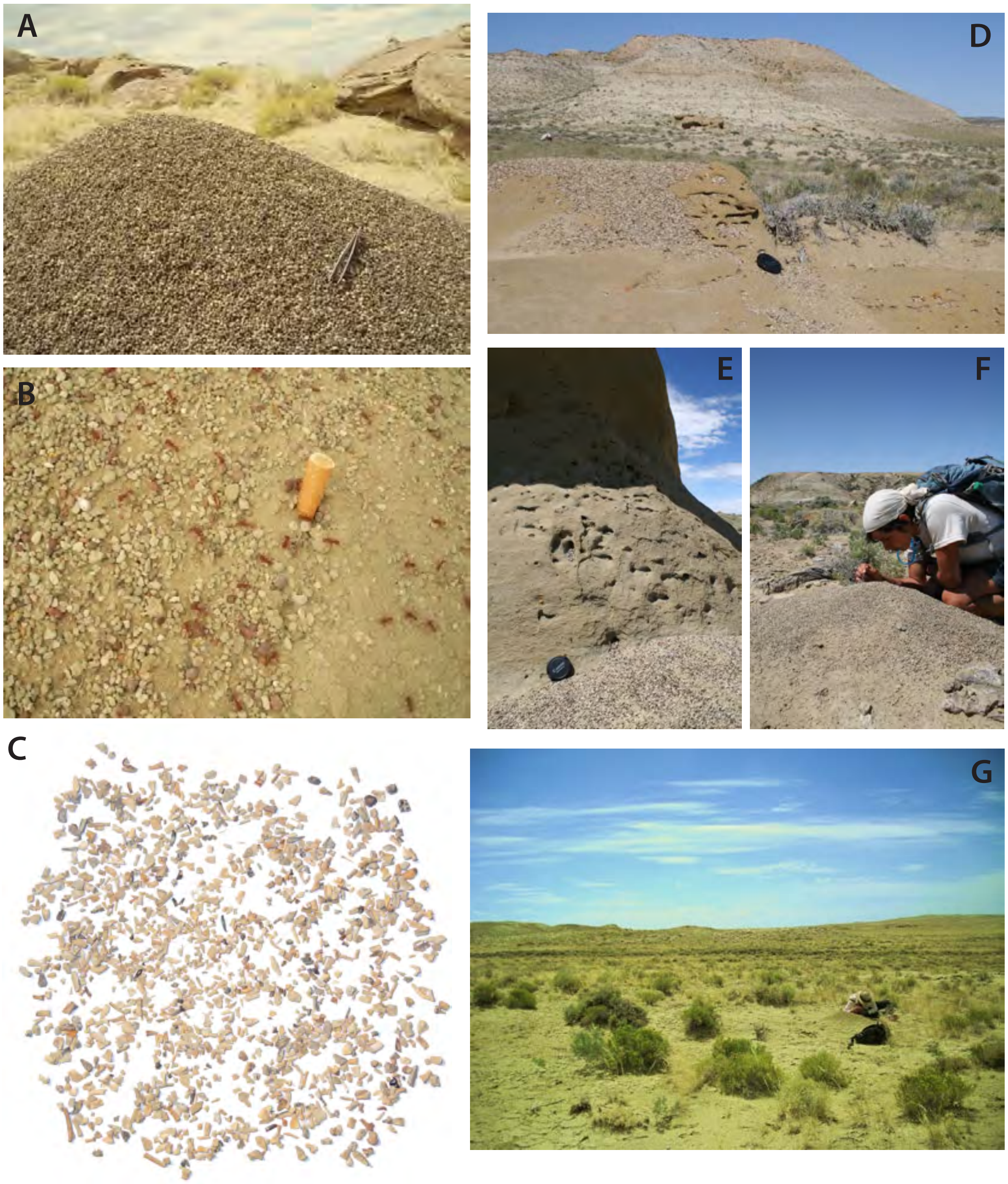

Figure 3.20 - Fossiliferous anthills. A: *Pogonomyrmrx* spp. anthill at locality SP 136. B: *Pogonomyrmrx* spp. on anthill surface C: Bone fragments from anthill wash at SP 136. D-E: Anthill burrows within Sstx sandstone lense at section 1104C and 1105A. F: SP Cairns collecting at SP 190. G: JK Adams collecting at SP 136.

ANTHILL SAMPLING

The anthills at SP 136, 75, 147, 125, 165, 187, 188, 189, 190 and 192 contain isolated elements collected by harvester ants from underlying and surrounding sediment (Fig. 3.20). Occurrence of modern insect burrowing consists of wasp larval chambers, black ant burrows and red ant mounds. The harvester ant *Pogonomyrmrx* spp. (likely *P. owyheei* or *P. occidental*; Wheeler and Wheeler 1988; MacMahon et al. 2000) exhumes coarse material during excavation and places lithoclasts and fossil material on the surface of the anthill. The anthills were a significant source of fossil material and many were utilized over several different field seasons.

Concentrated matrix from the mound created by harvester ants contains microscopic teeth, fragmented postcrania and even partial jaws. The anthills provide access to fossiliferous horizons by both distilling gravel-sized material (which includes microvertebrate remains) into an easily identifiable location and excavating into beds that may not be exposed at the surface. Productivity of an anthill is directly related to the nature and fossil content of the substrate in which the burrow was constructed. Ants that burrowed into lithified sandstone were observed to have a greater abundance of fossil bone than burrows in sediment eroded from unconsolidated sand substrata. The frequency of productive anthills in this area is well documented and coincides with success of surface collecting at fossiliferous horizons. Consequently, the method of using ants for collecting presents the possibility of sampling bias toward the collection. Fig. 3.20 C shows a sample of anthill bone fragments of similar size. the result of anthill sorting produces an abundance of small bones roughly 1-10mm in size, with most averaging about 4-5mm. Compared to other z misc samples (Fig. 3.22-3.25), anthill wash lacks large (10mm+) bone and skull fragments.

Prior to sampling, bones were erosionally removed from the original depositional horizon, incorporated into a fluvial channel lag, removed from these lags by ants

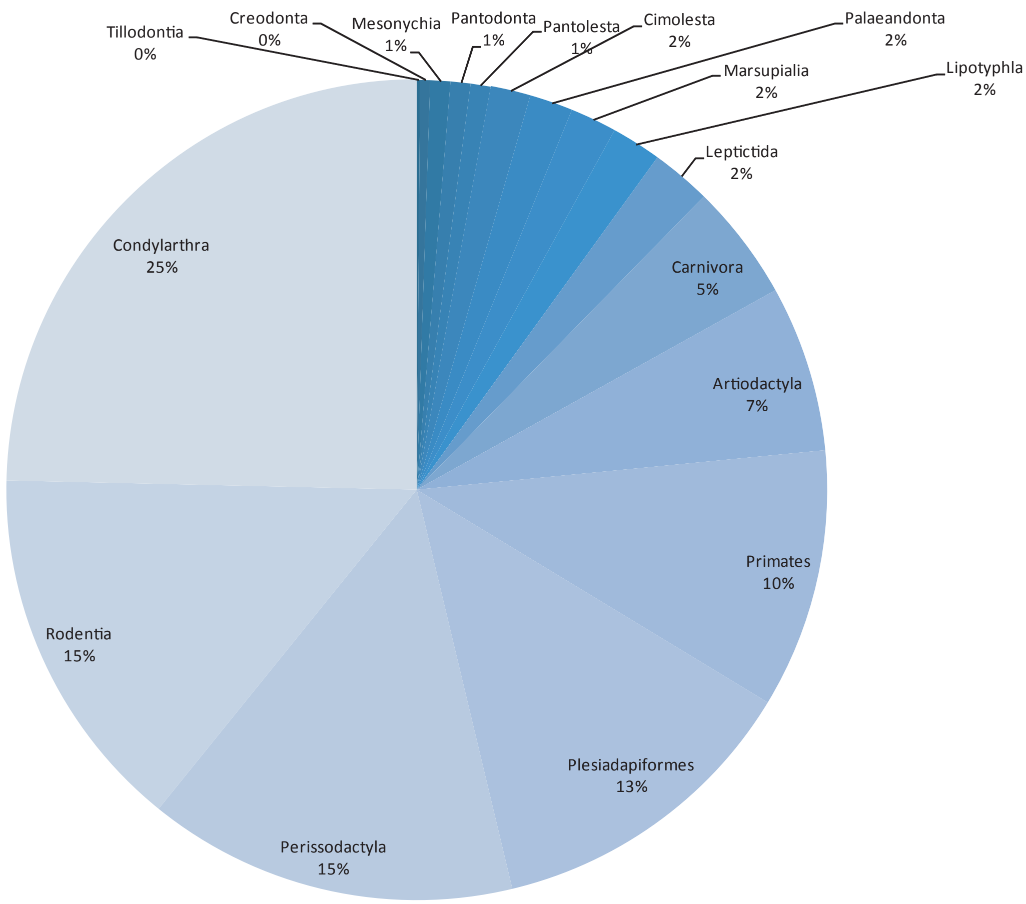

Figure 3.21 - Ordinal taxonomic composition of Pinnacles buttes assemblage based on number of specimens recovered from all localities. Condylarthra, Rodentia and Perissodactyla, Plesiadapiformes and Primates combined consist of 3/4 the collection due to large quantities of *Hyposodus*, *Hyracotherium*, *Microsyops* and *Cantius* recovered from these sites

and finally distributed onto the modern desert surface by both the ants and field collectors. The anthill collection is taxonomically biased to *Hyracotherium, Hyopsodus, Microsyops* and rodents with other genera represented by a few specimens (Fig. 3.21). The high abundance of few taxa may be the result of a size bias or erosion exaggerating ecological abundance from several smaller horizons. Fortunately the assemblage is represented by a diverse collection and the types of genera recovered are taken with higher regard than the exaggerated abundance of certain genera in the collection.

COMPARATIVE ABRASION ON SAMPLES FROM PALEOSOL AND CHANNEL LOCALITIES

The catalogued specimens consist of isolated and unabraded teeth, jaws and distal limb elements. The zmisc specimens are dominantly angular to subangular; fragmented and isolated; and are dominantly postcrania, skull and limb elements with some fractured or whole teeth. Small vertebrae from lizards or snakes are unabraded and typically not fractured. Rounded to subrounded pieces exist but are of lesser quantity in the zmisc samples. The largest teeth, such as those belonging to *Coryphodon*, are represented by fragments (UM 112936, 116115, 116107, 109003, 107979) ranging between 0.3 to 3.5 cm. The largest fossil fragment is a 6.5 cm subrounded astragalar fragment. Figures 3.22 to 3.25 show zmisc samples arranged into abrasion groups base on edge and surface degradation. The enamel of some teeth isintact, but not exceptionally well-preserved. Several teeth have no enamel and show degradation of the underlying dentine (Figs. 3.24 and 3.25; subrounded and subangular groups). SP 74 specimens are slightly more angular with unabraded edges, more associated material (Fig. 3.21 G) and fewer rounded or subrounded fragments than the samples of SP 75. UM 104507 from SP 74 is compared against UM 104709 in detail as both samples are relatively the same size (104507 V=215mL, 213 fragments; 104709 V=205mL, 306 fragments). In both samples, the majority of the fragments were observed to be angular to subangular. The paleosol sample

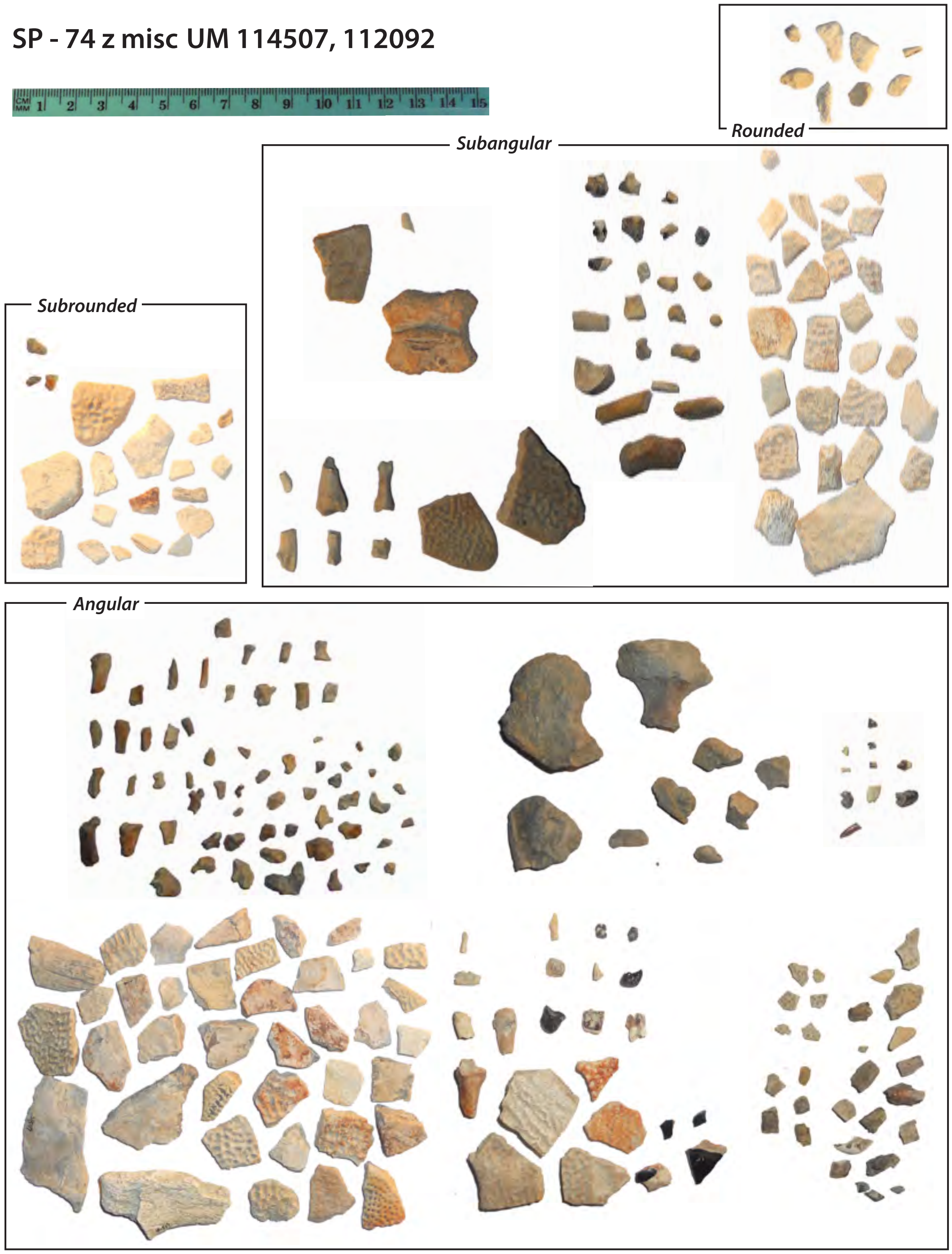

Figure 3.22 - Abrasion groups on z misc samples from SP 74

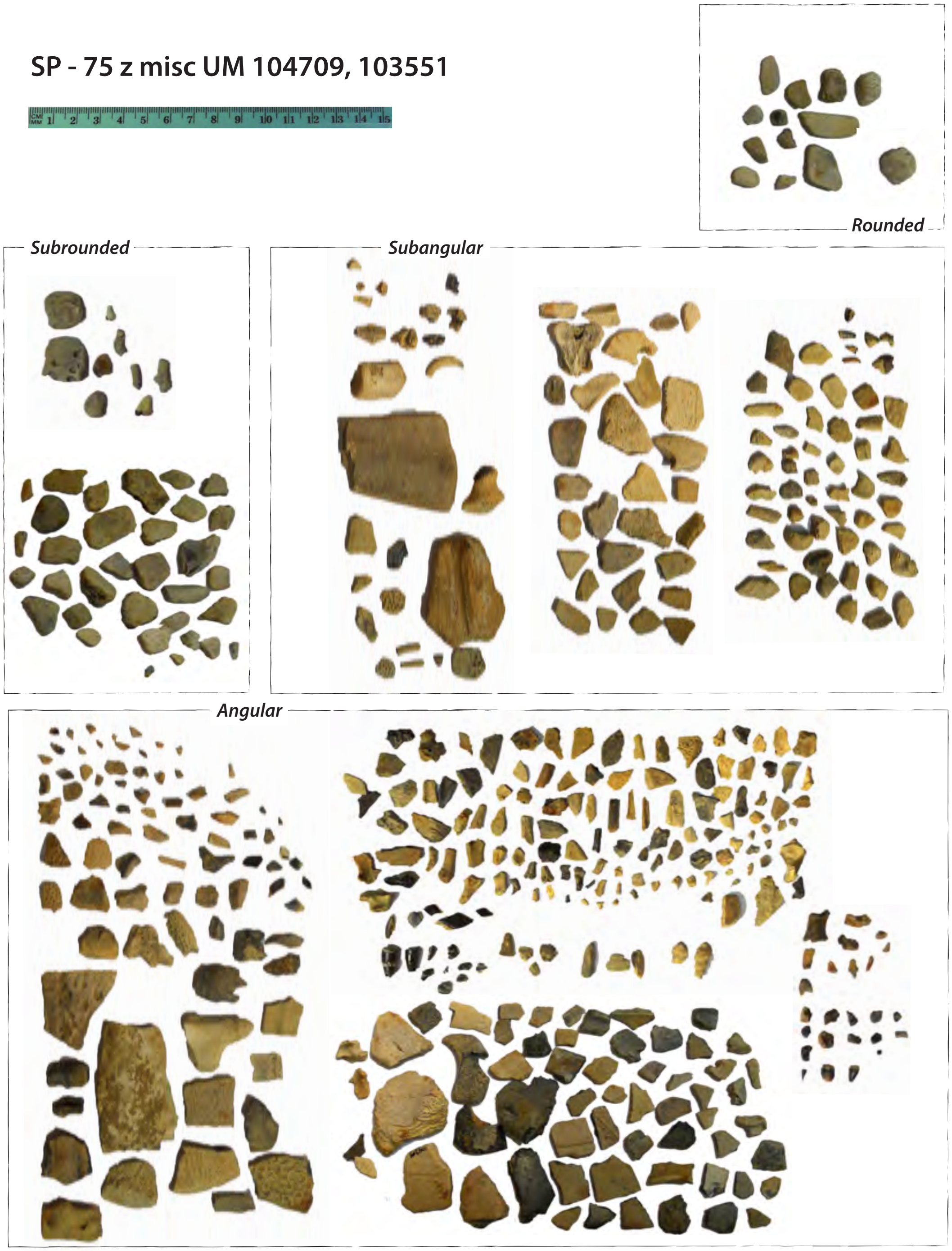

Figure 3.23 - Abrasion groups on z misc samples from SP 75

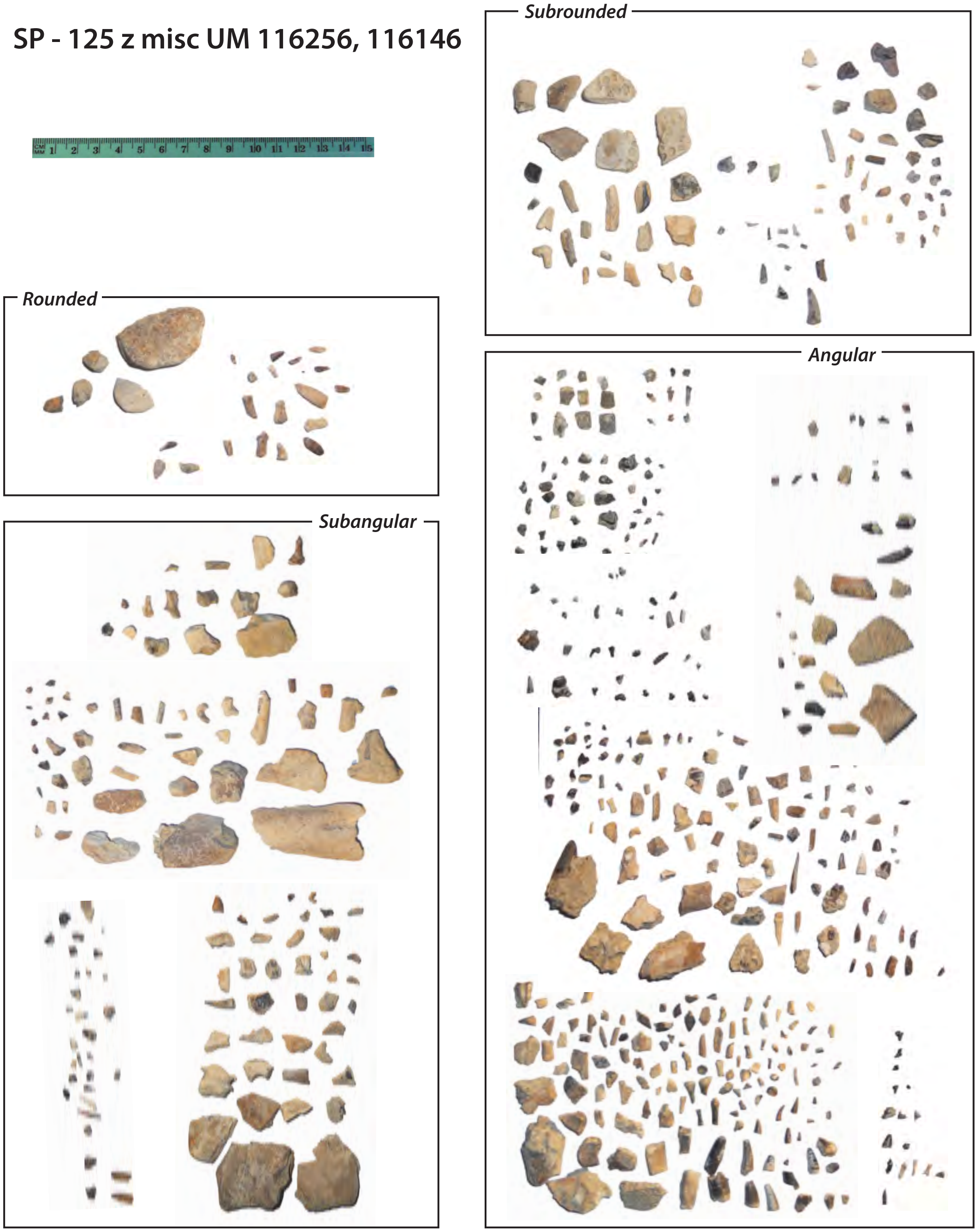

Figure 3.24 - Abrasion groups on z misc samples from SP 125

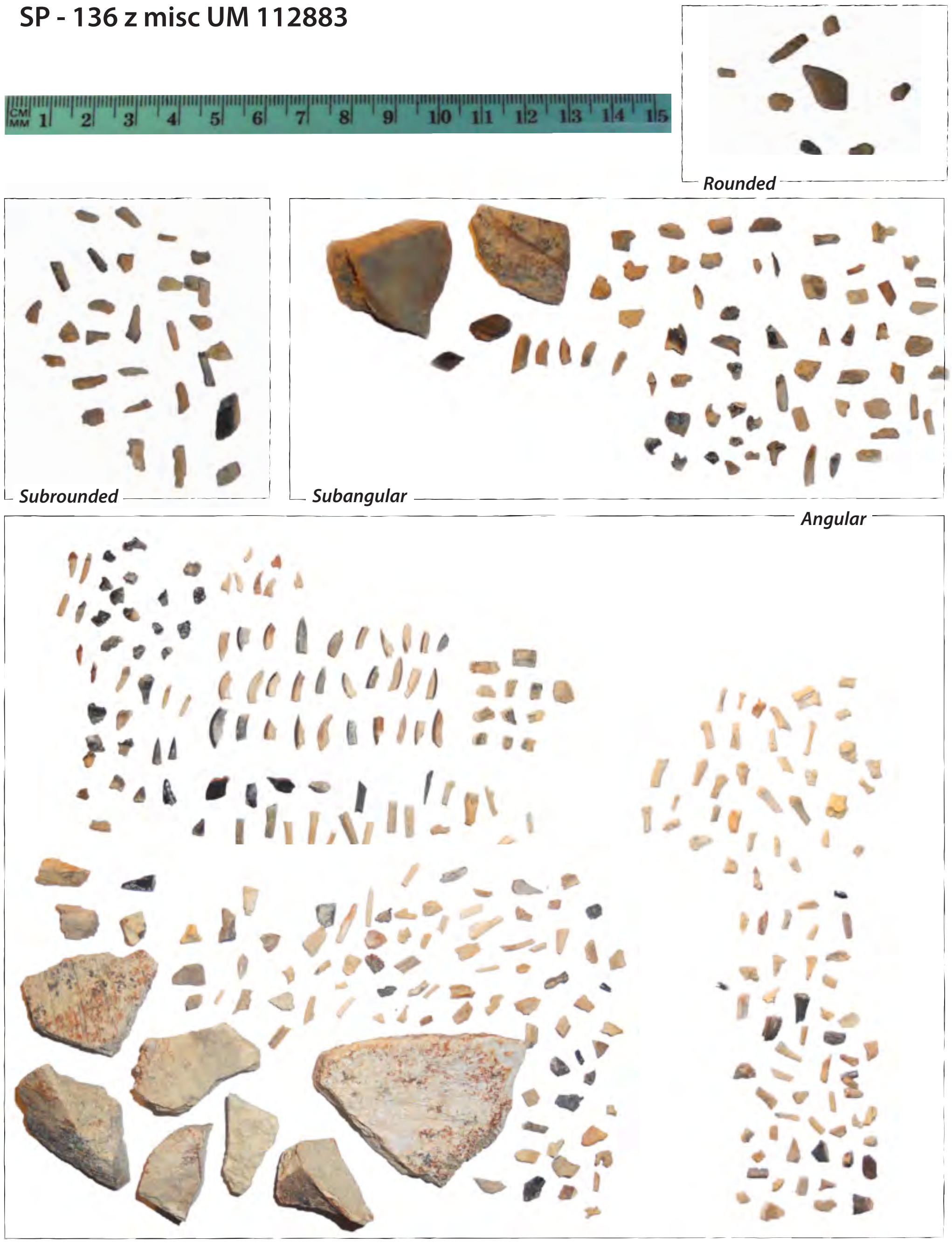

Figure 3.25 - Abrasion groups on z misc samples from SP 136

(104507) consisted of 69% angular, 19% subangular and 12% subrounded fragments. The channel sample (104709) was composed of 61% angular, 25% subangular, 10% subrounded and 4% rounded. The differences between surface abrasions are very slight, however, the overall shape of several SP 75 fragments are larger, rounded and more spheroidal than the SP 74 fragments.

Isolated and fragmented bone is mixed with mudstone and soil nodule intraclasts at the base of channel successions, crevasse splays, conglomerate beds and chute deposits. These intraclasts are composed of white siltstone, chert pebbles and green siltstone. SP 75, 147, 125, 189 and 165 contain *in situ* material within the base of Sstx, Sspx, Sqt, Gpo and Goo units (Fig. 3.14 H, 3.7 D, 3.26 A-E). The isolated and fragmented, although relatively unabraded, nature of most of the material may suggest that the assemblage was locally reworked but underwent a minimal level of hydraulic transport. Bone frequency is considerable in sandstone outcrops co-occuring with sand to pebble sized mudclasts and is highest where gravel-bearing, crossbedded chutes and scours occur (Fig. 3.13 B-D, 3.14). Intra-point bar reworking throughchutes during high water stages (possibly seasonal flooding) results in point-bar complexes with common lenticular scours (Galloway and Hobday, 1996). Periodic flooding, and incision of latertally-restricted chutes, would concentrate disarticulated teeth and skeletal debris into erosional lags at the bases of the chute depositsbut would produce minimalsurface and edge abrasion on fossil material. For instance, the effect of transport distance is reduced if fossil material is reworked locally within the point bar setting but would, as a result, cause skeletal pieces to break and fragment while accumulating bones in ‘pockets’ among the sandstone outcrop. Co-occurrence of fossil horizons within extensive sand sheets, channels and gravel complexes suggest stream processes played a dominant role in fossil preservation and accumulation.

Preservation of the fossil elements here differs from those found at the Lostcabinian type section in the Lost Cabin Member of the Wind River

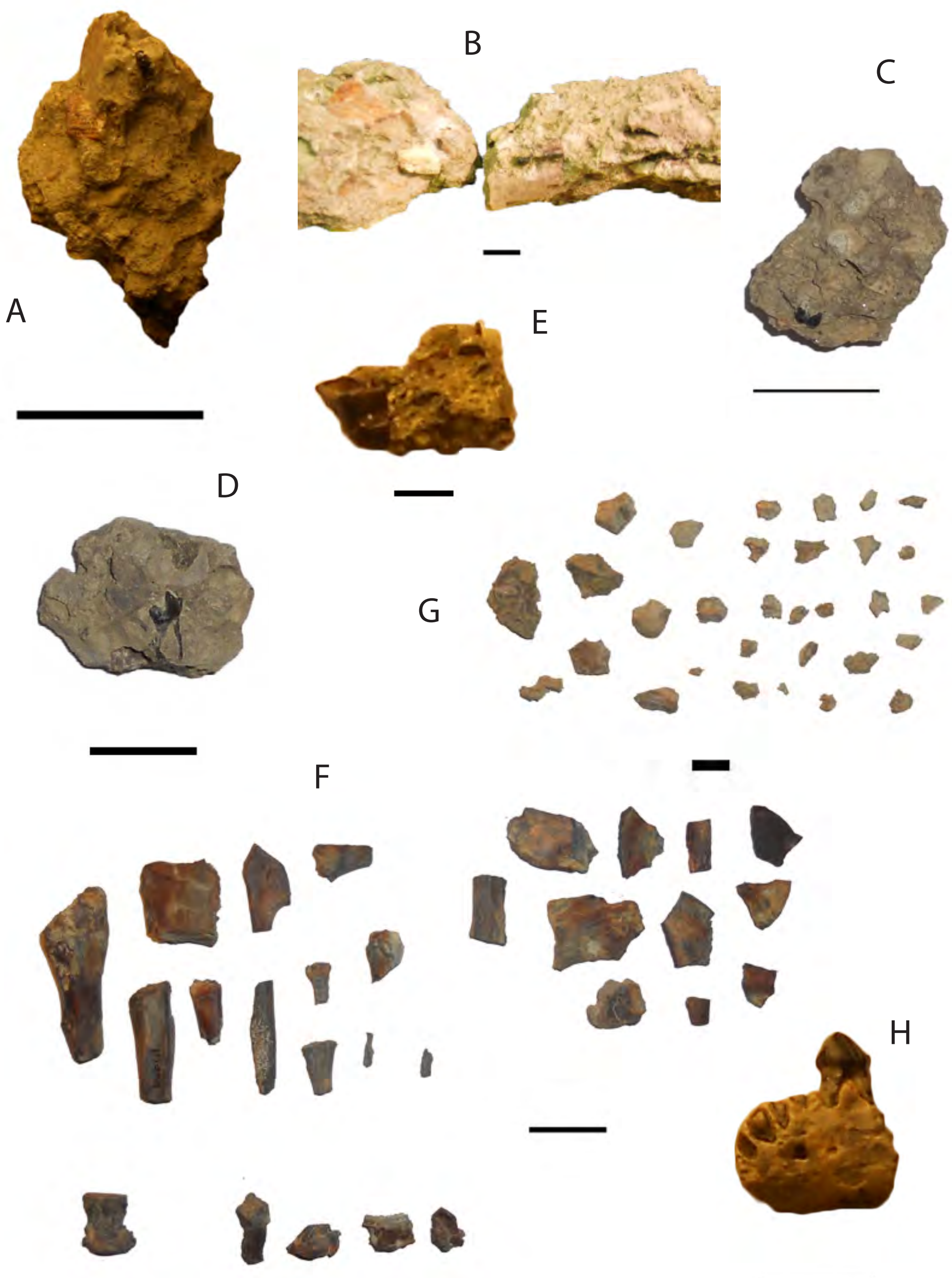

Figure 3.26 - Jaws and associated specimens from the quarry, paleosol and channel. A:*Paleosinopa lutreola*, 115819, in Gpo orthoconglomerate, scale 20mm. B:Horse jaw in Gpo orthoconglomerate, scale 5mm. C: *Hyopsodus*, 115823, Gpo orthoconglomerate, scale 20mm. D:*Paleosinopa lutreola*, 116254, Gpo orthoconglomerate, scale 10mm. E:*Peratherium*, 115156, Gpo orthoconglomerate, scale 2mm. F: Perissodactyl postcrania, 111909, from SP 165 quarry, scale 20mm. G:*Notharctus venticolis*, 104506, associated cranial fragments, SP 74 paleosol, scale 10mm. H: *Hyopsodus*, 104533, rounded dentary, SP 75 channel, scale 5mm.

Formation. Fossils recovered from Buck Springs Quarry occurin mudstone horizons, coprolites and in both bioturbated and laminated limestone beds (Stucky et al. 1990). The type assemblage is characteristically well-preserved as whole jaws, skulls, teeth, postcrania, partial skeletons and even eggshells (Stucky et al. 1990). Unlike the Pinnacles section, which lacks appreciable fossil material in floodplain associated beds, the fossils in Buck Springs Quarry were best preserved away from the stream in alkaline ponds and swamps (Stucky et al. 1990).

DISCUSSION

Fossil abundance varies between stratigraphic levels and between accumulation types. Sandstone beds at the base of the buttes are highly fossiliferous, while sandstone and mudstone beds at higher stratigraphic levels are less fossiliferous. Hypothetically, fossil preservation occurs more commonly in the floodplain environment in well-developed paleosols. However at the Pinnacles, less fossil material is found in the paleosols than in channels. The fluvial channel environment acted to collect and redistribute fossils from eroded sediment. Intrachannel processes also acted to isolate and fragment whole bones and teeth. The relatively low number of highly abraded and rounded fragments from the zmisc samples suggests that the source for many of these fossils was local to the final place of deposition. The z misc samples and teeth were collected in pockets along the base of the outcrops where chutes and scours occur. Reworking within the pointbar would fragment bones to the level witnessed in these samples while leaving the surface and edges of most fragments unabraded.

The upper Main Body of the Wasatch Formation at this location contains packages of green, grey and brown siltstone, claystone and siltstone paleosols, quartz-rich sandstone and conglomerate sheets; and both vertically and laterally aggregating sandstone complexes (Fig. 3.27). The Pinnacles section was deposited by meandering streams during an interval of lacustrine transgression and a concomitant rise in fluvial base level. The abrupt appearance of erosively-based (Pietras et al. 2003) Scheggs bed, sand-dominated beach deposits, immediately overlain by interbedded cyanobacterialand carbonaceous shale signifies the apex of this lacustrine transgression. The Pinnacles, and other fluvial units in the Green River and Uinta basins, are unique, in comparison to river systems which drain into the ocean. Similar to internally drained basins, depositional style of fluvial sequences in intermontane basins are affected by lake fluctuations rather than sea level (Nichols and Fisher 2013, Zonneveld et al. 2003). Stratigraphic sections from the Pinnacles demonstrate an increase in overall accommodation space prior to the incursion of the Tipton Member into the Greater Green River Basin (Great Divide Basin). Sublitharenite lenses with erosional bases at the bottom of the sections show up to 10 meters of incision into underlying strata. The thickness of sandstone lenses decreases progressively towards the top of the section as accommodation space increased. As the margin of Lake Gosiute approached, increasing volumes of overbank fines were preserved in the study area. Identifying bounding surfaces in the fluvial succession provides insight into the depositional history and fluctuations in lake level.

Stratigraphically important surfaces bisect distinct units in the Pinnacles section. The study interval is divided into three sub-units; a lower unit distinguished by thick, mature paleosols, an upper fluvial unit distinguished by channels and poorly developed paleosols and a lacustrine unit. The lowest bounding surface in the section occurs where the first set of FA2 sandstone lenses are marked by deeply incising channel bar deposits, fining-upward, lense-shaped sandstone complexes with multiple channels, basal gravel beds and high amounts of coarse biotite-rich lithic fragments. The lowest FA2 sandstone complexes appear as large, laterally-restricted, lense-shaped bodies, which may have been produced by a combination of avulsion, deep incision and slow to no migration. Crossbedded-sublitharenite units are underlain by thick and well-developed paleosols with thin, laminated sandstone beds. The ratio of fine to coarse sediment

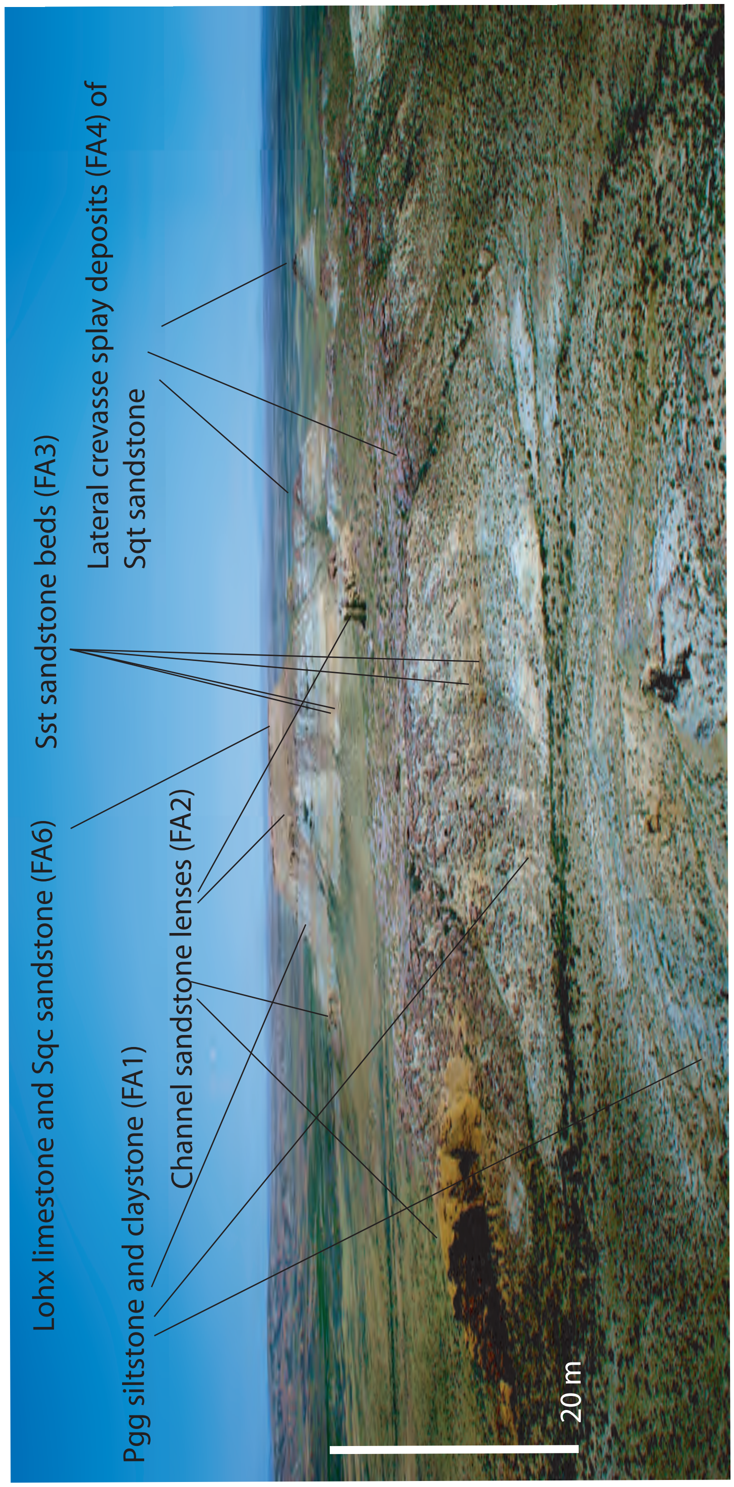

Figure 3.27 - Vertical and lateral relationship of fluvial facies on the eastern buttes. Sqt sandstone sheet underlain by siltstone (Pgg, FA1) and tabular sandstone (Sst, Fa3) and overlain by channel sandstone outcrops on butte 8 and 9.

of FA1 is approximately 1:6.5 in this unit.

Deep incision at the base of channel sandstone complexes in the lower part of the study interval produced a lowstand surface of erosion (Catuneanu et al. 2010) which may form under forced regression (Posamentier et al. 1988) such as lacustrine regression at the top of the Lumen phase (*sensu* Roehler, 1993). Erosional surfaces generated by lacustrine regression are present on the western side of the Green River Basin (Zonneveld et al. 2003). This interval has an overall high sandstone to mudstone ratio, indicative of a fluvial-lacustrine lowstands systems tract (Zonneveld et al. 2003). Approximately 40-50 meters above the lowest bounding surface of the sandstone lenses is a transgressive flooding surface. The dominance of siltstone and claystone increases in uppermost beds of the Main Body, where mud units are thicker with poorly developed paleosols. The presence of montmorillonite in uppermost strata of the Main Body suggests alteration of clay minerals after sediment saturation as a result of subaqueous inundation (El-Attar and Jackson 1973).

Deposits above this transgressive surface consist of hummocky cross-stratified sandstone to laterally extensive limestone and calcareous shale. The lacustrine flooding surface that marks the contact of the Main Body of the Wasatch Formation with the base of the Scheggs bed and its associated beach sandstone beds is regional in nature and may be correlatable with a similar surface identified on the opposite side of the Green River Basin in the Little Muddy area (Zonneveld et al. 2003). The lower Scheggs bed at Little Muddy and this study interval are characterized by littoral lacustrine facies thatinclude hummocky cross-bedded sandstone and oolitic grainstone. Abrupt changes in channel stacking patterns and paleosol maturity (reflected by paleosol color profiles) are also interpreted to reflect significant bounding surfaces, likely the landward equivalent of lacustrine flooding surfaces. The middle sandstone dominated unit may indicate that facies associated with alluvial deposition of the stream moved basinward and subsequently shifted upstream as base level rose and the lake

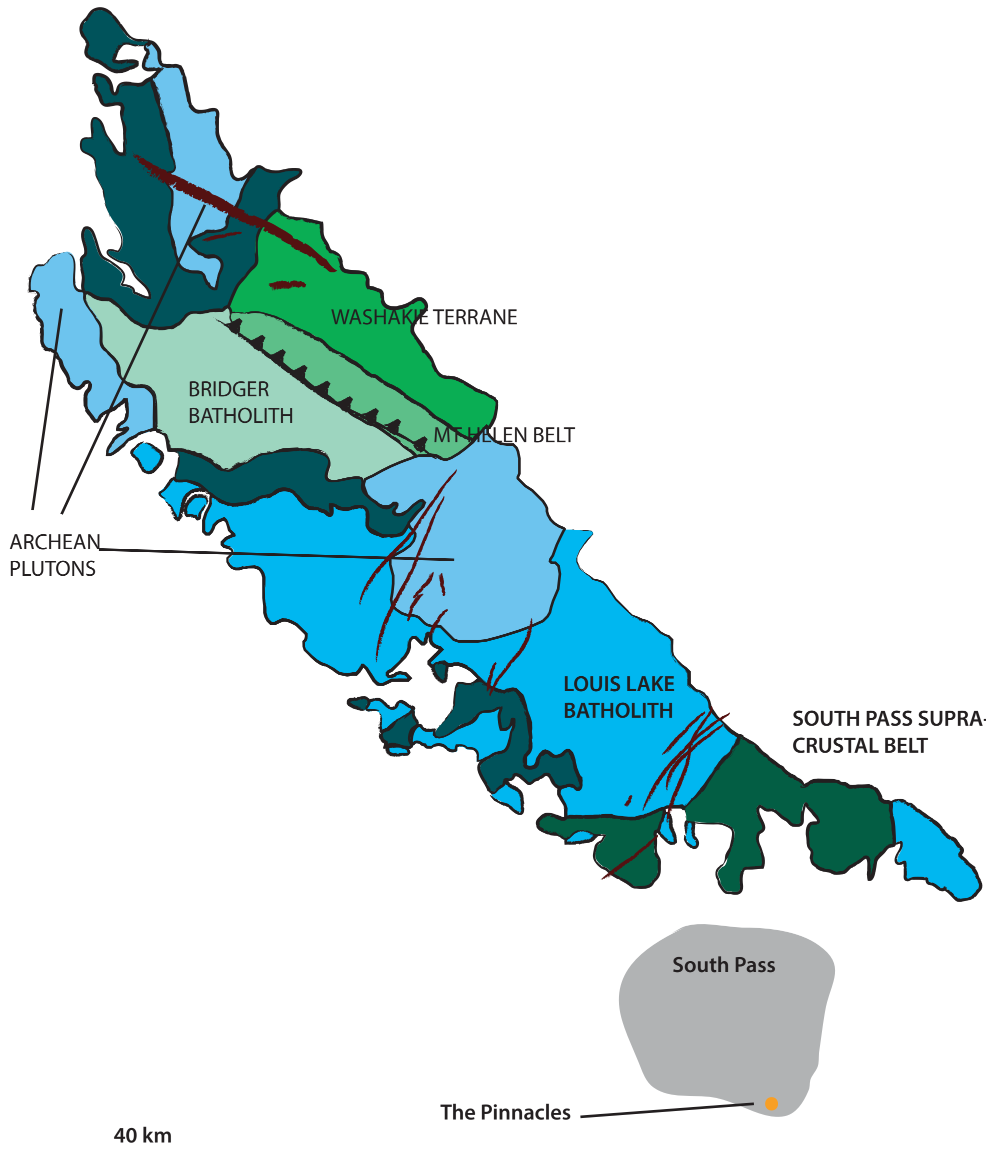

Figure 3.28 - Map of Proterozoic bodies in the basement core of the Wind River Range based off Chamberlin et al. (2003). The South Pass Supracrustal Belt and Louis Lake Batholith flank the southeastern edge of the mountain range, within 25 km of South Pass and the Pinnacles.

expanded toward the basin margin (Nichols and Fisher 2013, Nichols and Fisher 2007).

Erosion at the lowest bounding surface may represent an intra formational unconformity although this is not biostratigraphically resolvable. Crossbedded sandstone lense complexes are overlain by several thick, stacked, laterally continuous sandstone sheets followed by several thin, tabular sandstone sheets and immature paleosol units (floodplain/basin fines).

Considering that the Continental Fault and Wind River Thrust (Reds Cabin Monocline) were active at the time, it is possible that the erosion at the basin margin prior to the lake incursion was influenced by local or regional tectonism. With the Pinnacles residing near the northern margin of the Great Divide Basin, unconformities in the strata were likely influenced by movement on the Wind River Thrust. Pebble conglomerates, chert, feldspar and sand-sized biotite lithics are attributed to relative immaturity of the coarse sediment. The southeastern flanks of the Wind River Range are comprised of the volcanic and metamorphic complex of the South Pass Supracrustal Belt and the Louis Lake Batholith (Fig. 3.28). The South Pass Supracrustal Belt is mafic to ultramafic and consists of dacite, andesite, iron formation, schist, amphibole and quartzite (Frost et al. 2006). The Louis Lake Batholith is composed of diorite, granodiorite and granite (Frost et al. 2000). Louis Lake batholiths and South Pass Supracrustal Belt could have been sediment sources considering their proximity to South Pass. Displacement of Eocene beds on the Wind River Thrust only discontinued after Cathedral Bluffs deposition (Steidtmann and Middleton 1991). Uplift on the Wind River Range prior to this arrest in activity might have provided the influx of immature sediment.

Craven (2006) interpreted the lowest paleosol unit in the Pinnacles section as the Lumen Member of the Green River Formation and the middle sand-dominated successionas part of the Niland Member of the Wasatch Formation.

The Lumen Member is dominated by laminated organic-rich shale with subordinate amounts of coquina and calcareous mudstone. These lithologies suggest a lacustrine to marginal lacustrine depositional environment (Swanson and Carlson 2002). Instead, the interval assigned by Craven (2006) to the Lumen Member is dominated by variegated, pedogenically altered claystone with tabular sandstone, indicative of low to moderately mature paleosols and crevasse splay sandstone beds. The lack of planar lamination within the claystone interval and the dominance of features such as clay skins, cutans, mottling and root traces support the paleosol interpretation. Large ripples, lack of mud matrix and stratigraphic continuity of the tabular quartz arenite beds suggests that these are crevasse splay deposits related to overbank events in a moderate-sized fluvial system. The lack of freshwater lacustrine fossils within the bed and abundant micaceaous lithics suggests that the sediment source is the same as that of the meandering stream channel successions elsewhere in the succession. The Niland Tongue is a fluvially-dominated unit dominated by carbonaceous to coaly claystone (Roehler and Martin, 1987) which differs substantively from the lithologies encountered in the study interval. Thus, the entire succession discussed hereinis allocated to the Main Body of the Wasatch Formation following earlier workers (Roehler 1991) and contrary to the findings of Craven (2006).

During accommodation and base level changes, environments of deposition shifted from distal floodplain/alluvial plain to eroding meandering rivers,back to alluvial plain, and finally lacustrine shoreface, cyanobacterialmound/reef and proximal offshore. The Pinnacles buttes exemplify facies changes as the result of climatic shifts and tectonic activity onthe basin margin. Climaticlyand tectonicly (Smith et al. 2008, Pietras et al. 2003) induced regression of the Lumen member may have affected base level and erosion onthe basin margin. Laramide induced uplift of the southern Wind River Range, periodic movement on the Wind River Thrust Fault and the Continental Fault likelyinfluenced the degree of basinward migration of alluvial facies. Unroofing of Paleozoic sediments and the Precambrian core within the Wind River Range provided carbonate, quartz, biotite and feldspar rich sediments to the northern fringe of the basin. In the study area this is reflected in immature biotite and feldspar-rich sediments in fluvial channel sandstone beds. Grey-green to variegated paleosols and immature sediment in channel fills signifies proximity to both the Wind River Mountains and Lumen-Niland deposition.

CONCLUSIONS

The uppermost Main Body of the Wasatch Formation is separated into two units. The lower unit is mud dominated and associated with variegated paleosols and thin sand beds of FA1. The above unit is associated with conglomeratic sheets and scoured sandstone lenses of FA2, FA3, and FA4.

Two horizons exist at the Pinnacles buttes which produce abundant mammal fossils of late Wasatchian age. Horizons A and B correspond to crevasse splay sheets and channel lense associations. The sequences identified in the fluvial succession indicate two lower bounding surfaces caused by erosion and subsequent fill by vertically and laterally aggregating streams. It is along these two bounding surfaces that fossils appear in highest abundance. Fossil horizon A correlates with the lowstand surface of erosion. During the erosive meandering stream phase, underlying sediment was reworked and amalgamated into the base of the channel deposits. Extremely high fossil abundance at such localities occurred from the cannibalization and concentration of underlying and adjacent fossiliferous paleosols.

The fossil z misc samples are angular to subangular fragments with minor amounts of surface and edge abrasion. Most catalogued specimens are not fragmented or abraded. Reworking within the channel point bar by smaller scours and chutes at high water stages is interpreted to havebeen a significant process by which fossilvertebrate material was concentrated in the Pinnacles area.

REFERENCES

Allen JRL. 1964. Studies in fluviatile sedimentation: six cyclothems from the Lower Old Redstone, Anglo-Welsh Basin. Sedimentology. 3:163-198.

Allen JRL. 1965. A review of the origin and characteristics of Recent alluvial sediments. Sedimentology. 5:89-191.

Behrensmeyer AK. 1978. Taphonomic and Ecologic Information from Bone Weathering. Paleobiology. 4(2):150-162.

Bradley WH. 1964. Geology of Green River Formation and associated Eocene rocks in southwestern Wyoming and adjacent parts of Colorado and Utah. United States Geological Survey Professional Paper 496-A:1-86

Buchheim HP, Brand LR, Goodwin HT. 2000. Lacustrine to fluvial floodplain deposition in the Eocene Bridger Formation. Palaeogeography, Palaeoclimatology, Palaeoecology. 162:191-209.

Catuneanu O, Galloway WE, Kendall C, Miall AD, Posamentier HW, Strasser A, Tucker ME. Sequence Stratigraphy: Methodology and Nomenclature. Newsletters on Stratigraphy. 44(3):173-245.

Carroll AR, Bohacs KM. 1999. Stratigraphic classification of ancient lakes: Balancing tectonic and climatic controls. Geology. 27(2): 99-102

Chamberlin KR, Frost CD, Frost BR. Early Archean to Mesoproterozoic evolution of the Wyoming Province: Archean origins to modern lithospheric architecture. Canadian Journal of Earth Science. 40:1357-1374.

Clyde WC., Zonneveld JP., Stamatakos J., Gunnell GF., Bartels WS. 1997. Magnetostratigraphy across the Wasatchian/Bridgerian NALMA Boundary (Early to Middle Eocene) in the Western Green River Basin, Wyoming. Journal of Geology. 105: 657-669

Clyde WC., Sheldon ND., Koch PL., Gunnell GF., Bartels WS. 2001. Linking the Wasatchian/Bridgerian boundary to the Cenozoic Global Climate Optimum: new magnetostratigraphic and isotopic results from South Pass, Wyoming. Paleogeography, Paleoclimateology, Paleoecology. 75: 175-199.

Cole RD, Picard MD. 1978. Comparative mineralogy of nearshore and offshore lacustrine lithofacies, Parachute Creek Member of the Green River Formation, Piceance Creek Basin, Colorado, and eastern Uinta Basins, Utah. Geological Society of America Bulletin. 89:1441-1454

Craven A. 2006. Aquatic biota as an indicator of palaeoenvironment around the Paleocene-Eocene Boundary, within the Great Divide Basin of southern Wyoming, USA. Curtin University of Technology, Department of Applied Geology. Curtin University of Technology Publishing, Perth, Australia:1-172

Dunham RJ. 1962. Classification of carbonate rocks according to depositional texture. Ham WE (ed). Classification of carbonate rocks. American Association of Petroleum Geologists Memoir:108-121.

El-attar HA, Jackson ML. 1973. Montmorillonitic soils developed in Nile River sediments. Soil Science. 116(3):191-201.

Ferguson RJ, Brierley GJ. 1999. Levee morphology and sedimentology along the lower Tuross River, south-eastern Australia. Sedimentology. 46: 627-648.

Fiorillo AR. 1988. Taphonomy of Hazard Homestead Quarry (Ogallala Group), Hitchcock County, Nebraska. Contributions to Geology, University of Wyoming. 26(2):57-97

Fisher JA, Nichols GJ. 2013. Interpreting the stratigraphic architecture of fluvial systems in internally drained basins. Journal of the Geological Society, London. 170: 57-65.

Flugel E. 2010. Microfacies of carbonate rocks: Analysis, Interpretation and Application. Second edition. Springer Heidelberg Dordrecht London New York:1-928.

Folk RL. 1974. Petrology of sedimentary rocks. Hemphill Publishing Company. Austin, Texas:1-180.

Endlich FM. 1879. Report on the Geology of the Sweetwater District. United States Geological and Geographical Survey of the Territories Report. Ed, FV Hayden. 11: 3-158.

Fremont JC. 1845b. Report of the exploring expedition to the Rocky Mountains in the year 1842 and to Oregon and north California in the years 1843-44. United States Congress, the Senate. Gales and Seaton Printers Washington, DC: 1-693.

Fremont JC. 1848. Map of Oregon and upper California from the surveys of John Charles Fremont and other authorities. Drawn by Charles Preuss. United States Congress, the Senate. Edward Weber and Co. Baltimore, Maryland. Scale 1:3000000.

Frost BR, Frost CD, Hulsebosch TP, Swapp SM. 2000. Origin of the Charnockites of the Louis Lake Batholith, Wind River Range, Wyoming. Journal of Petrology. 41(12):1759-1776.

Frost ER, Frost CD, Cornia M, Chamberlain KR, Kirkwood R. 2006. The Teton – Wind River domain: a 2.68-2.67 Ga active margin in the western Wyoming Province. Canadian Journal of Earth Science. 43:1489-1510.

Galloway WE, Hobday DK. 1996. Terrigenous clastic depositional systems: Heidelberg, Springer-Verlag, 489 p.

Gunnell GF, Bartels WS. 2001. Basin margins, biodiversity, evolutionary innovation, and the origin of new taxa. Gunnell GF. Ed. Eocene Biodiversity: Unusual occurrences and rarely sampled habitats. Topics in Geobiology Series. Kluwer/Plenum, New York: 403-440.

Gunnell GF., Murphy PC., Stucky RK., Townsend KEB., Robinson P., Zonneveld JP., Bartels WS. 2009. Biostratigraphy and Biochronology of the Latest Wasatchian, Bridgerian, and Uintan North American Land Mammal "Ages". Papers on Geology, Vertebrate Paleontology, and Biostratigraphy in Honor of Michael O. Woodburne. Museum of Northern Arizona Bulletin 65. 279-330.

Keighley D, Flint S, Howell J, Moscariello A. 2003. Sequence stratigraphy in lacustrine basins: a model for part of the Green River Formation (Eocene), Southwest Uinta Basin, Utah, USA. Journal of Sedimentary Research. 73(6):987-1006.

Hayden FV. 1869. Chapter 11, Review of Leading Groups, etc. Preliminary Field Report of the United States Geological Survey of Colorado and New Mexico. Washington, DC:89-99

Hickin EJ. 1993. Fluvial facies models: a review of Canadian research. Progress in Physical Geography. 17(2):205-222

Hunt RM Jr. 1978. Depositional setting of a Miocene mammal assemblage, Sioux County, Nebraska (USA). Palaeogeography, Palaeoclimatology, Palaeoecology. 24:1-52.

Jackson RG. 1976. Depositional model of point bars in the Lower Wabash River. Journal of Sedimentary Geology. 46: 579-594.

Keighley D, Flint S, Howell J, Moscariello A. 2003. Sequence stratigraphy in lacustrine basins: a model for part of the Green River Formation (Eocene), Southwest Uinta Basin, Utah, USA. Journal of Sedimentary Research. 73(6):987-1006.

Kraus MJ. 1987. Integration of channel and floodplain suits, II Vertical relations of alluvial paleosols. Journal of Sedimentary Petrology. 57(4): 602-612.

Kraus MJ. 1999. Paleosols in clastic Sedimentary rocks: their geologic applications. Earth Science Reveiws. 47: 41-70.

Love JD, Christiansen AC. 1985. Geologic Map of Wyoming. U. S. Geological Survey, 1: 500,000

MacMahon JA, Mull JF, Crist TO. 2000. Harvester Ants (Pogonomyrmex SPP.): Their community and ecosystem influences. Annal Review of Ecology and Systematics. 31: 265-291.

Miall AD. 1977. A review of the braided-river depositional environment. Earth Science Reviews. 13:1-62.

Miall AD. 1978. Lithofacies types and vertical profile models in braided river deposits: a summary. Fluvial Sedimentology. Ed, AD Miall. Canadian Society of Petroleum Geologists, Memoir 5:597-604.

Miall AD. 1985. Architectural-element analysis: a new method of facies analysis applied to fluvial deposits. Earth Science Reviews. 2:261-308.

Miall AD. 1988. Facies architecture in clastic sedimentary basins. Ed, K Kleinspehn, C Paola. New Perspectives in basin analysis. Springer Verlag, New York, New York:67-81.

Miall AD. 1996. The Geology of Fluvial Deposits: Sedimentary Facies, Basin Analysis and Petroleum Geology. Springer:1-582.

Nace RL. 1939. Geology of the Northwest part of the Red Desert, Sweetwater and Fremont Counties, Wyoming. Geological Survey of Wyoming Bulletin 27:1-51.

Neumann AM., Bartels WS., Gunnell GF., Zonneveld JP. 2010. Comparison of Lostcabinian (Late Early Eocene) mammalian assemblages from the Green River and Wind River Basins, Wyoming. Geological Society of America Abstracts with Programs. Denver, Colorado. 42(5): p. 464

Nichols GJ, Fisher JA. 2007. Processes, facies and architecture of fluvial distributary system deposits. Sedimentary Geology. 195:75-90.

Ori GG. 1982. Braided to meandering channel patterns in humd-region alluvial fan deposits, River Reno, Po Plain (northern Italy). Sedimentary Geology. 31: 231-248.

Pietras JT, Carroll AR and Rhodes MK. 2003. Lake basin response to tectonic drainage diversion: Eocene Green River Formation, Wyoming. Journal of Paleolimnology. 30: 115-125.

Platt NH, Wright VP. 1991. Carbonates: facies models, facies distributions and hydrocarbon aspects. 13: 57-74.

Posamentier HW, Vail PR. 1988. Eustatic controls on clastic deposition. II Sequence and systems tract models. Sea Level Changes – An intergrated approach. Wilgus CK, Hastings BS, Kendall CGStC, Posamentier HW, Ross CA, Van Wagoner JC. SEPM Special Publication. 42: 125-154.

Roehler HW. 1991. Revised stratigraphic nomenclature for the Wasatch and Green River Formations of Eocene Age, Wyoming, Utah and Colorado. US Geological Survey Professional Paper 1506-B: 1.38.

Roehler HW. 1992. Introduction to the Greater Green River Basin. Geology, Physiography and History of Investigations. United States Geological Survey Professional Paper 1506-A:A1-A14

Roehler HW. 1993. Eocene climates, depositional environments and geography, Greater Green River Basin, Wyoming, Utah and Colorado. US Geological Survey Professional Paper 1506-F. p. F1-F72.

Roehler HW, Martin PL. 1987. Geological Investigations of the Vermillion Creek Coal Bed in the Eocene Niland Tongue of the Wasatch Fomation, Sweetwater County, Wyoming. US Geological Survey Professional Paper 1314A-L: 1-202.

Smith EM, Carroll AR, Singer BS. 2008a. Synoptic reconstruction of a major ancient lake system: Eocene Green River Formation, western United States. Geological Society of America Bulletin. 120(1/2):54-84.

Smith JJ, Hasiotis ST, Kraus MJ, Woody DT. 2008b. *Naktodemasis bowni*: new ichnogenus and ichnospecies for adhesive mensicate burrows (AMB) and paleoenvironmental implications, Paleogene Willwood Formation, Bighorn Basin, Wyoming. Journal of Paleontology. 82(2):267-278.

Smith JJ, Hasiotis ST, Kraus MJ, Woody DT. 2008c. Relationship of floodplain ichnocoenoses to Paleopedology, Paleohydrology and Paleoclimate in the Willwood Formation, Wyoming, during the Paleocene-Eocene Thermal Maximum.

Steidtmann RJ, Middleton LT. 1991. Fault chronology and uplift history of the southern Wind River Range, Wyoming: Implications for Laramide and post-Laramide deformation in the Rocky Mountain foreland. Geological Society of America Bulletin. 103: p. 472-485.

Stucky RK, Krishtalka L, Redline AD. 1990. Geology, vertebrate fauna and paleoecology of the Buck Spring Quarries (early Eocene, Wind River Formation), Wyoming.

Swanson BA, Carlson KJ. Walk, wade, or swim? Vertebrate traces on an Early Permian Lakeshore. Palaios. 17(2): 123-133.

Tanavsuu-Milkeviciene K, Sarg JF. 2012. Evolution of an organic-rich lake basin – stratigraphy, climate and tectonics: Piceance Creek basin, Eocene Green River Formation. 59:1735-1768.

Tsukui K, Clyde WC. Fine-tuning the calibration of the early to middle Eocene geomagnetic polarity time scale: Paleomagnetism of radioisotopically dated tuffs from Laramide foreland basins. Geological Society of America Bulletin. 124(5/6): 870-885.

Van Regenmorter J., Anemone R. 2008. Biostratigraphy of the Freighter Gap and Pinnacles areas, Great Divide Basin, southwestern Wyoming. Journal of Vertebrate Paleontology. 28 (3 supplement):156A.

Voorhies MR. 1969. Taphonomy and population dynamics of the early Pliocene vertebrate fauna, Knox County, Nebraska. Contributions to Geology, University of Wyoming, Special Paper 1:1-69.

Wheeler GC, Wheeler J. 1988. A checklist of the ants of Wyoming (Hymenoptera: Formicidae). Insecta Mundi. 2(3-4): 231-239.

White JA, Munn LC, Williams SE. 1989. Edaphic and Reclamation Aspects of Vesicular-Arbuscular Mycorrhizae in Wyoming Red Desert Soils. Soil Science Society of America Journal. 53:86-90.

Woodburne MO, Gunnell GF, Stucky RK. 2009. Land mammal faunas of North America rise and fall during the Early Eocene Climatic Optimum. Denver Museum of Nature and Science Annals, No 1, p. 1-74.

Zeller HD, Stephens EV. 1969. Geology of the Oregon Buttes Area Sweetwater, Sublette and Fremont Counties Southwestern Wyoming. United States Geological Survey Bulletin 1256:1-60.

Zonneveld JP, Bartels WS, Clyde WC. 2003. Stratal Archetecture of an Early Eocene Fluvial-Lacustrine Depositional System, Little Muddy Creek

Area, Southwestern Green River Basin, Wyoming. Cenozoic Systems of the Rocky Mountain Region. Ed Raynolds RG, Flores RM. Rocky Mountain SEPM, Denver, Colorado. 253-287.

CHAPTER FOUR

CONCLUSIONS

The objective of this study was to describe the fossil assemblage in the latest Wasatchian time interval from a unique geological setting in the basin margin of the Green River Basin. The descriptions provided on specimens from the Pinnacles add to the overall knowledge of genera known from the Lostcabinian. 46 genera and 30 families compose the mammalian assemblage.

The Pinnacles assemblage was recovered from the southeasternSouth Pass region on the northwest rim of the Great Divide Basin. The presence of brontothere*Lambdotheriumpopoagicum* and the absence of Gardnerbuttean index taxa such as *Eotitanops borealis, Hyrachyus*and *Trogosus* identifies the age of the assemblage as Lostcabinian (late Wasatchian; Wa7). In addition, the overlapping ranges of several other taxa such as *Palaeanodon, Copeleumur, Loveina, Trogoleumur, Artimonius* and *Northarctus*also confine the age to the latest Wasatchian (Woodburne et al 2009, Gunnell et al. 2009).

The Pinnacles assemblage overall is not as diverse or well preserved at the Lostcabinian type section in the Wind River Basin (Buck Springs Quarry, Lost Cabin member, Wind River Formation) (Stucky 1984, Stucky et al. 1990). The Pinnacles contain a less diverse sample of insectivores, more diverse sample of omomyids, with the absence of multituberculates, *Phenacodus, Shoshonius, Alveojunctus* and *Uintasorex.*

The Wasatchian/Bridgerian boundary in South Pass occursbetween Fossil horizon A at the Pinnacles and the first appearance of the *Eotitanops borealis* (Gunnell et al. 2009) Br1a representative in the Cathedral Bluffs at Honeycomb Buttes and Bush Rim. Based on paleomagneticanalyses of rocks sampled in the South Pass area by Clyde et al. (2001), the Wasatchian-Bridgerian boundary occursaround 52.2 Ma (Cr23r). The precise stratigraphic location of the

Wasatchian-Bridgerian contact cannot be ascertained from current fossil data from the Main Body at the Pinnacles although it can be narrowed down to at, or near the contactbetween the Main Body of the Wasatch Formation and the Scheggs Bed of the Tipton Shale Member, Green River Formation. The occurrence of *Lambdotherium* near Red's Cabin Monocline in the Farson sandstone (Roehler 1991) suggests that the end of the Wasatchian lies within the lower Tipton member. Further prospecting at the top of the Pinnacles section may provide more data to support this conclusion. Ongoing work in the Green River and Uinta basins in the future will better document the immense faunal change and effect of climate change during the Early Eocene Climate Optimum on the rise of modern mammals.

Several methods of fossil accumulation interact to provide the level of fossil abundance that characterizes the Pinnacles buttes. The presence of proximal channel facies associations such as point bars, crevasse splays and basal gravel lags coincides with dense horizons A and B. A likely accumulation scenerio involved the consolidationof surface remains and the erosional exhumation of older buried remnants into a contemporaneous depositional system. Local reworking within the chute-modified point bars, purged coarse lags into small scours and concentrated gravel and fossils into pocketed bonebeds. Lastly the anthills further reconcentrated scattered and buried material into a discretelocations, concentratingthe smallest elements of the succession (i.e. those that the ants could carry) into discrete surface accumulations.

Though the collection represents a diverse array of taxa, the quality of many samples is poor and fragmented, albeit with minimal surface abrasion. The comparative abrasion between SP 74 and SP75 is slightly different with the channel locality (SP75) represented by large, spheroidal fragments. Chute reworking in the point bar setting is a method of concentrating bone debris into discrete pockets while minimizing the effects of transport.

Fossil horizons A and B are also coincident with bounding surfaces in the succession that may represent lowstand erosional surfaces from fluctuating fluvial base level (*sensu* Roehler 1993, Catuneanu et al. 2010). Fossil horizon A rests at the base of incising meandering stream bar sandstone complexes that separate the Main Body at this site into two units: a lower mud-dominated paleosol unit and a higher sand-dominated proximal channel unit. A third lacustrine unit, dominated by calcareous sand, grainstone, micrite and carbon-rich shale is identified at the top of the section. This unit is seperatedfrom the channel deposits by a lacustrine flooding surface thatmarks the formational boundary between the Main Body of the Wasatch Formation and lower Scheggs bed, Tipton shale, Green River Formation.

Knowledge of the stratigraphic occurrence of fossils in this section of the Wasatch Formation is essentialfor future collectors and authors working in the Green River or Great Divide Basin and is crucial for analyses of climate change on vertebrate faunas in central North America. The association between fossil horizons and tecoupled occurrence of channel scours and conglomeratic sheets provides a geologic basis for future fossil prospecting. Further fossil recovery in this area willprovide more information by which to compare faunas from the Wasatchian and Bridgerian and may potentially lead to the discovery of additional new genera.

REFERENCES

Anemone RL, Dawson MR, Beard KC. 2012. The Early Eoence Rodent *Tuscahomys* (Cylindrodontidae) from the Great Divide Basin, Wyoming: Phylogeny, Biogeography and Paleoecology. Annals of the Carnegie Museum. 80(3):187-205.

Clyde WC., Sheldon ND., Koch PL., Gunnell GF., Bartels WS. 2001. Linking the Wasatchian/Bridgerian boundary to the Cenozoic Global Climate Optimum: new magnetostratigraphic and isotopic results from South Pass, Wyoming. Paleogeography, Paleoclimateology, Paleoecology. 75: 175-199.

Gunnell GF. 2012. New Uintasoricine (?Primates, Plesiadapiformes) from the Earliest Bridgerian, Latest Early Eocene of Wyoming. Journal of Paleontology. 86(6):973-978.

Gunnell GF., Murphy PC., Stucky RK., Townsend KEB., Robinson P., Zonneveld JP., Bartels WS. 2009. Biostratigraphy and Biochronology of the Latest Wasatchian, Bridgerian, and Uintan North American Land Mammal "Ages". Papers on Geology, Vertebrate Paleontology, and Biostratigraphy in Honor of Michael O. Woodburne. Museum of Northern Arizona Bulletin 65. 279-330.

Roehler HW. 1991. Revised stratigraphic nomenclature for the Wasatch and Green River Formations of Eocene Age, Wyoming, Utah and Colorado. US Geological Survey Professional Paper 1506-B: 1.38.

Stucky RK, Krishtalka L, Redline AD. 1990. Geology, vertebrate fauna and paleoecology of the Buck Spring Quarries (early Eocene, Wind River Formation), Wyoming.

Stucky RK. (1998). Eocene bunodont and bunoselenodont Artiodactyla ("dinobunids"). Evolution of Tertiary Mammals of North America Volume 1: Terrestrial Carnivores, Ungulates and Ungulatelike Mammals. Ed. Janis CM, Scott KM, Jacobs LL. Cambridge University Press, New York.

Woodburne MO, Gunnell GF, Stucky RK. 2009. Land mammal faunas of North America rise and fall during the Early Eocene Climatic Optimum. Denver Museum of Nature and Science Annals, No 1, p. 1-74.

APPENDIX A

A.1 – ARTIODACTYLA

A.1.1 – *Bunophorus* sp.

Specimen number	Description	Width	Length	Remarks
103529	Left m1	-	-	Broken anterior cingulum, tiny hypoconulid and paraconid
104496	Left P3	-	-	
115684	Left p4	-	-	
103538	Right MX	7.35	6.45	Small hypocone
104524	Right astragalus	-	-	
104698	Right MX	7.90	5.65	Cusps completely worn
109065	Right m1	-	-	Broken hypoconid and paraconid
(associated?)	Right p4	-	-	
112101	Right p4	-	-	
112133	Left M1	6.30	5.70	Small hypocone
112174	Right M2	8.10	5.60	
116245	Left m3	5.95	8.35	Elongate talonid
115810	Right m3	5.10	7.45	
116100	Right m3	5.85	8.60	Elongate talonid
116263	Left P3, Left P4 unassociated			
115724	Left p3			
115725	Left m1	5.30	6.00	

A.1.2 – *Bunophorus sinclairi*

Specimen number	Description	Width	Length	Remarks
104530	Right m1	6.45	7.30	Large hypoconid and tall metaconid, very bulbous cusps, medial trough

A.1.3 – *Diacodexis* sp.

Specimen number	Description	Width	Length	Remarks
103524	Left M1	4.95	4.00	
104687	Right M1	4.95	3.60	Cusps completely worn
104692	Left p3	-	-	
109050	Right M3	5.70	4.20	
112117	Right p4	-	-	
112137	Left m1	-	-	Broken trigonid
112193	Left M3	4.95	3.20	
115162	Left m2	3.55	4.20	
115163	Left MX	-	-	Broken paracone
115702	Right M1	4.65	3.75	Tiny cusp on posterior side of protocone, cusps on posterior and anterior cingula
111902	Left P4	-	-	
115834	Left p4	-	-	
116109	Right M3	5.65	3.95	Cusps on posterior and anterior cingula
116255	Right m2		3.80	Labial side buried in quarry block
112863	Right M3	5.50	4.30	
112879	Left m3	2.70	4.60	No paraconid, posteriorly protruding hypoconulid
115183	Left P4	-	-	
115723	Left P4	-	-	
112837	Left M3	5.55	3.90	Cusps completely worn
116123	Left M3	5.70	4.25	

A.1.4 - *Hexacodus pelodes*

Specimen number	Description	Width	Length	Remarks
104490	Right M1 or M2	5.05	4.25	
115165	Left p4			Twinned paraconid
116246	Right M1 or M2	5.10	4.10	Broad cingulum
116271	Right MX	4.90	3.40	Small hypocone
115653	Left m1	3.05	4.20	
115656	Left MX	4.25	2.80	Tiny hypocone, strong preprotocrista
115886	Right m2	2.80	3.65	

A.1.5 – *Antiacodon vanvaleni*

Specimen number	Description	Width	Length	Remarks
104700	Right p3			
115718	Left m2	4.05	4.95	Narrow trigonid
115746	Right M1	6.30	5.05	Small hypocone, strong pre and postprotocrista
116103	Right p4			
115196	Left m1	3.15	3.75	Distinct paraconid, worn metaconid

A.2 – CARNIVORA

A.2.1 – *Vulpavus* sp.

Specimen number	Description	Width	Length	Remarks
115194	Right m2	2.60	3.55	Tall protoconid, dinstinct paraconid, twinned metaconid, narrow talonid, distinct anterior cingulum, serration on entocristid

A.2.2 – *Vulpavus australis*

Specimen number	Description	Width	Length	Remarks
103532	Right dentary m2	3.20	4.30	Total length of dentary fragment 16.35; heavy wear on cusps, low talonid, large protoconid, distinct paraconid
112170	Right M2	6.60	3.65	Posteriolingual hypocone, labially protruding parastyle, broad lingual cingulum
116251	Left M2	4.40	2.15	Overall elongate, hypocone lingual to protocone, labally protruding parastyle

A.2.3 – *Miacis* sp.

Specimen number	Description	Width	Length	Remarks

115121	Right p4	1.55	4.60	Tall sectoral protoconid, metaconid taller and larger than paraconid

A.2.4 – *Miacis latidens*

Specimen number	Description	Width	Length	Remarks
104688	Left M2	7.10	4.60	No hypocone, strong pre and postprotocrista, paracone larger than metacone, distinct metastyle, strong postparacrista and labially protruding parastyle

A.2.5 – *Uintacyon* sp.

Specimen number	Description	Width	Length	Remarks
115779	Left m3	1.45	1.85	Very small and reduced, tall trigonid, distinct paraconid, no entoconid or hypoconulid, small talonid

A.2.6 – *Viverravus* sp.

Specimen number	Description	Width	Length	Remarks
115730	Right M1	10.35		Broken paracone, very elongate trigon basin
105195	Left M2	3.65	1.70	Distinct pre and post cingula
109071	Right p4	2.20	5.90	Low worn cusps, metaconid and

				paraconid small
112103	Right m2 (or m3?)	2.15	4.15	Distinct paraconid, elongate talonid, serrated entocristid
115713	Left M1	6.10	3.70	Paracone larger than metacone, strong preprotocrista and postparacrista with labially protruding parastyle
115765	Right p3	1.50	5.45	Low worn cusps, metaconid larger than paraconid
116247	Right P4	6.70	3.40	Tall protocone with crest-like hypocone, metacone larger than paracone
108048	Left P4	6.10	3.20	Large protocone, crest-like hypocone, protruding paracone
112893	Right p4	1.60	4.55	Metaconid larger than paraconid
116125	Left p4	1.60	4.65	Metaconid larger than paraconid
116126	Left m1			Buried in quarry block, tall paraconid
116127	Right M1 fragment			Broken paracone, distinct pre and postcingula
116136	Left m2	1.60	2.70	Tall inflated trigonid, low talonid, distinct paraconid, protoconid taller than metaconid
116272	Left m1	2.80	5.10	Tall inflated trigonid, distinct labially protruding paraconid, sharp paracristid, low talonid
112854	Left p3	1.50	3.60	Medially placed protoconid
112856	Right p3			Broken metaconid
115112	Left p3	1.30	3.65	Tall protoconid, metaconid larger than indistinct paraconid
115875	Left p2			Broken metaconid
115887	Left M2	3.10	4.90	Low indistinct cusps with strong preprotocrista, postprotocrista and postparacrista with labially protruding prastyle

A.2.7 – *Didymictis* sp.

Specimen number	Description	Width	Length	Remarks
116275	Right mX trigonid	-	-	Distinct lobate paraconid, strong paracristid, protoconid taller than metaconid

A.3 – CIMOLESTA

A.3.1 – *Apatemys* sp.

Specimen number	Description	Width	Length	Remarks
105199	Right M1	2.70	2.45	Distinctly triangular, anteriorly protruding parastyle, posteriorly protruding metastyle and distinct hypocone
116278	Right I1	-	-	
115111	Left I1	-	-	
115123	Left I1	-	-	
115660	Left i1	-	-	
115847	Left I1	-	-	
115150	Right I1	-	-	

A.3.2 – *Didelphodus* sp.

Specimen number	Description	Width	Length	Remarks
115832	Left m3	1.85	2.95	Inflated trigonid, worn cusps
115127	Right m3	1.90	2.85	Tall trigonid, distinct hypoconulid
115652	Left m3	1.90	3.10	Tall trigonid, inflated protocone, reduced talonid

A.3.3 – *Paleosinops* cf. *P. lutreola*

Specimen number	Description	Width	Length	Remarks
115819	Right M3	-	-	Small hypocone and labially protruding paracone, buried in quarry block
116254	mX	-	2.90	Tall trigonid, buried in quarry block
115132	Left P3	3.55	2.25	
116092	Left m1 or m2	2.70	4.10	Distinct cusps, tall trigonid

A.4 – CONDYLARTHRA

A.4.1 – *Hyopsodus* sp.

Specimen number	Description	Width	Length	Remarks
103528	Left M2	5.60	4.25	
103534	Left dentary p3-4	p3=1.60, p4=1.85	p3=2.40, p4=2.60	Total length of dentary 7.35
104491	Left M2	5.50	4.25	
104492	Right M1	4.85	4.10	
104494	Right mX	2.29	2.95	
104498	Left M3	5.10	3.85	
104500	left MX	-	-	likely M1, broken protocone and paracone
(unassociated)	left p2 or p3	-	-	Broken
	left mX (m1?)	2.65	3.45	
	left mX (m1?)	2.60	3.75	
103545	Left M2	5.80	4.35	
103550	Right dP4	-	-	
104516	Right P4	-	-	
104517	Left M2	5.75	4.10	white silt in between conules
104519	Left M2	4.65	3.20	
104525	Right mX	3.10	3.85	slight lingual protruding of entoconid, possibly m1
104527	Right mX	2.90	3.45	Total length of dentary fragment 4.20; anteriorlaterally compressed talonid, possibly m2
104528	Left P3	-	-	
104531	Left M2	5.20	3.40	
104532	Right MX	4.65	3.20	
104533	dentary p3	1.50	2.20	Total length of dentary fragment 6.75
104685	Left M3	4.60	3.40	

104699	Right M2	5.80	4.30	
104900	Left M2	5.05	3.20	
104901	Left MX	5.10	3.55	
109028	Right m1	2.55	3.40	
109048	Left m2	3.45	4.55	
109051	Right m3	2.65	3.60	
109057	Right M2	4.45	3.20	
109059	Left m3	2.70	5.00	
109062	Right m1	3.50	4.10	
109064	Left M1	5.20	3.95	
109070	Left M3	4.70	3.45	
109072	Right P4	-	-	
112094	Left m3	2.85	4.90	
112096	Left MX	6.10	4.30	heavy wear, broken metacone
112102	Left mX	3.40	4.30	broad talonid, anterior crest with tiny paraconid bump
112104	Left MX	4.90	3.50	
112105	Left mX	-	-	broken hypoconid
112106	Left mX	3.10	3.75	slightly expanded talonid, possibly m1
112107	Right M3	4.10	2.85	
112124	Left p4	-	-	
112135	Right mX	3.35	3.95	lingually protruding entoconid, possibly m1; vertebrate in capsule with molar, associated?
112139	Left MX	3.80	2.80	slightly oblique, possibly M2
112171	Left MX	3.55	4.35	heavily worn cusps
112178	Left MX	-	-	very small, broken metacone and paracone
112179	Right mX	2.85	3.90	bulbous steep cusps, possibly m2
112184	Left mX	2.45	3.15	slightly broad talonid and posteriolingually offset entoconid, m1
112186	Left P3	-	-	
112194	Right mX	3.00	3.60	broad talonid, protruding entoconid, possibly m1
112195	Right m3	2.10	3.70	
112197	Right M1	4.25	3.25	
112198	Left P4	-	-	
112200	Left mX	3.60	4.60	slightly expanded talonid, possibly m1
115164	Left m1	2.80	3.40	
115688	Right M3	4.80	3.45	
115689	Right M3	4.95	3.35	
115690	Left MX	4.80	3.65	
115696	Left MX	6.65	4.40	
115703	Left MX	3.80	3.00	
115704	Left mX	2.40	3.60	anterior crest with bump, broad talonid

115706	Left p4	-	-	
115707	Right MX	4.60	3.45	right MX possibly M2
115708	Left M3	4.95	3.30	
115709	Left P2	-	-	
115710	Left MX	5.05	3.45	heavily worn, possibly M1
115711	Right M3	3.95	2.90	
115714	Right P3	-	-	
115715	Left M3	4.70	3.55	
115736	Right mX	2.50	3.25	broad talonid, anterior crest and bump, white silt in talonid
115738	Right MX	5.65	4.15	
115739	Left MX	4.60	3.60	
115750	Right m1	3.60	5.25	
115757	Right p4	-	-	
115758	Right MX	4.75	3.30	fine sand and silt cemented between cups
115759	Right m2	3.60	4.60	
115760	Right MX	4.65	3.15	
115764	Left M3	4.90	3.35	
115767	Right M3	3.55	2.55	
108042	Left mX	2.60	3.40	m1? Small, but has steep cusps like m2
108043	Left mX	3.60	4.10	bulbous cusps but lingually protruding entoconid, possibly m1
111906	Left P4	-	-	
112886	Left P3	-	-	
112891	Right MX	4.55	3.65	
112894	Right p4	-	-	
115215	Left M2	6.15	4.10	
115786	Right MX	4.30	3.55	
115789	Left p4	-	-	
115803	Left m3	3.05	5.01	
115817	Right mX	3.20	4.10	quadrate shape, possibly m2
115818	Right m3	-	-	m3 buried in quarry block
115821	Left P4	-	-	In block from quarry
115823	Left mX	-	-	buried in quarry block
115824	Left P3	-	-	
115828	Left p4	-	-	
115829	Right dp4	-	-	
115836	Right m3	2.50	4.20	
115838	Left m3	3.10	5.50	medium quartz sand and white silt clast cemented around crown, enough tooth exposed to take measurement
116098	Right MX	4.20	3.15	
116102	Right p4	-	-	
116105	Right MX	-	-	broken hypocone, fine sand under crown
116108	Right mX	3.05	3.90	quadate shape, possibly m2
116112	Left MX	4.05	3.20	
116122	Right m2	3.60	4.10	
116130	Left MX	3.70	3.10	

116132	Right M3	4.70	3.10	
116133	Left MX	4.80	4.10	
116135	Left m3	2.65	3.95	
111919	Right mX	2.25	3.15	broad talonid, possibly m1
111921	Left MX	4.75	3.55	
111922	Left m3	2.30	3.90	
111923	Left MX	3.95	3.15	
111924	Right M3	4.20	2.70	
111931	Left mX	2.35	3.10	m1?
111932	Left MX	4.50	3.55	
111936	Left M3	4.90	3.50	
111943	Right mX	2.55	3.35	talonid slightly wider than trigonid, possibly m1
111948	Right m3	-	-	broken protoconid and metaconid
112850	Right P4	-	-	
112852	Right dp4	-	-	
112853	Right p4	-	-	
112855	Right P3	-	-	
112860	Right P4	-	-	
112862	Left mX	3.20	3.85	wide talonid, lingually protruding entoconid, possibly m1
112867	Right P4	-	-	
112870	Left m3	-	-	worn hypoconid and metaconid
112871	Left mX	-	-	broken hypoconid and hypoconulid
112876	Right m3	2.40	4.15	
112878	Left P2	-	-	
112925	Right MX	-	-	broken protocone, paracone and metacone
112926	Right MX	4.50	3.20	
112927	Right MX	6.10	4.15	
112928	Left MX	-	-	broken protocone and hypocone
115092	Unassociated lot			Anthill wash
115186	Left MX	5.45	3.70	
115201	Left P3	-	-	
115657	Left M3	3.55	2.70	
115658	Left p4	-	-	
115661	Right M3	4.30	3.20	
115665	Right m3	2.25	3.55	
115666	Left MX	4.25	3.10	
115669	Left P4	-	-	
115672	Right m1	2.35	3.40	
115674	Left M3	4.10	2.80	
115675	Right M3	3.50	2.45	
115676	Left MX	5.10	3.90	
115843	Left M3	4.95	3.65	
115850	Left dp4	-	-	
115851	Left P3	-	-	
115854	Right M3	5.15	3.55	
115856	Left p4	-	-	
115857	Right M3	4.90	3.95	

115860	Left M1	4.20	3.35	
115870	Right P3	-	-	
115874	Right P4	-	-	
115876	Left mX	2.60	3.30	slightly broad talonid, anterior crest with bump
115881	Left P3	-	-	
115884	Left M3	4.60	3.10	triple rooted, listed as M3 but could be either p3 or p4
115885	Right MX	4.20	3.40	very worn
116086	Left M1 or M2	4.40	3.45	
116090	Right M3	4.70	3.55	
116093	Right MX	3.80	3.05	
116095	Right M3	4.65	3.20	
112076	Left m1	2.30	2.95	
112077	Left P4	-	-	
112941	Right MX	3.85	2.95	heavily worn
112081	Left m3	2.50	3.70	
112166	Left m3	3.40	5.15	
115153				
115155	Right M2	6.20	4.00	coarse sand with white silt clasts cemented around roots
115801	Left MX	4.15	3.20	
112838	Right mX	3.10	4.25	rectangular, possibly m1?
112840	Left M3	4.55	2.75	
112843	Left MX	4.30	3.15	
112844	Right m3	2.25	3.90	
115773	Left p4	-	-	
115776	Left m1	2.35	3.20	
115782	Right m1	2.40	3.15	
115784	Right MX	4.60	3.70	
115151	Right MX	6.70	4.30	
108047	Right M3	3.90	2.65	
109014	Right M1	3.95	2.60	
109026	Right P3	-	-	
115149	Left MX	4.20	3.20	

A.4.2 – *Meniscotherium* sp.

Specimen number	**Description**	**Width**	**Length**	**Remarks**
115733	Left m1	7.30	-	Fractured metaconid and protoconid
107995	Left MX fragment	-	-	Fractured posterior surface
107996	Left m1 talonid	-	-	Fractured trigonid, distinct cusp on posterior side of metaconid

111899	Left M3	10.70	8.90	Lingually protruding parastyle and mesostyle
111916	Left M3	9.40	11.90	Broad cingulum, distinct, mesostyle and parastyle
115888	Left dentary p4-m2	p4=5.20 m1=6.20 m2=6.35	p4=7.45 m1=7.80 m2=8.05	Total length of dentary 30.75; Heavily worn teeth, no hypoconulid, trigonid and talonid produces triangular crests
112939	Left M3	11.65	-	Large bulbous cusps, distinct conules, mesostyle and crista, no hypocone, fractured metacone
115769	Right m1	5.60	8.50	

A.5 – CREODONTA

A.5.1 – *Prolimnocyon antiques*

Specimen number	Description	Width	Length	Remarks
104495	Left m1 or m2	3.70	6.40	Very tall inflated trigonid and low talonid, distinct paraconid with vertical crest protruding lingually from parconid, protoconid and metaconid broken, small hypoconid, serrated postcristid

A.5.2 – *Tritemnodon whitiae*

Specimen number	Description	Width	Length	Remarks

116260	Left c1	5.65	7.50	19 mm tall excluding root, posteriorly curved, large

A.6 – LEPTICTIDA

A.6.1 – *Palaeictops* sp.

Specimen number	Description	Width	Length	Remarks
116282	left mX	-	-	worn or broken trigonid, possibly m1 because of small precingulid
116261	fractured right MX	-	-	broken, shallow talon, short hypocone and protocone
112931	left m3	1.65	2.65	anterioposteriorly elongate talonid, very tall and sharp protoconid and metaconid
115093	right M1	4.35	3.85	distinct hypocone, deep talon, small parastyle, protruding postmetacrista
115095	right p3	-	-	
115097	right m1 or m2	1.80	2.65	worn but distinct paraconid
115098	right m1 or m2	1.75	2.65	cusps worn or broken, paraconid present
115099	left m1 or m2	1.90	2.40	hypoconulid and entoconid tall, paraconid and metaconid completely worn down
115108	right P4	-	-	
115115	right m1 or m2	1.80	2.60	distinct sharp cusps, paraconid present, tall entoconid, hypoconulid and hypoconid
115198	right p4	-	-	
115844	left M1	4.05	2.30	broken hypocone and preparacrista making length shorter as measured
116088	left p3	-	-	

116096	left m2	1.80	2.65	completely worn or absent paraconid, protoconid and metaconid sharp, little wear
112923	left m2	2.12	2.70	paraconid is present, distinct cristid oblique, tall protoconid and metaconid

A.6.2 – *Prodiacodon* sp.

Specimen number	Description	Width	Length	Remarks
115808	left m2	2.10	3.60	tall narrow trigonid with paraconid, broad talonid with protruding hypoconulid and bulbous entoconid. A very tiny <0.2mm cusp exists anteriolingually to the entoconid

A.7 – ERINACEOMORPHA

A.7.1 – *Scenopagus* sp.

Specimen number	Description	Width	Length	Remarks
105185	Right m3	1.00	1.50	Tall trigonid, anterior crest and tiny paracondi, protruding hypoconulid
105186	Left mX	0.75	1.30	Tall trigonid, distinct paraconid, reduced talonid
105198	Right dentary m1	0.95	1.45	Tall entoconid, paraconid present, tall trigonid
105207	Left p4			
116138	Left MX	2.00	1.15	Tiny conules, distinct hypocone,

				postparacrista
115096	Left MX	2.00	1.50	Distinct hypocone, tiny conules
115114	Left M1 or M2	1.50	0.95	Distinct hypocone and tiny conules
115116	Left P4			
115852	Left dentary p4-m2 (p3-p4?)	=0.35 =0.70	=0.95 =1.30	Total length of dentary 3.90
116315	Left MX	1.55	1.15	Distinct hypoconid, anteriorly protruding parastyle
116322	Right mX (m2)	1.75	2.45	Tall trigonid, distinct paraconid, low talonid, large compared to other specimens
(unassociated)	Right mX (m3)	1.65	2.80	Elongate talonid, protruding hypoconulid, tall trigonid, anterior crest, large compared to other specimens

A.7.2 – *Talpavus* sp.

Specimen number	Description	Width	Length	Remarks
115125	Right m1	0.80	1.40	Sharp anterior crest with small paraconid, distint talonid cusps, metaconid taller than protoconid

A.8 – MARSUPIALIA

A.8.1 – *Herpetotherium* sp.

Specimen number	Description	Width	Length	Remarks
105182	Right mX trigonid	-	-	Broken talonid
105189	Right mX	1.65	2.40	Heavily worn

105203	Left mX	1.25	2.45	Narrow trigonid, anteriorly protruding paraconid, lingual hypoconulid
116248	Left MX	-	-	Broken paracone and metacone
115094	Right MX	2.10	2.45	Wide protocone, broad shelf on metacone
115100	Left MX	2.75	2.65	Broad metacone shelf and parastyle
115156	Right MX	3.10	3.30	Broad metacone shelf and tiny conules

A.8.2 – *Peradectes* sp.

Specimen number	Description	Width	Length	Remarks
105193	Left MX (right?)	1.75	1.10	Labially protruding paracone (metacone if right)
115089	Left dentary m3-m4 talonid	0.45	1.05	Total length of dentary 8.85; distinct paracond, reduced talonid
115119	Right mX	0.70	1.25	Tall hypoconid and protoconid
115131	Right m4	0.50	1.25	Total length of dentary fragment 3.00; very tall paraconid (metaconid) and hypoconid, elongate and open talonid
116021	Right maxilla MX	1.10	0.95	Three cusps, labially protruding metacone

A.9 – CETE

A.9.1 – *Hapalodectes* sp.

Specimen number	Description	Width	Length	Remarks
104691	P3	4.65	5.40	Small lingual cusps, wide trigon basin
(associated?)	P4	5.40	-	Broken paracone, compressed rounded cusps, wide trigon basin, distinct protocone and hypocone
111926	Left mX	1.25	3.95	Compressed cusps, slightly pointed, small cusp on anterior crest
115766	Left p3	1.80	3.10	Slightly pointed paraconid
115218	Right mX	1.35	4.55	Rounded protoconid and metaconid, no talonid
116110	Right P3	2.60	3.60	Distinct hypocone, tall metacone
112080	Right m2	1.70	6.20	Rounded compressed cusps, paraconid larger than metaconid

A.10 – PALAEANODONTA

A.10.1 – *Palaeanodon* sp.

Specimen number	Description	Width	Length	Remarks
116283	Metatarsal II			
116128	Dentary fragment			19 mm part of mandibular ramus, no teeth
116257	Left c1			
116265	Metacarpal II			
112100	Metatarsal fragment			
115814	Right c1			
112875	Distal radius			

A.11 – PERISSODACTYLA

A.11.1 – *Hyracotherium* sp.

Specimen number	Description	Width	Length	Remarks
103525	Left p3	-	-	
103526	Left p4	-	-	
103530	Unassociated left and right astragalus	-	-	
103540	right M2			
103542	right M3	8.10	6.95	
103546	Left p2	-	-	
103549	left M3	3.75	5.80	
104502	left m1 or m2	4.55	7.10	
104505	Right P2	-	-	
104515	left M1 or M2	8.80	7.25	
104520	right M3	8.00	6.85	
104523	right m3	4.85	10.45	protocolnid broken but length still measureable
104529	Left P3	-	-	
104680	right m1	4.20	6.60	
104681	right M3	7.70	6.60	completely worn cusps, protocone and hypocone replaced by shallow basin
104682	right M3	8.05	6.20	cusps completely worn, tooth is shallow basin
104683	left m3	-	-	broken
104686	Left P4 fragment	-	-	
104696	left M2	8.90	7.10	
104697	right m1	-	-	broken right mX trigonid
104701	Left P1	-	-	
107981	Right p3	-	-	
107983	broken right mX trigonid	-	-	
107988	left M2	8.30	7.20	
107991	Right P2	-	-	
109005	Right m3	4.30	8.85	
109022	Left dp4	-	-	
109024	Right m3	4.40	8.65	
109025	Right M3	8.45	7.01	
109045	left M1	8.45	6.80	very strongly developed ectoloph, protoloph and metaloph
109049	Left p4	-	-	

109053	Left I1	-	-	
109055	Distal tibia		-	
109069	right m1	4.70	7.25	
111912	Left P4	-	-	
111917	right dentary p3-4	p3=3.15 p4=5.55	p3=6.10 p4=8.60	total length of dentary is 21.15
111950	Left p2	-	-	
112082	Left P3	-	-	
112084	Left M1	7.90	6.85	
112085	Right M1	7.80	7.15	
112086	left MX	p	p	broken
112088	right MX	8.50	7.15	well developed protoloph and metaloph
112089	left MX	9.35	8.15	M2 or M1
112090	left MX	8.70	7.20	M2, assessory cusp anteriolabially to the paracone
112093	right MX	8.20	6.90	
112095	Right P2	-	-	
112098	left MX	-	-	broken
112125	Right p3	-	-	
112126	Left m1	4.05	6.60	
112132	Left dP4	-	-	
112134	left MX	8.40	6.95	lophate paraconule and oblique tooth, possibly M3 but intensely worn
112167	Right p3	-	-	
112172	right m1	5.25	7.55	
112173	Right dP4	-	-	
112202	Left dP4	-	-	
112848	Right dp3	-	-	
112861	Right dp4	-	-	
115154	Left m3	5.05	9.65	
115160	right m1	4.80	6.70	
115683	right MX			Fractured
115685	Right dP3	-	-	
115691	right mX	4.60	6.50	
115692	left MX	8.35	6.65	protoloph strongly developed
115694	left M3	8.00	7.05	
115698	Left P3	-	-	
115705	left MX	8.10	7.05	broken paracone, but does not impare measurement
115726	left m1	8.60	7.40	
115727	Left MX	8.55	7.10	protocone broken, does not impare measurement

115731	Right p4	-	-	
115734	Left p3	-	-	
115743	Right M1	8.50	7.05	
115744	Right dp4	-	-	
115752	Left p4	-	-	
115754	Right P3	-	-	
115755	Right p4	-	-	
115756	Left dp4	-		
115805	left M1	8.10	7.00	
115809	right m1	4.55	7.20	
115822	Left p3	-	-	In block of Gom conglomerate
115826	Left P3	-	-	
115830	Left MX	8.75	7.10	
115833	Left m3	5.80	10.20	anteriorly compressed hypoconulid, possibly *H. vasacciense*
115861	Right pX	-	-	
116101	Right p4	-	-	
116111	left M1	6.85	5.00	
116114	Right astragalus	-	-	
116119	Left M3	8.65	7.25	
116121	Left p4	-	-	
116137	right m1	4.35	6.25	
116139	left m3	5.50	9.85	
116140	right m2	5.45	7.65	
116141	left m1	4.80	7.55	
116143	left dentary fragment p1-2	p1=1.90 p2=3.15	p1=5.35 p2=6.45	total length of dentary is 14.55
116249	Right dP4	-	-	
116266	Right dp4	-	-	
116274	Right dP4	-	-	

A.11.2 – *Orohippus* sp.

Specimen number	**Description**	**Width**	**Length**	**Remarks**
112839	Right dp2?	2.20	4.60	Elongate, large protoconid (no metaconid), distinct paraconid, entoconid and hypoconid

A.11.3 – *Lambdotherium popoagicum*

Specimen number	Description	Width	Length	Remarks
103527 (associated?)	Left P2	8.20	7.95	
	Right P3	10.00	8.85	
	Right M3	16.80	12.95	
112118	Right m3	8.10	15.95	Fine sand between cusps
107976	Left astragalus			White silt in between trabiculae
111907	Right p4	7.25	9.95	
111913	Left M3	17.80	13.05	Fine sand under crown
115807	Left M1	14.65	12.65	
115825	Right mX	-	12.20	Broken paraconid and hypoconid
116113	Right m1 or m2	9.40	12.90	
116118	Left p4	6.60	8.90	In green silt clast
116262	Left P3	10.50	9.45	
116267	Right m3	9.00	17.00	Medium sand and silt clast under crown

A.11.4 – *Helaletes* sp.

Specimen number	Description	Width	Length	Remarks
115728	Right mX	-	-	Broken paraconid, entoconid and hypoconid

A.11.5 – *Heptodon*

Specimen number	Description	Width	Length	Remarks
115192	Left p4	6.55	9.55	Heavily degraded on labial side
112165	Left m1	6.60	10.10	

A.12 – PLESIADAPIFORMES

A.12.1 – *Microsyopsps* sp.

Specimen number	Description	Width	Length	Remarks
104510	Left m3	2.35	3.75	
104690	Right dp4	-	-	
105197	Right m3	2.50	3.80	enamel completely worn off cusps
105201	Right P3	-	-	
107990	Left dP4	-	-	
108049	Left M1	-	-	Fractured or sheared paracone and metacone
108050				
109058	Left M3	3.90	3.50	small hypocone and parastyle, indistinct metastyle
109061	Left M1	3.90	3.65	extreme wear on the labial side of the tooth, shearing off the paracone
109067	Left m2	2.60	3.75	Medial hypoconulid, indistinct mesoconid and low paraconid
111900	Right m1	2.90	3.60	large linguomedial hypocone, distinct paraconid
111903	Right m1	2.20	3.20	distinct paraconid, hypoconulid pair to entoconid
111910	Left m1	2.05	3.45	Medially placed hypoconulid
111920	Right M1	4.45	3.65	tiny hypocone, conules and mesostyle
111929	Left dp4	-	-	
111933	Right m2	2.20	3.15	no protoconid, linguomedial hypoconulid, worn
111935	Right m3	2.45	4.60	Posteriolabially placed hypoconulid and distinct paraconid
111937	Left M1	3.85	3.30	small hypocone, indistinct mesostyle and metastyle, fine sand cemented between the paraconule and metaconule

111938	Left m2	1.80	2.85	distinct paraconid relative to small tooth, paired ligual entoconid and hypoconid
111945	Left m2	2.85	3.45	low paraconid, low medially placed hypoconulid
112091	Right m3	2.60	4.60	low tiny paraconid, grouped hypoconulid and entoconid, mesoconid present, tiny bump between hypoconid and hypoconulid
112119	Right dp4	-	-	
112123	Left m3	-	-	hypoconulid broken
112138	Left p4	2.55	3.65	Heavily worn deuterocone and posteriorly centered hypoconulid
112177	Left p4	2.15	3.55	medially located hypoconulid
112190	Right p4	2.45	3.45	indistinct hypoconulid
112866	Right p4	2.15	3.10	
112868	Right p4	1.65	2.90	molarform, indistinct medial hypoconulid
112869	Right M3	3.65	3.10	no hypocone, very tiny conules and stylar cones
112877	Left m1	2.35	3.10	tall trigonid, low paraconid. Lingually placed hypoconulid
112885	Left m2	2.60	3.55	Coupled hypoconulid and entoconulid
112888	Right p4	2.00	3.05	steep deuterocone, narrow precingulum, hypoconulid closer to entonconid than hypoconid
112889	Left m1	2.75	3.60	low paraconid, hypoconulid closely paired with entoconid
112892	Left M1	3.55	3.10	no hypocone or mesostyle, tiny

				metaconule and metastyle
112895	Left M1	3.80	3.20	distinct hypocone, mesoconid and metastyle
112896	Right M1	3.60	4.30	indistinct hypocone and conules, extreme wear on labial cingulum
112897	Left m1	2.90	4.05	very low trigonid (protoconid and mesoconid equiheight), distinct paraconid, medial hypoconulid
112920	Right M1	3.35	3.10	low hypocone, metastyle and mesostyle, distinct relative to the small tooth size
112930	Left M3	3.70	3.15	no hypocone, indistinct metaconule and metastyle, tiny mesostyle
112933	Left m1	2.20	3.45	short trigonid, steep unworn cusps
112934	Right M1	3.75	3.10	distinct hypocone, extreme wear on the labial side, sheared at centrocrista
112940	Left m1	2.25	3.20	large bulbous mesoconid, distinct paraconid, closely approximated entoconid and hypoconulid
115091	right MX or P4 (or even dP4?)	3.30	2.65	small non descript, worn cusps, lacking metaconule, paraconule and hypocone
115091 Unassociated lot	left P4	3.50	3.15	closely approximated paracone and metacone, enamel worn off
115091	left inscisor	-	-	
115091	left p4	2.15	3.20	white silt cemented in talonid
115091	left M3	3.45	3.40	mesostyle present, tooth a oblique

				angle, distinct protostyle
115091	right M1 or M2	4.10	3.20	no mesostyle
115091	right m1 or m2	2.35	3.50	wide talonid, tiny mesoconid and paraconid, hypoconulid paired to entoconid
115091	right p4 or m1	2.25	3.45	
115091	right p4 or m1	1.50	2.50	heavily worn, hypoconulid and entoconid closely paired, distinct parconid
115091	right m3	2.20	3.90	posteriolingually projecting hypoconulid
115091	right p2	-	-	
115091	canine	-	-	
115091	m 1 or 2	2.20	3.20	indistinct hypoconulid
115091	left p4	2.95	3.10	
115091	left M3?	-	-	broken cingulum
115091	left M3	3.10	2.70	
115091	P4 or dP4?	3.20	3.05	
115091	left p2	-	-	
115091	right m1	2.40	3.40	indistinct hypoconulid, worn crista
115091	left M1 or M2	4.10	3.35	degraded enamel
115091	right M3	3.20	2.70	no hypocone or conules
115091	right P4	3.55	2.70	
115091	left m1 or m2	2.25v	3.15	
115091	left mX	-	-	broken protocone and mesoconid
115091	left MX	-	-	broken metacone and paracone
115091	right m1	2.20	3.20	distinct anterior protruding paraconid and closely paired hypoconid and entoconid
115144				
115181	Right i1	-	-	
115184	Right p4	2.40	3.80	medial hypoconulid
115191	Left p4	2.15	3.75	
115195	Right M1	2.60	2.50	low paraconid, indistinct linguomedial hypoconulid
115216	Right m3	2.65	4.10	low paraconid, hypoconid worn,

115217	Right M2	3.80	3.15	large linguall hypoconulid distinct metastyle on the postmetacrista
115219	Left p4	2.45	3.65	medially placed and distinct hypoconulid
115654	Right M1	-	-	broken paracone
115655	Right M3	3.55	2.90	no hypocone, extreme wear on labial side on the metacone
115662	Left m2	-	-	Fractured hypoconulid and entoconid
115679	Left distal calcaneum	-	-	
115682	Right m1	2.30	3.40	distinct paraconid, no hypocone on postcingulum (or broken off?)
115712	Right M1	3.60	3.15	tiny hypocone, metaconule and mesostyle
115735	Right dentary m3	2.65	4.60	total dentary length of 10.14; distinct paraconid, low hypoconid, large lingual hypoconulid
115741	Left m2	2.85	3.70	low paraconid, low to no hypoconulid
115747	Left M1	3.60	2.75	no hypocone, conules or stylar cusps
115761	Right M1	4.35	3.55	small but present mesostyle
115762	Right m3	2.55	4.30	no parconid on precigulm and linguomedially placed hypoconulid
115780	Left p4	1.70	2.80	molarform, medially placed tiny hypoconulid between mesoconid and entoconid
115787	Right m2	2.55	3.50	worn protoconid and mesoconid, linguomedial hypoconulid
115788	Right M1	4.65	3.85	low hypocone and parastyle, indistinct mesostyle

115806	Right m3	2.65	4.25	tall shallow trigonid, linguomedially positioned hypoconulid
115835	Right i1	-	-	
115845	Right m2	2.90	3.60	low paraconid, linguomedial hypoconulid
115849	Left dP4	-	-	
115855	Right m3	2.15	3.75	low paraconid, linguomedial hypoconid
115862	Right M2	4.10	3.40	enamel degraded, distinct metastyle and mesostyle, parastyle present
115863	Right dP4	-	-	
115867	Left M3	3.55	3.10	indistinct hypocone, tiny mesostyle, metaconule and metstyle
115871	Right m2	2.65	3.40	low paraconid, linguomedially positioned hypoconulid
115873	Right m2	2.90	4.15	indistinct paraconid, tiny medial hypoconulid
115878	Right M3	4.25	3.75	no hypocone or conules, protocone completely worn off
116094	Left m2	2.40	3.70	low paraconid, medial postitoned hypoconulid
116116	Left m2	2.65	3.95	indistinct paraconid, low lingually placed hypoonulid
116120	Left M3	3.95	3.60	tiny hypocone, metastyle and mesostyle present
116134	Right M1	4.05	3.20	low hypocone, no metastyle, distinct mesostyle and parastyle
116145	Left m3	2.65	4.40	shallow trigonid, hypoconulid ligually next to entoconid, fine sand cemented in talonid

116253	Left m2	2.60	3.40	low paraconid, tiny mesoconid, hypoconulid paired with entoconid
116279				
116622	Left M1	4.10	3.45	distinct hypocone and metastyle
109007	Right M1	4.05	3.20	indistinct hypocone, cusps worn
109027	Left M1	3.45	2.90	low hypcone, indistinct mesostyle
109029	Right m2	2.10	2.95	low entoconid and hypoconulid, forms a crest
109012	Right p4	2.30	3.80	indistinct medially placed hypconulid
115228	Right m2	2.50	3.15	distinct hypoconulid, worn cusps
112916	Left mX	2.65	3.60	heavily worn cusps, no paraconid

A.12.2 – *Microsyops knightensis*

Specimen number	Description	Width	Length	Remarks
103548	left m2	2.65	3.60	tall trigonid, low paraconid, linguomedially placed hypoconulid
115107	right M1	3.70	3.10	enamel worn off
103544	right p4	2.10	3.25	molarform
103543	left M1	4.10	3.45	distinct hypoocone, metaconule and paraconule, tiny metastyle and mesostyle

A.12.3 – *Niptomomys* sp.

Specimen number	Description	Width	Length	Remarks
115763	Right dentary p4	0.60	1.10	Total length of

116314	Left m2	0.80	0.90	dentary 6.55 Narrow trigonid, no paraconid, wide talonid, lingually placed hypoconulid

A.12.4 – *Phenacolemur* sp.

Specimen number	Description	Width	Length	Remarks
111901	Left MX	3.55	2.90	Broad posterior cingulum
115804	Left M1	2.60	2.00	Broad postcingulum and no conules
115118	Right m3	1.10	2.55	Tall metaconid and trigonid, elongate talonid, inflated hypoconulid
115126	Left dentary fragment m2	1.60	1.95	Total length of dentary fragment 2.65, tall trigonid, no paraconid, distinct lingual cingulum
116074	Left M3	2.20	1.40	Tiny hypocone, inflated paracone
116316	Right MX	2.15	1.65	Broad posterior cingulum, no conules
116319	Right I1	-	-	
109008	Left m3	1.90	3.80	Tall metaconid, very wide bulbous hypoconulid

A.13 – PRIMATA

A.13.1 – *Notharctus* sp.

Specimen number	Description	Width	Length	Remarks
109056	Right m2	3.95	4.70	Narrow labial cingulum, narrow trigonid, wide talonid, small lingual paraconid

				and cusp on paracristid, cristid obliqua medially intersects the protocristid, indistinct hypoconulid, lingually protruding entoconid
109068	Left M2	6.45	4.45	Medially coupled hypocone and protocone, broad cingulum around tooth, distinct mesostyle, parastyle, metastyle, metaconule and paraconule
116252	Left m2	3.25	4.20	Low indistinct cusps, no paraconid, no hypoconulid, cristid obliqua extends anteriolabially to the base of the protoconid
116259	Right P4	4.65	3.45	
(unassociated lot)	Right m1 or m2	3.20	3.55	Low indistinct cusps, broad talonid, metaconid larger than paraconid, cristid obliqua intersects protocristid at base of the protoconid
	Left M1	6.10	3.55	Narrow cingulum, medially placed hypocone and protocone, distinct mesoconid, no metaconule, indistinct paraconule
	Left M2	5.60	4.15	Narrow cingulum, small hypocone, large metacone, metastyle, mesostyle, paraconule and metaconule present
116264	Left m3	3.15	5.40	Wear on

				protoconid and hypoconid, labially placed hypoconulid, three indistinct cusps on lingual crest, narrow precingulum
116276	Right m1	3.20	4.50	Narrow trigonid, wide talonid, large hypoconid, indistinct hypoconulid, distinct lingually situated paraconid with small cusp on the paracristid, metaconid taller than protoconid, cristid oblique meets protocristid at the base of the metaconid
116277	Right m3	3.05	5.05	Narrow precingulum aroung protoconid and hypoconid, posteriolabally protruding hypoconulid, sharp posteriolingual crest with three indistinct cusps, very short cristid oblique which extends to the base of the protoconid
115105	Right m3	2.95	5.30	Narrow precingulum around the protoconid and hypoconid, labially situated hypoconulid, protoconid worn and lower than metaconid, no entoconid, low and sharp posteriolingual crest, short cristid obiqua which intersects medially at the protocristid

A.13.2 – *Notharctus venticolus*

Specimen number	Description	Width	Length	Remarks
112192	Right p4	3.30	4.35	
115088	Left m1	3.20	4.20	
104506				
107977	Right MX fragment			Broken above the protocone
108041	Right dP4			
109020	Right M2	6.30	4.10	

A.13.3 – *Copelemur* sp.

Specimen number	Description	Width	Length	Remarks
112192	Right p4	3.30	4.35	
115088	Left m1	3.20	4.20	
104506				
107977	Right MX fragment			Broken above the protocone
108041	Right dP4			
109020	Right M2	6.30	4.10	

A.13.4 – *Cantius* sp.

Specimen number	Description	Width	Length	Remarks
112131	Left M1	5.60	4.15	
112140	Right m3	3.10	4.65	
112175	Right M3 (m3)	3.15	4.55	
112180	Right M3	5.35	3.60	
112185	Right M3	4.20	3.35	
112189	Right M3	3.95	2.70	
112196	Left m1	3.10	4.15	
115687	Left m1	3.20	4.15	
115697				
115748				
115749	Left m3	3.00		Broken hypoconulid
115753				
115213	Right M1	5.60	3.80	
115214	Right p4	2.20	3.55	

115831	Left m1			Broken talonid
111930	Right M1	5.70	3.60	
111934				
112880	Right M1	5.15	3.85	
112882	Distal phalanx			
112915	Right m3	2.70	4.65	
112929				
115187	Left P4	3.80	2.80	
115670	Left m1	3.15	3.95	
115840	Right m1	3.20	4.15	
115858	Right m3	3.10	5.35	
115859	Left M1	4.90	2.90	
115868				
115869	Right m1	3.10	4.00	
115872	Left M3	4.90	3.60	
112083	Left m1	3.20	4.25	
115158				
115777	Left MX	3.20	2.75	Heavily worn protocone and hypocone
115781				
115145				
116621	Left M3	4.60	3.10	

A.13.5 – *Cantius nunienus*

Specimen number	Description	Width	Length	Remarks
103539				
103541	Right m3	3.20	5.55	
103547				
104684	Left m2	3.15	3.80	Heavy wear on cusps
112865	Right M3	3.10	4.60	
116317	Left m3	3.05	4.60	
116318	Left P4	4.20	3.10	
116320	Left m1	2.70	4.00	
115142				

A.13.6 – *Trogolemur*

Specimen number	Description	Width	Length	Remarks
111942	left dentary m3	0.90	1.80	Total length of dentary fragment 3.80; tall narrow trigonid, no

				paraconid, low posteriorly elongate talonid, metaconid taller than protoconid, labial hook on hypoconulid

A.13.7 – *Artimonius nocerai*

Specimen number	Description	Width	Length	Remarks
104501	Left m3	1.35	2.10	Tall and narrow trigonid, lingually placed paraconid, elongate talonid posteriolabial hook on hypoconulid
104678	Right dentary m2	1.75	2.10	Total length of dentary 12.20; tall and narrow trigonid with lingual paraconid, wide talonid, indistinct hypoconulid
109063	Right dentary m2-3	m2=1.80, m1=1.20	m2=1.90, m1=1.75	Total length of dentary 9.50; tall and narrow trigonids, lingual paraconid on m2, no paraconid on m3, labial cingulum on m2-3, posteriorly expanded talonid with posteriolabially hooked hypoconulid, no hypoconulid on m2
109011	Left maxilla M2	3.60	1.90	Total length of maxilla 4.85; lingually elongate protocone, no hypocone, narrow pre- and postcingula, paraconule and

				metaconule present

A.13.8 – *Absarokius* sp.

Specimen number	Description	Width	Length	Remarks
116268	Right dentary m2	1.90	2.15	Total length of dentary 4.10; very tall and narrow trigonid, no paraconid, small protoconid and metaconid, no hypoconulid, narrow labial cingulum, short cristid obliqua
116269	Left p4	2.10	2.20	
116270	Left M1 fragment			Broken protocone, metastyle an parastyle present, tiny conules

A.13.9 – *Absarokius gazini*

Specimen number	Description	Width	Length	Remarks
115745	Left p4	2.00	1.85	

A.13.10 – *Anemorhysis* sp.

Specimen number	Description	Width	Length	Remarks
115220	Left M1	2.85	1.80	Lingually elongate protocone, tiny metaconule and paraconule
115837	Left M2	2.80	1.65	Tiny paracone and metacone, no metaconule and

				paraconule

A.13.11 – *Anemorhysis sublettensis*

Specimen number	Description	Width	Length	Remarks
115101	Left M1	2.05	1.50	Sharp postprotocrista, very tiny metastyle and conules
115109	Right M1	2.85	1.75	Sharp pre and postprotocrista, tiny conules
115110	Left m1	1.65	2.30	Tall trigonid, distinct paraconid, large metaconid posterior to protoconid, labial hypoconulid (or twinned hypoconid)
115113	Right M2	3.15	1.80	Broad posterior cigulum, lingually elongate protocone, tiny conules

A.13.12 – *Loveina* sp.

Specimen number	Description	Width	Length	Remarks
115700	Right m1	1.20	1.90	Small paraconid, no hypoconulid, tall trigonid, cristid obliqua medially intersects protocristid
105184	Right P4	2.15	1.15	

A.13.13 – *Loveina zephyri*

Specimen number	Description	Width	Length	Remarks

116030	Left m2	1.15	1.25	Tall trigonid, wide talonid, no paraconid, metaconid twinned and taller than paraconid, no hypoconulid, cristid obliqua intersects at base of protoconid

A.14 – RODENTIA

A.14.1 – *Sciuravus* sp.

Specimen number	Description	Width	Length	Remarks
105183	Left p4			
105188	Left mX	1.40	1.60	Mesoconid, low pointed cups
105190	Right p4			
105192	Left MX	1.35	1.35	Broad pre?cingulum
105200	Left MX	1.55	1.45	Conules present, broad postcinuglum
105205	Right P4			
105206	Right mX	0.90	1.05	Cusps worn down, metaconid and protoconid into lophs
108044	Right MX	2.15	1.70	Conules, mesostyle and parastyle present, quadrate
112849	Right mX	1.60	2.10	
112851	Right mX	2.10	2.15	Tall metaconid, no mesoconid
112857	Left p4			
112859	Left P4			
112918	Left p4			
112919	Right m1	1.65	1.95	Wide talonid, no mesoconid
112932	Left M1	2.15	2.20	Conules and mesostyle
112841	Right MX	2.35	1.95	

A.14.2 – *Paramys* sp.

Specimen number	Description	Width	Length	Remarks
105194	Right mX	2.10	2.30	Flat/worn?
105209	Right mX	2.25	2.90	
115770	Right m1	2.80	3.10	Distinct mesoconid

A.14.3 – *Microparamys* sp.

Specimen number	Description	Width	Length	Remarks
105204	Right mX	0.70	0.80	Wide shallow talonid, no hypoconulid or mesoconid
115719	Left mX	2.35	2.35	Wide talonid, hypoconulid and mesoconid
116104	Right M3	1.80	2.20	Very wide with conules, hypocone and anteriorly protruding parastyle
115128	Right m3	1.20	1.60	
115130	Left M1 or M2	1.30	1.15	precingulum
115651	Left m3	1.05	1.25	Flat worn cusps
115883	Left p4			
116087	Right p4			
115772	Left m1	1.20	1.40	Indistinct mesocnid

A.15 – TILLODONTIA

A.15.1 – *Esthonyx acutidens*

Specimen number	Description	Width	Length	Remarks
115815	Left i2	5.10	6.20	9.30 mm tall excluding root, robust and slightly curved, transverse crest

APPENDIX B

APPENDIX B.1 - Section 1001, Butte 2 of the North Pinnacles buttes. 42˚ 04’ 19’’ N 108˚ 42’ 32’’ and Section 1002 Butte 13 of the South Pinnacles buttes 42˚ 03’ 29’’ N 108˚ 42’ 46’’ W.

Measured by LP McHugh, J Schoengut, JP Zonneveld in 2010. Composed by ZP Zonneveld and AM Neumann

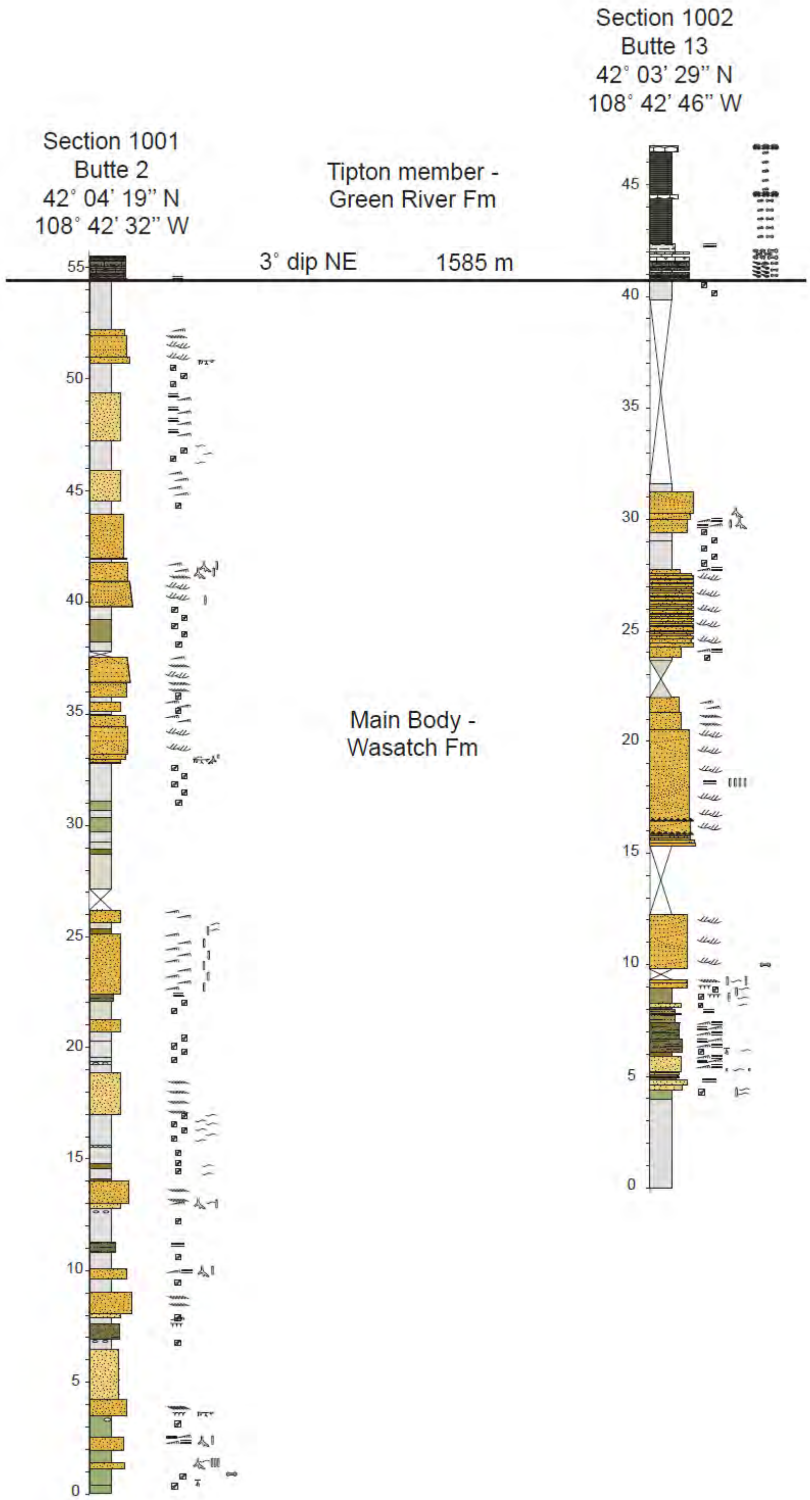

APPENDIX B.2 - Section 1101, Butte 1 of the North Pinnacles buttes. 42˚ 04' 21'' N 108˚ 42' 19'' W. Measured by C Hodgson, SP Cairns, AM Neumann in 2011; composed by AM Neumann

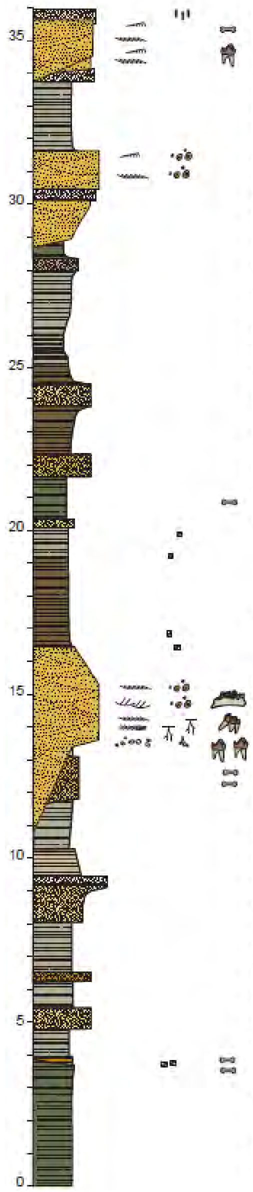

Coarse sandstone; quartz rich, mica lithics, vertical burrows; white, weathers red	0.46m
Fine to medium sandstone; tabular and trough crossbedding (4-12cm sets), outcrops only on south face of butte; golden to amber hue	1.40m
Medium sandstone; quartz rich, tabular, outcrops only on south face of butte; white, weathers red	0.40m
Medium to coarse sandstone; mica lithics, tabular and trough cross bedding, outcrops only at north face of butte; amber to golden hue	1.90m
Silt to sand; massive, exfoliated weathering, mica lithics; grey hue	2.10m
Medium to coarse sandstone; chert and mica lithics, trough cross bedding at top, large iron concretions (1-50cm); golden to amber hue	1.15m
Medium sandstone; quartz rich, tabular; white, weathers red	0.35m
Very fine to medium sandstone; coarsens upward, mica lithics, massive to cross bedded; tan to golden hue	1.18m
Silt to clay; fines upward, massive; grey hue	0.61m
Very fine sand; brown to yellow hue	0.35m
Silt; coarsens upward, massive; grey hue	1.95m
Clay; massive to bedded; grey hue, orange weathering	0.50m
Silt to clay; fines upward, massive; grey hue	0.43m
Sand to silt; fining upward, massive; brown to grey hue	0.61m
Fine to medium sand; mica lithics, quartz rich; yellow tan hue	0.70m
Silt to fine sand; coarsens upward, massive; grey to brown hue	1.48m
Fine to medium sand; mica lithics; yellow orange hue	0.70m
Silt to clay; massive; green grey hue	1.24m
Very fine to fine sand; quartz rich; yellow beige hue	0.32m
Silt; massive; brown at base and grey at top	3.60m
Medium to coarse sandstone; mica lithics, fining upward, parallel bedding at bottom overlain trough cross bedding, clay nodules, round to oval iron concretions (2-10 cm); amber to golden hue	5.67m
Medium to coarse sandstone; mica lithics, parallel and trough cross beds, iron concretions, clay clasts; golden to amber hue	1.25m
Silt; massive; grey hue, orange weathering	1.54m
Silt to fine sand; massive; tan hue	0.83m
Medium to coarse sandstone; tabular shaped; tan, weathers red	0.26m
Very fine sand; coarsens upward; tan hue	1.15m
Silt; massive; grey hue, orange weathering	1.52m
Fine to medium sand; mica lithics; yellow orange hue	0.25m
Silt; massive; grey hue	0.82m
Medium to fine sand; mica lithics; yellow orange hue	0.65m
Silt; massive; grey hue	0.85m
Silt to very fine sand; pedogenic mottling; grey hue, with variegated colors	1.15m
Silt; massive; green grey hue	1.48m
Silt; laminated, bioturbated; green grey hue	1.30m

APPENDIX B.3 - Section 1102 Butte 3 of North Pinnacles buttes. 42˚ 04’ 09.5’’ N 108˚ 42’ 38.5’’ W. Measured by C Hodgson, SP Cairns, AM Neumann, 2011. Composed by AM Neumann

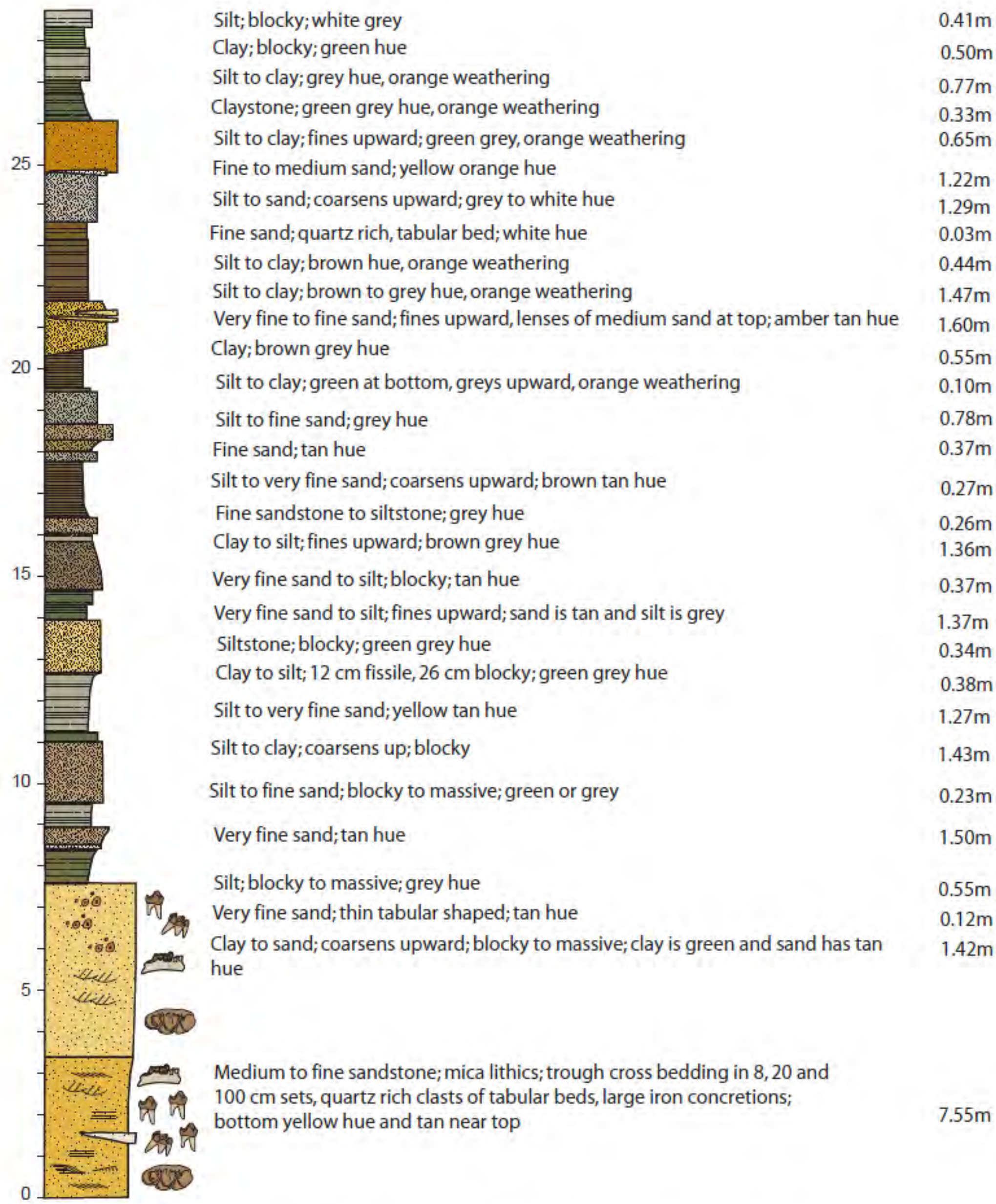

APPENDIX B.4 - Section 1103 Butte 4 of the North Pinnacles buttes. 42˚ 04’ 02’’ N 108˚ 42’ 45’’ W. Measured by C Hodgson, SP Cairns, LP McHugh, AM Neumann in 2011. Composed by AM Neumann

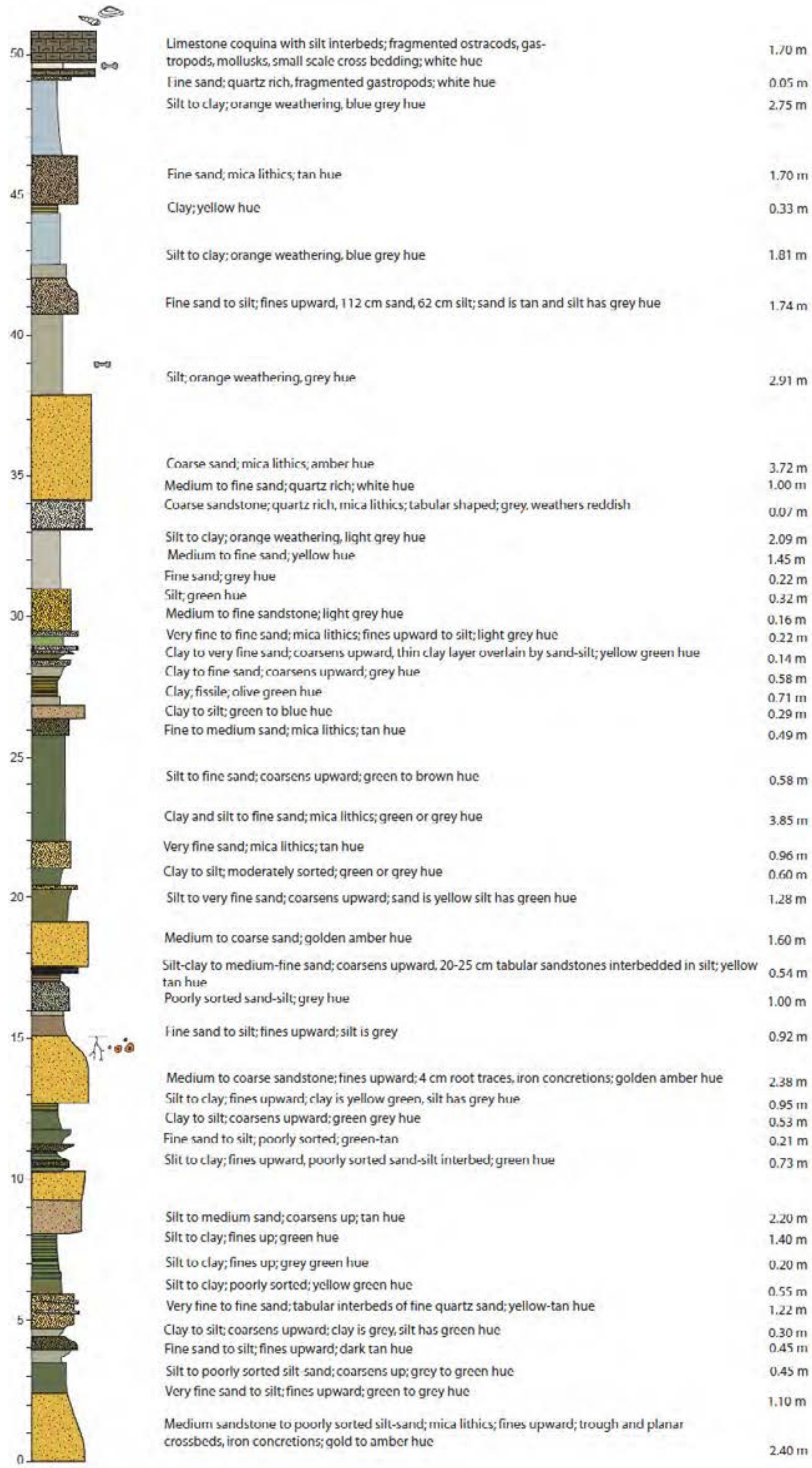

APPENDIX B.5 - Section 1104C Butte 5 of the East Pinnacles buttes. 42˚ 03' 46'' N 108˚ 41' 25'' W. Measured by C Hodgson, SP Cairns, LP McHugh, AM Neumann in 2011. Composed by AM Neumann, Section 1104 A at the Pinnacles quarry. 42˚ 03' 48'' N 108˚ 41' 22'' W. Measured by SP Cairns, LP McHugh in 2011. Composed by AM Neumann

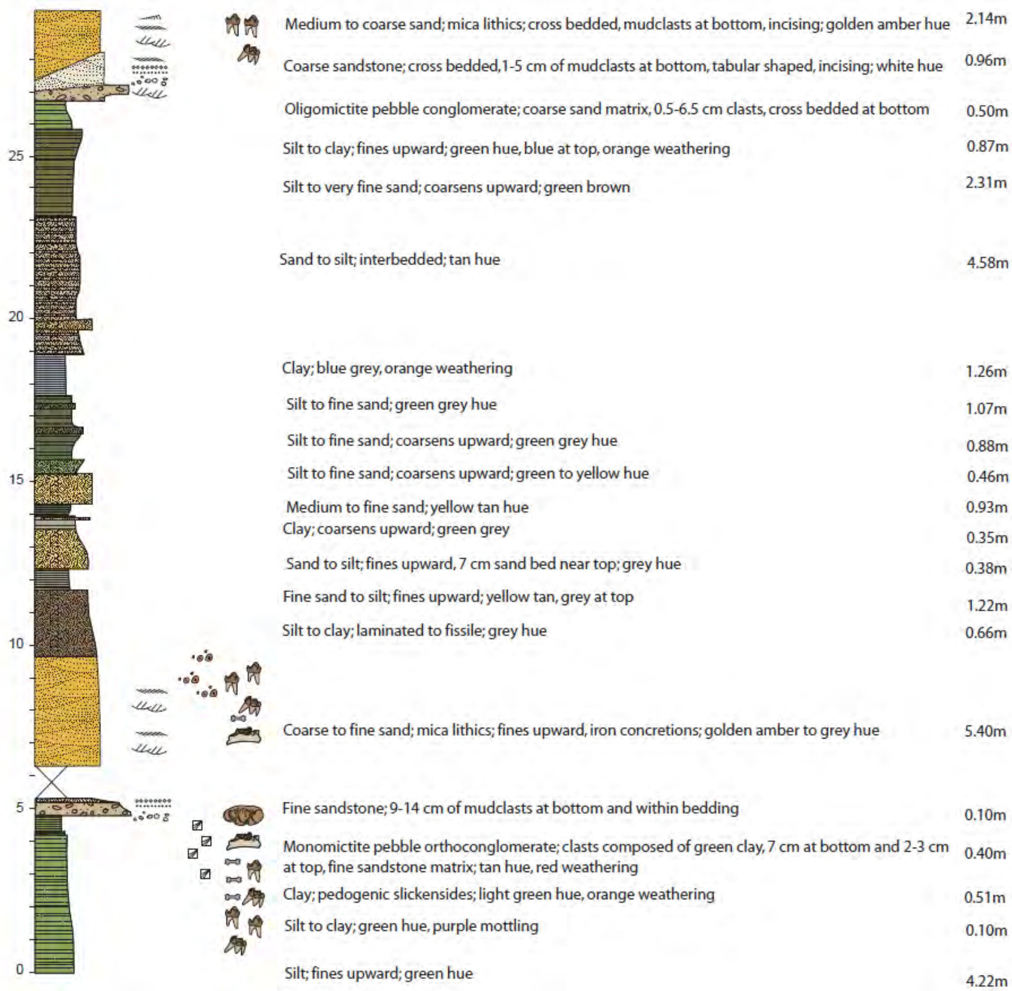

APPENDIX B.6 - Section 1104 B at the Pinnacles east quarry. 42˚ 03’ 52’’ N 108˚ 41’ 12’’ W. Measured by C Hodgson, AM Neumann in 2011. Composed by AM Neumann

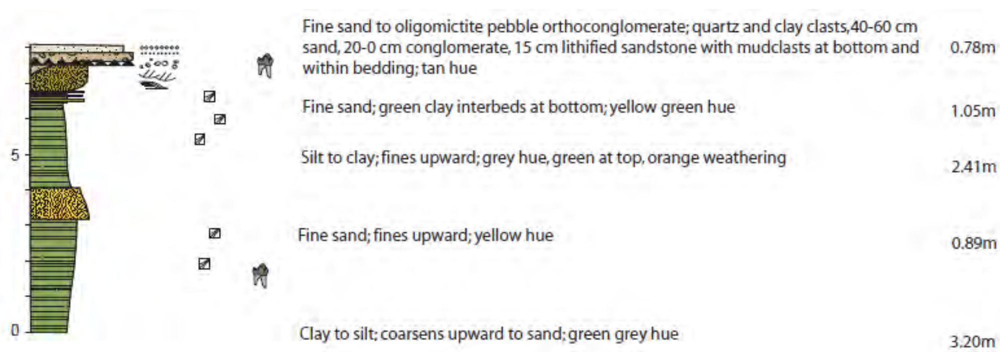

APPENDIX B.7 - Section 1105A Butte 6 of the East Pinnacles buttes. 42˚ 03’ 57’’ N 108˚ 41’ 37.5 W. Measured by SP Cairns, LP McHugh. Composed by AM Neumann

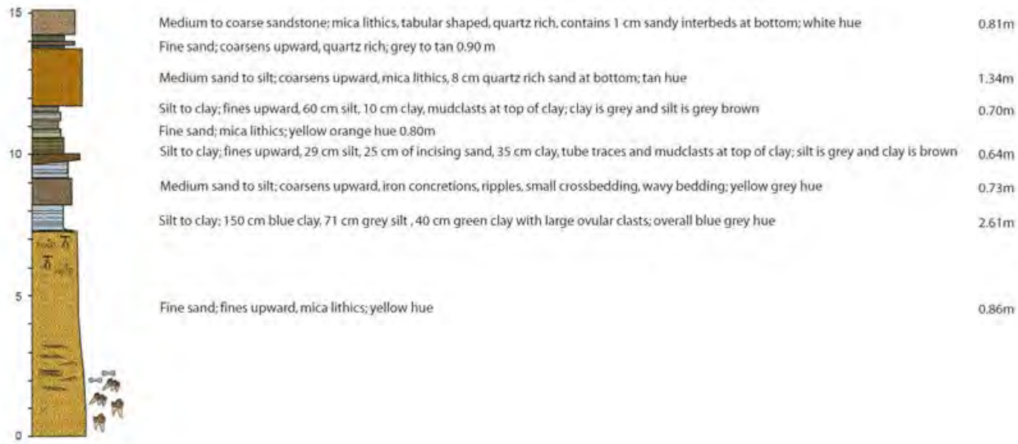

APPENDIX B.8 - Section 1105B Butte 7 of the East Pinnacles buttes. 42˚ 03' 48'' N 108˚ 41' 33'' W. Measured by SP Cairns, AM Neumann. Composed by AM Neumann

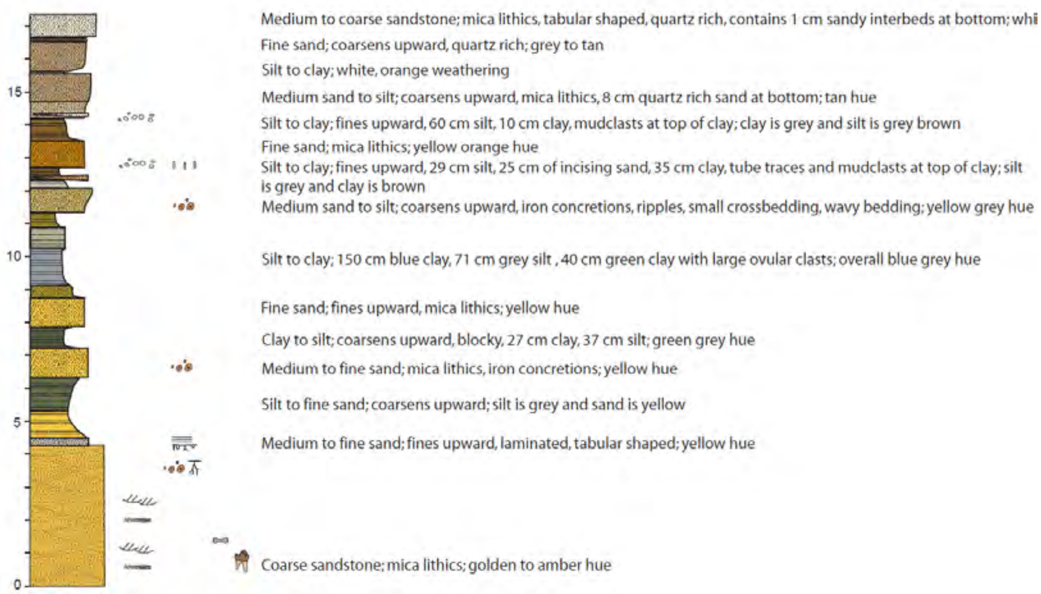

APPENDIX B.9 - Section 1105C Butte 8 of the East Pinnacles buttes. 42˚ 03' 52'' N 108˚41' 42'' W. Measured by SP Cairns, AM Neumann. Composed by AM Neumann

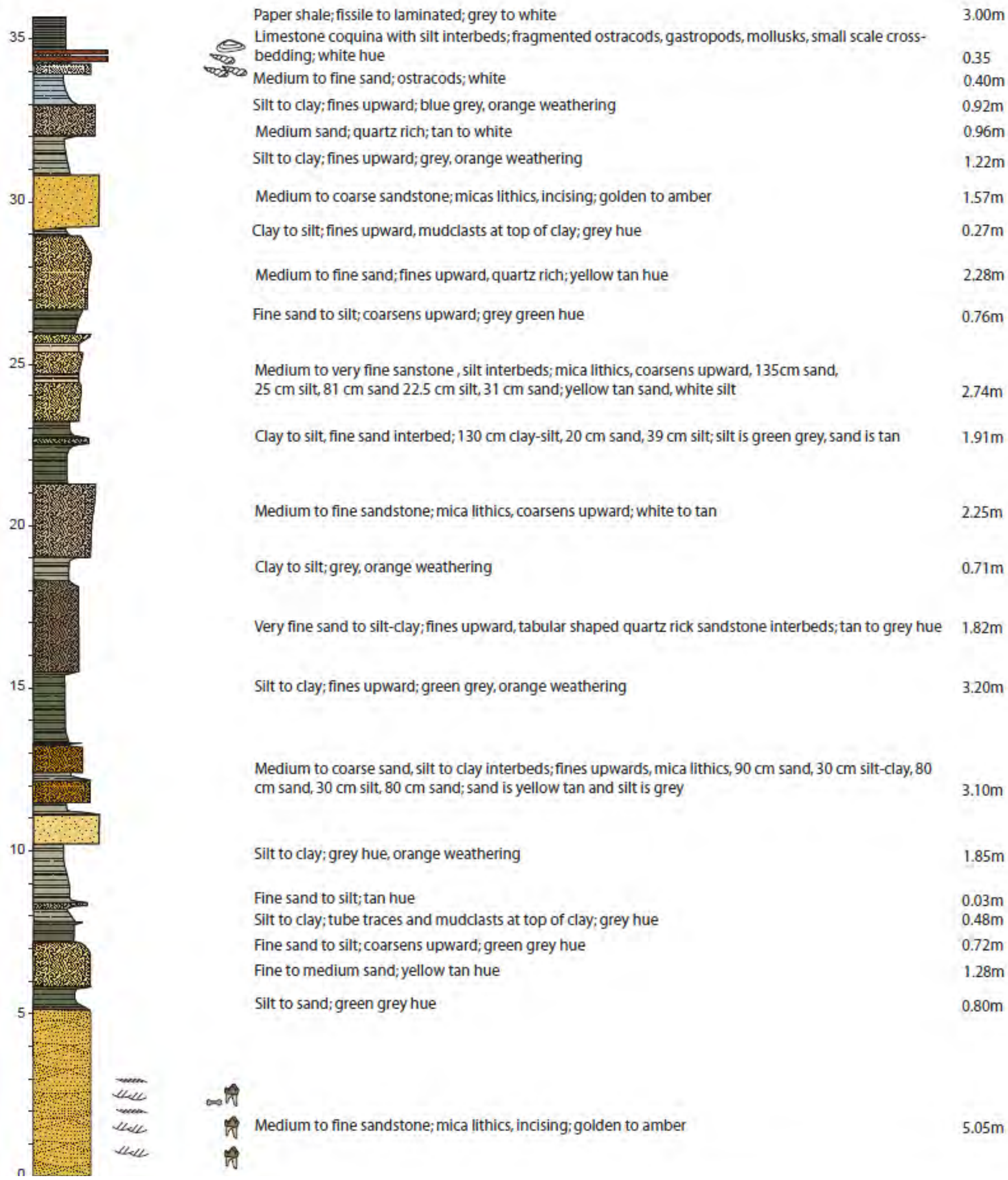

APPENDIX B.10 - Section 1106A Butte 15 of the West Pinnacles buttes. 42˚ 04’ 09’’ N 108˚ 44’ 04’’ W. Measured by C Hodgson, SP Cairns, LP McHugh, AM Neumann. Composed by AM Neumann

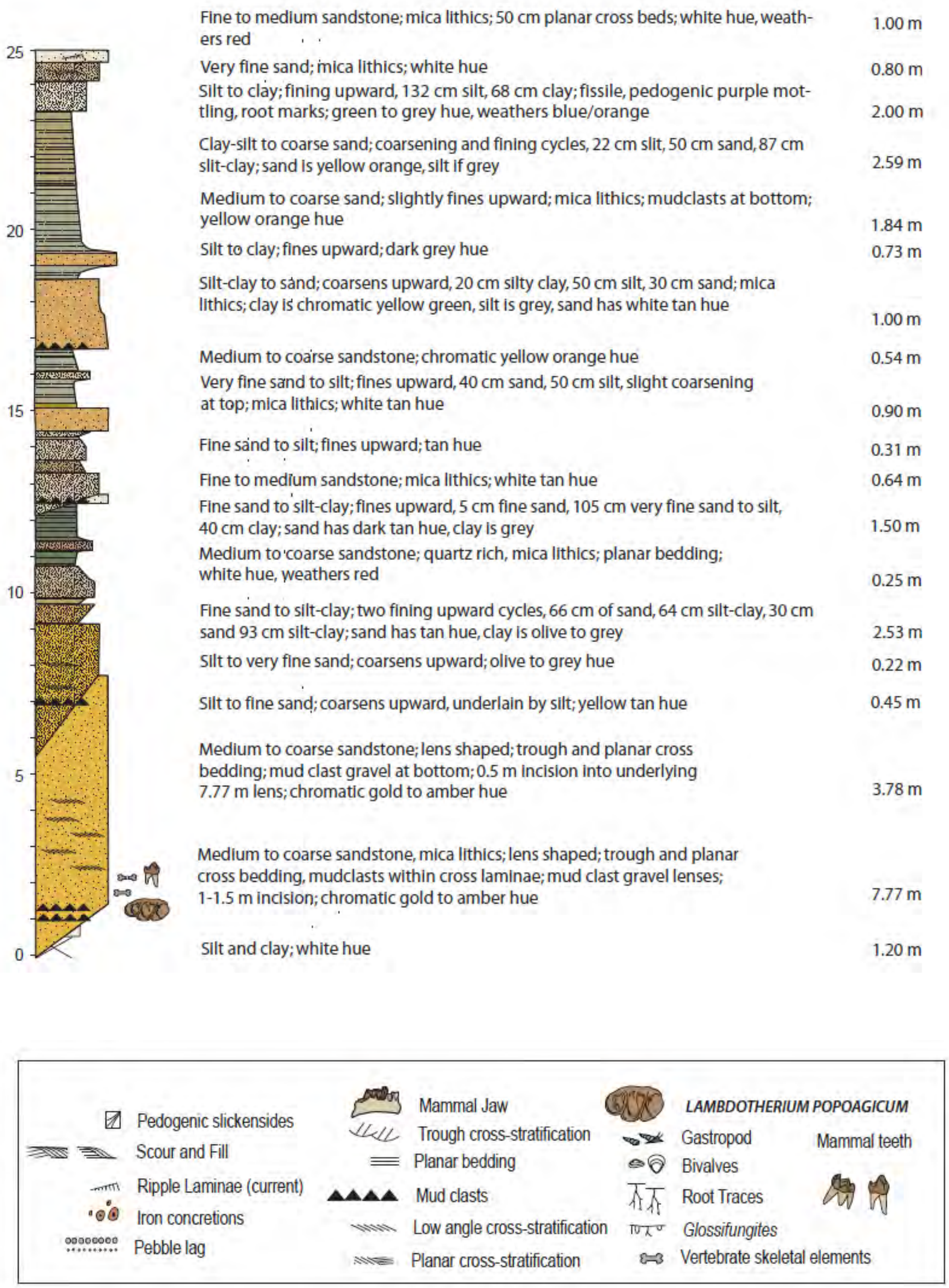

APPENDIX B.11 - Section 1106B Butte 16 of the West Pinnacles buttes. 42˚ 04' 03'' N 108˚ 44' 19'' W. Measured by C Hodgson, LP McHugh, AM Neumann. Composed by AM Neumann

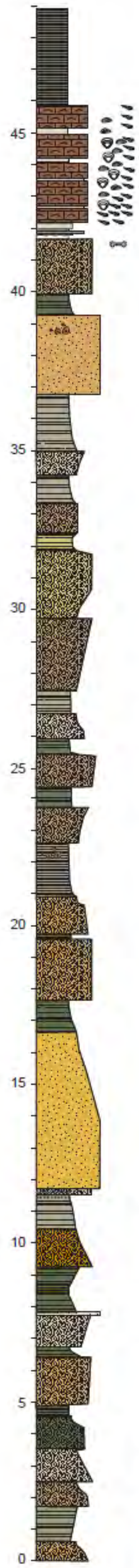

Paper shale; fissile to laminated; grey to white hue	3.00m
Limestone coquina with silt interbeds; ostracods, gastropods, mollusks, 0.5 cm interbeds of sand; white to orange hue	3.60m
Calcareous silt to chalk; fossiliferous, orange laminations; grey white hue	0.195m
Silt and fine sand; 6 cm fossiliferous silt, 2 cm sand, 7-9 cm fossiliferous silt; grey hue	0.185m
Calcareous silt to chalk; wave ripples; white hue	0.12m
Fine to medium sand; mica lithics; grey tan hue orange at top	1.75m
Silt to clay; sand lenses and interbeds; green hue	0.65m
Medium to coarse sand; mica lithics, iron concretions; yellow tan hue	2.50m
Silt to clay; fines upward; grey hue	1.76m
Silt to very fine sandstone; mica lithics, coarsens upward; tan white hue	0.75m
Silt to clay; fines upward; grey hue	0.92m
Very fine sand; mica lithics, tan hue	1.00m
Sand to silt; fines upward; green tan hue	0.55m
Silt to medium sand, mica lithics, coarsens upward; green tan hue	2.10m
Silt to medium sandstone; coarsens upward; tan hue	2.26m
Clay to silt; grey, orange weathering	0.73m
Fine sand to silt; fines upward; tan white hue	0.80m
Clay to silt; green grey hue	0.47m
Fine to medium sandstone; mica lithics, coarsens upward; tan hue	1.11m
Clay to silt; green grey hue	0.65m
Silt to very fine sandstone; coarsens upward, fissile at top; tan hue	1.10m
Silt to clay; fines upward, iron concretions; grey, orange weathering	1.70m
Fine sand; mica lithics, fines upward; tan yellow hue	1.17m
Clay to silt; green grey, orange weathering	0.14m
Fine to medium sandstone; mica lithics; yellow orange hue	1.95m
Silt to clay; fines upward; green grey hue	0.98m
Coarse to medium sandstone; mica lithics, fines upward, incising; golden amber hue	4.95m
Medium sandstone; quartz rich, tabular shaped, mudclasts at base, incising; white hue	0.20m
Sand to silt; mica lithics, fines upward, 83 cm blocky, 20 cm fissile silt; grey hue	1.03m
Medium to fine sand; mica lithics, fines upward; orange tan hue	1.19m
Fine sand to clay; 56 cm fining sand, 17 cm clay, 72 cm coarsening sand; green grey hue	1.45m
Very fine to medium sand; mica lithics, coarsens upward, tabular shaped at top; white tan hue	1.10m
Silt to clay; fines upward, 30 cm silt, 4 clm clay; green grey hue	0.34m
Fine sand; mica lithics, coarsens upward, incising; yellow tan hue	1.42m
Clay to silt; green grey hue	0.33m
Fine sand to silt; mica lithics, fines upward; green grey hue	1.12m
Medium to fine sand; mica lithics, fines upward; white tan hue	1.03m
Fine sand; mica lithics, fines upward, 58cm sand, 20cm silt; tan hue	0.78m
Clay-silt; coarsens upward; grey green hue	1.10m
Fine sand; fines upward; yellow tan hue	0.62m